Cytotoxic study of Poly-N-vinyl-2-pyrrolidone-based polymeric drug delivery system

Martin B. Rosenlund

Master thesis in Nanobiotechnology, 07 February, 2019 Department of Materials and Production, Aalborg University

Master's Project

Copyright © Aalborg University 2019

Department of Materials and Production
The Faculty of Engineering and Science
Aalborg University
http://www.aau.dk

AALBORG UNIVERSITY
STUDENT REPORT

Title:
Cytotoxic study of poly-N-vinyl-2-pyrrolidone-based polymeric drug delivery system

Theme:
Advanced Nanobiotechnology

Project Period:
Fall Semester 2018- Fall semester 2019

Project Group:

Participant(s):
Martin B. Rosenlund

Supervisor(s):
Leonid Gurevich
Christian Pablo Pennisi

Copies:

Page Numbers: 165

Date of Completion:
October 23, 2019

Abstract:

This Master project focuses on the cytotoxicity of polyvinylpyrrolidone-based polymer micelles as a drug delivery system. Among the many focuses of preparation for a drug delivery system is checking each possibility of requirements, among these are cytotoxicity. It has previously been reported to be non-toxic. However, a previous master project found that the polymer micelles formed via a sonification method was toxic. This was investigated further in this thesis, where sonification method and co-solvent evaporation method was used to create micelles from 1 kDa,3 kDa, 6 kDa and 12 kDa PVP-OD at 10xCMC. The co-solvent evaporation method showed a significant portion of smaller aggregates 10-100 nm for 12 kDa, in comparison to the other method and polymer sizes. Cytotoxic assay was performed on fibroblast (CRL 2429) and glioblastoma (U87) and it was found that the sonification method for 6 kDa micelles was toxic at concentrations above 0.08 mg/ml regardless if it was loaded or empty. For 12 kDa, the toxicity was at 0.1 mg/ml for loaded micelles and 0.08 mg/ml for empty micelles on fibroblast cells, while for glioblastoma cells they were only toxic with loaded micelles at the concentration of 0.1 mg/ml. It was also shown that the cytotoxic assay kit used in this thesis is sub-optimal for these polymeric micelles.

The content of this report is freely available, but publication (with reference) may only be pursued due to agreement with the author.

Department of Materials and Production
The Faculty of Engineering and Science
Aalborg University
http://www.aau.dk

AALBORG UNIVERSITET
STUDENTERRAPPORT

Titel:
Cytotoksisk undersøgelse af poly-N-vinyl-2-pyrrolidone-baseret polymert medikamentleveringssystem

Tema:
Avanceret nanobioteknology

Projektperiode:
Efterårssemestret 2018 - Efterårssemesteret 2019

Projektgruppe:

Deltager(e):
Martin B. Rosenlund

Vejleder(e):
Leonid Gurevich
Christian Pablo Pennisi

Oplagstal:

Sidetal: 165

Afleveringsdato:
23. oktober 2019

Abstract:

Dette master-projekt fokuserer på cytotoksicitet af polyvinylpyrrolidon-baserede polymermiceller som et lægemiddelleveringssystem.Blandt de mange fokus på forberedelse til et lægemiddelafgivelsessystem er at kontrollere hver mulighed for krav, blandt disse er cytotoksicitet. Det er tidligere rapporteret at polyeret skal være ikke-giftigt. Imidlertid fandt et tidligere masterprojekt, at polymermicellerne dannet ved hjælp af en sonificeringsmetode var giftige. Dette blev undersøgt nærmere i denne afhandling, hvor sonificeringsmetode og co-opløsningsmiddeldampningsmetode blev anvendt til at skabe miceller fra 1 kDa, 3 kDa, 6 kDa og 12 kDa PVP-OD ved 10xCMC. Fremgangsmåde til fordampning med co-opløsningsmiddel viste en betydelig del af mindre aggregater 10-100 nm i 12 kDa i sammenligning med den anden fremgangsmåde og polymerstørrelser. Cytotoksisk assay blev udført på fibroblast (CRL 2429) og glioblastoma (U87), og det blev fundet, at sonificeringsmetoden for 6 kDa miceller var toksisk i koncentrationer over 0,08 mg /ml, uanset om den var indlæst eller tom. For 12 kDa var toksiciteten 0,1 mg/ml for indlæste miceller og 0,08 mg/ml for tomme miceller på fibroblastceller, mens de for glioblastomaceller kun var toksiske med indlæste miceller i koncentrationen på 0,1 mg / ml. Det er også vist, at det cytotoksiske assay-kit, der er anvendt i denne afhandling, er suboptimalt for disse polymere miceller.

Rapportens indhold er frit tilgængeligt, men offentliggørelse (med kildeangivelse) må kun ske efter aftale med forfatterne.

Contents

Preface

This thesis project was written by Martin B. Rosenlund a master student studying Nanobiotechnology, at the department of materials and production at Aalborg University. The master project began the 01/09-2018 and ended 22.10-2019. The theme for the project is "Advanced Nanobiotechnology".

References to various sources, throughout this project are listed as [*], where the number refers to a specific source in the bibliography. The bibliography is placed in the end of the project, where the sources will be listed with their title, athor and other relevant information, depending on the form of the source (Book, article etc.). For the most parts the references are listed after a specific section in which they are used. indication that the reference applies to the entire section.

Tables and figures are numbered in the order of appearance per chapter e.g. Figure 4.1, denotes the first figure in chapter 4. Each table and figure has a brief caption, which can also contain a reference.

Special thanks are given to *Christian Pablo Pennisi* for his help and guidance at the Laboratory for Stem Cell Research at Aalborg univiersity. I would also like to thank *Mari Utigard* for being my support in these trying times.

Aalborg University, October 23, 2019

Martin B. Rosenlund
<mbrenn16@student.aau.dk>

Chapter 1

Introduction

Buchanan described the effect that ether anaesthesia had on the depth of narcosis in 1847, and this sparked the understanding that therepeutic agents had on the body. Pharmacokinetics is the field of study that describes drugs after delivery to the body, the distribution and the metabolical changes among. This is to better understand the effect of the materials that are put into to the body to optimise the treatment against the specific diseases. Among the diseases that keep researchers busy is the umbrella term, cancer. Cancer can be traced back to documented cases in Egyptian mummies and the number of cancer patients is high. In 2008 there was an estimate of 7 million cancer-related deaths with over 25 million people living with the disease. This number is also expected to increase in the future [47, 42, 19, 40, 12, 20, 8, 2]

Today the treatment for cancer include chemotherapy and radio therapy, but these treatments also come with concerns. In the case of chemotherapy the problem lies with the fact that the therapeutic agent is reacting throughout the whole system in the hopes that it will weaken the cancer cells enough before doing too much damage to the body. An interesting approach to this problem is a delivery system to manage the therapeutic agent directly to the cancer cells. This approach comes with different potential delivery methods, among them there have been research into delivering a killer gene via viruses or bacteria [42].

For this thesis the focus have been on the miceller drug delivery system, getting inspiration from *Polymeric Drug Delivery system* by Camilla Lystlund Andersen [4]. Where she showed the possibility of using amphiphilic thiooctadecyl-terminated poly-N-vinyl-2-pyrrolidone, PVP-od as a form of delivery system. Curcumin was chosen a model hydrophobic drug, by dissolving it in acetone before mixing it with PVP-od dissolved in water it was possible to incorporate it into the micelles. In a recent study done by Luss A. et al [27] it was shown that PVP-od micelles formed by two different methods, emulsification and ultrasonic-dispersion, showed different size distributions and the micelles smaller than 100 nm penetrated the nuclei through biologically independent mechanisms.

It was of interest then too look into the possibility of fractioning the different sized particles. This to to check the different cytoxic behaviour between the sizes and creation methods.

1.1 Curcumin

Plants have evolved throughout history to protect themselves from the enviroment, infections and diseases via different metabolites and some of these metabolites have been shown to beneficial to humans. Among the plant based treatments we find Turmeric. Turmeric, also known as *Curcumua longa*, is a plant of the ginger family. It is very present in Indian cooking as a spice, but it has also been documented as a medical herb for thousand of years. It is a major part of Ayurveda (alternative medicine based in the Indian subcontinent), Siddha medicine, Chinese traditional medicine and more [35, 33].

From Turmeric, the compound with most interest is Curcumin, which is a chemical that are used in food coloring, food flavoring and as an cosmetic agent. It was first isolated by Vogel and Pelletier in 1815 and has been since then studied extensively [1]. It's chemical composition is $\mathbf{C_{21}H_{20}O_6}$
and the chemical structure is *diferuloylmethane [1,7- bis(4-hydroxy-3-methoxyphenyl)-1,6-heptadiene-3,5-dione]*. The commercial availablity of curcumin consists of three different analogues of curcumin which also vary between their keto and enol form: 77% of Curcumin I (figure 1.1a) 17% of Curcumin II (figure 1.1b) and 3% of Curcumin III (figure 1.1c).

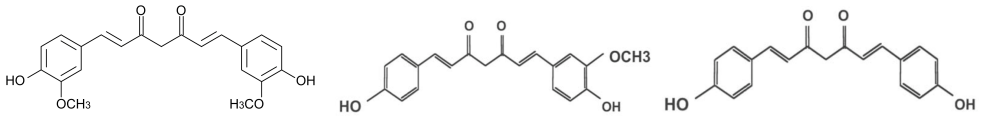

(a) Curcumin I in keto form **(b)** Curcumin II **(c)** Curcumin III

Figure 1.1: The chemical structure of the commercially available curcumin. Retrieved from [3, 4]

It's molecular weight is 368,37gmol and has a melting point at 183 °C. The color of curcumin is dependent on the enviroment and the pH. In an aqueous enviroment it will either have a yellow color at pH 2.5-7 and above pH 7 it will appear red. Curcumin shows great stability and solubility in organic solutions at acidic pH. When dissolved in acetone it shows a maximum absorbance between 415nm and 420nm.

The record from thousand of years of use on curcumin indicate that it has a great benefit in many different medical situations. To mention some benefits; it repress symptoms of type II diabetes, reduce blood cholesterol and speed up wound healing, to mention a few. More of it's medical properties can be seen in (figure 1.2).

From this it can be gathered that curcumin has a multi-targeting ability, which can explain its anti-cancerous properties. When looking into malignant glioblastoma cells it has been shown by Aoki et al [18] to reduce the size of a induced tumor by a threefold in comparison with the control [18, 32]. This makes it an interesting drug to look into for furthere development.

The problem with curcumin lies in its poor solubility, its fast degradation and poor oral bioavailability [50, 26]. To combat this poor solubility there are mutliple researches looking into the possibility of incorporating curcumin within different nanoparticles [43]. Among these there have been research into loading solid lipid nanoparticles, SLN, with curcuminoids. In this article by Tiyaboonchai [43], they showed an prolonged release of

curcumin *in vitro* up to 12h. It also showed a great storage capability, even after 6-months there were no significant difference between the stored and newly created curcuminoid loaded SNL.

Another possible curcumin loaded nanoparticle that researchers have shown a huge interest in are micelles. In the recent study by Luss A. [27] they showed that the two most common methods for micelle preperation, emulsification and ultrasonic dispersion, showed a difference in size distribution. It further proved that by managing the size of the loaded micelles, different mechanisms of crossing the cellular membrane was showed. This opens the intriguing possiblity of tailoring particles for different penetration mechanisms.

1.2 Targeted drug delivery

There are many routes of delivering therepeutical drugs to a patient; it can be delivered gastroinestinal (oral or rectal), parenteral (intramuscular, intravenous, intra-arterial) or pulmonary just to mention a few. However, most of the therapeutical drug is distributed evenly throughout the body and the active component of the therapeutical drug has to cross many barriers to get to the target of treatment. This exposes the agent to possibilities

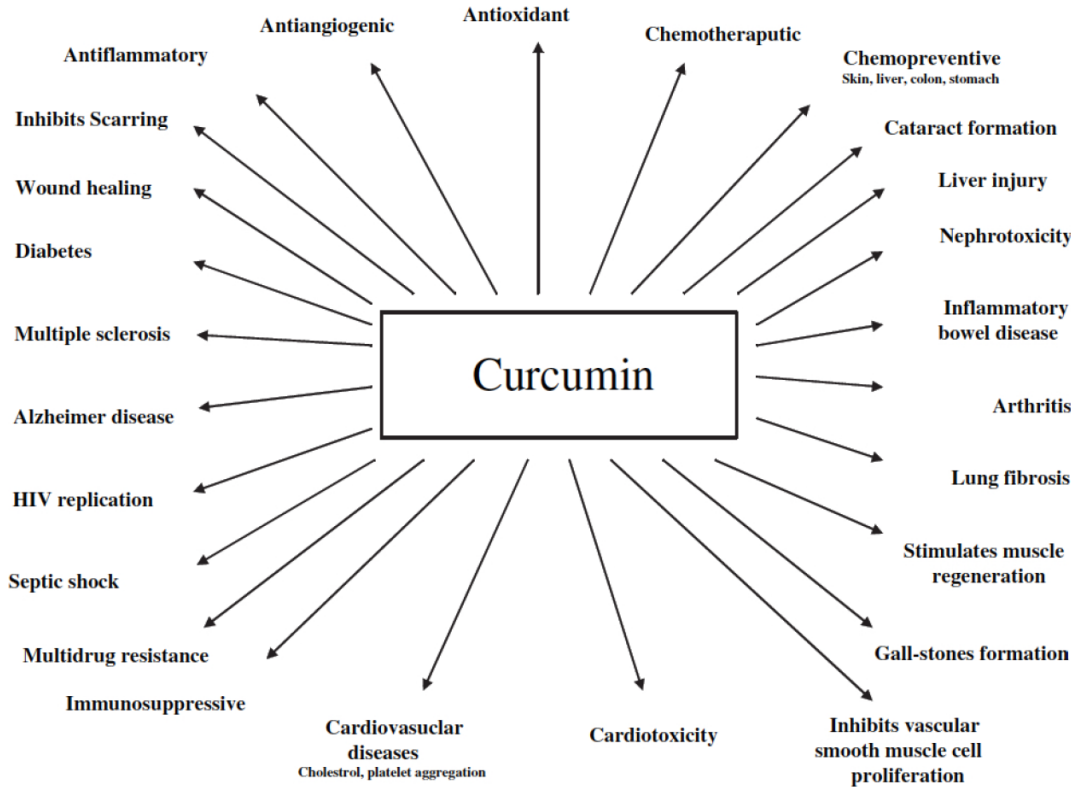

Figure 1.2: An image representation of the different medical benefits that curcumin has shown. Retrieved from [4]

that may inactivate the component or produce unintended effects to organs or tissues that are not a part of the treament. To overcome the possibility of parts of the drug being inactivated, the dosage is increased to up the chance of enough agent reacting with the target of treatment. This again increases the unintended effects of the therapeutic agent [31, 36].

To decrease the unintended effects of drugs it could be optimised to deliver it directly to the targeted cells, targeted drug delivery. This is defined as the ability to accumulate the agent at the targeted organ or tissue, independent on how the drug is delivered. By achieving a sufficient accumulation at the target site the side effects of the drug is reduced and the efficacy is increased. Some requirements for the drug delivery system is expected, it should not release any amount of the drug until it is has gathered at the target site (minimal to no leakage during transit), it should have a controllable release rate of the drug or a precise and consistent realese rate and should be stable in storage, *in vivo* and *in vitro* [36, 34].

There are multiple ways to carry a therapeutic agent for a targeted delivery. There are liposomes, antibody-drug conjugates, microspheres and nanoparticles, modified plasma proteins and micelles, to mention a few. There are also two distinct approaches to get it to the target site. One of the methods is based on the drug reaction to physiological properties that are around or at the active site, this is called passive targeting. The other method is to use a specific receptor on the delivery system attatching it or releasing the agent when it interacts with the target, active targeting.

1.2.1 Passive targeting

For a passive targeting delivery system, one of the requirements is that it is stable enough to keep the drug for a long period of time. This is to make sure that the drug has enough time to be able to accumulate enough at or in the target. This can be achieved by modyfing the delivery system in such a way that the opsonization is slowed down or prevented all together. This was proven possible by Torchillin and Trubetskoy [46], where they investigated the possibility, and effect, of using a water-soluble polymer to mask a drug delivery system.

One of the major effect utilized by a passive targeting delivery system is the Enhanced Permeability and Retention, EPR. This is an effect that can occur in cases with tumors. When the tumor grows quickly, the endothelial cell junctions become defective which creates gaps (200-800 nm) that the drug carriers can pass through from the blood stream. An example of this can be seen in figure 1.3. Another important part of this effect is reduced lymphatic drain that tumor tissue has. Allowing the drug carriers to accumulate within the tumor growth. This is the basis for passive targeting, and drug carriers can then be created with that gap size in mind, allowing them to accumulate inside the tumor cells.

1.2.2 Active targeting

Not all situations enable the use of passive targeting, some may not create defects in the endothelial cells making the EPR effect not an available method. Antoher possibility is that the affected cells may not differe too much from the healthy cells, thus not creating any significant changes that might make a drug delivery system accumulate and realese the drug in the affected area. In such situations a more direct approach is needed, where the

system can actively bind to the cells or penetrate specific cellular structures. This is called active targeting and it has a wide variety of ways to interact with the affected cells.

One of the methods of active targeting is utilising different moieties to interact with the enviroment it is in and among these the more popular choice is often antibodies. Antibodies utilises the fact that certain proteins can be expressed on the outside of affected cells, which creates a metaphorical harbour for the delivery system to dock to the cell. However, many problems may also arrive with the use of antibodies, such as size of the complete system. Since antibodies have a large size (150 kda) this might be one limiting factor. There are other moieties that are also a possibility. Such as, lipoproteins, sugars, hormones and lectins [7, 36, 21, 38, 39, 44, 22].

1.3 Polymer

Polymers are larger molecules that consist of a chain of multiple subunits that are repeated in different patterns. Some polymers, called biopolymers, can be found naturally occurring in the nature or in living organisms. Some of the biopolymers can be found as cellulose (polysaccharides) or proteins (polypeptides). Polymers can also be produced in a laboratory environment or larger production facilities, often described as synthetic polymers. Synthetic polymers can be derived from petroleum oil and it is the main component of plastics. Among the synthetic polymers we have polyethylene, nylon and polyvinyl chloride.

As mentioned previously, a polymer is composed of repeated subunits called monomers, and can be the same monomer repeated throughout the whole structure. In that case it is referred to as a homopolymer. If there are different monomers creating the larger structure, then the whole structure is referred to as a copolymer or heteropolymer. The monomers

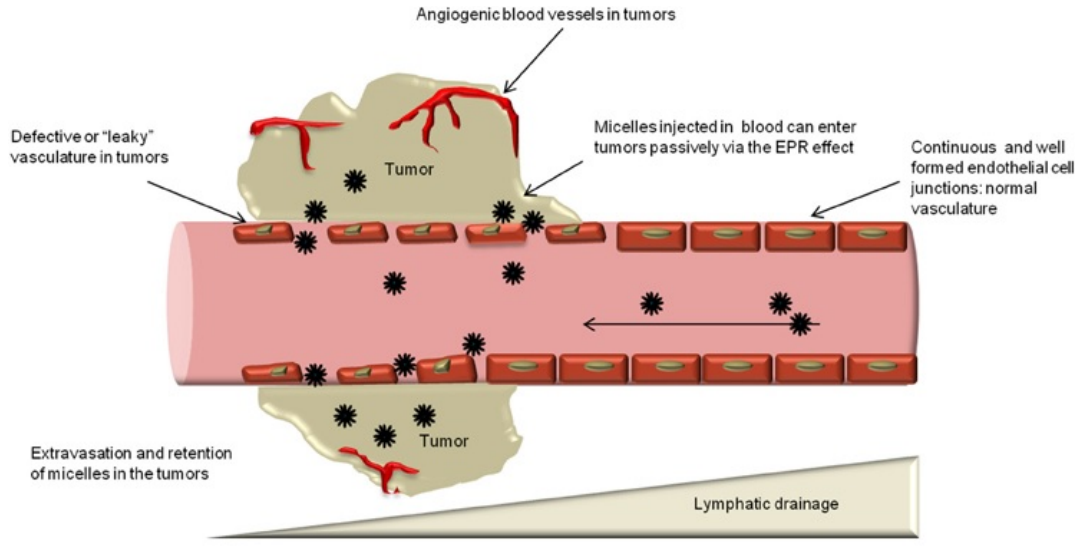

Figure 1.3: A view on the blood stream showing the effects of EPR. Retrieved from [21]

in a copolymer can be arranged in specific ways, and the behaviour of the polymer in different environments is dependent on both the monomer and the distribution of the monomers. A schematic of representation of the different copolymeric structures can be seen in figure 1.4.

By synthesizing the polymers we can affect the physical and chemical properties of the end product, further optimising them for specific drug delivery systems. There are two main groups of methods for creating polymers synthesis. The chain-growth polymerization is a chain reaction where one monomer will attach to the initiated monomer, this attachment will then generate an active site at the other end of the attached monomer. This allows another monomer to attach, and this continues in a chain until the reaction is terminated. The second methodology is where all the monomers are active and reacting at the same time by two active sites on each monomer. This will form dimers, trimers and more until they form a long polymer by combining all the "pieces" [41].

1.4 Polymers in medicine

There is a long list of medical applications of polymers, since the number of different polymers is also rather vast. Even narrowing it down to the synthetical polymers is not helping in the large varieties of different applications that polymers do have. The different applications in clinical medicine can be divided into the following groups; bulk material, coatings and carriers.

In the bulk materials we see polymers functioning as containers or sutures or even prostheses. Coating utilises the innate ability of some polymers to hinder or reduce inter-

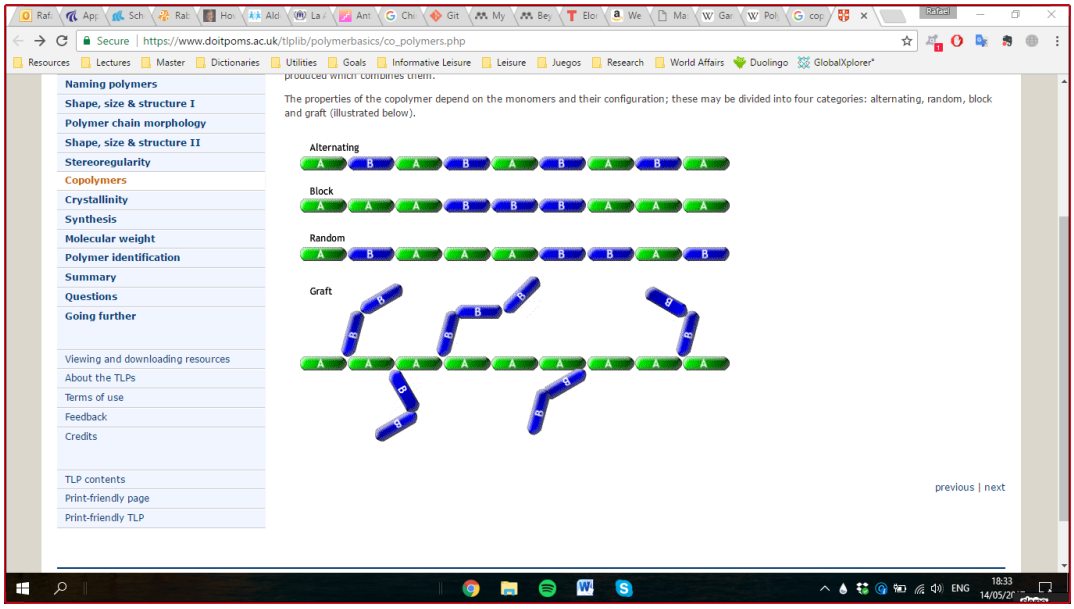

Figure 1.4: A schematic representation of different copolymeric structures. Retrieved from University of Cambridge 2004-2015 [11]

actions between the coated material and the body, or even alter the physical properties of other polymers or materials. This comes in the form such as a plasticizer and is often used in with poly (vinyl chloride), making it more flexible and durable [10, 28].

The last application that we find polymers in clinical medicine is the carriers and this is the focus of this master thesis. The pharmaceutical carriers is a wide field, but narrowing it down to the polymeric section gives us an easier overview. We have polymer-protein conjugates, drug-polymer conjugates, supramolecular drug delivery systems, and these are just some of the main groupings [13]. They all have different strengths and uses as drug delivery systems, and they have been researched for a long time.

1.5 Drug-polymer conjugates

Among the polymeric delivery systems we have is the drug-polymer conjugates. There are several ways that a polymer can be utilised as a cnojugate, but the general consensus is that the chosen polymer should be rather inert, not affecting the cells or system around it, water-soluble and having functioning groups that can be used for attaching the drug of choice. Other things that should be considered is the attachability of different moieties that can target the disease of choice. There are multiple different structures of drug-polymer conjugates being investigated. Among them is the traditional monofunctional linear conjugates. Here the drug is attached at the end of a single polymer or on a linker between the polymer and the drug. We also have polyfunctional linear, where the polymer is still a linear shape, but drugs are attached multiple places along the polymer. Starlike architecthure is also a possibility, here several polymers are surrounding the drug [13].

1.6 Micelles

Micelles gives a possibility of having a stable structure that can carry a drug throughout the system. It also offers the possibility of carrying hydrophobic therapeutic drugs and delivering them to the target cell. There are some important characteristics that needs to be considered for the micelles to function optimal as a drug delivery system. The biodegradability and biocompatability are to major factors, along with the size of the structure. The outer layer of the micelles created do not react with the blood or other tissue. This makes the micelles have a longer time in the blood stream[45, 16].

Micelles can be formed by self-assembly in an aqueous enviroment due to the monomer components of the copolymer are hydrophilic and hydrophobic. This creates an outer shell where the the hydrophilic parts are located and interacts with the medium, in the core the hydrophobic part creates a nucleous. The self-assembly happens through due to energy minimization and can be understood with thermodynamics as a balance between entropy and enthalpy. There are two factors that has to be reached before the micelles start self-assembling. The concentration of the amphiphilic polymer has to be over a certain threshold called the critical micelle concentration, CMC, and the temperature have to be greater than the critical micelle concentration, also known as the Krafft temperature. Now the main contributor to the entropy and enthalpy comes from the hydrophobic part of the polymer, while the hydrophilic will affect the size and interaction parameters [**doi:10.1021/bm015574q**, 29].

When a system is below the CMC there will be a small amount of the polymer acting as a surfactant on the surface, and the more surfactant there is the higher the surface tension will get. After reaching the CMC the surface tension will stay the same, but the surfactants will start to gather in the liquid until they spontanously start to form micelles. The CMC can be seen when you create a logarithimic response between the surface tension against the surfactant concentration. It will show two distinct regions, and in the intersect of this region you see the CMC point. This can be seen in figure 1.5.

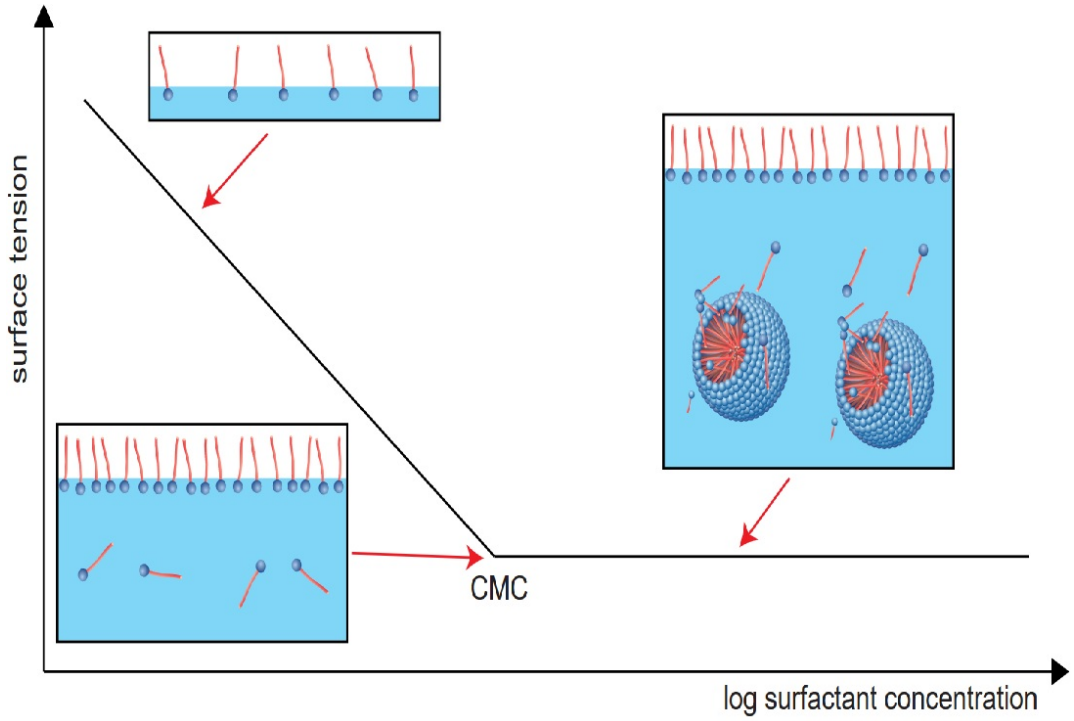

Figure 1.5: A logarithmic representation of the surface tension compared to the surfactant concentration. Retrieve from DataPhysics - Surfactants & critical micelle concentration https://www.dataphysics-instruments.com/knowledge/understanding-interfaces/surfactants-cmc/

The solvent is a vital point in the micellization, since the surfactant will act accordingly to the polarity of the solvent by having the same polarity part of the surfactant be submerged. However, it has been shown that the CMC for the chosen polymer for this thesis is given at 0.065mmol/l [27]. Micelles vary in the size range between 60-200 nm, but the optimal range for treatment of tumor growth has been shown to between 100-160nm. This is due to the fact that larger micelles will not be able to enter the cells, and the smaller will not remain in the cells long enough for the therapeutic agent to have a substantial effect [49].

1.7 Fibroblast

In animal tissue the basic types of cells can be divided into four major groups, or families. It is the muscle-tissue, nervous-tissue, epithelial-tissue and the connective-tissue. Among the connective-tissue family we find cells such as fat cells, bone cells, firboblast cells, cartilage cells and smooth muscle cells. The connective tissue is an important and vital part of the support system in the body. It's ability to reshape itself, adopting to each situation, makes it a vital part of tissues and organs reperation and support. It also support the other tissues in the body and is spread out through the system by the collagenous extracellular matrix (ECM).

The ECM is compromised of macromolcules, such as collagen and glycoproteins which create a extracellular network that gives structural support. The fibroblast cells are a central part of the ECM since they secreete precursor components of the ECM and they synthesize, and maintain the framework. Fibroblasts also play key parts when there is injury in the surrounding tissue, since the damage stimulates the fibrocytes producing more fibroblast. By migrating into the wound after multiplication they start an inflammation to battle the invading microorganisms. They also play a role in immune suppression in tumors by changing the ECM components, causing a remodeling of the ECM [9, 23, 37].

1.8 Glioblastoma

The nervous system is mainly built up of two classification of cells, it is the nerve cells and the glia cells. The nerve cells have the task of transferring the signals that occur in high speed through the nerve path. The glia cells are mainly small cells and have been long thought to just have the task of being a binding tissue in the nervous system. However, it has been later shown that they also have active functions. Such as destroying pathogens and removing dead neurons, support the neurons by supplying oxygen and nutrients and also have a role in neurotransmission [17]. They have a huge presence in the nervous system and they can be divided into multiple different cells. Such as; oligodendrocytes, astrocytes, ependymal cells, microglia, Schwann cells and satellite cells. Of these the Schwann cells and satellite cells are found in the peripheral nervous system, while the rest is in the central nervous system. There are also been recent discoveries that conflict with the previous idea that the glia cells outnumber neurons by a ratio of 10:1, stating that the ratio is most likely less than 1:1. They also state that they reviewed the previous data and that it also support the <1:1 ratio of glia to neurons [6].

When a tumour occurs from the glia cells it is called a glioma and it can further be classified depending on its grade, which cells the share features with and the location. The grade is determined by a evaluation of the tumour and the most common grading system is the World Health Organization (WHO) grading system. Where the least active or advanced disease is given the I grade and the most advanced and malignant is given IV grade. The IV grade of glioma is given the name glioblastoma multiforme (GBM) or glioblastoma. It is also the most common form of glioma.

The standard treatment after diagnosis is surgical removal of as much of the tumour tissue that is possible followed with chemotherapy and radiation if deemed possible with the patient's condition. The radiation is often given at a wide range, even covering the

whole brain. This is due to the growth pattern that glioblastoma has, it spreads diffusely over the brain tissue. The prognosis is serious with glioblastoma and as few as around 25 percentage of the diagnosed patients live 2 years after diagnosed and fewer than 5% live longer than 5 years. This is grim numbers considering that 3 per 100000 gets the diagnosis each year [25, 24, 6, 17, 14, 48]

1.9 Endocytosis pathways

In the case of drug uptake into the cells there are multiple pathways they can take, and endocytosis the cellular process in which an object is brought into the cell. These pathways can be categorised within the three different categories: clathrin-mediated endocytosis, pinocytosis and phagocytosis. Phagocytosis is the process in which particles to be uptaken into the cell is marked in the blood stream making it possible to be targeted by phagocytes. The marked particles are then recognised by the phagocytic receptors, before the particle is engulfed and forms a vesicle, a phagosome. This cannot occur without a trigger. A system that occurs naturally without a trigger is the pinocytosis group. Pinocytosis absorb soluble materials from the enviroment, creating small vesicles with extracellular fluids [15].

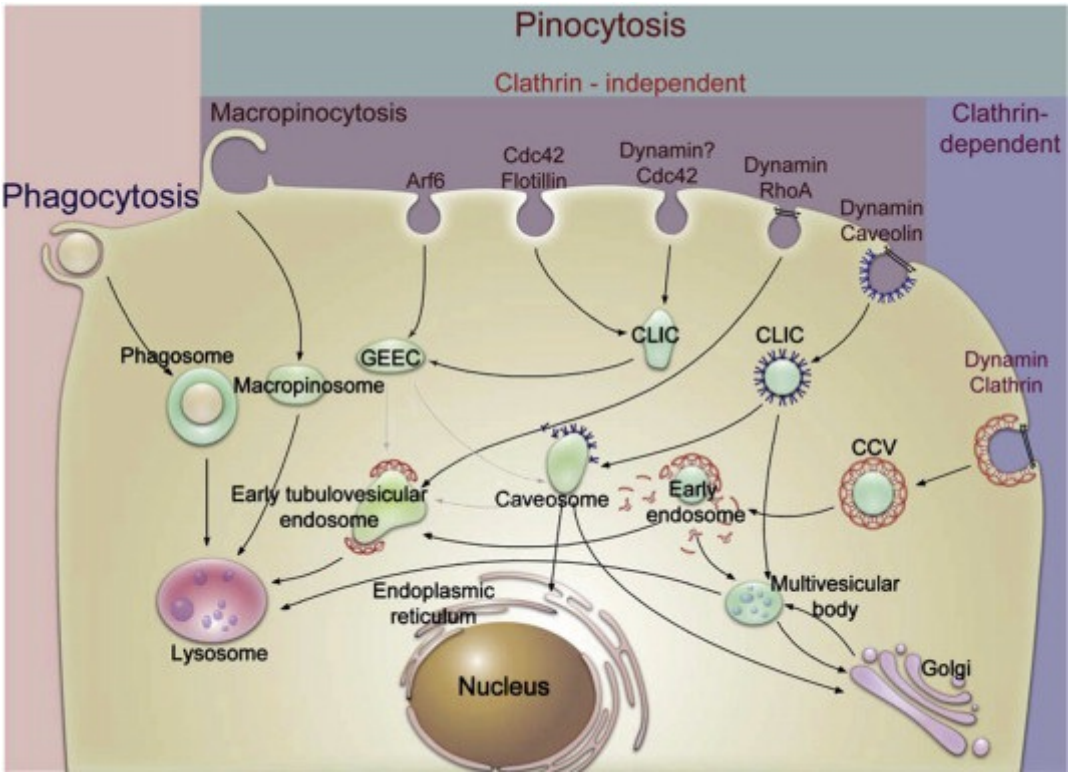

Figure 1.6: A representation of the different endocytosic pathways from outside of the cell to inside. CCV: Clathrin-coated vesicles. CLIC: Clathrin-independent carriers. GEEC: Glycophosphatidylinositol-anchored protein. Taken from Sahaya et al.[15]

Chapter 2

Materials and Methods

2.1 Materials

The chemicals and materials in this project is presented in table 2.1 and the list of machines can be seen in table 2.2

Table 2.1: Table containing the materials and chemicals used in the master thesis

Name	Manufacturer
0.2 µm filter	
Acetone	Sigma-Aldrich
Amicon 15 mL Spin filter	Merck
BSA-polystyrene conjugates	
Curcumin	Sigma Aldrich
CytTox-ONE	Promega
Ethanol	Kemetyl
Fibroblast (CRL 2429)	
Growth Medium	
Glioblastoma (U87)	
Phosphate-buffered saline (PBS)	Gibco
PVP-OD	Provided from Mendeleev University of Chemical Technology of Russ
Water LiChrosolv	Merck

Table 2.2: Overview of the instruments and programs used during this master thesis.

Name	Manufacturer - Description
Centrifuge	Eppendorf 5804R
Cooler system	Lauda - Variocol VC600
DLS Malvern Zetasizer nano-ZS	Malvern
Freeze-dryer	Christ Alpha 1-4 LD plus
Multimode plate reader	Perkin Elmer
PixelLink Digital camera	PixelLink
PixelLink Capture OEM (program)	PixelLink
Rotary Evaporator	Ika - RV10 digital
Sonicator (machine)	Sonics Vibracell
Sonicator (probe)	Sonics Vibracell

2.2 Methods

2.2.1 Micelles

The preperation for micelles were the same for the most part. Some differences were done in regards to concentration and order of filtration, but the following procedures were the general.

2.2.1.1 Sonification method

PVP-OD was dissolved in milliQ-water to achieve 10x the CMC value (exact values can be seen in table 2.3
Stock solution of curcumin was created by dissolving 0,0630 g curcumin in 15 mL acetone before adding 5 mL of stock solution to PVP-OD solution
Solution was transfered to a greiner tube, before sonicating (pulse, 1s on 2s off, amplitude 40%, 10 min) in ice bath
The sonicated solution was the run through a 0.2 µm syringe filter
The solution was then lyophilised

Table 2.3: List of the masses required of the different PVP-OD polymers to achieve 10xCMC at 50 mL

	1 kDa	3 kDa	6 kDa	12 kDa
g	0,0325	0,0975	0,1950	0,3900

For creating empty micelles the creation and addition of curcumin dissolved in acetone was bygone

2.2.1.2 Co-solvent evaporation

Adjust the pH of filtered LiChrosolv (10kMWCO centrifuge filter) with nAOH to 9.5-10 pH. Add 5 drops of pH adjusted water to ethanol (96%, 100 ml), and dissolve the polymer and drug (if loading the polymers) in the solution. Add pH adjusted water to the solution dropwise until the concentration of ethanol reaches 80%
Add the solution to a rotary evaporator, water batch at 40 degrees, and run it until there is just around 3 mL left. Run the remaining solution through a 0.2 µm syringe filter before freese-drying

Table 2.4: List of the masses required of the different PVP-OD polymers to achieve 10xCMC at 3 mL through the rotary evaporator.

	1 kDa	3 kDa	6 kDa	12 kDa
g	0.0020	0.0059	0.0117	0.0234

2.2.2 Cytotoxic assay

Prepare a multiwell-plate with cells in growth medium.

Incubate the plate containing the cells until 80% confluence is reached.

1. Photograph each well
2. Discard growth medium
3. Wash once with PBS

Add the prepared micelle solution, see chapter 2.2.2.2, to the appropriate wells. Incubate the plate at 37 °C for 24 hours. Then add 2 µL of lysis solution per 100 µL of original solution to create forced positivies. Incubate at 37 °C for 5 minutes, before equilibrating to 22 °C. Photograph each well. Transfer 100 µL of medium to a multiwell-plate. Add 100 µL of CytoTox-ONE reagent to each well and shake for 30 sec. Add 50 µL of stop solution to each well, in the same order of addition that was used for adding the CytoTox-ONE reagent. Shake plate for 10 seconds. Record the fluorescence with excitation wavelength of 560 nm and emission wavelength of 590 nm in a multi-plate reader.

2.2.2.1 CytoTox-ONE Reagent

The CytoTox-ONE reagent was prepared in the following way:

1. Thaw and equilibrate Substrate Mix and Assay buffer to room temperature (22 °C).
2. Add 11 mL Assay buffer to a vial of substrate mix to prepare The CytoTox-ONE reagent.
3. Gently mix to dissolve the substrate mix

2.2.2.2 Growth medium for micelle solution

The growth medium for the micelle solution was prepared by adding 1 mL P/S solution and 2 mL Horse Serum were added to 100 mL DMEM growth medium. The solution is then filtered for sterilization. To this the prepared micelles was added to create a batch with the concentration of 5,0 mg/ml. From this further dilutions was made as needed.

Chapter 3

Results and Discussion

3.1 Micelle preperation

Several batches of micelles were prepared with PVP-OD of different sizes (3 kDa, 6 kDa and 12 kDa). These were also prepared either loaded or not loaded with curcumin as a therapeutic agent and in two different methods. The specific co-solvent evaporation methodology that was used for this thesis was developed by Levi Nelemans at our group [30]. He has found out that the co-solvent evaporation method showed great promise in creating a substantial fraction of smaller aggregates of the PVP-OD at around the 30-60 nm range. By following his technique, I observed smaller aggregates in the co-solvent method than for the sonification method, as can be seen in [et eller annet]. However, there is a larger concentration of bigger aggregates also present in both methods. This can be attributed to the difference in choice of model drug, as for this thesis the choice was laid upon curcumin. Another possibility is that the micelles formed by the co-solvent evaporation method are smaller before lyophilised, and aggregate to larger structures when re-hydrated. Adding lyoprotectants might inhibit this aggregation.

1 kDa of PVP-OD was excluded from comparisons. In both methods there is filtration using 200 nm syringe filter, and it was quickly discovered that micelles prepared with the 1 kDa PVP-OD had trouble being filtered. More on this in later sections

3.2 Physical observations

One of the major concerns that came when preparing the curcumin loaded micelles with co-solvent evaporation method was the colour change in the solution when comparing it to the other method. This coincides with the pKa_1 , pKa_2 and pKa_3 of curcumin respectively at pH 7.8, 8.5 and 9.0 [5]. As the method required an alkaline solution at 10 pH to increase the nagative charge on the micelles. The colour change is easily explained with this. It do, however, raise the concern of the solubility of curcumin. As it changes colour it also becomes water soluble, indicating the detoriation of curcmin into different derivatives. There was no longer a possibility to discern with the naked eye if the curcumin was incorporated into the micelles or was loose in the solution, as this was made possible by the insolubility

in water.

As a quick confirmation test, the pH was dropped below the pKa_1 to check if the colour would change back or if there would be some precipitation. This gave varying results, but nothing ever precipitated. Sometimes the colour did change back to the yellow and other times it did not change colour even into highly acidic solutions. This pointed in the direction that after lyophilisation the curcumin would be incorporated into the micelles, and that it also protected the curcumin sometimes from the environment. Keeping the water-soluble form when it would change back. Another important point about this water-soluble form of curcumin is that it is less stable and most likely decomposes rapidly in this form.

Another quick observation that was made in regards to the differences between the two method and is relevant for both the empty and loaded micelles. The lyophilised product from the different methods was highly different. Where the sonification method gave a denser and more compact product, the co-solvent evaporation gave a more powdered form, like coarse sand. This can be that there is a small percentage of ethanol left in the solution before freezing the samples, and since the ethanol would be among the first liquids to evaporate it creates "small pockets of air". The other option is that there is a larger solution in the greiner tubes

3.3 DLS results

Looking into particle sizes in the mdium (Milli-Q water and 10k MWCO filtered LiChrosolv water) that was used for re-hydrating the powdered micelles, it was shown that there are particles present in both cases, as can be seen in figure 3.1 &(figure 3.2. The figure shows the average of three DLS measurements as presented by the software. However, when looking into the BSA-conjugates in the same medium there is no presence of these particles shown in the graph. The same liquids was used when diluting the PBS to 20mM.

To be on the safer side of things, the filtered LiChrosolv water was still used. Since it showed the smalles amount of intereference width and the presence of particles in the range of interest was the least for LiChrosolv water. As the particles of interest is in the range of 50-300 nm it would be better to have the smallest amount of impact in that range.

3.3.1 BSA-polymer conjugates

The BSA-polymer conjugates show a clear peak at around 136 nm with a low PDI, as can be seen in figure 3.3 which shows all 3 graphs from the DLS software. In figure 3.3 the 3 distributions are presented in the colours red, blue and green. The red and blue graphs are right atop each other. The conjugates was dissolved in 20mM PBS that was diluted from 40mM PBS with LiChrosolv water. The DLS results from LiChrosolv water can be seen in 3.1. This can attribute to the low presence of any of the same peaks that were present in both figure 3.1 & 3.2. It can also be the intensity of the peak making the other peaks that would have been presented, but diluted, a lot smaller. This could make them masked on the graph.

This can be attribted to the polymer and the production of that polymer giving a smaller size distribution. This makes the size more controlled since BSA is of a specific size, when comparing it to the pvp-od micelles which is a self-assembled process that shows a wide size distribution that is dependent on several factors.

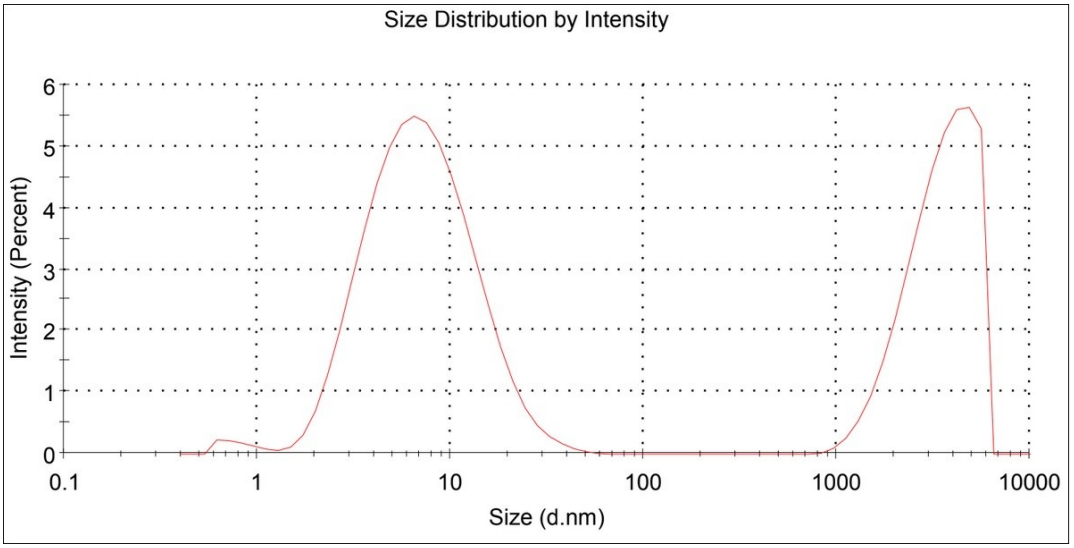

Figure 3.1: Size distribution by intensity for the filtered LiChrosolv water with the average of three measurements given by the DLS software done with attenuation factor 9. Individiual readings and a table with information can be seen in Appendix A and Appendix B

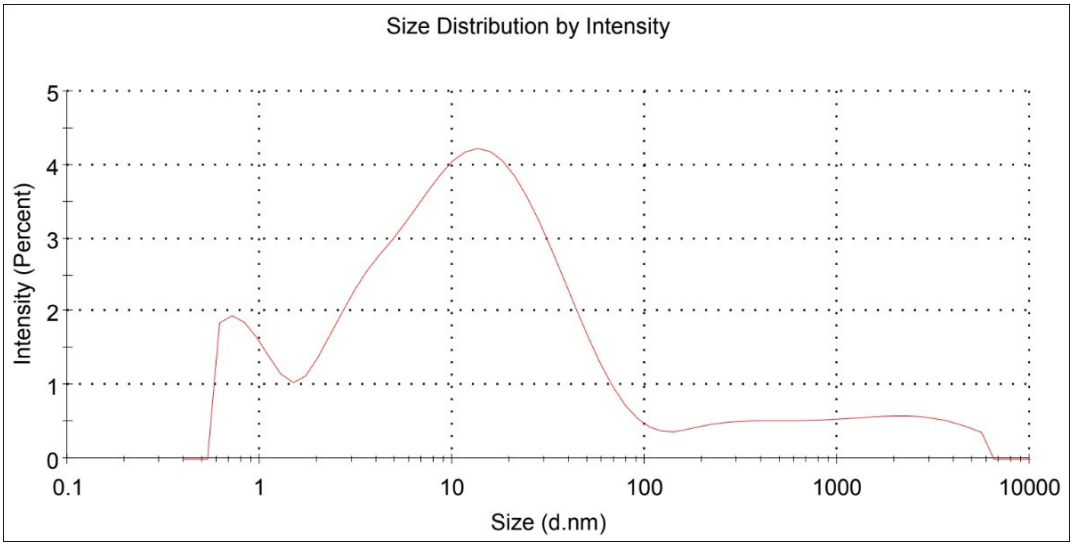

Figure 3.2: Size distribution by intensity for the Milli-Q water with the average of three measurements given by the DLS software done with attenuation factor of 7. Individiual readings and a table with information can be seen in the Appendix A and Appendix B

3.3.2 PVP-OD micelles

3.3.2.1 1 kDa micelles

When creating the 1 kDa polymeric micelles, the solution was very viscous compared to the other sized polymeric micelle solutions. This made it impossible to filter it through the 200 nm syringe filter and further tests was deemed unnecessary for comparisons with the 1 kDa polymeric micelles. The solution was still of interest to check in the DLS to see what created the viscous sample. This gave the graph presented in figure 3.4.

This clearly shows a wide range of different sized particles, with peaks present around the 100-300, 1000 and 5000-6000 nm range. It is clear that it would be difficult to filter it through a 200 nm filter with the higher peaks for the larger aggregates.

This can indicate that the process would be better focused on doing a comparison between same concentrations at mass in solution instead of molecular concentration.

3.3.2.2 3 kDa micelles

3.3.2.2.1 Sonification method Comparatively to the BSA-polymer conjugates, the results from the DLS shows a wider spread. Just like in the case of the 1 kDa micelles, as seen in figure 3.4. However, what can be seen from the graphs in figure 3.5 - 3.7 is a higher concentration of particles in the range around 100-200 nm and less of the particles close to 1000 nm. There is still a presence of aggregates or particles in the 5000 nm range, but this can also be attributed to the solvent used, as can be seen in figure 3.1. The graph for the BSA-polymer conjugates was 20mM PBS with the same solvent used for diluting the

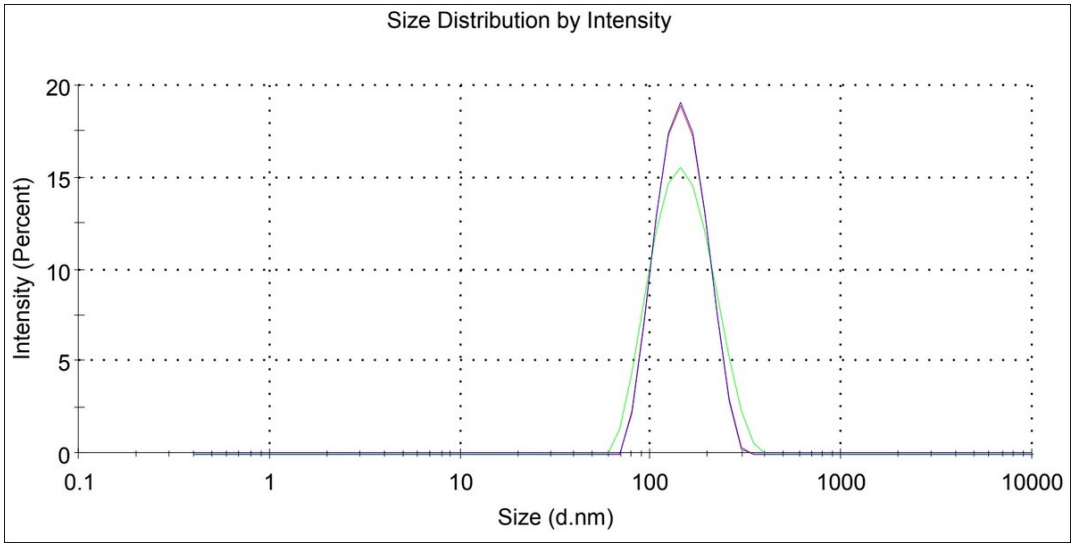

Figure 3.3: Size distribution by intensity for the BSA-polymer conjugates with the three measurements given by the DLS software done with attenuation factor 3. Individiual readings and a table with information can be seen in the Appendix A and Appendix B

PBS from 40mM to 20mM and thus should have some small presence of particles in both ranges. This is the case for the polymeric micelles, the loaded and not loaded.

When comparing the different micelles created with 3 kDa, both the loaded and unloaded micelles, there is a small difference in the graphs. This can also be seen in the values

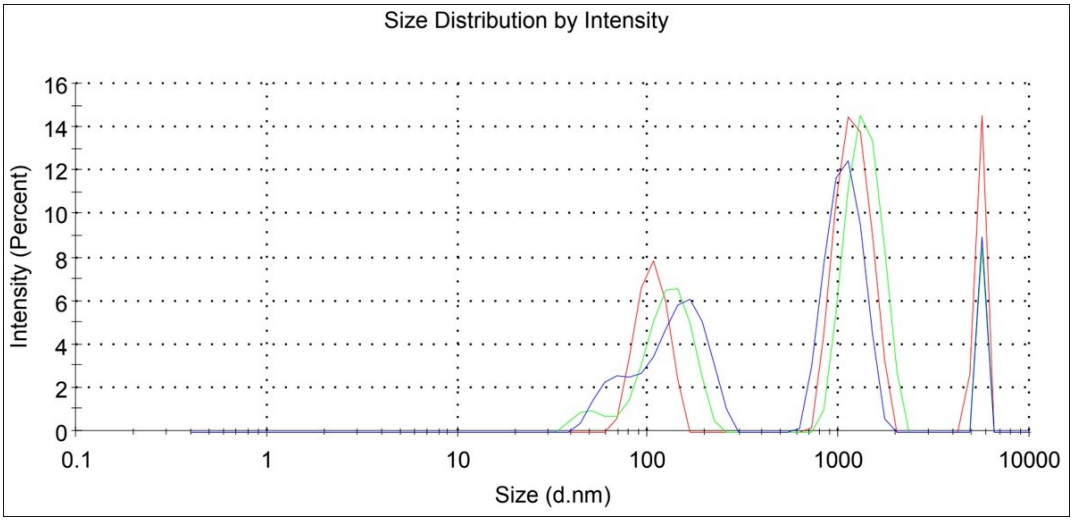

Figure 3.4: Size distribution by intensity for the 1 kDa polymeric micelles of pvp-od with the three measurements given by the DLS software done with attenuation factor 4. Individiual readings and a table with information can be seen in the Appendix A and Appendix B

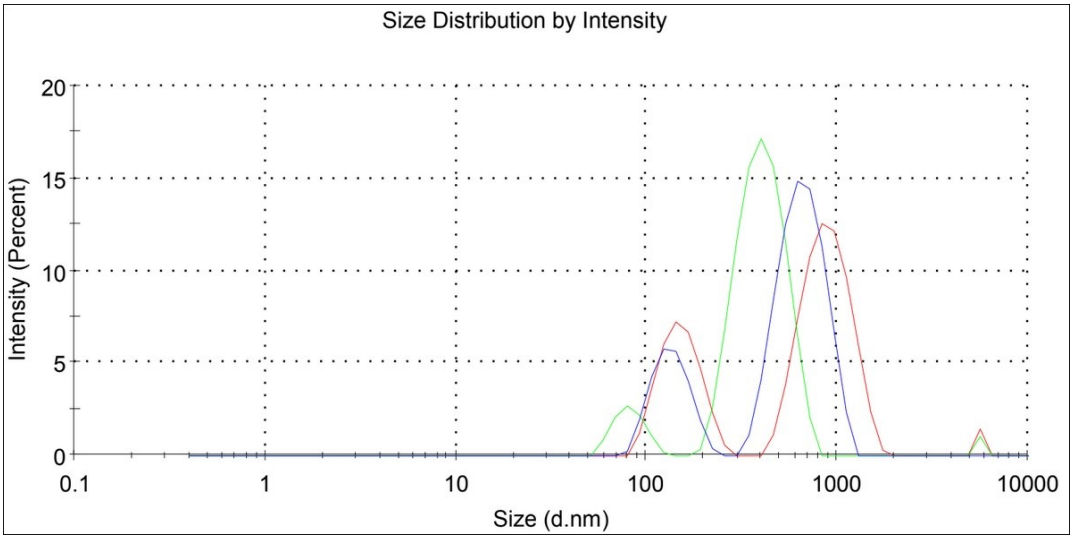

Figure 3.5: Size distribution by intensity for first iteration of the triplicates of the not loaded 3 kDa polymeric micelles of pvp-od with the three measurements given by the DLS software done with attenuation factor 5. The micelles were formed by the sonification method. Individiual readings and a table with information can be seen in the Appendix A and Appendix B

presented in the tables B.2, in Appendix A and Appendix B. Looking at DLS graphs and peak values presented, one must use a little caution since the graphs are not alwasy displayed with the range in the y axis. Take the 3 of the triplicates of the loaded 3 kDa

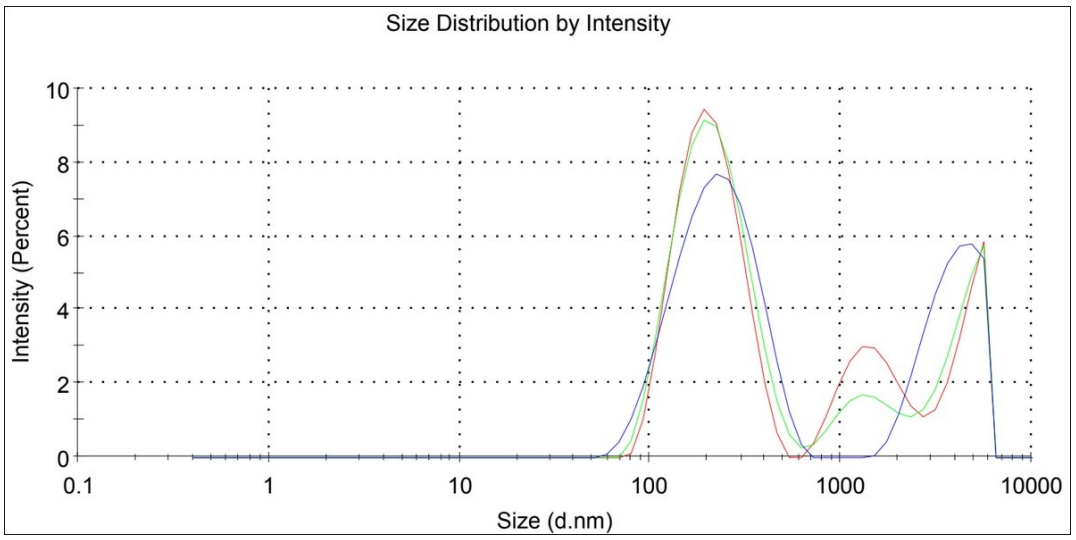

Figure 3.6: Size distribution by intensity for second iteration of the triplicates of not loaded 3 kDa polymeric micelles of pvp-od with the three measurements given by the DLS software done with attenuation factor 6. The micelles were formed by the sonification method. Individiual readings and a table with information can be seen in the Appendix A and Appendix B

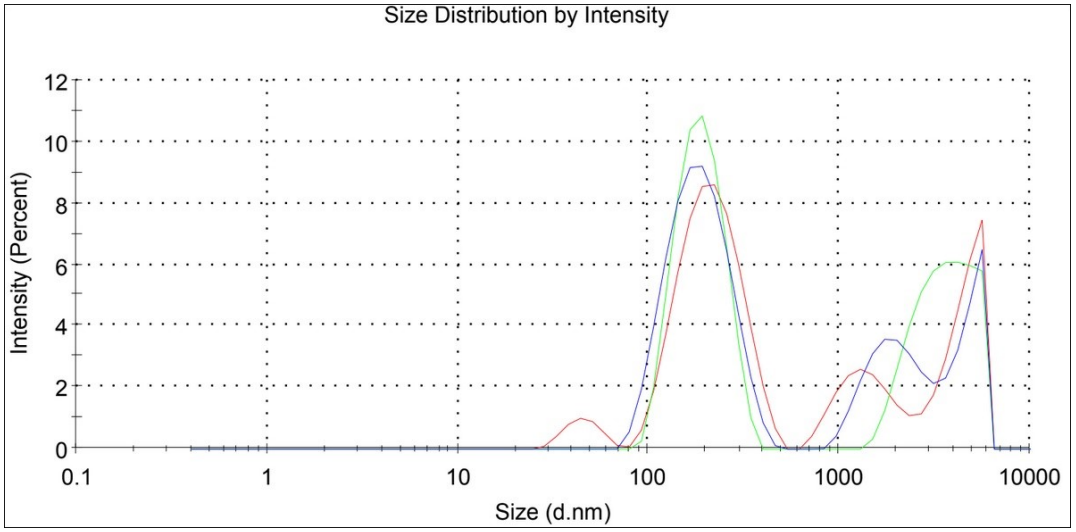

Figure 3.7: Size distribution by intensity for third iteration of the triplicates of not loaded 3 kDa polymeric micelles of pvp-od with the three measurements given by the DLS software done with attenuation factor 6. The micelles were formed by the sonification method. Individiual readings and a table with information can be seen in the Appendix A and Appendix B

micelles, there is clearly a huge peak present at a bit below the 200 nm mark, but the peak presented with values is closer to the 400 nm mark. Due to this, one should use bothe the values given by the program as well as the graph presented with caution. Utilising the knowledge of both to avoid conflicting values presented.

The loaded micelles created with 3 kDa pvp-od polymer shows a slight difference in creating larger aggregates, but they also have a wider spread around those areas. The wider spread can be seen in the graphs in figure 3.8, 3.9 and 3.10, or they can be extrapolated with the standard deviation given in table B.5, B.6 and B.7 in the Appendix A and Appendix B, taking care to compare both the graph and table.

Given the average values; 138.2, 223.0 and 199.8 for the empty micelles and; 277.9, 220.2 and 178.3 for the loaded micelles. It can be clearly seen that there is a difference in the peaks for the sizes and a difference between the samples. This might be attributed to the presence of a drug loaded into the micelles, causing a slight sell in seize and in the spread by having a difference in the amount loaded into the aggregates.

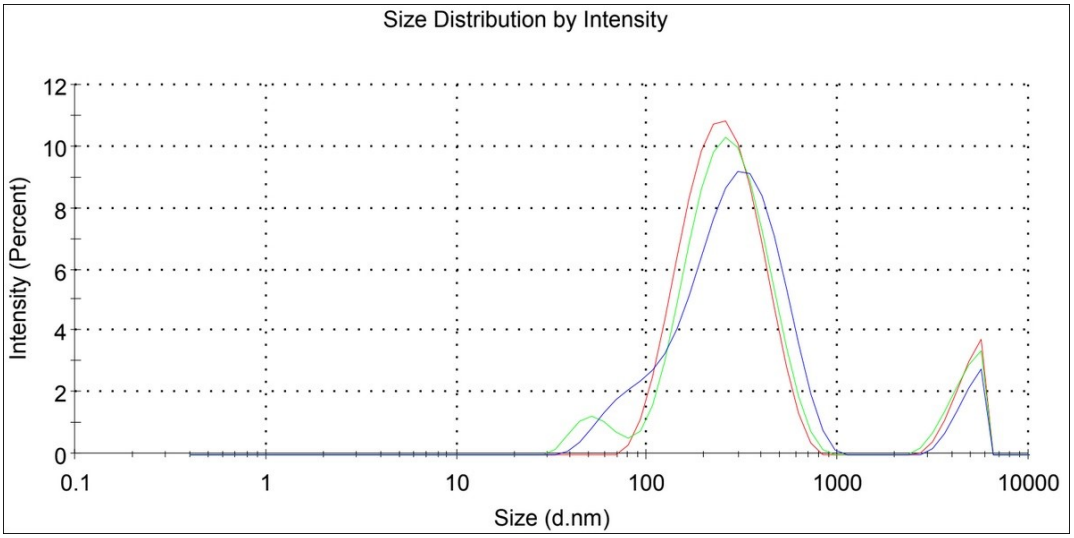

Figure 3.8: Size distribution by intensity for first iteration of the triplicates of the not loaded 3 kDa polymeric micelles of pvp-od with the three measurements given by the DLS software done with attenuation factor 5. The micelles were formed by the sonification method. Individiual readings and a table with information can be seen in the Appendix A and Appendix B

3.3.2.2.2 Co-solvent evaporation method Quikly looking at the graphs in figure 3.11 - 3.13 it can be seen that they are showing even larger aggregates than that of the sonification method, by showing high peaks closer to the 300-500 nm mark. It could also be argued that they show a larger presence of particles already at the 30-60 nm mark, but this is varying too much between the triplicates to be concluded as a good proof of anything. The presence of aggregates close to the 5000 nm mark is still evident even in the co-solvent evaporation method.

The interesting things with these particles happen when we add the curcumin to the mixture in the rotary evaporator. The DLS clearly shows a higher presence of the loaded

micelles in comprison to the previous samples. This can clearly be seen in figure 3.15 and 3.16, by the higher intensity of the particles. However, figure 3.14 shows that there is still a presence of particles at the 5000 nm mark. Unlike what happened with the sonification

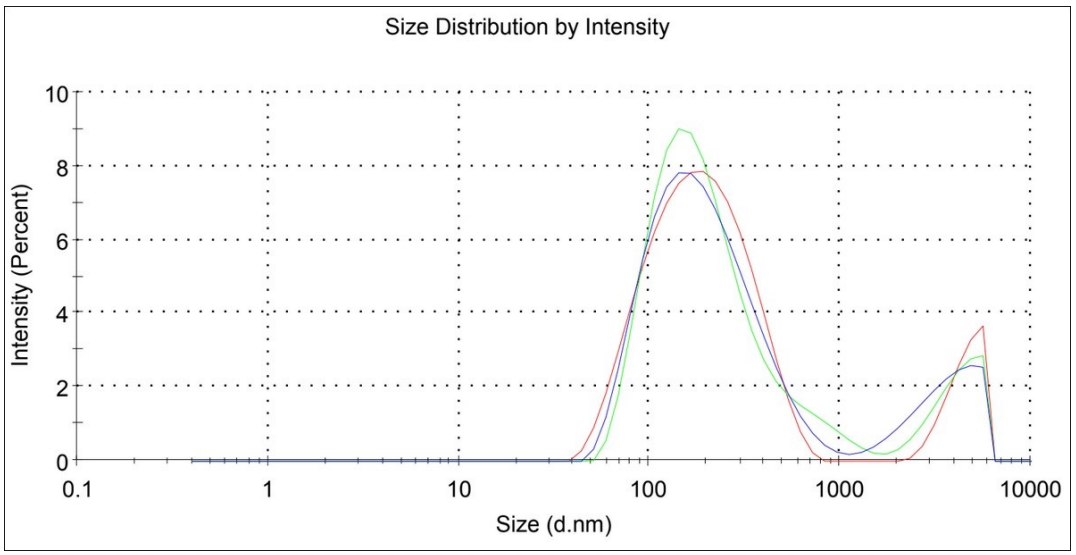

Figure 3.9: Size distribution by intensity for second iteration of the triplicates of not loaded 3 kDa polymeric micelles of pvp-od with the three measurements given by the DLS software done with attenuation factor 6. The micelles were formed by the sonification method. Individiual readings and a table with information can be seen in the Appendix A and Appendix B

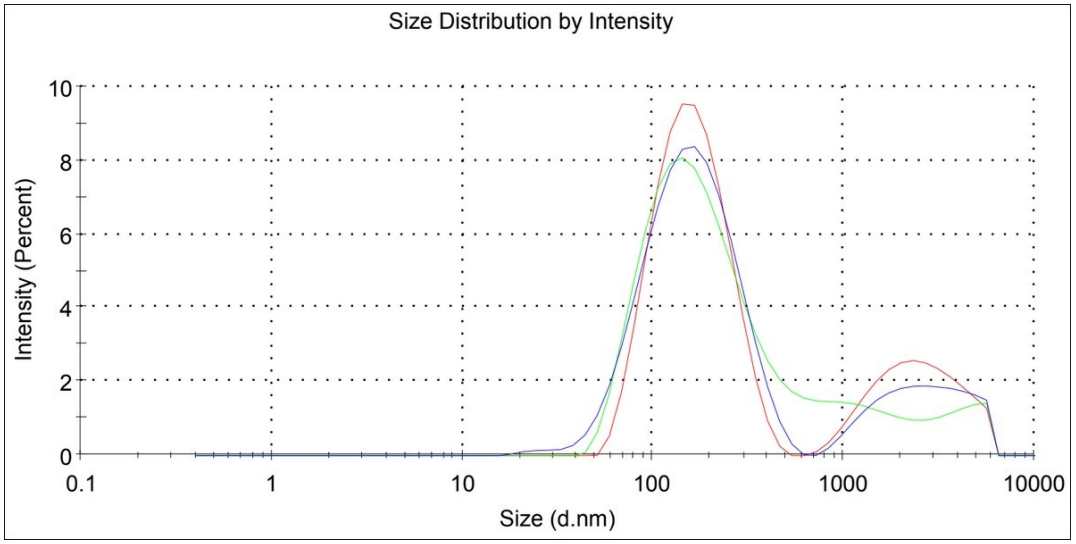

Figure 3.10: Size distribution by intensity for third iteration of the triplicates of not loaded 3 kDa polymeric micelles of pvp-od with the three measurements given by the DLS software done with attenuation factor 5. The micelles were formed by the sonification method. Individiual readings and a table with information can be seen in the Appendix A and Appendix B

method for 3 kDa pvp-od micelles, where the presence of curcumin enlarged the micelles, the presence of curcumin in co-solvent evaporation method creates smaller sized micelles. The size is closer to that of the empty micelles of the sonification method for the loaded

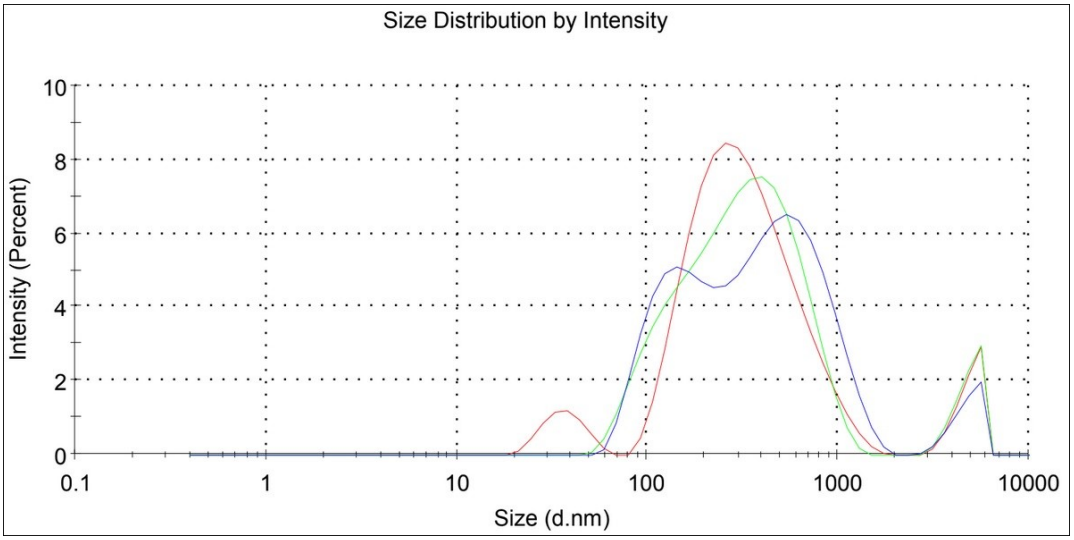

Figure 3.11: Size distribution by intensity for first iteration of the triplicates of the not loaded 3 kDa polymeric micelles of pvp-od with the three measurements given by the DLS software done with attenuation factor 7. The micelles were formed by the co-solvent evaporation method. Individiual readings and a table with information can be seen in the Appendix A and Appendix B

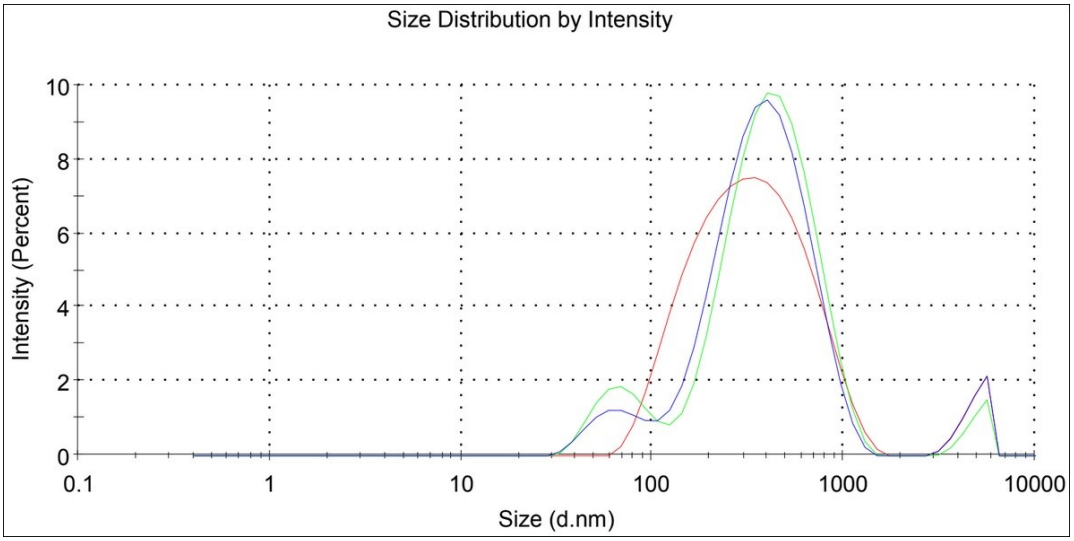

Figure 3.12: Size distribution by intensity for second iteration of the triplicates of not loaded 3 kDa polymeric micelles of pvp-od with the three measurements given by the DLS software done with attenuation factor 7. The micelles were formed by the co-solvent evaporation method. Individiual readings and a table with information can be seen in the Appendix A and Appendix B

micelles formed by the co-solvent evaporation method. While the empty micelles formed by the co-solvent evaporation method is even larger than the loaded micelles formed with the sonification method.

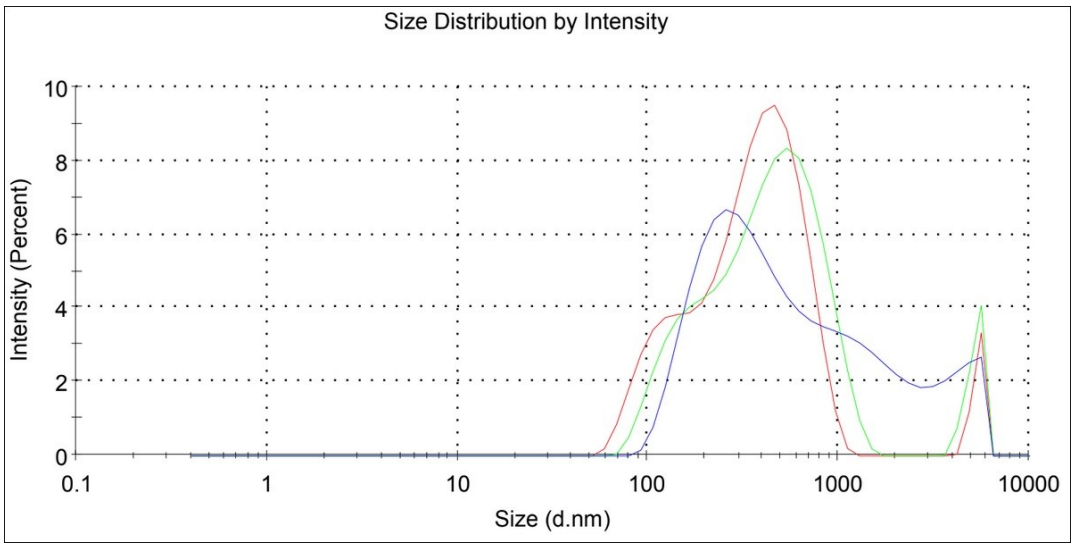

Figure 3.13: Size distribution by intensity for third iteration of the triplicates of not loaded 3 kDa polymeric micelles of pvp-od with the three measurements given by the DLS software done with attenuation factor 6. The micelles were formed by the co-solvent evaporation method. Individiual readings and a table with information can be seen in the Appendix A and Appendix B

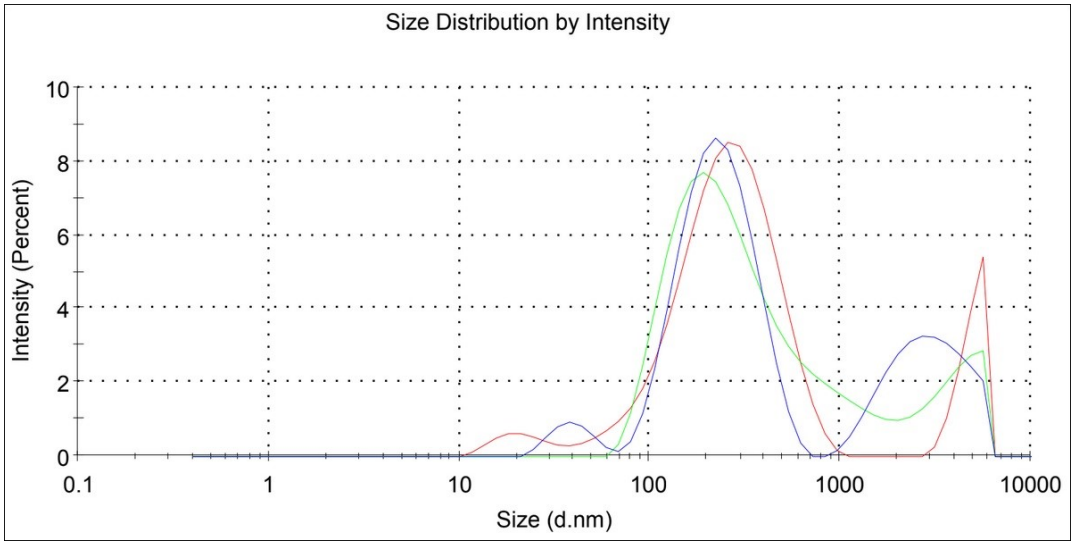

Figure 3.14: Size distribution by intensity for first iteration of the triplicates of the loaded 3 kDa polymeric micelles of pvp-od with the three measurements given by the DLS software done with attenuation factor 8. The micelles were formed by the co-solvent evaporation method. Individiual readings and a table with information can be seen in the Appendix A and Appendix B

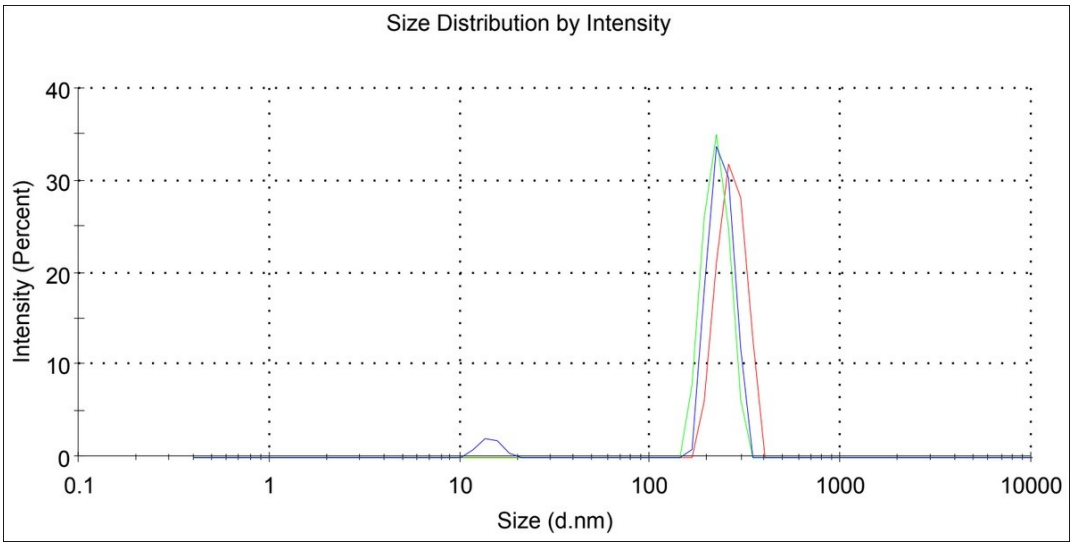

Figure 3.15: Size distribution by intensity for second iteration of the triplicates of loaded 3 kDa polymeric micelles of pvp-od with the three measurements given by the DLS software done with attenuation factor 9. The micelles were formed by the co-solvent evaporation method. Individiual readings and a table with information can be seen in the Appendix A and Appendix B

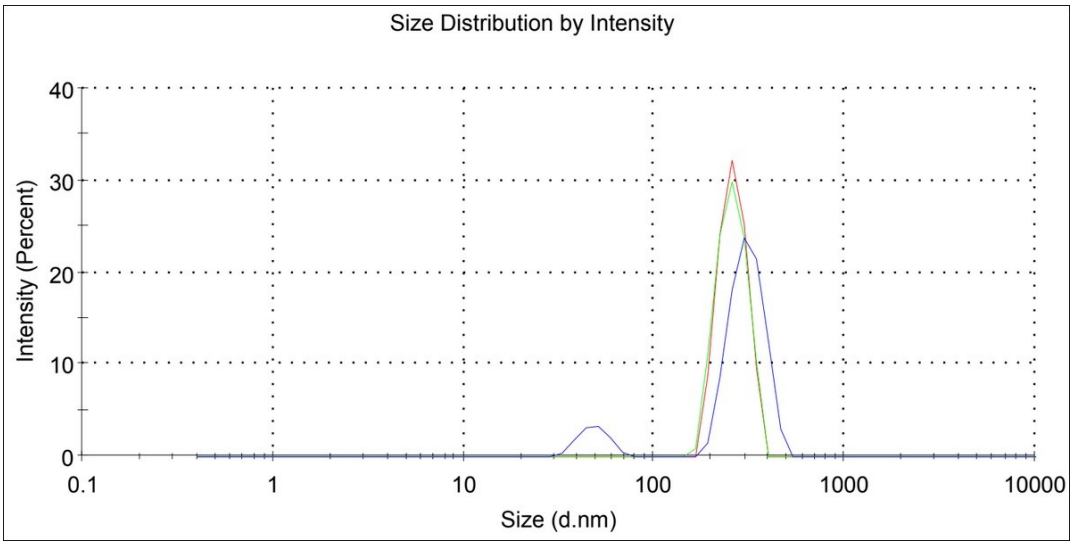

Figure 3.16: Size distribution by intensity for third iteration of the triplicates of loaded 3 kDa polymeric micelles of pvp-od with the three measurements given by the DLS software done with attenuation factor 9. The micelles were formed by the co-solvent evaporation method. Individiual readings and a table with information can be seen in the Appendix A and Appendix B

3.3.2.3 6 kDa micelles

3.3.2.3.1 Sonification method The micelles for the 6 kDa polymer show similar properties to that of the 3 kDa. They have a nice gathering around the 200 nm range and a low spread. There might be a difference in the presence, as seen by the intensity in each figure. However, this difference is too small to have any major effect on the samples differences. As most of the previous samples there is a presence at the 5000 nm mark.

Going by each reading for each triplicates as different samples shows that there is less presence of aggregates around the 900-1000 nm range for 6 kDa samples. This is unreliable, since the 3 readings is done for the same sample. This can be artefacts present in the water that gets hidden by the larger aggregates or artefacts. Since this only shows up on 2 of the 9 readings of the empty micelles of 6 kDa formed by the sonification method, it can be said to not be a major part of the solution or anything of significant interest.

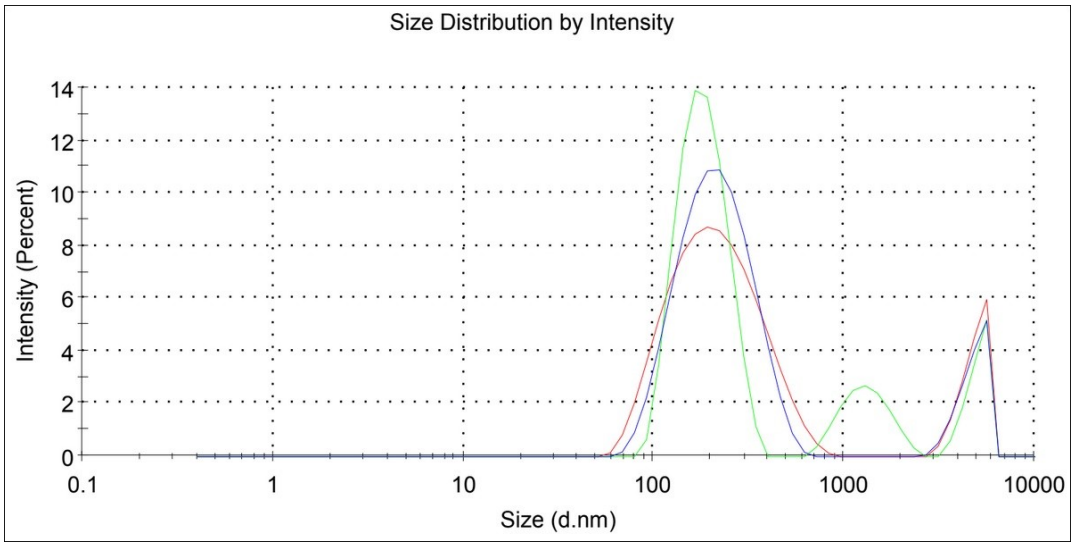

Figure 3.17: Size distribution by intensity for first iteration of the triplicates of the not loaded 6 kDa polymeric micelles of pvp-od with the three measurements given by the DLS software done with attenuation factor 6. The micelles were formed by the sonification method. Individiual readings and a table with information can be seen in the Appendix A and Appendix B

When adding curcumin to the solution, the samples seems to be at the same range, but slightly wider spread. This can also come from the intensity being slightly lower than for the empty micelles, but looking at the relevant tables in the Appendix A and Appendix B we can see that there is a slight increase in the overall standard deviation for the relevant peaks in comparison to the empty micelles. It can also be said that the larger and smaller end of the graph is more stretched out than for the empty micelles. Going down closer to the 800-1000 nm range for the loaded micelles, whereas the empty micelles comes closer to the 500-700 nm range. The smaller end starts at closer to the 40-50 nm range and 70-90 nm range. This might be of the difference in the graph range by the higher intensity in the empty micelles.

3.3.2.3.2 Co-solvent evaporation method When using the co-solvent evaporation method for 6 kDa pvp-od polymers, something interesting starts to happen. The presence of the peak at 5000 nm does not show up for the empty micelles. It does come back for

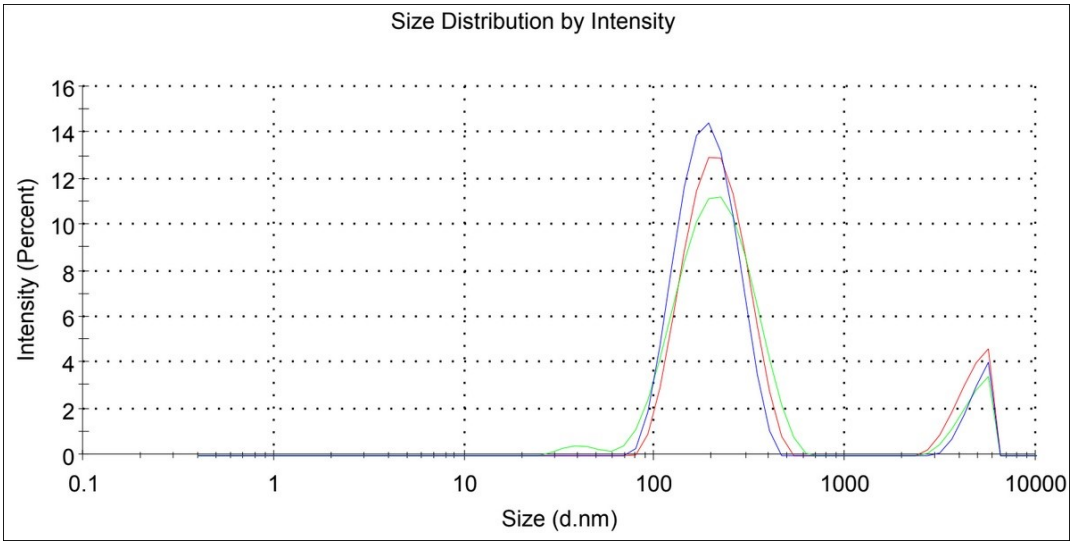

Figure 3.18: Size distribution by intensity for second iteration of the triplicates of not loaded 6 kDa polymeric micelles of pvp-od with the three measurements given by the DLS software done with attenuation factor 6. The micelles were formed by the sonification method. Individiual readings and a table with information can be seen in the Appendix A and Appendix B

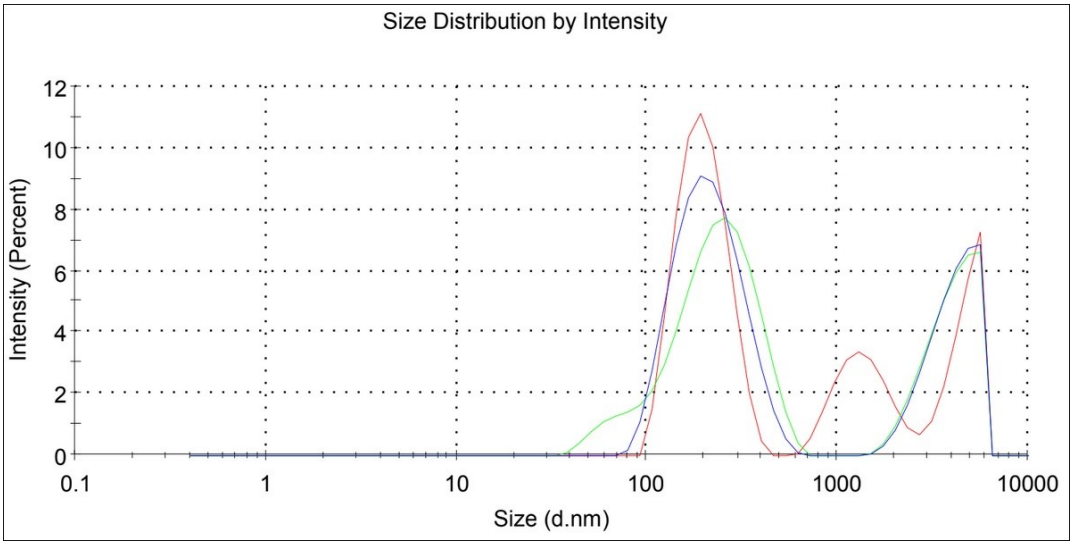

Figure 3.19: Size distribution by intensity for third iteration of the triplicates of not loaded 6 kDa polymeric micelles of pvp-od with the three measurements given by the DLS software done with attenuation factor 6. The micelles were formed by the sonification method. Individiual readings and a table with information can be seen in the Appendix A and Appendix B

the loaded micelles. The second iteration of the triplicates show a nice peak in the 200-300 nm range with a low dipsersity, as well as a high intensity. Only comparable to the BSA-conjugates. Looking at table B.21 in Appendix A and Appendix B shows the low standard

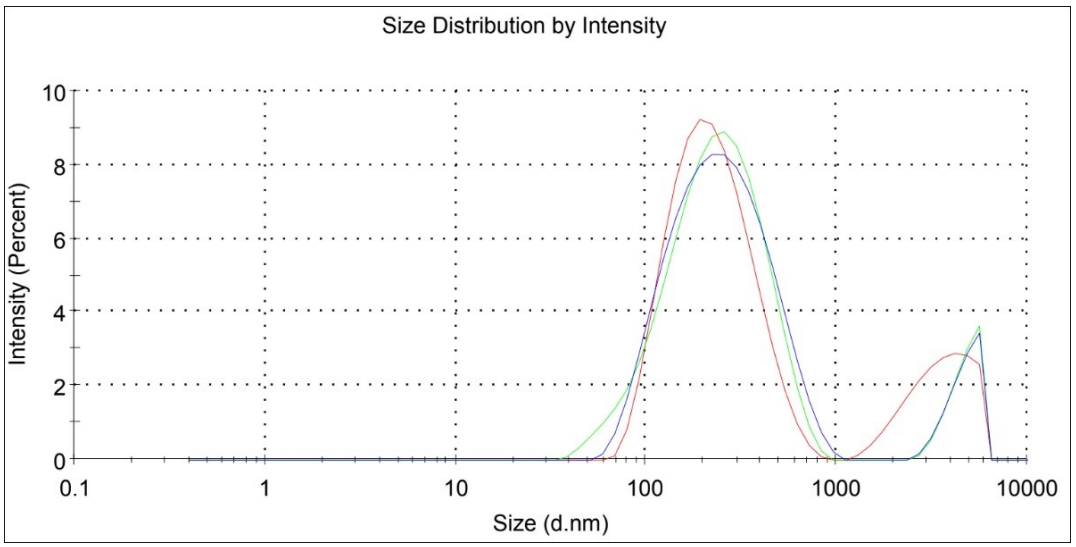

Figure 3.20: Size distribution by intensity for first iteration of the triplicates of the loaded 6 kDa polymeric micelles of pvp-od with the three measurements given by the DLS software done with attenuation factor 6. The micelles were formed by the sonification method. Individiual readings and a table with information can be seen in the Appendix A and Appendix B

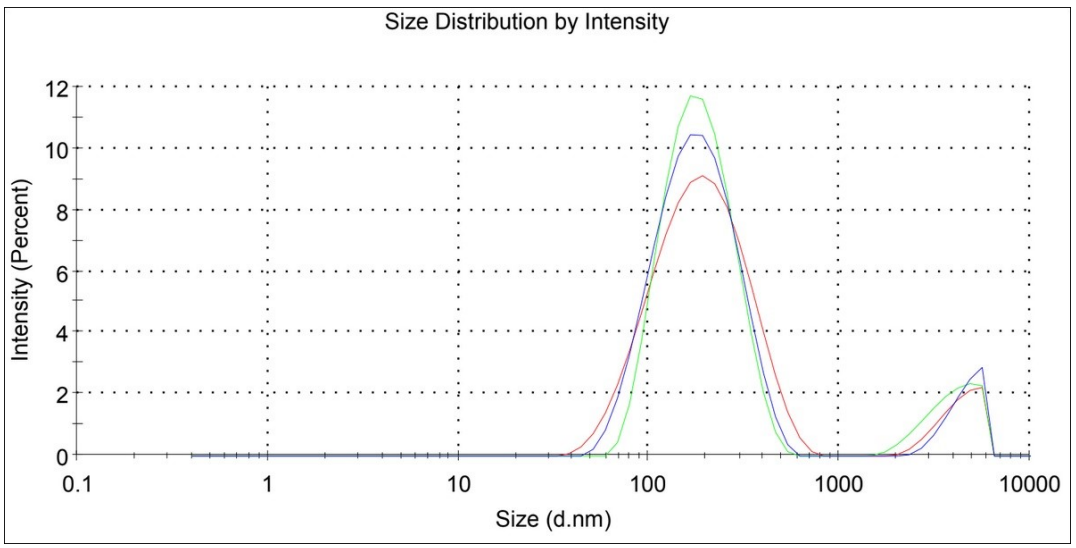

Figure 3.21: Size distribution by intensity for second iteration of the triplicates of loaded 6 kDa polymeric micelles of pvp-od with the three measurements given by the DLS software done with attenuation factor 6. The micelles were formed by the sonification method. Individiual readings and a table with information can be seen in the Appendix A and Appendix B

deviation comparatively for such a large aggregate. This confirms the low dispersity that is shown.

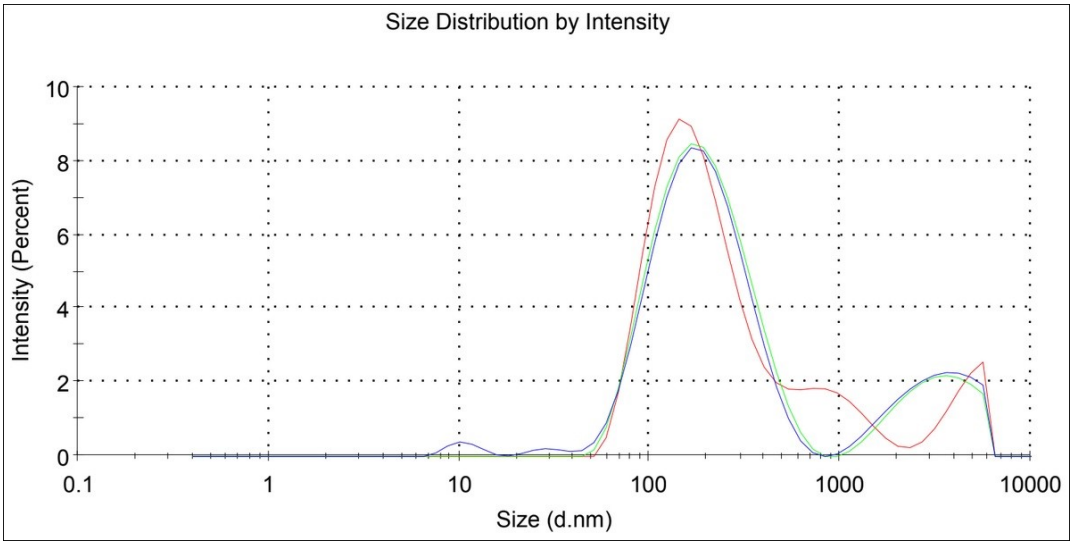

Figure 3.22: Size distribution by intensity for third iteration of the triplicates of loaded 6 kDa polymeric micelles of pvp-od with the three measurements given by the DLS software done with attenuation factor 6. The micelles were formed by the sonification method. Individiual readings and a table with information can be seen in the Appendix A and Appendix B

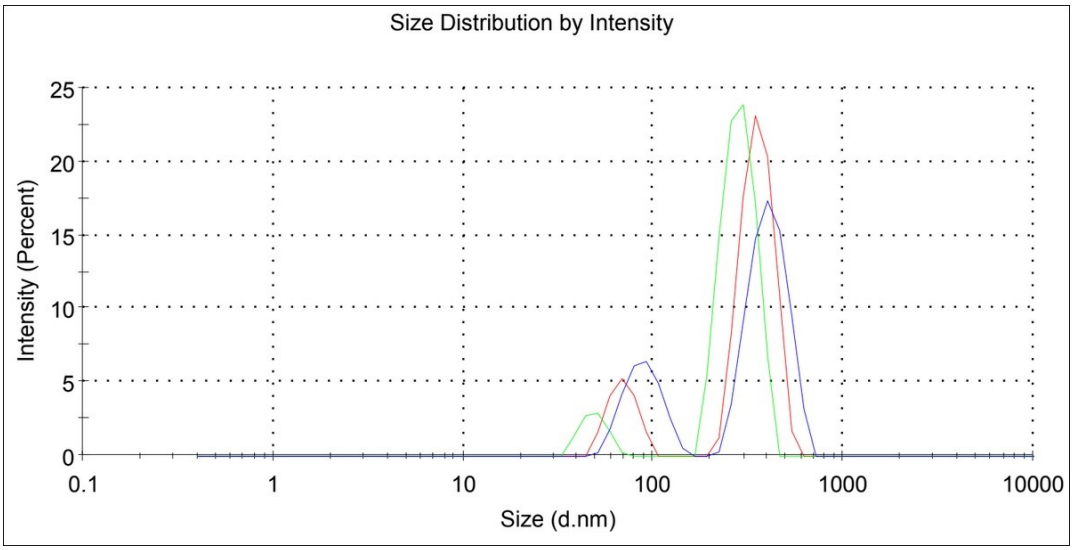

Figure 3.23: Size distribution by intensity for first iteration of the triplicates of the not loaded 6 kDa polymeric micelles of pvp-od with the three measurements given by the DLS software done with attenuation factor 8. The micelles were formed by the co-solvent evaporation method. Individiual readings and a table with information can be seen in the Appendix A and Appendix B

The other two samples of the triplicates give a slight difference in the peak, they are much more disperse and have two peaks present in the samples. The smaller peak in the first iteration is in the range from 30-100+ nm, with the average being at 76 nm with a

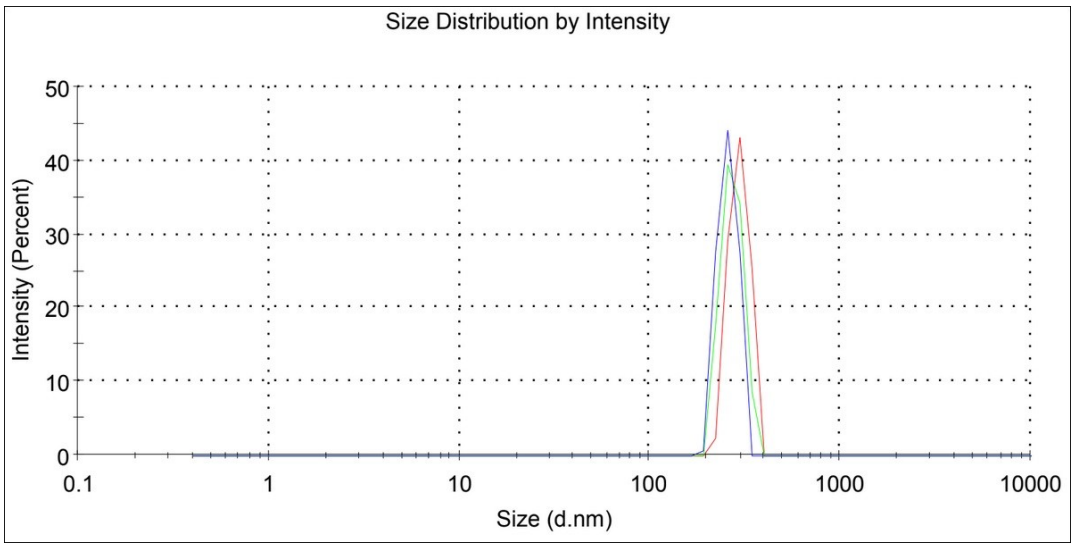

Figure 3.24: Size distribution by intensity for second iteration of the triplicates of not loaded 6 kDa polymeric micelles of pvp-od with the three measurements given by the DLS software done with attenuation factor 8. The micelles were formed by the co-solvent evaporation method. Individiual readings and a table with information can be seen in the Appendix A and Appendix B

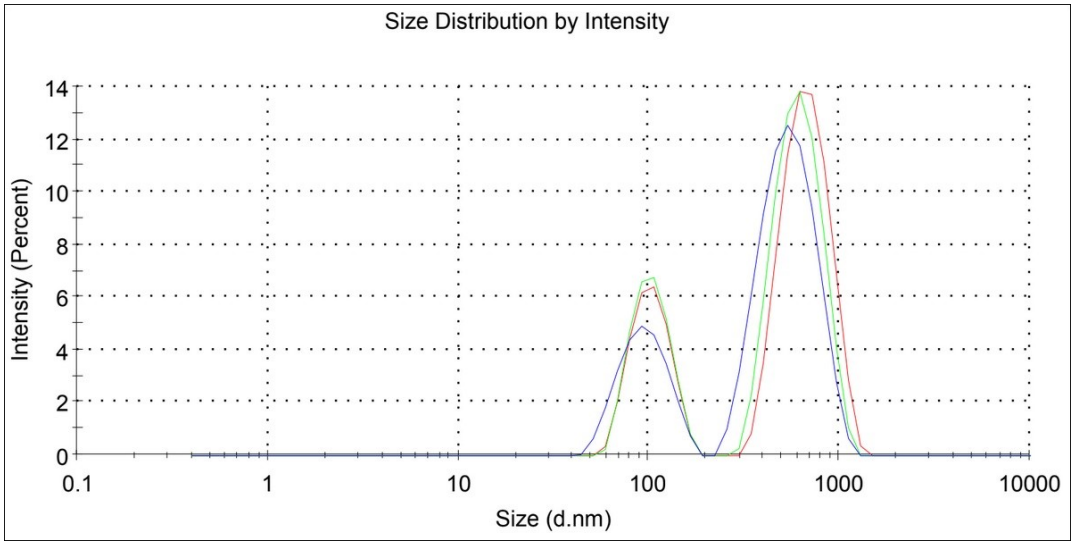

Figure 3.25: Size distribution by intensity for third iteration of the triplicates of not loaded 6 kDa polymeric micelles of pvp-od with the three measurements given by the DLS software done with attenuation factor 7. The micelles were formed by the co-solvent evaporation method. Individiual readings and a table with information can be seen in the Appendix A and Appendix B

high standard deviation for such a small aggregate at 22. The larger peak is in the 300-400 nm range, and the average is given at 343 with a standard deviation at 87. It also shows a higher intensity than the third iteration.

the third iteration have larger aggregates than the first, with the smaller going from 60-100+ nm closer to the 200 nm on the end. The average is given at 101 with a standard deviation of 25. The larger aggregate is in 500-700 nm range, with the average peak given at 617 with a standard deviation of 184.

As mentioned previously, the presence of aggreagtes at the 5000 nm range is present again, the presence of curcumin also gives a much more disperse spread all over the graph. With samples showing presence of aggregates down to the 10 nm with a varied spread up to the 5000 nm range where everything drops off. There is a significant drop in the intensity, but this comes from the higher spread in the dispersion.

The difference between each triplicate indicates that the samples create a larger array of aggregates with 6 kDa and curcumin in the rotary evaporator. Due to the nature of the rotary evaporator used, makes controlling the exact pressure used for evaporation difficult to contrl. This also affects the time used for creating the samples and the time spent in solution with a higher ethanol content than water, where the pvp-od have formed few aggregates. This should also be present in the loaded micelles formed with the 3 kDa pvp-od, but the samples created there shows clearer peaks and less dispersity.

This might indicate that the length of the 6 kDa pvp-od is creating a more varied range of aggregates when using the co-solvent evaporation method, with the curcumin being encapsulated. Since the empty micelles shows less dispersity.

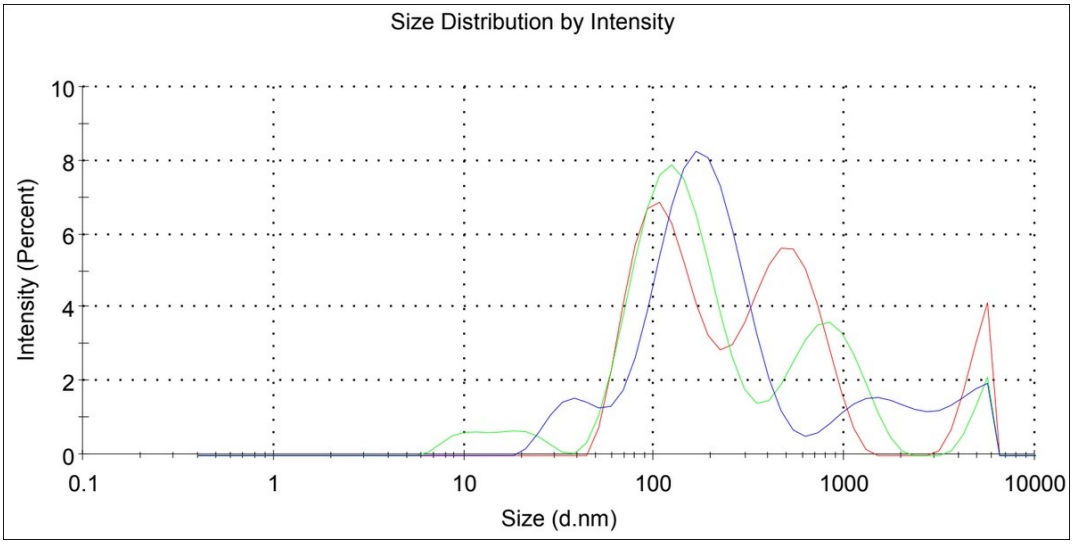

Figure 3.26: Size distribution by intensity for first iteration of the triplicates of the loaded 6 kDa polymeric micelles of pvp-od with the three measurements given by the DLS software done with attenuation factor 7. The micelles were formed by the co-solvent evaporation method. Individiual readings and a table with information can be seen in the Appendix A and Appendix B

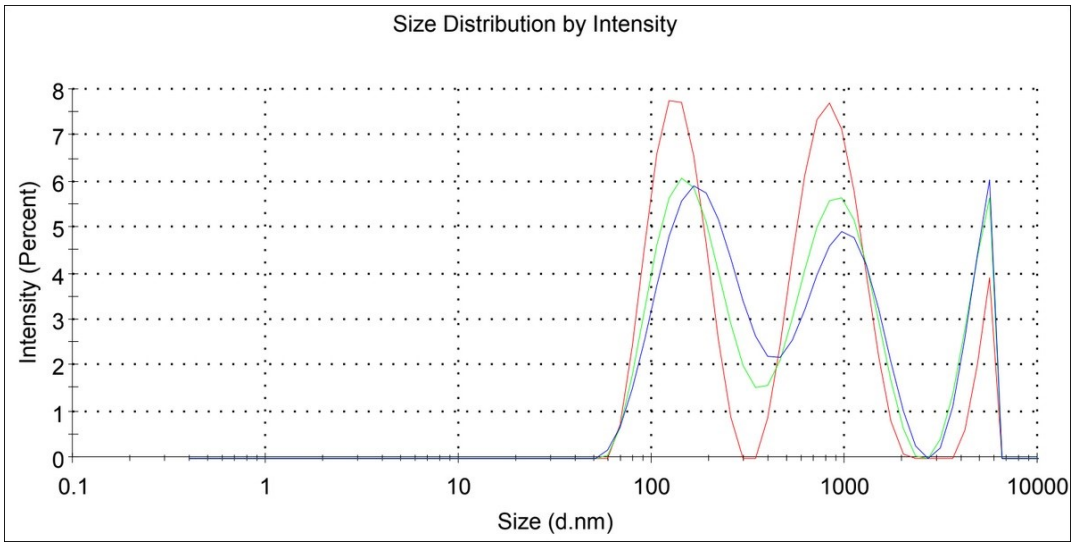

Figure 3.27: Size distribution by intensity for second iteration of the triplicates of loaded 6 kDa polymeric micelles of pvp-od with the three measurements given by the DLS software done with attenuation factor 7. The micelles were formed by the co-solvent evaporation method. Individiual readings and a table with information can be seen in the Appendix A and Appendix B

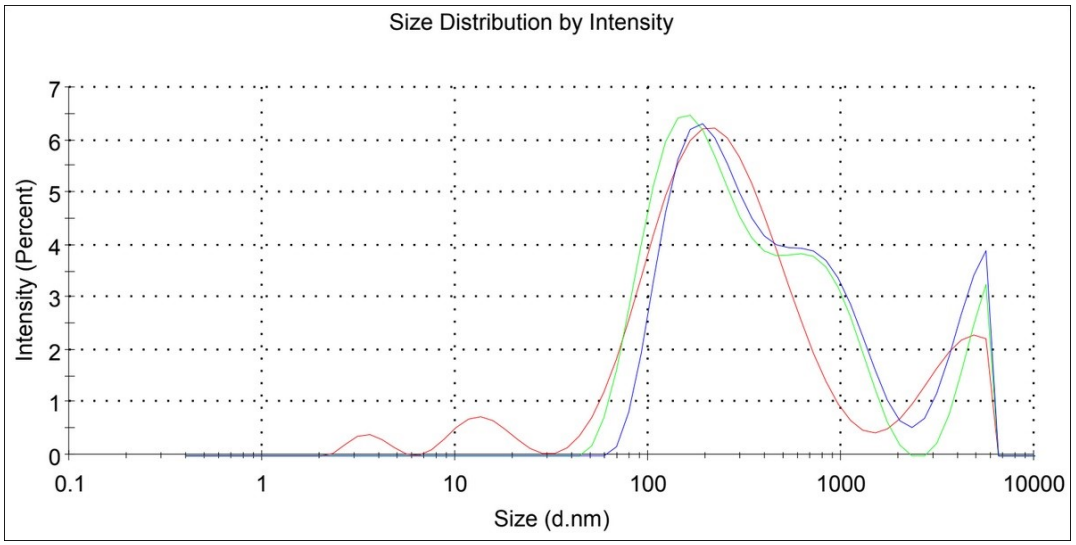

Figure 3.28: Size distribution by intensity for third iteration of the triplicates of loaded 6 kDa polymeric micelles of pvp-od with the three measurements given by the DLS software done with attenuation factor 6. The micelles were formed by the co-solvent evaporation method. Individiual readings and a table with information can be seen in the Appendix A and Appendix B

3.3.2.4 12 kDa micelles

3.3.2.4.1 Sonification method 12 kDa shows a wider spread in the empty micelles with the sonification method, than for the same micelles created with 3 kDa and 6 kDa pvp-od. However, 12 kDa also shows a presence of aggregates closer to the 10 nm range and shows a distinct presence of particles aggregating in the smaller range below the 100 nm range. This has been shown with the other polymer lengths, but not to this degree.

There is still a significant peak in the 200 nm range for 12 kDa, which is the same range that one expects the aggregates if looking at the previous polymers. However, the dispersity is much higher than the other empty micelles with same method.

There is a weird "rest" in the graph on the right side of the peaks, indicating that there might be 2 peaks that are closer together and bleeding into each other with their respective aggregates. This "rest" is present in all of the triplicates, but is easier to see in figure 3.29 and 3.31.

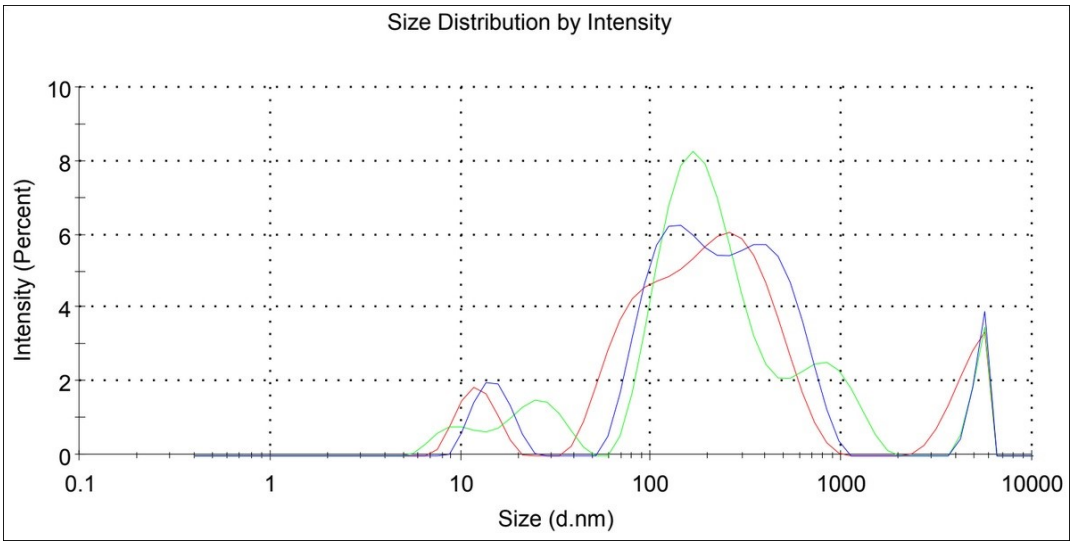

Figure 3.29: Size distribution by intensity for first iteration of the triplicates of the not loaded 12 kDa polymeric micelles of pvp-od with the three measurements given by the DLS software done with attenuation factor 7. The micelles were formed by the sonification method. Individiual readings and a table with information can be seen in the Appendix A and Appendix B

When adding curcumin to the mixture, the solution gets less disperse with the peak generally being around the 200 nm range, just as for the empty micelles. The samples are still more disperse than their counterparts with the other polymer lengths and is slightly larger for their peaks.

3.3.2.4.2 Co-solvent evaporation method The empty micelles created with the co-solvent evaporation method for 12 kDa pvp-od shows the same presence of smaller aggregates at the 10 nm range, and some are even shown to be smaller. The 200 nm range is still the major peak present, with the exception the first iteration of the triplicates where

the major peak is closer to the 600-700 nm range and showing the smaller aggregates in the range from 5 nm to slightly above 100 nm.

When adding the curcumin with the co-solvent evaporation, the dispersion seems to

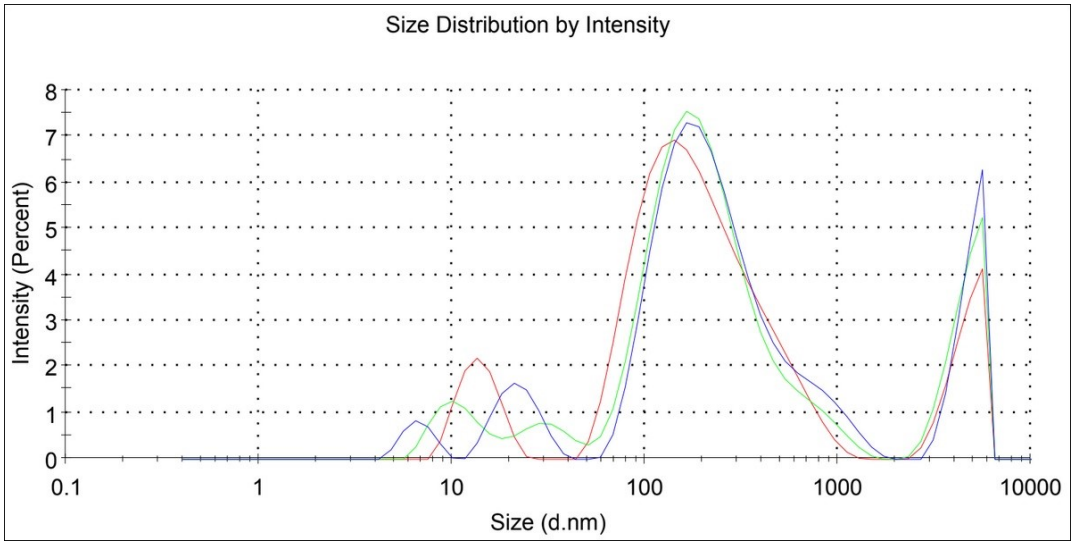

Figure 3.30: Size distribution by intensity for second iteration of the triplicates of not loaded 12 kDa polymeric micelles of pvp-od with the three measurements given by the DLS software done with attenuation factor 6. The micelles were formed by the sonification method. Individiual readings and a table with information can be seen in the Appendix A and Appendix B

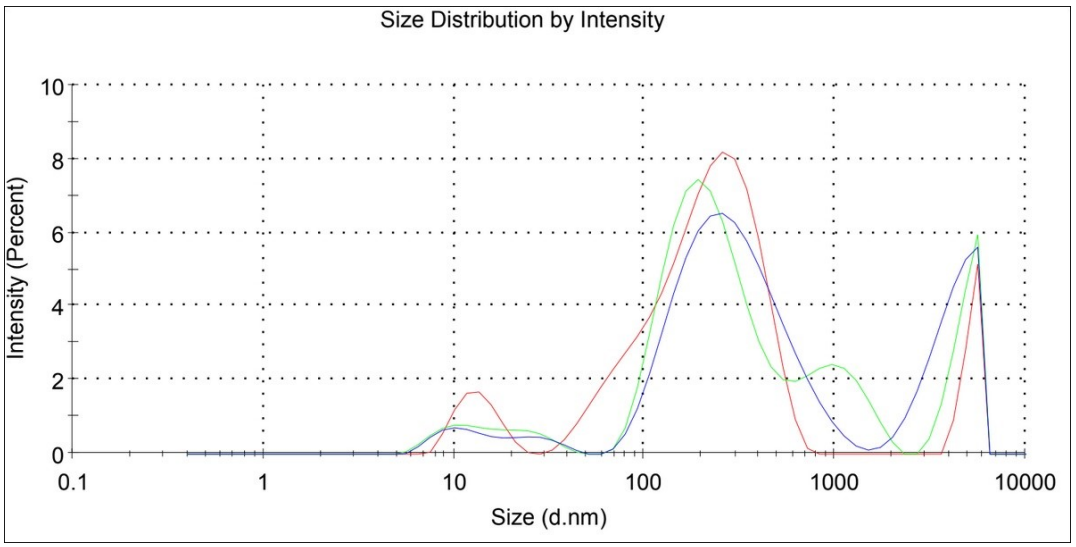

Figure 3.31: Size distribution by intensity for third iteration of the triplicates of not loaded 12 kDa polymeric micelles of pvp-od with the three measurements given by the DLS software done with attenuation factor 6. The micelles were formed by the sonification method. Individiual readings and a table with information can be seen in the Appendix A and Appendix B

lower for the aggregates, even giving more distinction between the smaller and larger aggregates. However, the changes overall is not much different to the third iteration of the empty 12 kDa micelles formed with the co-solvent evaporation method. There might be

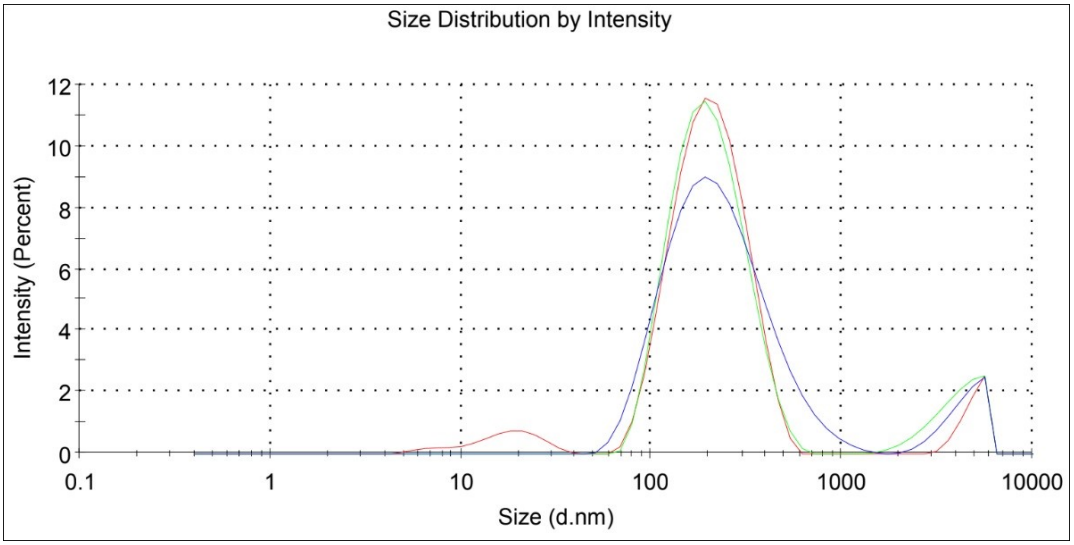

Figure 3.32: Size distribution by intensity for first iteration of the triplicates of the loaded 12 kDa polymeric micelles of pvp-od with the three measurements given by the DLS software done with attenuation factor 6. The micelles were formed by the sonification method. Individiual readings and a table with information can be seen in the Appendix A and Appendix B

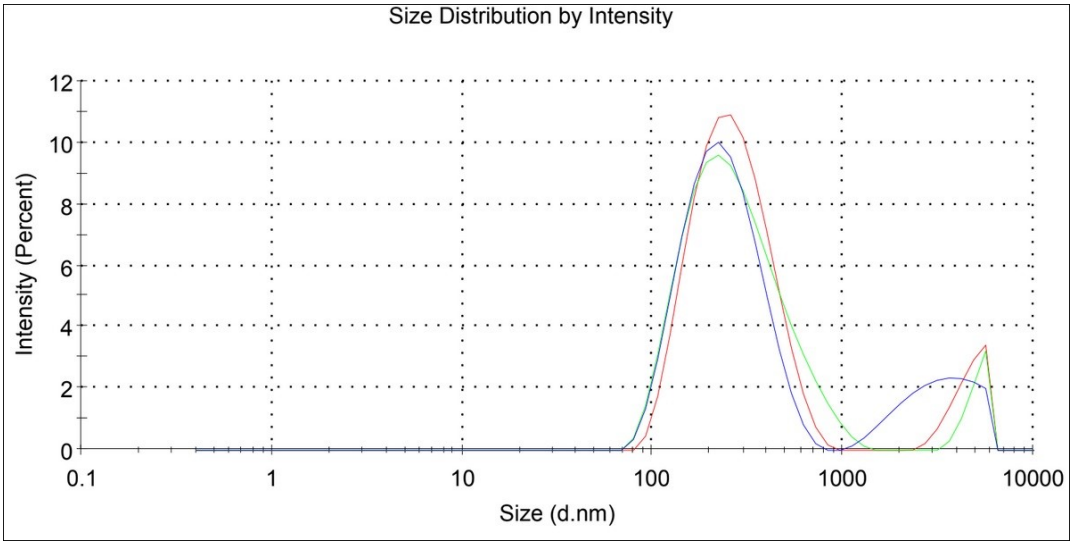

Figure 3.33: Size distribution by intensity for second iteration of the triplicates of loaded 12 kDa polymeric micelles of pvp-od with the three measurements given by the DLS software done with attenuation factor 6. The micelles were formed by the sonification method. Individiual readings and a table with information can be seen in the Appendix A and Appendix B

a slight difference in the presence of the smaller aggregates, but this becomes difficult to compare directly due to the the differences in intensity between each sample.

Comparatively with the empty 3 kDa micelles formed with co-solvent evaporation, the

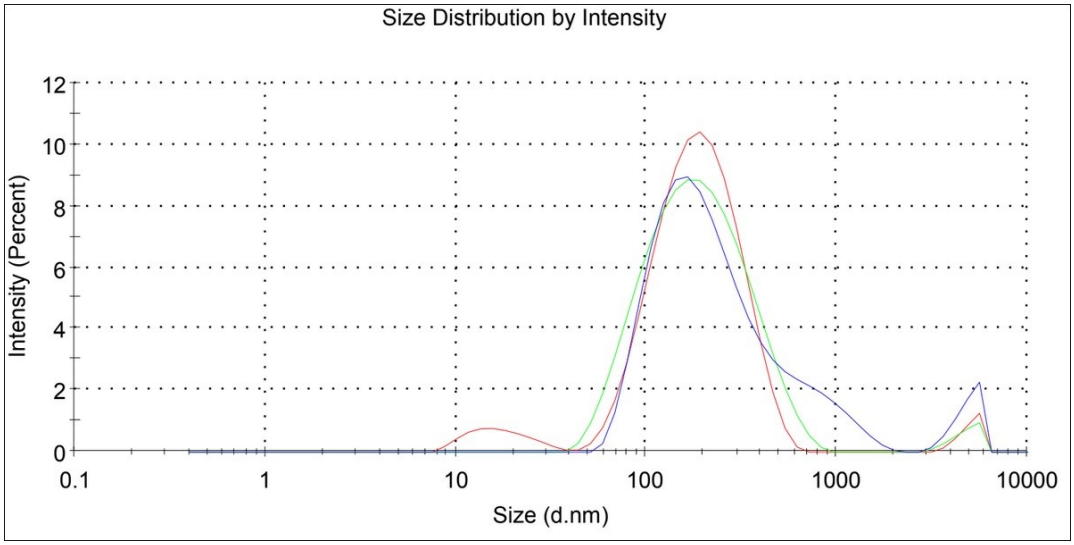

Figure 3.34: Size distribution by intensity for third iteration of the triplicates of loaded 12 kDa polymeric micelles of pvp-od with the three measurements given by the DLS software done with attenuation factor 6. The micelles were formed by the sonification method. Individiual readings and a table with information can be seen in the Appendix A and Appendix B

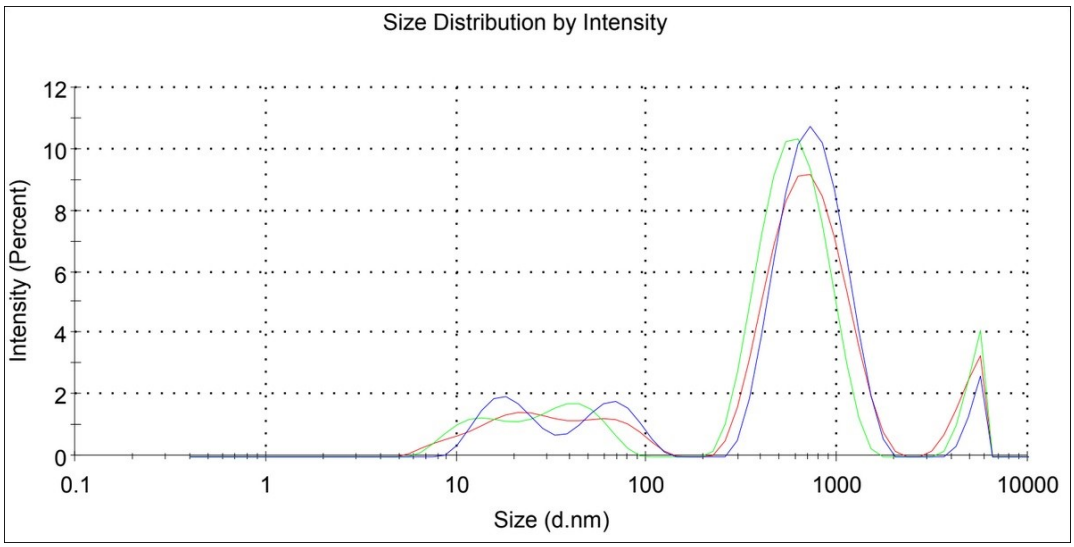

Figure 3.35: Size distribution by intensity for first iteration of the triplicates of the not loaded 12 kDa polymeric micelles of pvp-od with the three measurements given by the DLS software done with attenuation factor 7. The micelles were formed by the co-solvent evaporation method. Individiual readings and a table with information can be seen in the Appendix A and Appendix B

dispersion is larger and there is a presence of the smaller aggregates in the samples for empty 12 kDa micelles formed with co-solvent evaporation. When looking at the samples for empty 6 kDa micelles formed with the co-solvent evaporation method it is clear that

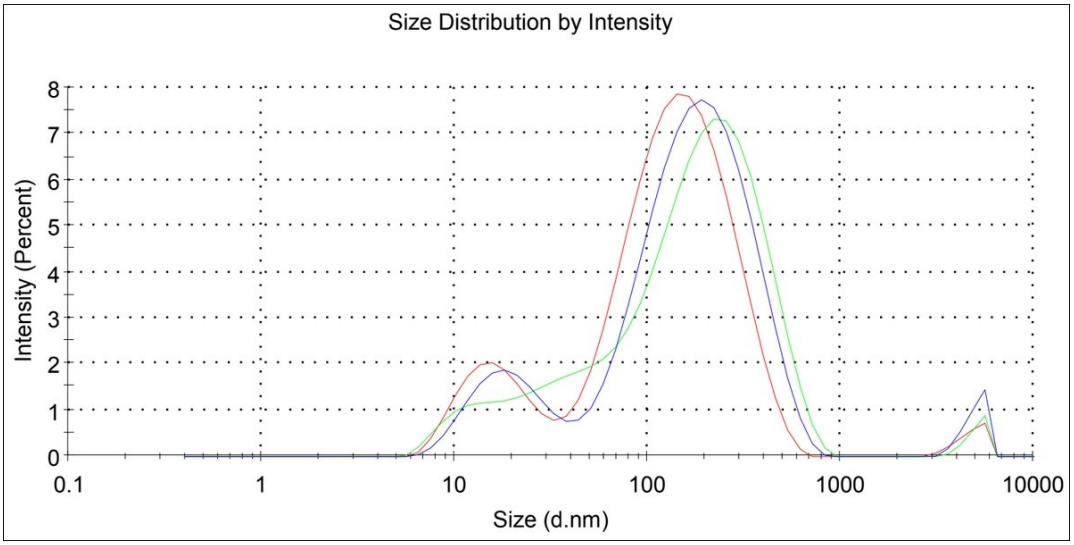

Figure 3.36: Size distribution by intensity for second iteration of the triplicates of not loaded 12 kDa polymeric micelles of pvp-od with the three measurements given by the DLS software done with attenuation factor 8. The micelles were formed by the co-solvent evaporation method. Individiual readings and a table with information can be seen in the Appendix A and Appendix B

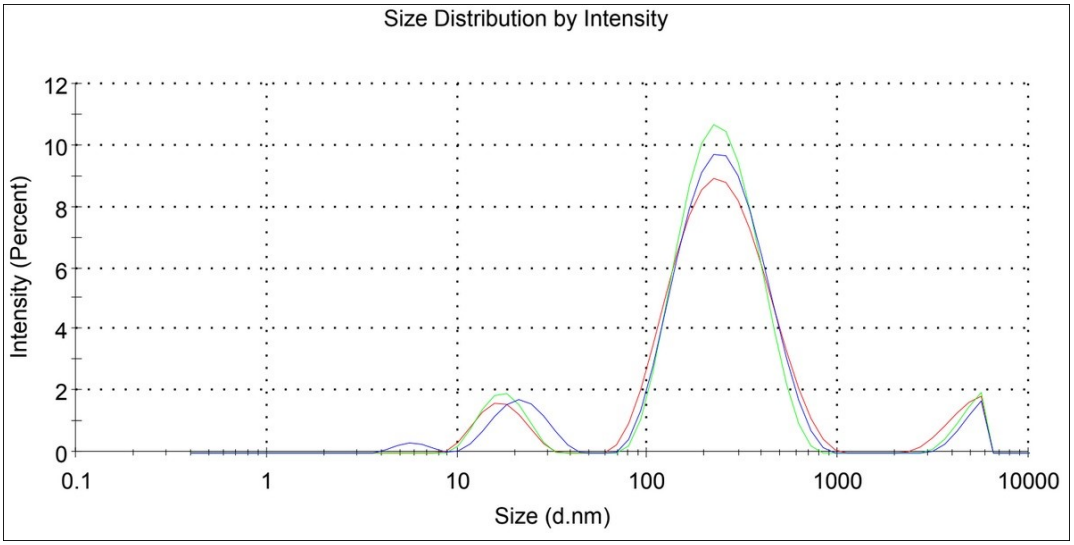

Figure 3.37: Size distribution by intensity for third iteration of the triplicates of not loaded 12 kDa polymeric micelles of pvp-od with the three measurements given by the DLS software done with attenuation factor 7. The micelles were formed by the co-solvent evaporation method. Individiual readings and a table with information can be seen in the Appendix A and Appendix B

the dispersion is much more contrllled for the 12 kDa micelles of the same method.

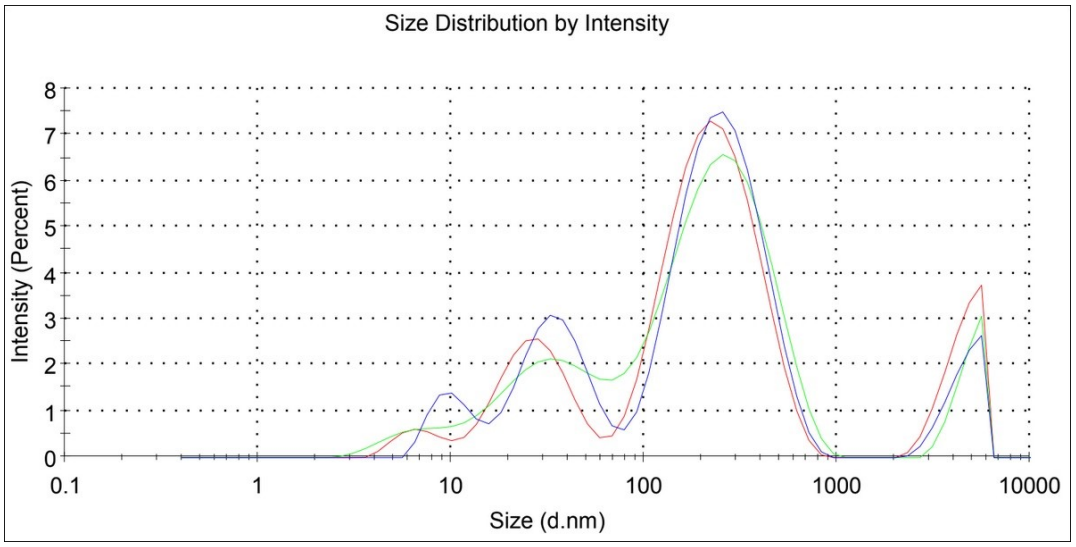

Figure 3.38: Size distribution by intensity for first iteration of the triplicates of the loaded 12 kDa polymeric micelles of pvp-od with the three measurements given by the DLS software done with attenuation factor 7. The micelles were formed by the co-solvent evaporation method. Individiual readings and a table with information can be seen in the Appendix A and Appendix B

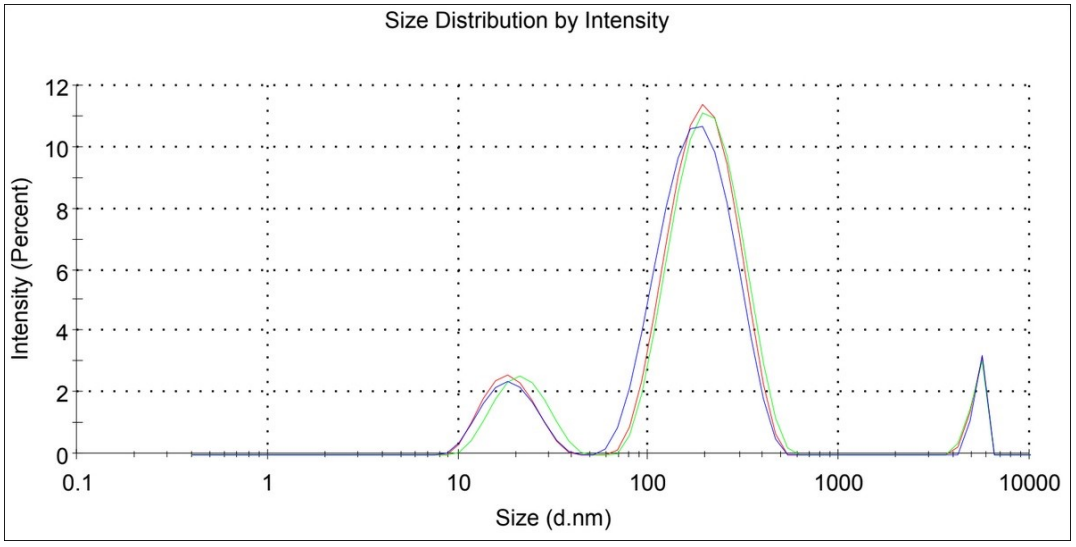

Figure 3.39: Size distribution by intensity for second iteration of the triplicates of loaded 12 kDa polymeric micelles of pvp-od with the three measurements given by the DLS software done with attenuation factor 7. The micelles were formed by the co-solvent evaporation method. Individiual readings and a table with information can be seen in the Appendix A and Appendix B

Another thing to note is the higer attenuation factor for the co-solvent evaporation

method. This indicates that even if all of the samples are treated equally when re-hydrating them, by using the same solvent and concentration, there is a difference in the light needed for reading. A higher attenuation factor indicates that there is a need for more light, as the concentration of particles is lower.

3.4 Preliminary cytotoxic assay

The preliminary life-death assay performed on the fibroblast cells for 24 hours gives us interesting results for 6 kDa micelles, and especially for the sonification method without curcumin. This sample yields a percentage of 44.3% of cells were dead after incubation, while the co-solvent evaporation method yielded much lower results; 12,4 and 5,2 % for loaded and empty micelles respectively. For the other results they are in the range of 1-4%, with the exception of co-solvent evaporation method for loaded 12 kDa micelles, that have -1,9% for 0.08 mg/ml and 0,8% for 0,04 mg/ml.

Another interesting thing to note about the results is that looking at 12 kDa, the general trend is that the lower concentrations yields higer cell death, with the exception for loaded 12 kDa micelles formed with the sonification method. While the BSA-polymer conjugates gives us a stable 1,1% for both concentration, with a slight difference between them of 0,06% wich is negligible.

The control readings gives us a quite large standard deviation considering the results, this makes the readings have a larger maring of error when looking at the results. Still the results from 6 kDa is noteworthy. This can be due to the polymer length. It might create a sub-optimal aggregations structure in regards to energy balance, making it a large

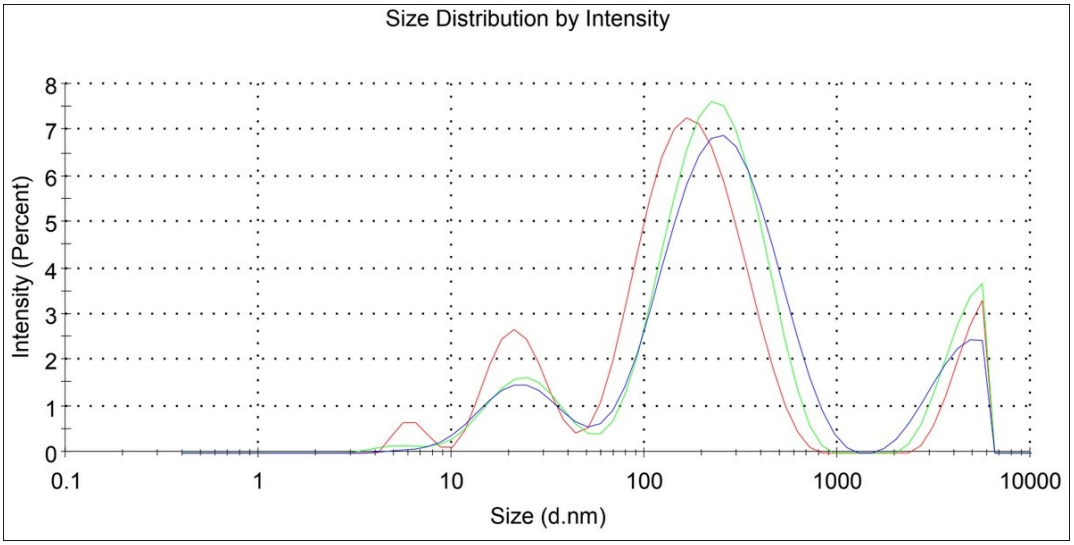

Figure 3.40: Size distribution by intensity for third iteration of the triplicates of loaded 12 kDa polymeric micelles of pvp-od with the three measurements given by the DLS software done with attenuation factor 7. The micelles were formed by the co-solvent evaporation method. Individiual readings and a table with information can be seen in the Appendix A and Appendix B

possibility that the aggregates reshape themselves into other aggregates with small changes in the environment. All of the triplicates of loaded micelles of 6 kDa for the co-solvent evaporation method shows a wide range of dispersion and aggregate sized and is the least uniform of the samples between each triplicates. The high toxicity given by the 6 kDa required further life-death assays.

The percentage is calculated from the samples difference from the negative control, divided by the difference between the positive and negative control.

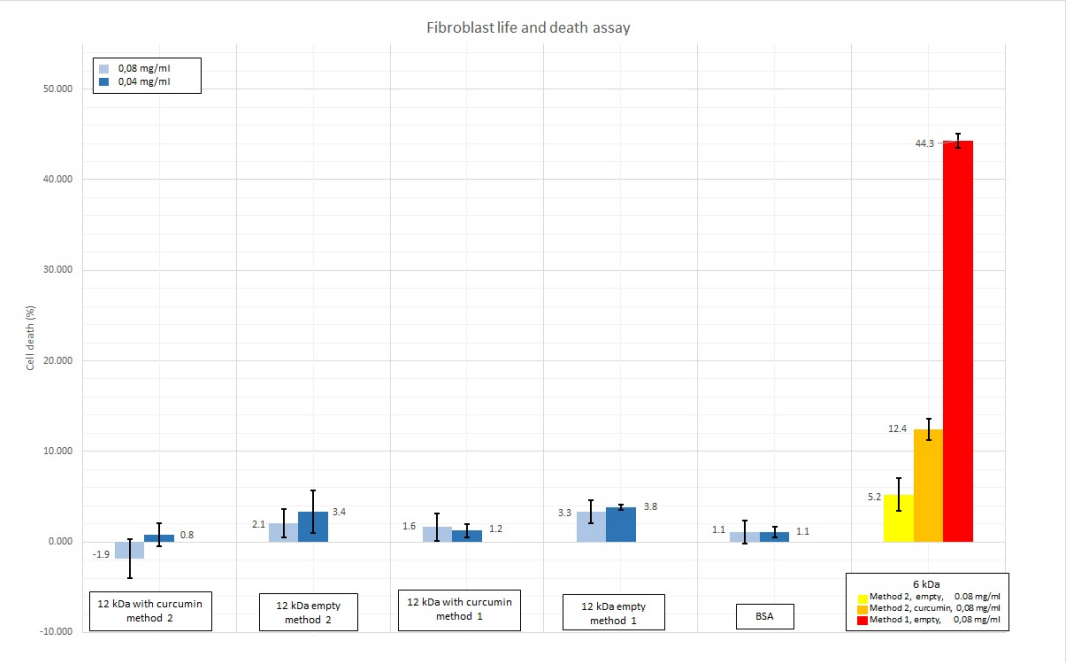

Figure 3.41: Graph of the cytotoxic assay performed on fibroblast cells, incubated for 24 hours. With triplicates for each sample and concentration. Values for the graph can be seen in table C.1

3.5 Cytotoxic assay

After the high toxicity from the 6 kDa micelles it was interesting to see the effect on both glioblastoma and fibroblast cells. The assay was performed the same way as previously done by Camilla [Cam], and as the preliminary assay. The cells were incubated at 24 hours with micelles of 6 kDa for the concentrations of 0.01 mg/ml, 0.04 mg/ml, 0.08 mg/ml,0.1 mg/ml and 5 mg/ml to check the extreme. There were also performed assay on 6 kDa of co-solvent evaporation method at the concentrations of 0.01 mg/ml, 0.04 mg/ml, 0.08 mg/ml.

3.5.1 6 kDa

3.5.1.1 Sonification method

As can bee seen by both the graphs from figure **??** and **??** the 6 kDa created with the sonification method is rather toxic to the cells. There is however, a discrepency between the images and the graph presented. When looking at images in figure 3.43, 3.44, 3.46 and 3.47 and comparing them directly with the results from the graph it does not match up at the higher concentrations. In regards to the glioblastoma cells, almost all can be said to be dead at the concentration of 0.08 mg/ml whereas the graph sets the percentage of dead cells at 35,1%. This is also the case for higher concentrations, as can be seen in the graph in figure **??**. All the cells incubated at above 0.08 mg/ml are dead, where the highest percentage from the graph is given at 35,1%, for 0.08 mg/ml and goes lower with higher concentrations. This is also the case for the fibroblast cells, even thou there are still some cells alive at 0.1 mg/ml and 0.08 mg/ml, the percentage of living cells shown from the images are much closer to each other than the 50,7% and 29,5% that the graph gives.

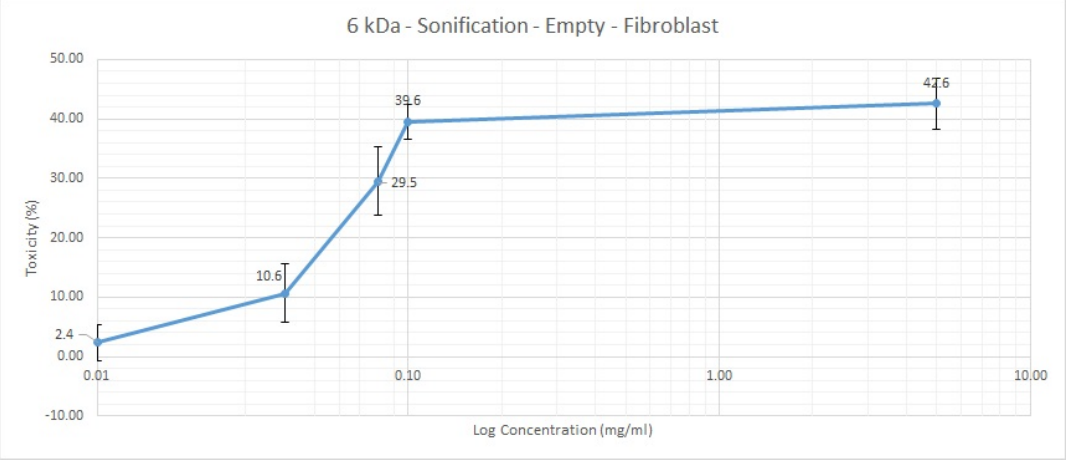

Figure 3.42: Graph of the cytotoxic assay for fibroblast cells incubated with empty micelles formed from 6 kDa pvp-od polymers with the sonification method, with added standard deviation. The values can be seen in table C.2

This is also present in the loaded micelles of the same method, and it might be that even more of the cells are dead for the loaded micelles when looking at the images. Where the percentages is even lower than the other graphs, this can be seen in the graphs in figure **??** and **??** and comparing them to the images in figure 3.48, 3.56 and 3.49.

However, it is clearly seen that cytotoxicity starts at a concentration between 0.04 mg/ml and 0.08 mg/ml. The issue with the mismatch in values presented by the assay and that might be due to intereference from the polymeric aggregates on the enzymatic reaction that occur in the assay. Either through absorbing the nescessary product for the full enzymatic conversion to resorfin, or inhibiting the enzymes through other means. This should be tested by doing two positive controls, where one use lysis solution on 1 control

before adding a micelle solution and the other control is done as mentioned in the methods section.

3.5.1.2 Co-solvent evaporation method

An interesting point to note is that with the co-solvent evaporation method the micelles do not appear to be cytotoxic at the same concentrations as for the sonification method. This can be seen by comparing the previous figures and figure 3.53 and 3.54, and the cell images also confirm this. This opens up the possibility of using different methods of creating less toxic drug delivery systems, making them more optimal to use. The difference between the micelles can be in the aggregations, as mentioned previously Levi found that the polymer formed smaller aggregates before freeze-drying, but after re-hydrating they "returned" back to the larger aggregates. The micelles formed via the co-solvent evaporation might be very stable inthemselves compared to the sonification method, and as discussed they are closer to the true micelle size, and when they aggregate to larger aggregates again they might be a super structure of smaller "true" micelles forming a larger aggregate. Whereas the sonification method creates a super structure, or simply large aggregates, that are not as stable as the super structure of true micelles. This might explain the difference in cytotoxicity through the 2 different methods. However, no sign has been seen of a super structure of "true" micelles, and this is purely speculation.

3.5.2 12 kDa

After the high toxicity from the 12 kDa micelles it was interesting to see the effect on both glioblastoma and fibroblast cells. The assay was performed the same way as previously done by Camilla [Cam], and as the preliminary assay. The cells were incubated at 24 hours with micelles of 6 kDa for the concentrations of 0.01 mg/ml, 0.04 mg/ml, 0.08 mg/ml,0.1 mg/ml.

The 12 kDa micelles also shows similar signs of intereference on the assay, this can clearly be seen in the graph in figure 3.57 and the cell images in figure **??**. Where the graph shows at around 16% of the cells are dead for both 0.04 mg/ml and 0.08 mg/ml, the images shows that for 0.04 mg/ml the cells seems almost unaffected, where at 0.08 mg/ml alot of the cells are dead. The glioblastoma cells are unaffected it seems, from both the graph in figure 3.58 and cell images 3.60, where for the 6 kDa the glioblastoma cells were also affected similary to the toxicity.

Unlike the the unloaded 12 kDa micelles, there is an effect on glioblastoma. However, it is only seen when the concentration is at 0.1 mg/ml, indicating that at that concentration with loaded micelles it is toxic to the glioblastoma cells. Since the empty micelles at the same concentration had no effect on the glioblastoma cells, this can be attributed to the curcumin loaded into the micelles. As previously discussed, curcumin have shown abilities to reduce the size of induced tumor by a threefold in comparison a control [Cam 52, 53].

Another important point to note is that from the cell images as seen in figure **??** the concentration of 0.08 mg/ml is showing little to non toxicity, whereas with the empty micelles of the same method and polymer showed a high toxicity in this range. This

might be due to the curcumin binding the polymer better together, creating a more stable structure that is favorable to the cells. Another point to note is that almost all the cells are dead at 0.1 mg/ml for fibroblast cells while the graph in figure 3.61 show only a mortality percentage of 29,1%. This is much lower than the results gained from the 6 kDa sonification method micelles. Where the highest percentage was at 50,7%. Indicating that the polymer length might have an impact on the inhibition of accurate measurement by the assay.

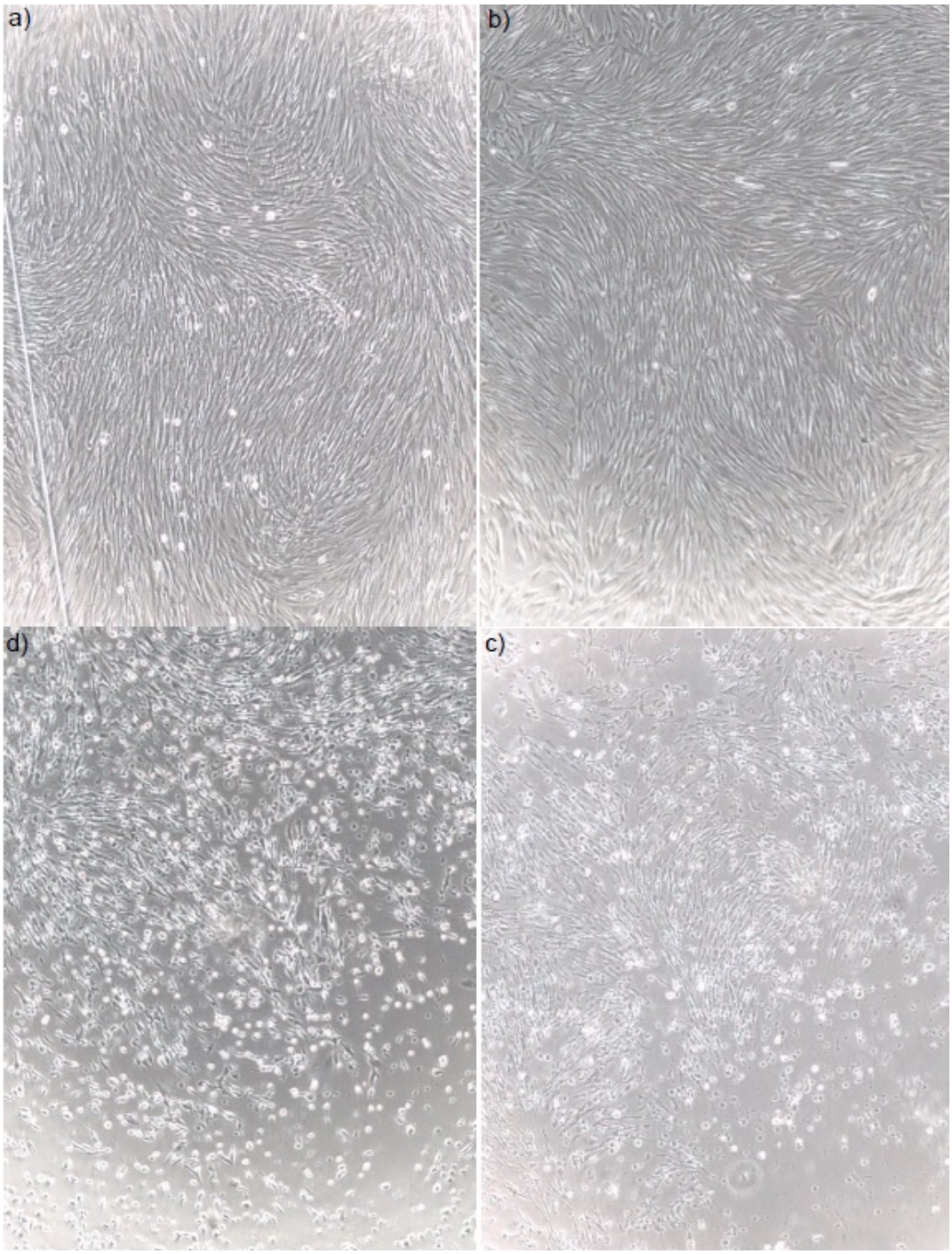

Figure 3.43: Light micrograph of fibroblast cells after 24 h incubation with empty micelles formed with 6 kDa pvp-od with the sonification method at a) 0.01 mg/ml, b) 0.04 mg/ml, c) 0.08 mg/ml and d) 0.1 mg/ml.

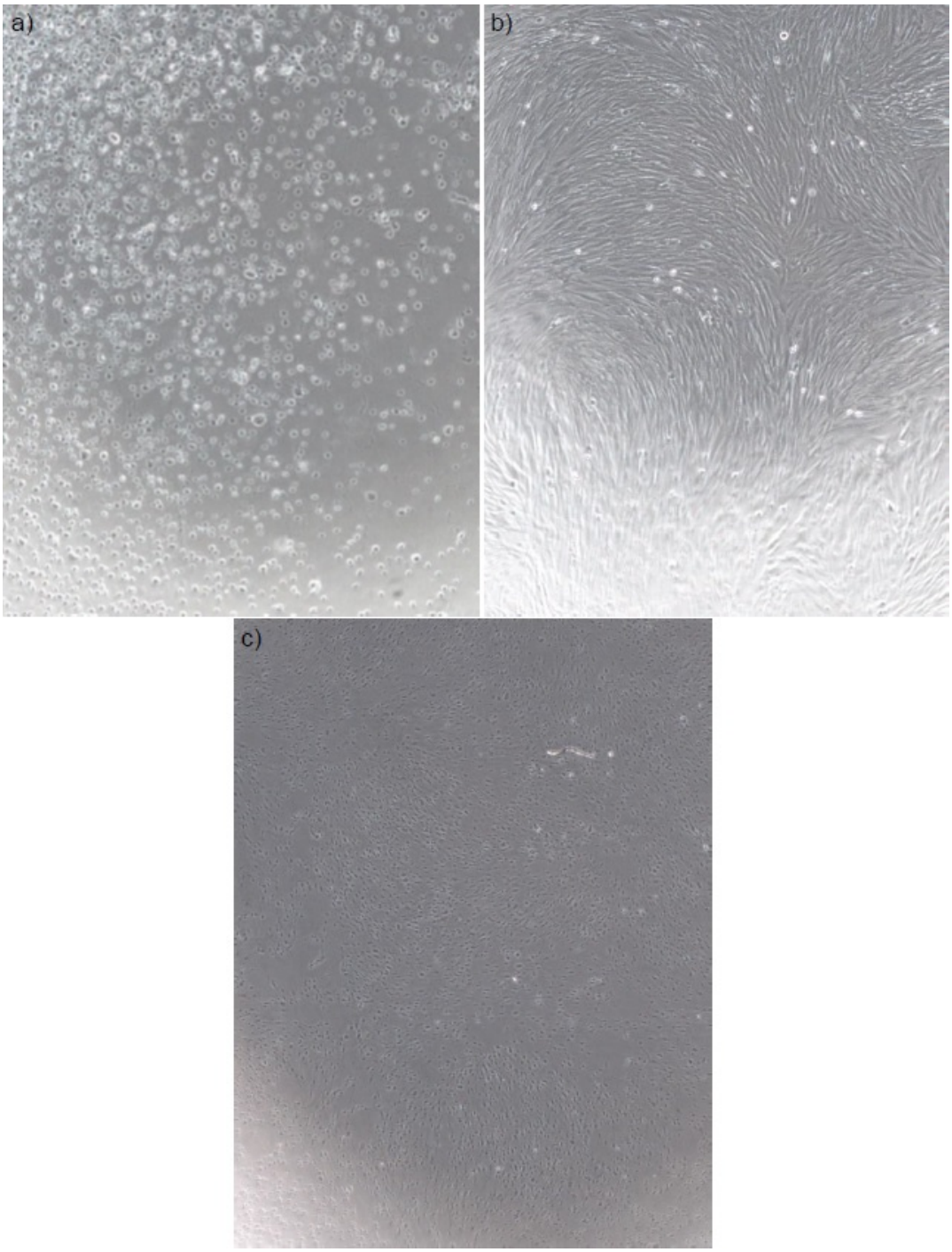

Figure 3.44: Light micrograph of fibroblast cells after 24 h incubation with empty micelles formed with 6 kDa pvp-od with the sonification method at a) 5 mg/ml while b) is the negative control cells and c) positive control cells.

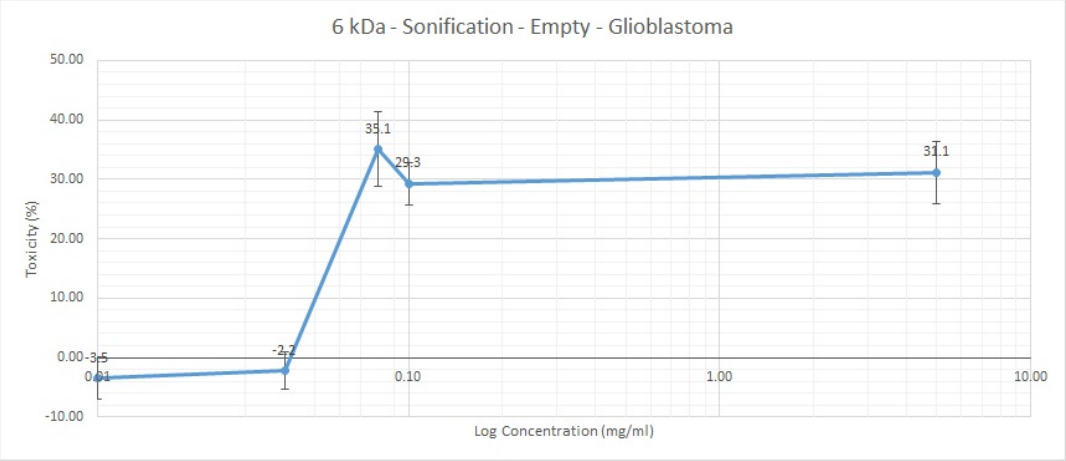

Figure 3.45: Graph of the cytotoxic assay for glioblastoma cells incubated with empty micelles formed from 6 kDa pvp-od polymers with the sonification method, with added standard deviation. The values can be seen in table C.3

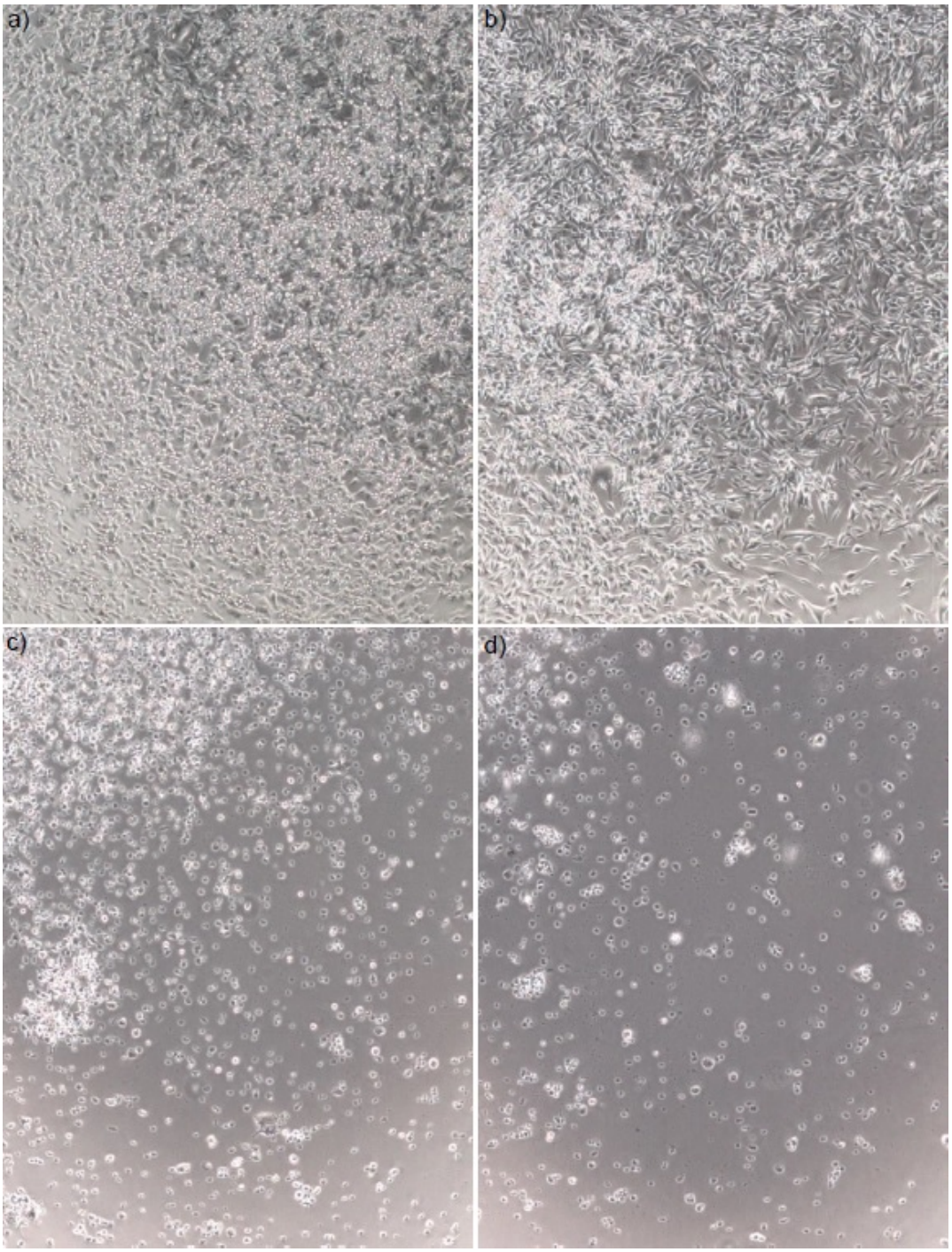

Figure 3.46: Light micrograph of glioblastoma cells after 24 h incubation with empty micelles formed with 6 kDa pvp-od with the sonification method at a) 0.01 mg/ml, b) 0.04 mg/ml, c) 0.08 mg/ml and d) 0.1 mg/ml.

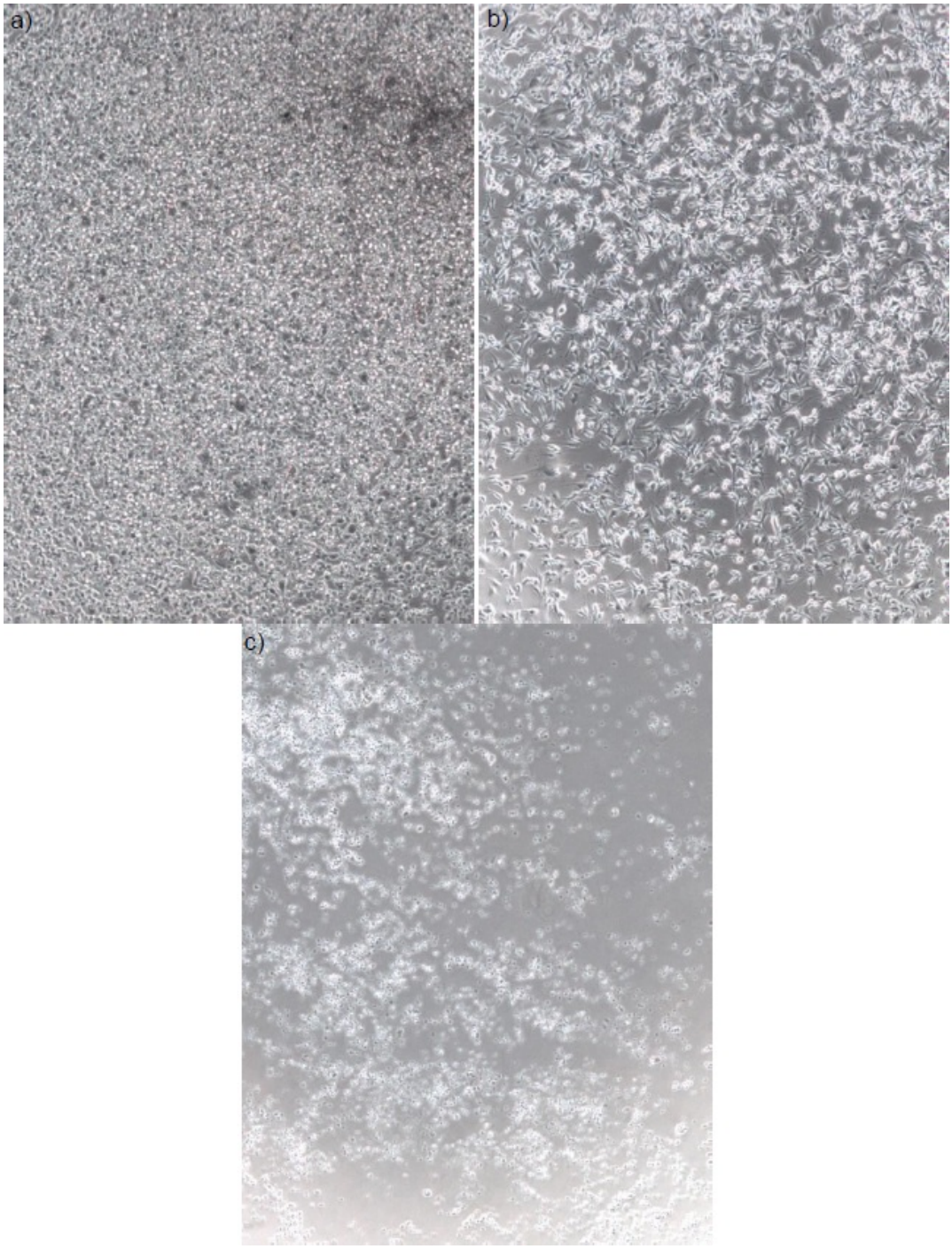

Figure 3.47: Light micrograph of glioblastoma cells after 24 h incubation with empty micelles formed with 6 kDa pvp-od with the sonification method at a) 5 mg/ml while b) is the negative control cells and c) positive control cells.

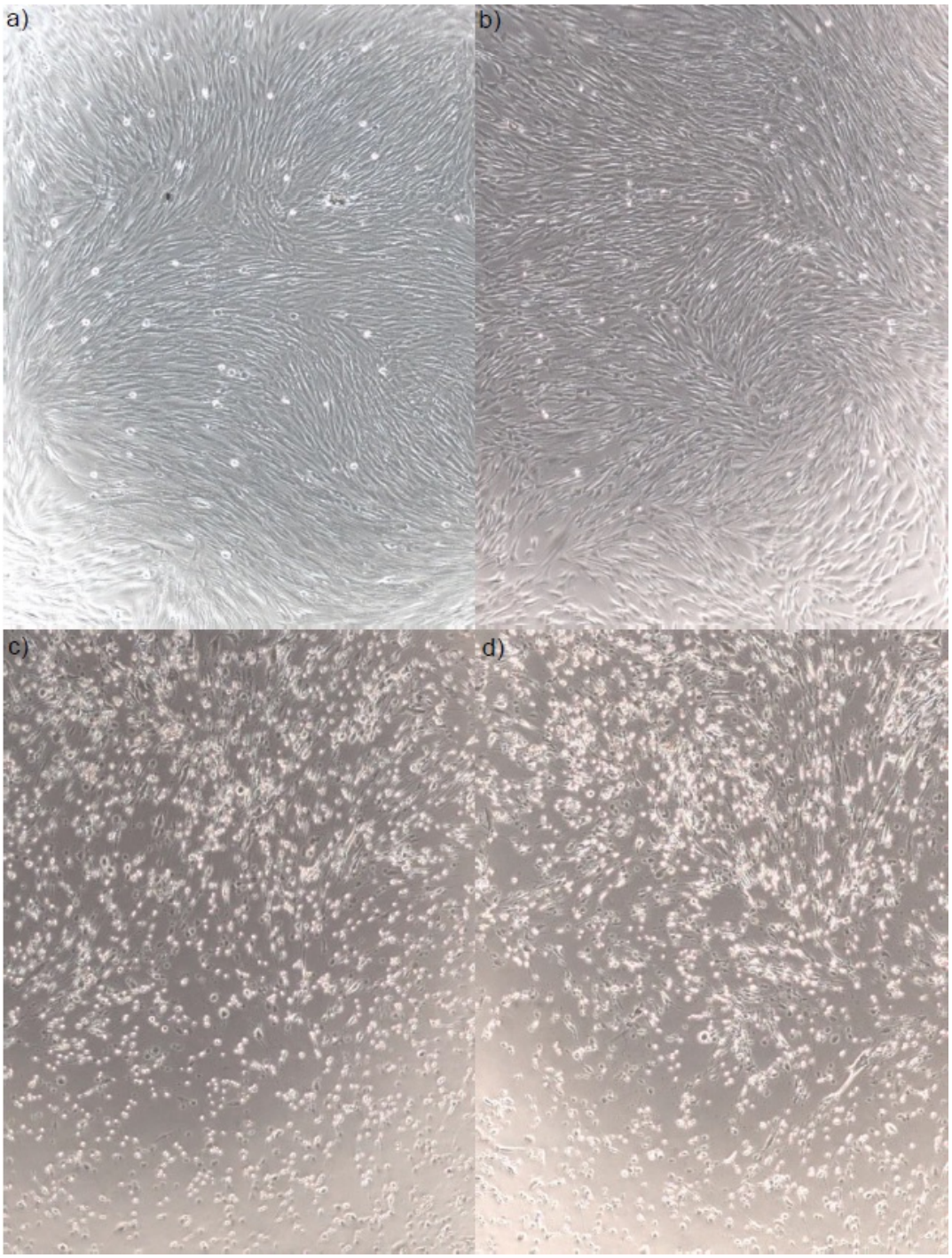

Figure 3.48: Light micrograph of fibroblast cells after 24 h incubation with loaded micelles formed with 6 kDa pvp-od with the sonification method ata) 0.01 mg/ml, b) 0.04 mg/ml, c) 0.08 mg/ml and d) 0.1 mg/ml.

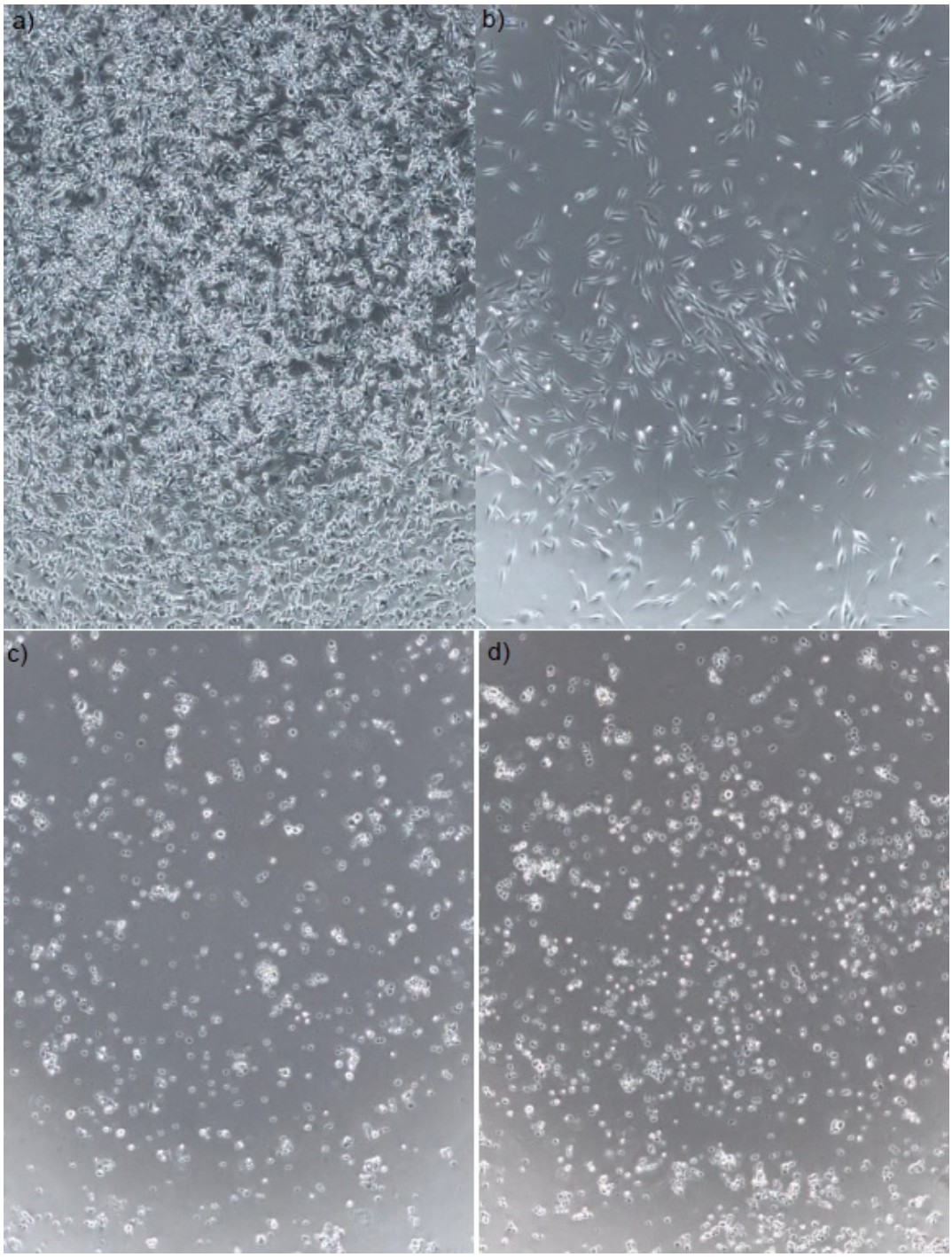

Figure 3.49: Light micrograph of glioblastoma cells after 24 h incubation with loaded micelles formed with 6 kDa pvp-od with the sonification method at a) 0.01 mg/ml, b) 0.04 mg/ml, c) 0.08 mg/ml and d) 0.1 mg/ml.

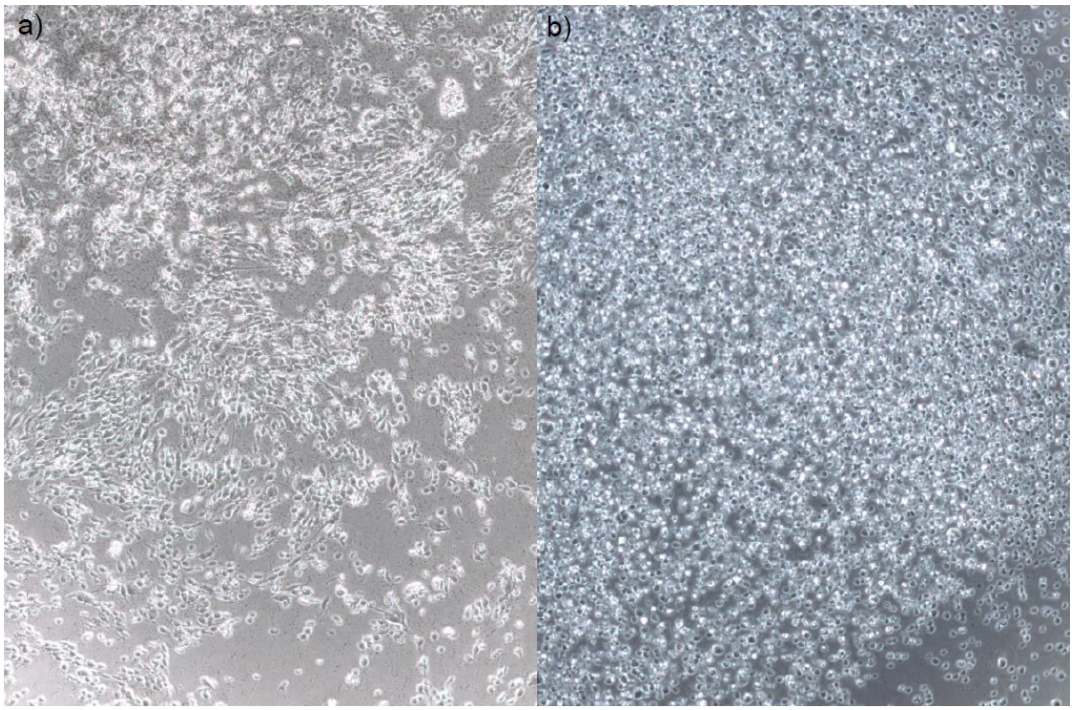

Figure 3.50: Light micrograph of fibroblast a) and glioblastoma b) cells after 24 h incubation with loaded micelles formed with 6 kDa pvp-od with the sonification method at 5 mg/ml.

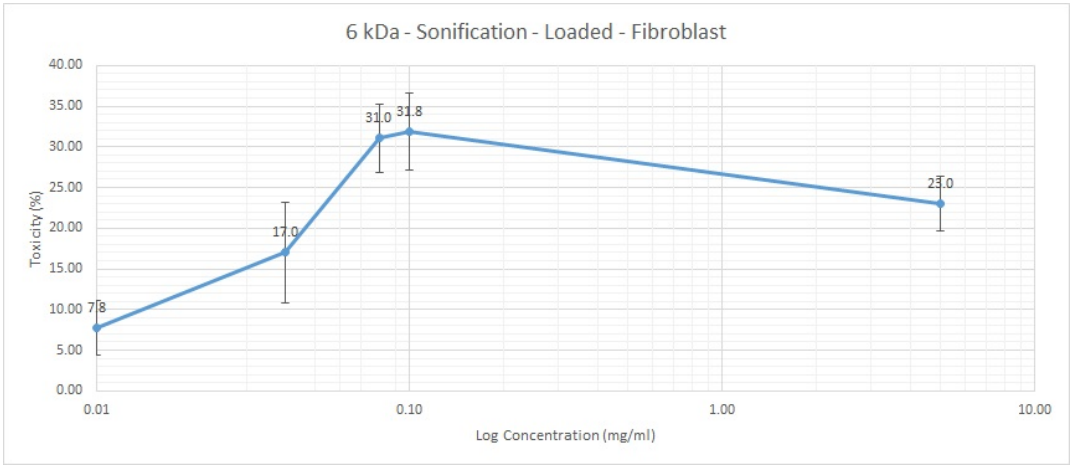

Figure 3.51: Graph of the cytotoxic assay for fibroblast cells incubated with loaded micelles formed from 6 kDa pvp-od polymers with the sonification method, with added standard deviation. The values can be seen in table C.4 in Appendix C

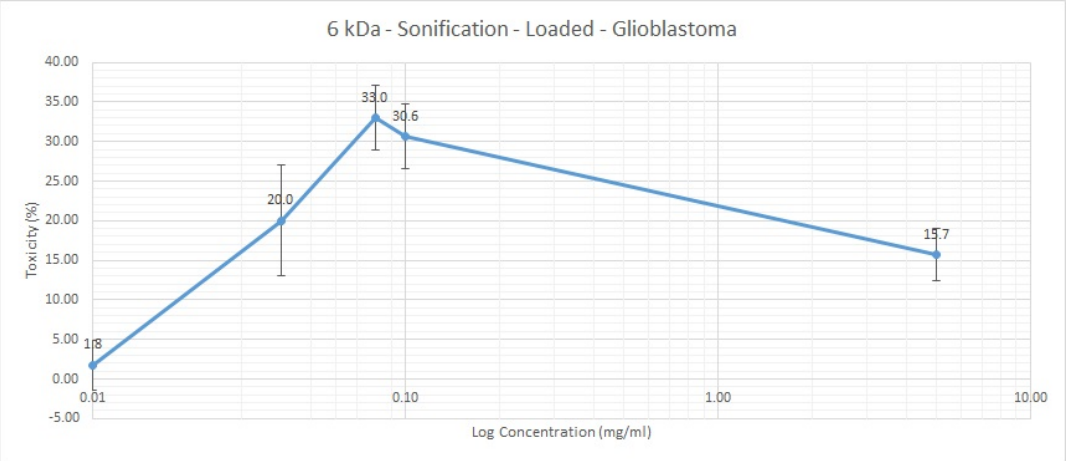

Figure 3.52: Graph of the cytotoxic assay for glioblastoma cells incubated with loaded micelles formed from 6 kDa pvp-od polymers with the sonification method, with added standard deviation. The values can be seen in table C.5 in Appendix C

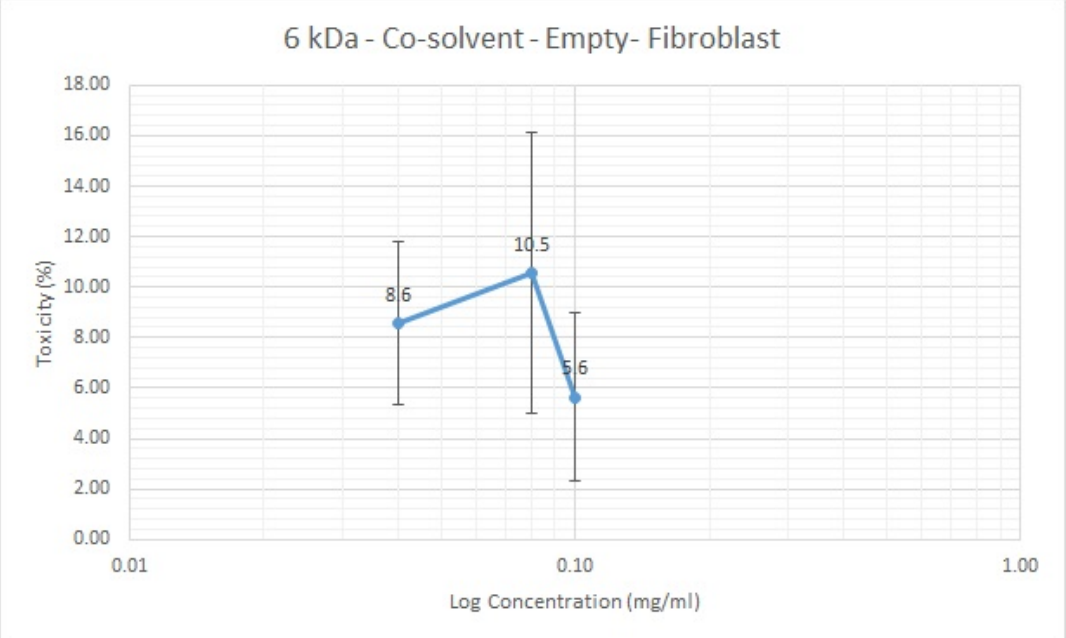

Figure 3.53: Graph of the cytotoxic assay for fibroblast cells incubated with empty micelles formed from 6 kDa pvp-od polymers with the co-solvent evaporation method, with added standard deviation. The values can be seen in table C.6 in Appendix C

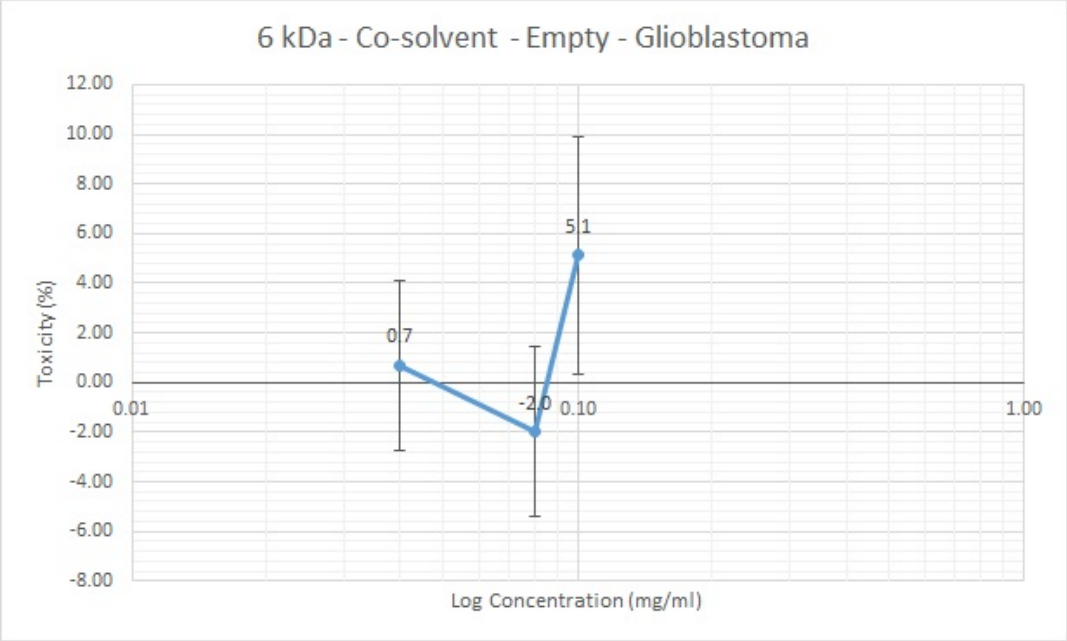

Figure 3.54: Graph of the cytotoxic assay for glioblastoma cells incubated with empty micelles formed from 6 kDa pvp-od polymers with the co-solvent evaporation method, with added standard deviation. The values can be seen in table C.6 in Appendix C

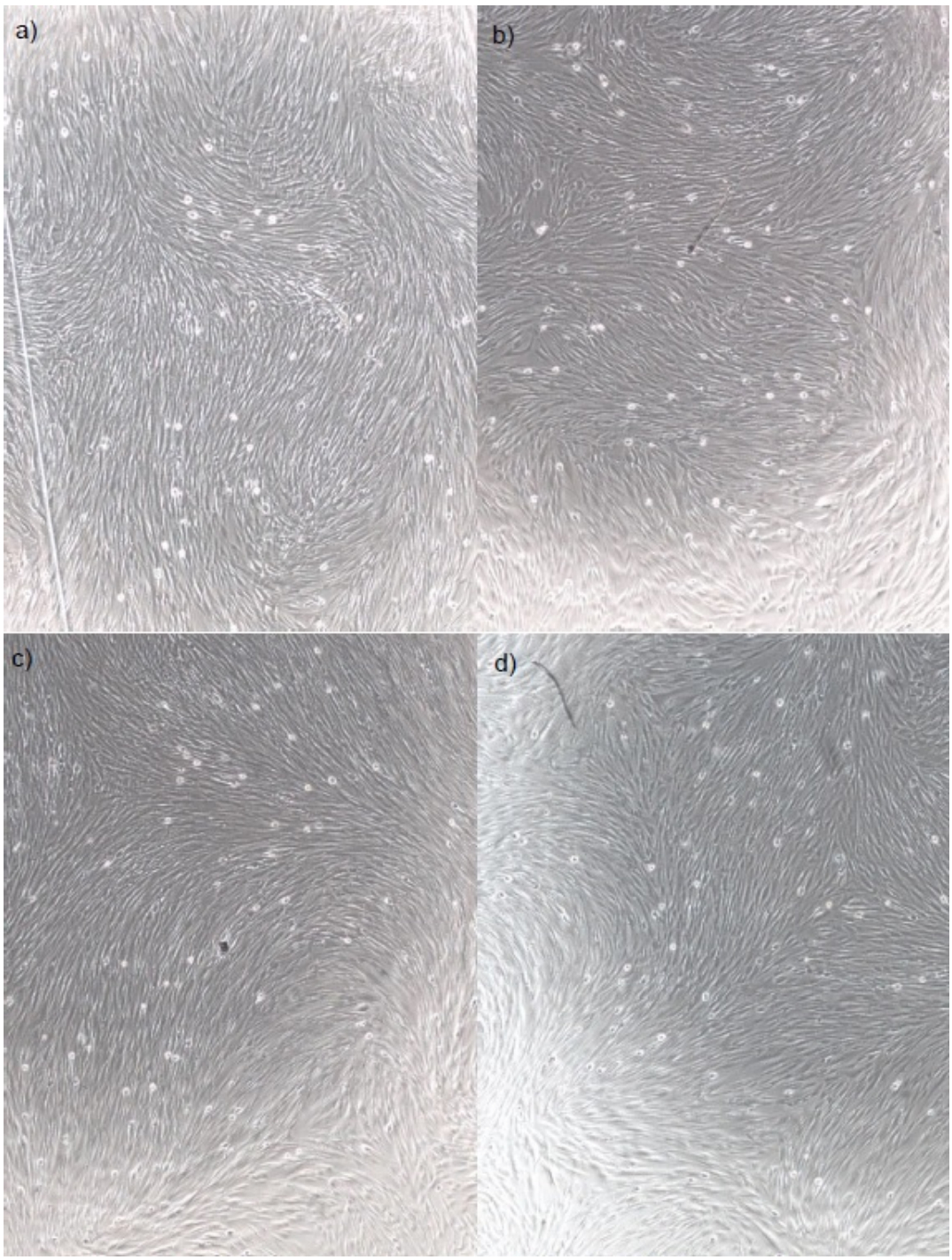

Figure 3.55: Light micrograph of fibroblast cells after 24 h incubation with empty micelles formed with 6 kDa pvp-od with the co-solvent evaporation method at a) 0.01 mg/ml, b) 0.04 mg/ml and c) 0.08 mg/ml.

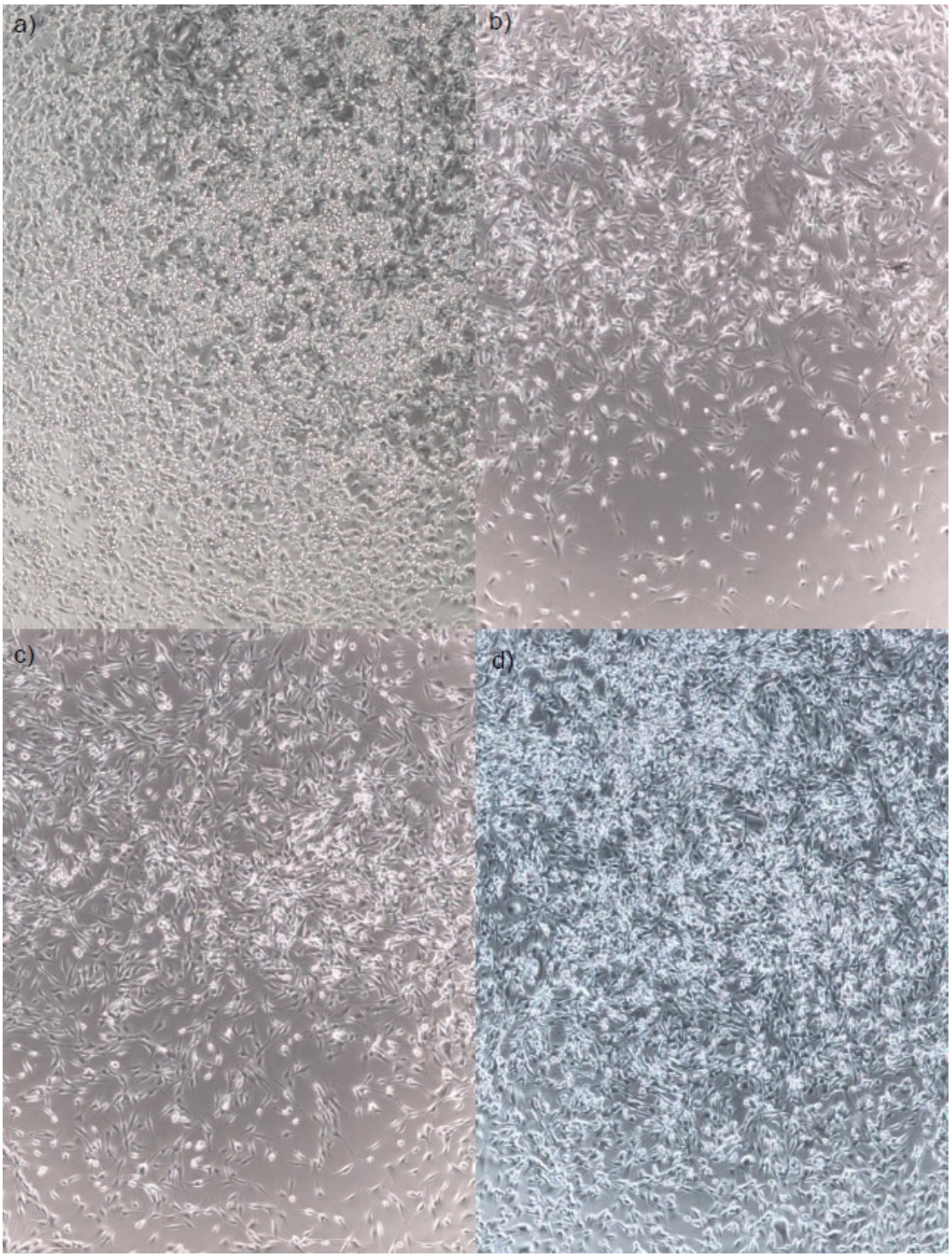

Figure 3.56: Light micrograph of glioblastoma cells after 24 h incubation with loaded micelles formed with 6 kDa pvp-od co-solvent evaporation method at a) 0.01 mg/ml, b) 0.04 mg/ml and c) 0.08 mg/ml.

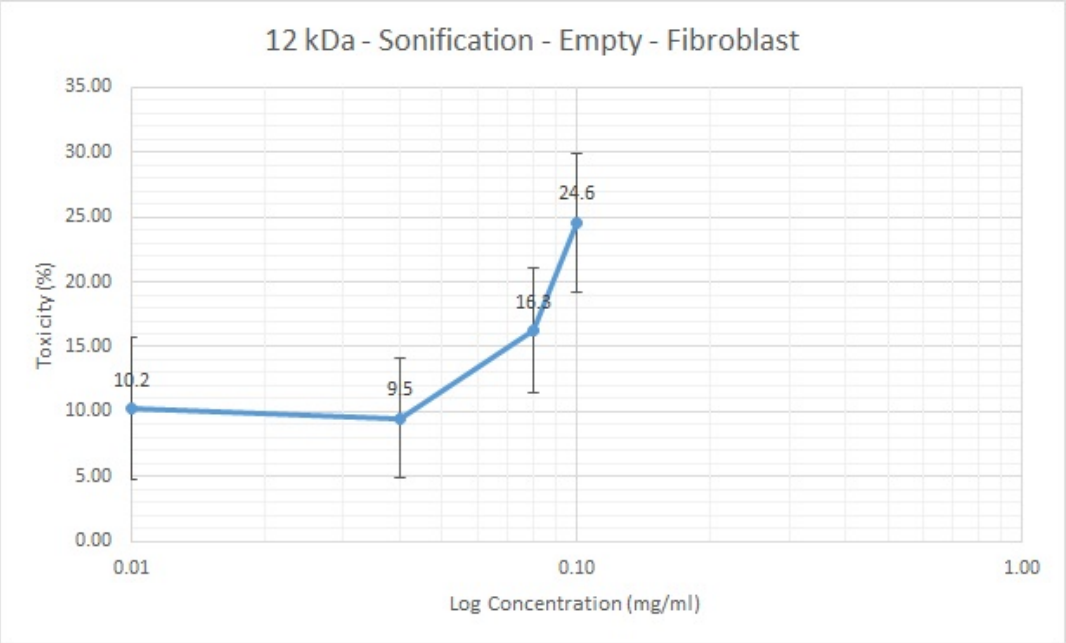

Figure 3.57: Graph of the cytotoxic assay for fibroblast cells incubated with empty micelles formed from 12 kDa pvp-od polymers with the co-solvent evaporation method, with added standard deviation. The values can be seen in table C.6 in Appendix C

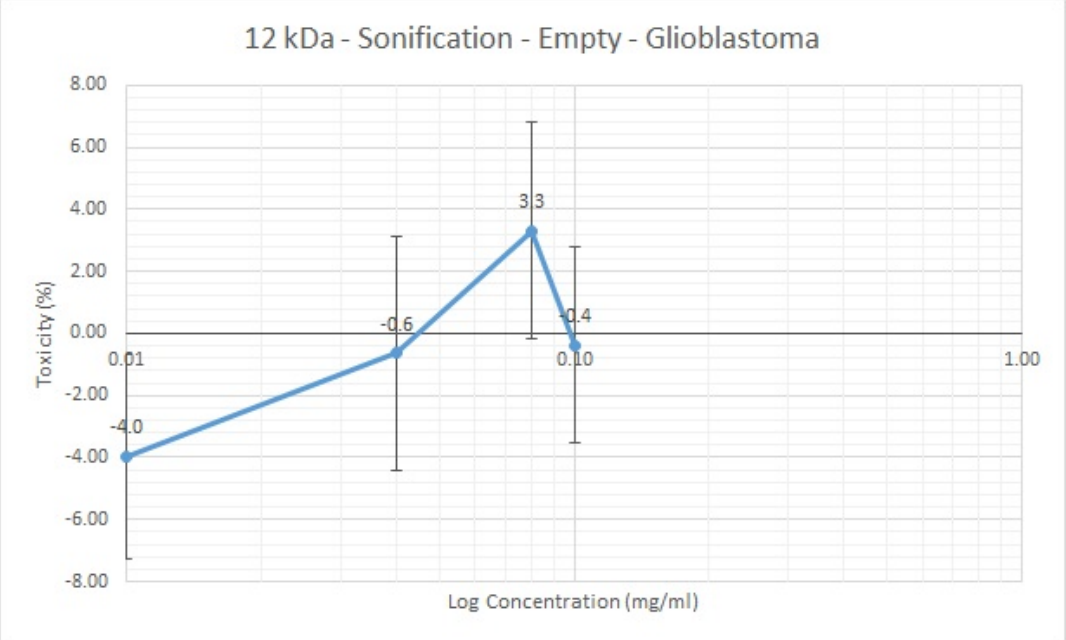

Figure 3.58: Graph of the cytotoxic assay for glioblastoma cells incubated with empty micelles formed from 12 kDa pvp-od polymers with the co-solvent evaporation method, with added standard deviation. The values can be seen in table C.6 in Appendix C

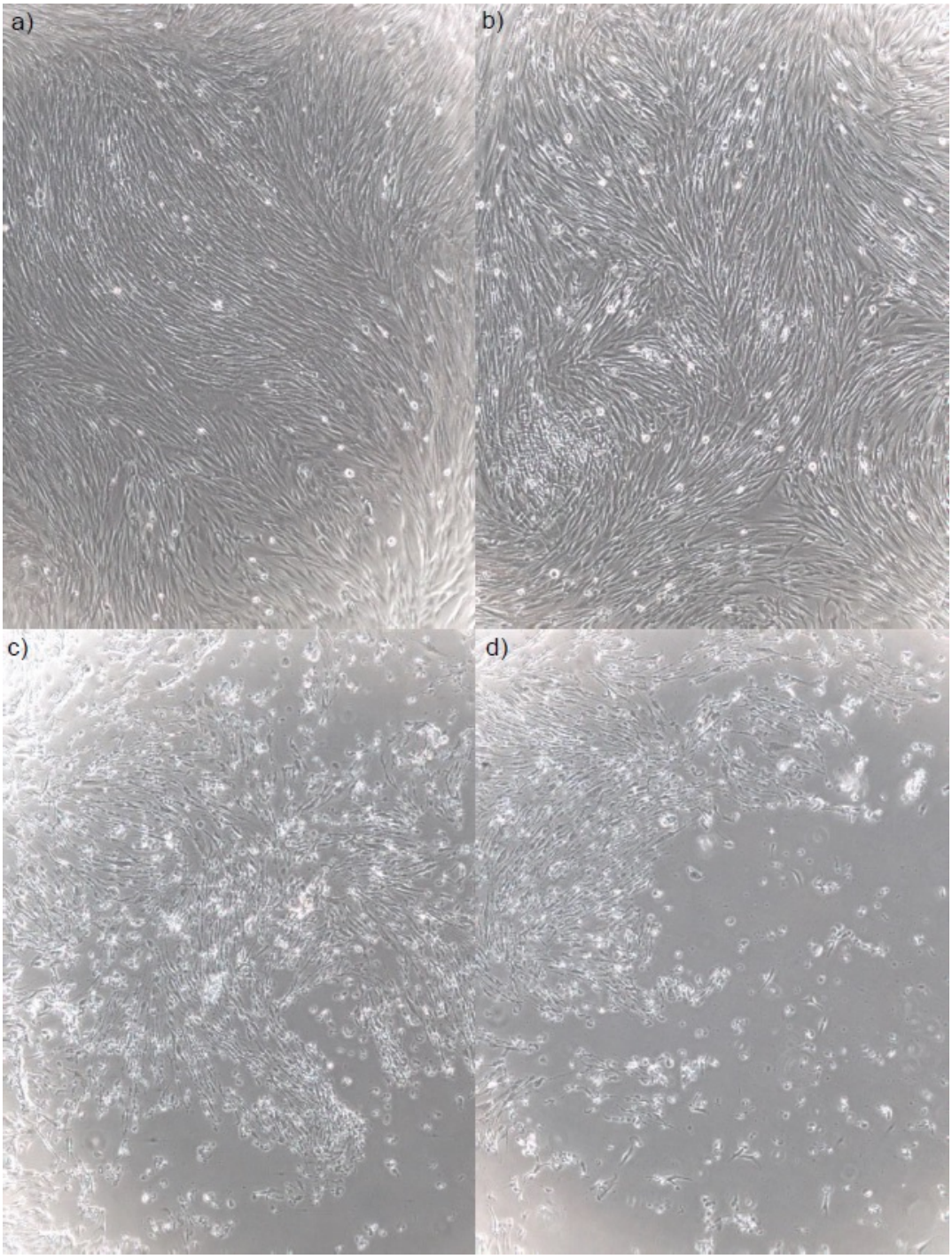

Figure 3.59: Light micrograph of fibroblast cells after 24 h incubation with loaded micelles formed with 12 kDa pvp-od sonification method at a) 0.01 mg/ml, b) 0.04 mg/ml, c) 0.08 mg/ml and d) 0.1 mg/ml.

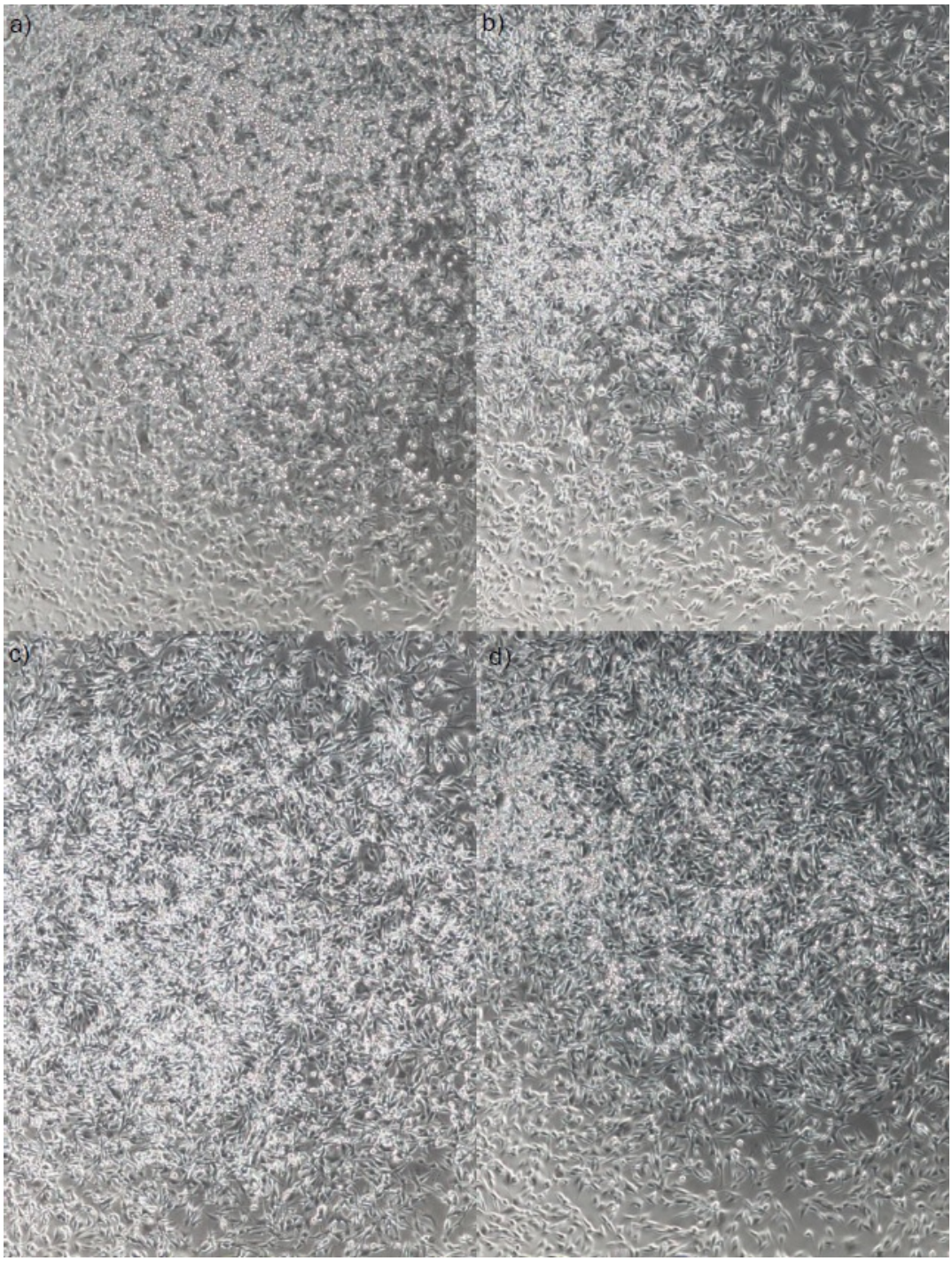

Figure 3.60: Light micrograph of glioblastoma cells after 24 h incubation with loaded micelles formed with 12 kDa pvp-od sonification method at a) 0.01 mg/ml, b) 0.04 mg/ml, c) 0.08 mg/ml and d) 0.1 mg/ml.

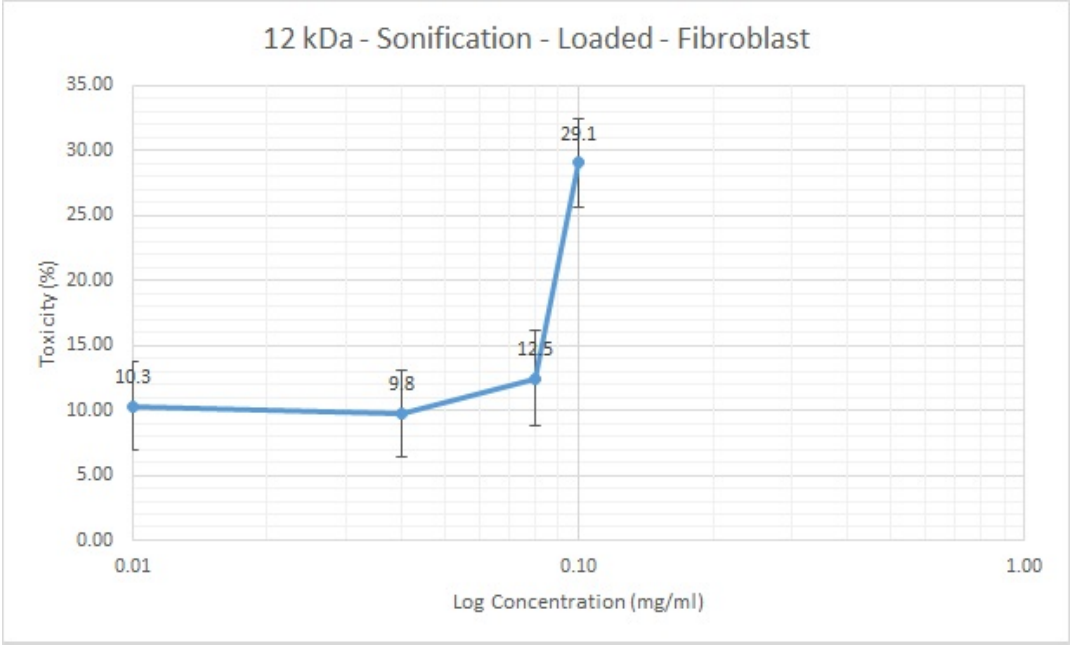

Figure 3.61: Graph of the cytotoxic assay for fibroblast cells incubated with loaded micelles formed from 12 kDa pvp-od polymers with the co-solvent evaporation method, with added standard deviation. The values can be seen in table **??**

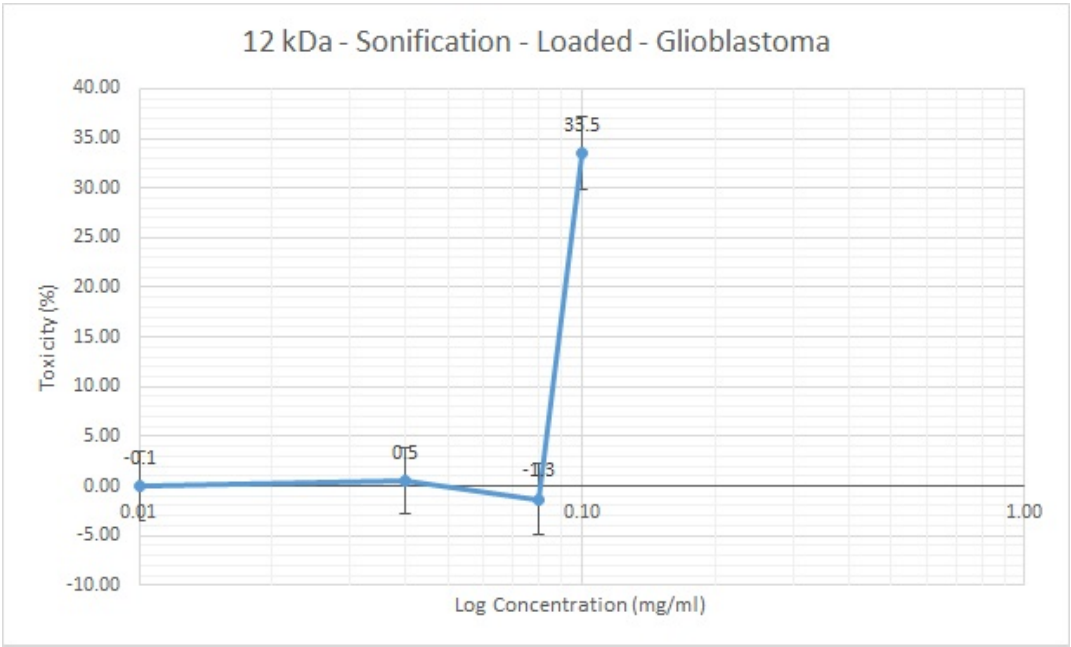

Figure 3.62: Graph of the cytotoxic assay for glioblastoma cells incubated with loaded micelles formed from 12 kDa pvp-od polymers with the co-solvent evaporation method, with added standard deviation. The values can be seen in table **??**

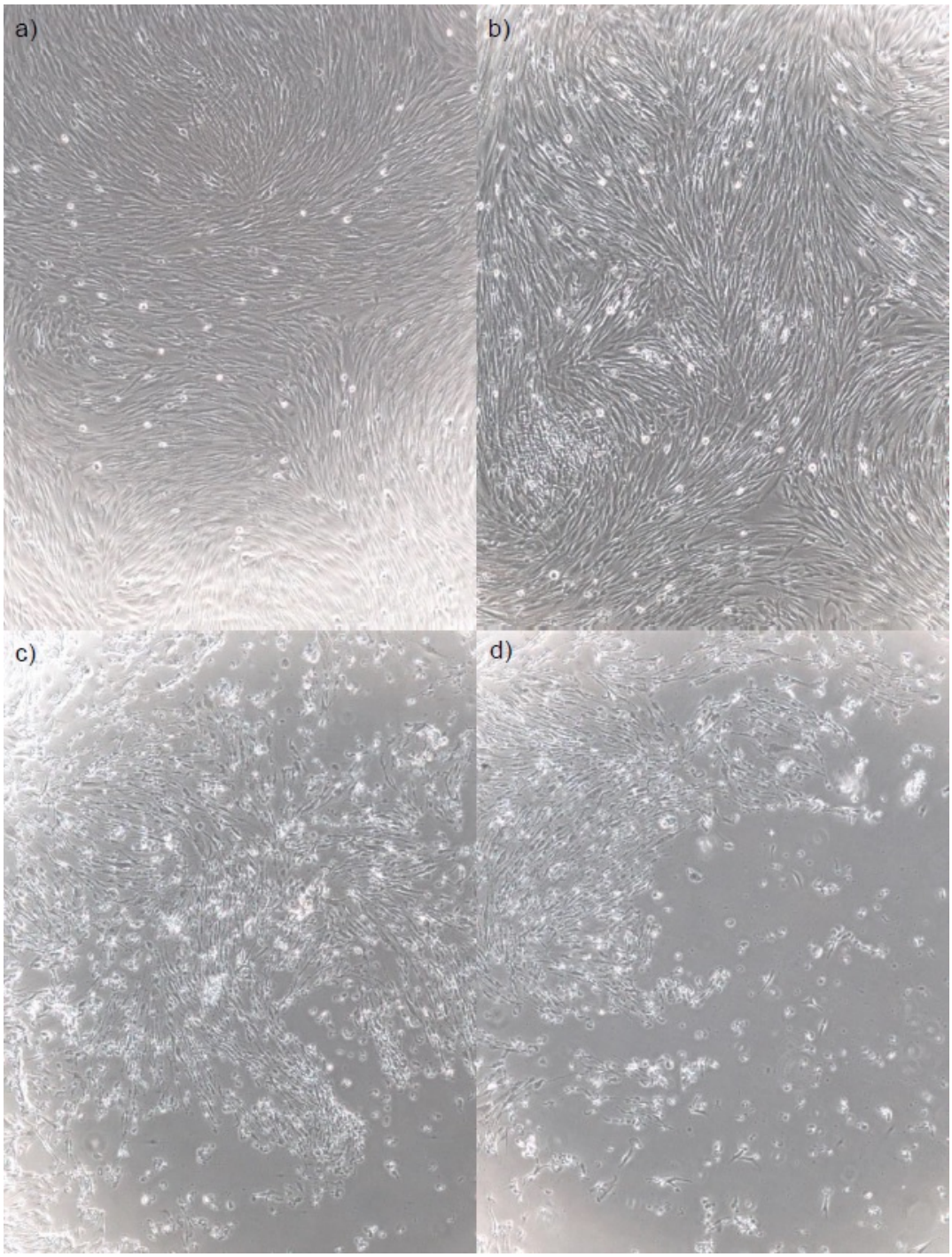

Figure 3.63: Light micrograph of fibroblast cells after 24 h incubation with loaded micelles formed with 12 kDa pvp-od sonification method at a) 0.01 mg/ml, b) 0.04 mg/ml, c) 0.08 mg/ml and d) 0.1 mg/ml.

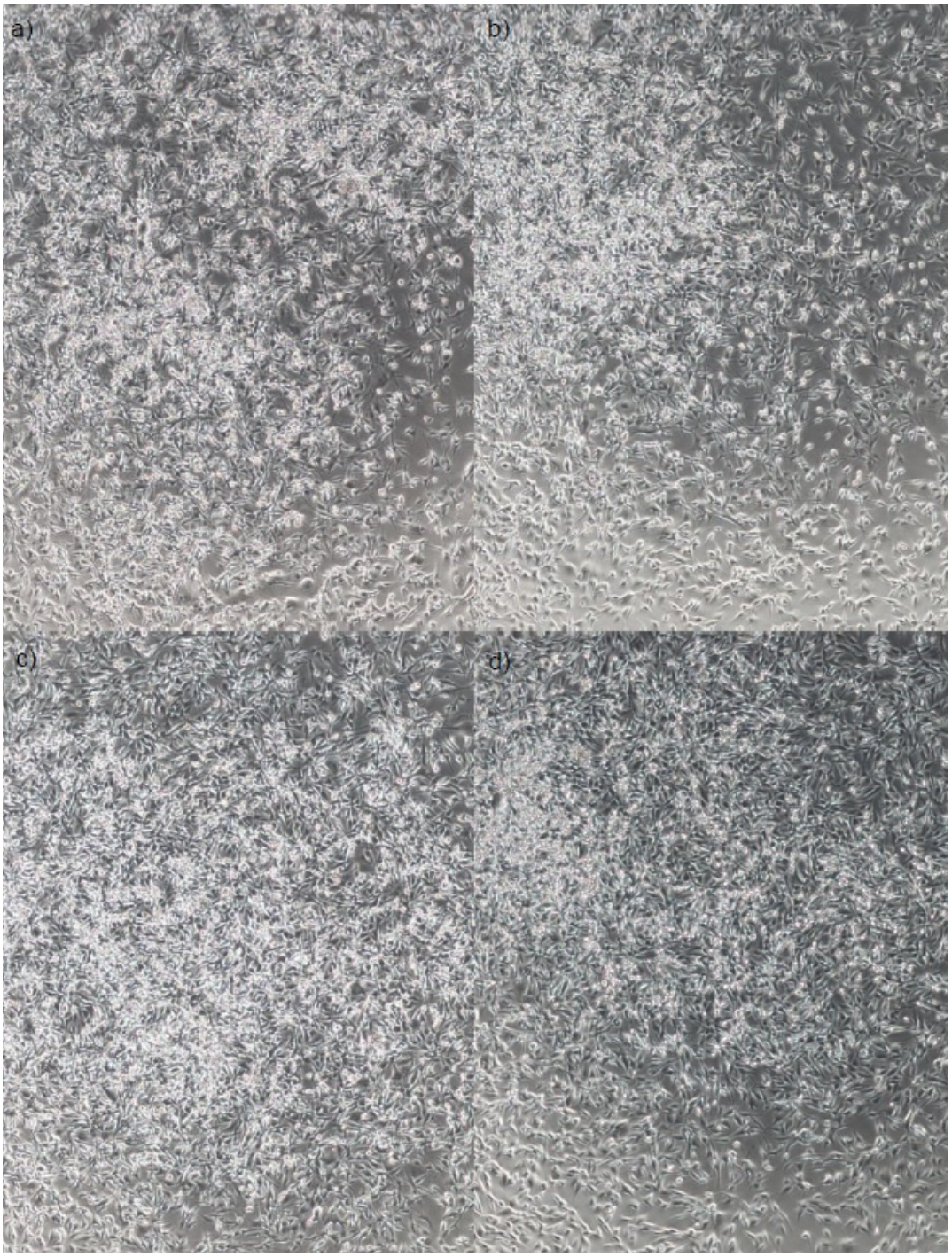

Figure 3.64: Light micrograph of glioblastoma cells after 24 h incubation with loaded micelles formed with 12 kDa pvp-od sonification method at a) 0.01 mg/ml, b) 0.04 mg/ml, c) 0.08 mg/ml and d) 0.1 mg/ml.

Chapter 4

Conclusion

In this master thesis the cytotoxicity of PVP-OD micelles were examined via CytTox-ONE life and death assay kit. The micelles were formed via either sonification method or co-solvent evaporation method, and in both cases they were either loaded or not loaded with curcumin, as it has shown it's great ability at being a model drug. There were created micelles of PVP-OD polymers with the lengths of 1 kDa, 3 kDa, 6 kDa and 12 kDa at 10x the CMC value. It was shown that 1 kDa created larger fraction of bigger aggregates in the range of 1000 nm and 5000-6000 nm, in comparison to the other micelles were the larger fraction of aggregates were found at sub 1000 nm. It was also shown that the different methods had impact on both the sizes of the aggregates present in solution, as well as the polydispersity. For 12 kDa polymers, there were a substantial fraction present in the range between 10 nm and 100 nm that became more expressed when using the co-solvent evaporation method, or loading the aggregates when using the sonification method. The size and distribution were analyzed via DLS.

For the cytotoxic assay the mammalian cells fibroblast (CRL 2429) and glioblastoma (U87) were used for comparisons. Here it was shown that there is a discrepancy between the obtained percentage from the assay to the amount of dead cells shown in light micrographs. It was shown that the polymer size has an impact on this discrepancy, due to the lower percentage obtained with 12 kDa in comparison to 6 kDa where the light micrographs showed similar amount of cellular death (24,6%, 12 kDa PVP-OD micelles at 0.1 mg/ml concentration, 50,7%, 6 kDa PVP-OD micelles at 0.1 mg/ml). Further it was shown that both loaded and empty micelles of 6 kDa PVP-OD polymer, created with the sonification method, were cytotoxic above 0.08 mg/ml to both glioblastoma and fibroblast cells. While the co-solvent evaporation method did not create any cytotoxic aggregates in the same concentrations. For 12 kDa, the toxicity was at 0.1 mg/ml for loaded micelles and 0.08 mg/ml for empty micelles on fibroblast cells, while for glioblastoma cells they were only toxic with loaded micelles at the concentration of 0.1 mg/ml. Due to the non-toxicity against glioblastoma with empty micelles at the same concentration, it can be concluded that this is due to the curcumin present in the loaded micelles.

Due to the inhibitation of the assay by the aggregates formed, it is not possible to determine exact amount of dead cells after incubation. It comes down to human observation, which can be unreliable at times and creates different opinions on the approximate amount

of dead cells. This inhibitation of the assay do require further study to determine cause to better optimise the assay, or find a more suited method for the polymer. Further study is also required on the difference in toxicity between the 2 methods presented in this master thesis.

Bibliography

[1] In: ().

[2] James P. Allen. *Edwin smith papyrus*. https://ceb.nlm.nih.gov/proj/ttp/ flash/smith/smith.html. last read on 28th of May. 1600 BC.

[3] Preetha et al. Anand. "Design of Curcumin-Loaded PLGA Nanoparticles Formulation with Enhanced Cellular Uptake, and Increased Bioactivity in Vitro and Superior Bioavailablility in Vivo". In: *Hiochemical Pharmacology 79(3): 330-38* (2010).

[4] Camilla Lystlund Andersen. "Polymeric Drug Delivery Systems". PhD thesis. Department of Physics and Nanotechnology, Aalborg University, 2017.

[5] Virginie Noirot Bachar Zebib Zéphirin Mouloungui. "Stabilization of Curcumin by Complexation with Divalent Cations in Glycerol/Water System". In: *Bioinorganic Chemistry and Applications* (2010).

[6] Suzana Herculano-Houzel Christopher S. von Bartheld Jami Bahney. *The search for true numbers of neurons and glial cells in the human brain: A review of 150 years of cell counting*. https://onlinelibrary.wiley.com/doi/full/10.1002/cne.24040. 2016.

[7] Elvin Blanco et al. "Multifunctional micellar nanomedicine for cancer therapy." In: *Experimental biology and medicine (Maywood, N.J.)* 234.2 (2009), pp. 123–31. ISSN: 1535-3702. DOI: 10.3181/0808-MR-250.

[8] Peter Boyle and Bernard Levin. "World Cancer Report 2008". In: *International Agency for Research on Cancer (IARC)* (2008).

[9] Julian Lewis Martin Ra-Keith Roberts Bruce Alberts Alexander Johnson and Peter Walter. "Molecular Biology of the Cell". In: *GS Garland Science* (2002).

[10] David F. Cadogan and Christopher J. Howick. "Plasticizers". In: *Ullmann's Encyclopedia of Industrial Chemistry* (2000).

[11] University of Cambridge.

[12] Beata Chertok et al. "Drug Delivery Interfaces in the 21st Century: From Science Fiction Ideas to Viable Technologies". In: *Molecular Pharmaceutics* 10.10 (2013), pp. 3351–3543. DOI: 10.1021/mp4003283.

[13] Rainer Haag Prof. Dr. Felix Kratz Dr. *Polymer Therapeutics: Concepts and Applications*. https://onlinelibrary.wiley.com/doi/abs/10.1002/anie.200502113. 2006.

[14] O. Gallego. *Nonsurgical treatment of recurrent glioblastoma*. https://current-oncology.com/index.php/oncology/article/view/2436. visited 12th of april.

[15] Daria Y. Alakhovaa Gaurav Sahaya and Alexander V. Kabanov. "Endocytosis of nanomedicines". In: *Journal of Controlled Release* (2010).

[16] Karlheinz Graf Hand-JÃrgen Butt and Michael Kappl. "Physics and Chemistry of interface". In: *WILEY-VCH* (2003).

[17] Livia Balan Veronika N.Foltyn Herman Wolosker Elena Dumin. "d-Amino acids in the brain: d-serine in neurotransmission and neurodegeneration". In: *The FEBS Journal* (2008).

[18] Seiji Kondo Raymond Sawaya-Bharat B. Aggarwal Hiroshi Aoki Yasunar Takada and Yasuko Kondo. "Evidence that curcumin suppress the growth of malignant gliomas in vitro and in vivo through induction of autophagy: Role of akt and extracellular signal-regulated kinase signaling pathways". In: *Molecular Pharmaceutics* (2007).

[19] Wang Chao Hu Quanyin Sun Wujin and Gu Zhen. "Recent advances of cocktail chemotherapy by combination drug delivery systems". In: *Advanced Drug Delivery Reviews* (2015).

[20] Kewal K Jain. "Drug Delivery Systems â An Overview". In: *Methods in Molecular Biologyâ* 437 (2008).

[21] Aditi M. Jhaveri and Vladimir P. Torchilin. "Multifunctional polymeric micelles for delivery of drugs and sirna". In: *Frontiers in - Pharmacology* (2014).

[22] Marie-Christine Jones and Jean-Christophe Leroux. "Polymeric micelles +/- a new generation of colloidal drug carrier". In: *European Journal of Pharmaceutics and Biopharmaceutics* (1999).

[23] Ryan T. Kendall and Carol A. Feghali-Bostwick. "Fibroblasts in brosis- novel roles and mediators". In: *Frontiers -In Pharmacology* (2014).

[24] OlbjÃ¸rn Klepp. *Glioblastom*. https://sml.snl.no/glioblastom. retrieved 10th of april. 2018.

[25] OlbjÃ¸rn Klepp. *Gliom*. https://sml.snl.no/gliom. visited 10th of april. 2009.

[26] Qinjie Wu Wenhao Guo-Ling Li YiShan Chen yuchen Li Changyang Gong Zhiyong Qian Lei Liu Lu Sun and Yuquan Wei. "Curcumin loaded polymeric micelles inhibit breast tumor growth and spontaneous pulmonary metastasis". In: *International journal of pharmaceutics* (2012).

[27] Anna L. Luss et al. “Nanosized carriers based on amphiphilic poly-N-vinyl-2-pyrrolidone for intranuclear drug delivery.” eng. In: *Nanomedicine (London, England)* 13 (7 2018), pp. 703–715.

[28] M.F.Maitz. *Applications of synthetic polymers in clinical medicine*. https://www.sciencedirect.com/scienc

[29] Abbas Khan Muhammad Usman and Mohammad Siddiq. “Thermodynamic and Solution Properties of Amphiphilic Anti-Allergic Drug Cetirizine HCl”. In: (2008).

[30] Levi Nelemans. “Characterization of 12 kDa PVP-OD nanocarriers and the influence of their size on the uptake in mammalian cells”. PhD thesis. Department of Materials and Production, Aalborg University, 2019.

[31] Jayanth Panyam and Vinod Labhasetwar. “Biodegradable nanoparticles for drug and gene delivery to cells and tissue”. In: *Advanced Drug Delivery Reviews* 55.3 (2003), pp. 329–347. ISSN: 0169409X. DOI: 10.1016/S0169-409X(02)00228-4.

[32] Sonia Hurani Ajaikumar B. Kunnumakkara Preetha Anand Chitra Sundaram and Bharat B. Aggarwal. “Curcumin and cancer: An "old-age" disease with and "age-old" solution”. In: *Cancer letters* (2008).

[33] K. Indira Priyadarsini. “Photphysics, photochemistry and photobiology of curcumin: Studies from organic solutions, bio-mimetics and living cells”. In: *Journal of Photochemistry and Photobiology C: Photochemistry Reviews* (2019).

[34] K Rani and S Paliwal. “A Review on Targeted Drug Delivery: its Entire Focus on Advanced Therapeutics and Diagnostics”. In: *Scholars Journal of Applied Medical Sciences* 2.1 (2014), pp. 328–331.

[35] P. N. Ravindran. “Turmeric - The genus curcuma”. In: *CRC Press* (2007).

[36] Seymour Reichlin. *Handbook of Experimental Pharmacology*. Vol. 258. 5. 1969, p. 366. ISBN: 354022565X. DOI: 10.1097/00000441-196911000-00008.

[37] Timothy M. Blieden Roger S. Smith Terry J. SMith and RIchard P. Phipps. “Fibroblasts as Sentinel Cells”. In: *American Journal of Pathology* (1997).

[38] Sharon Sagnella and Calum Drummond. “Drug delivery - a nanomedicine approach”. In: *Australasian Biochemist* (2012).

[39] Monika SchÃfer-Korting, ed. *Drug Delivery - Passive and Active Drug Targeting - Drug Delivery to Tumors as an Example*. Vol. 197. Handbook of experimental pharmacology. Springer, 2010.

[40] American Cancer Society. *The history of cancer*. http://www. cancer.org/acs/groups/cid/documents/pdf.pdf. last downloaded on 23rd of May. 2014.

[41] Sperling. *Introduction to Physical Polymer Science*. http://doi.wiley.com/10.1002/0471757128.ch9. 2006.

[42] Drug Delivery Systems et al. “Drug Delivery Systems : Getting Drugs to Their Targets in a Controlled Manner”. In: *NATIONAL INSTITUTE OF BIOMEDICAL IMAGING AND BIOENGINEERING* October (2016).

[43] Waree Tiyaboonchai, Watcharaphorn Tungpradit, and Pinyupa Plianbangchang. “Formulation and characterization of curcuminoids loaded solid lipid nanoparticles”. In: 337 (2007), pp. 299–306. DOI: 10.1016/j.ijpharm.2006.12.043.

[44] V. P. Torchilin. “Drug targeting”. In: *Pharmaceutical Sciences* (2000).

[45] Vladimir P. Torchilin. “Structure and design of polymeric surfactant-based drug delivery systems”. In: *Elsevier - Journal of controlled release* (2001).

[46] Vladimir P. Torchilin and Vladimir S. Trubetskoy. “Which polymers can make nanoparticulate drug carriers long-circulating?” In: *Advanced Drug Delivery Reviews* (1995).

[47] John G Wagner. “HISTORY OF PHARMACOKINETICS was entitled the Kinetics of Drug Absorption , Distribution , Metabolism and Excretion and at d / + VkC”. In: (1964), pp. 537–562.

[48] *World Cancer Report*. Vol. 5.16. World Health Organization, 2014.

[49] Zhuo Chen Dong M. Shin Xu Wang Lily Yang. “Application of Nanotechnology in Cancer Therapy and Imaging”. In: *CA: A Cancer Journal for Clinicians* (2008).

[50] Ommoleila Molavi Afsaneh Lavasanifar Raymond Lai Zenshuan Ma Azita Haddadi and John Samuel. “Micelles of poly/ethylene oxide)-b-poly(-caprolactone) as vehicles for solubilization, stabilization, and controlled delivery of curcumin”. In: *Journal of biomedical materials research* (2007).

Appendix A

DLS graphs

A.1 3 kDa polymeric micelles

A.1.1 Sonification method

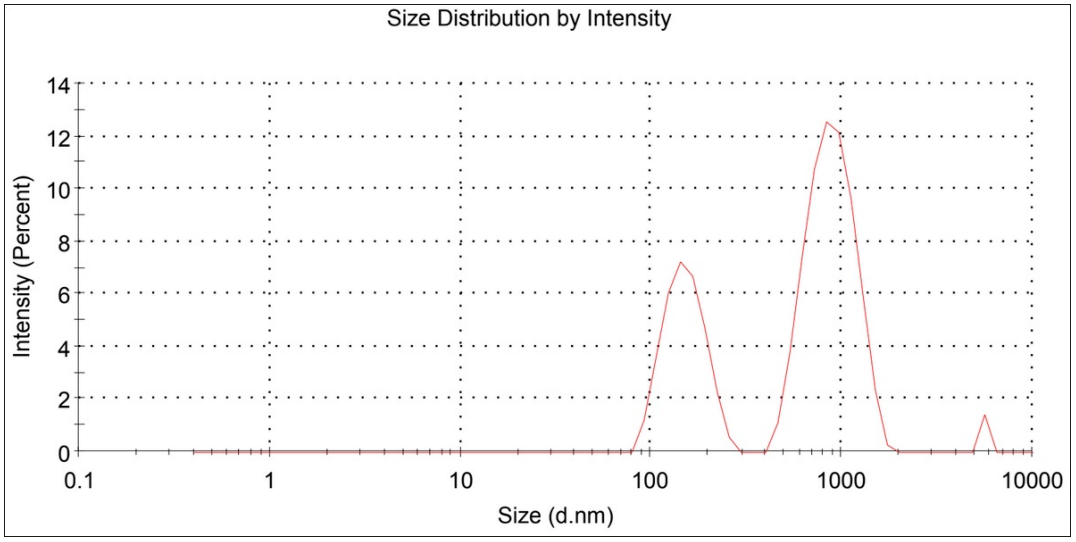

Figure A.1: First reading of size distribution by intensity for empty micelles created with the sonification method for 3 kDa, first iteration of the triplicates, done by the DLS software done with attenuation factor 5. A table with information on peaks, intensity and standard deviation can be seen in Appendix B as readings 1.3.0.1 - 1

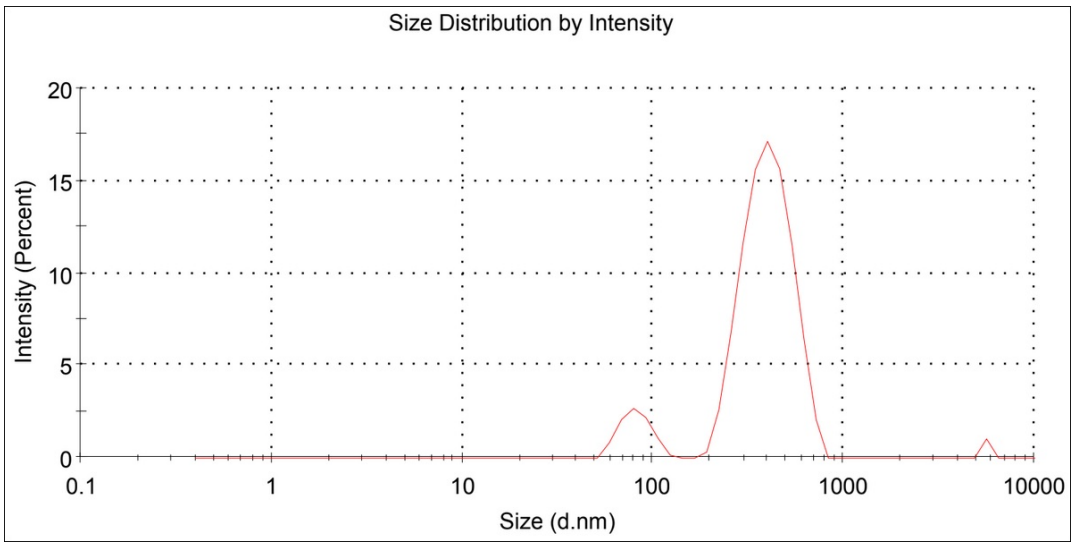

Figure A.2: Second reading of size distribution by intensity for empty micelles created with the sonification method for 3 kDa, first iteration of the triplicates, done by the DLS software done with attenuation factor 6. A table with information on peaks, intensity and standard deviation can be seen in Appendix B as readings 1.3.0.1 - 2

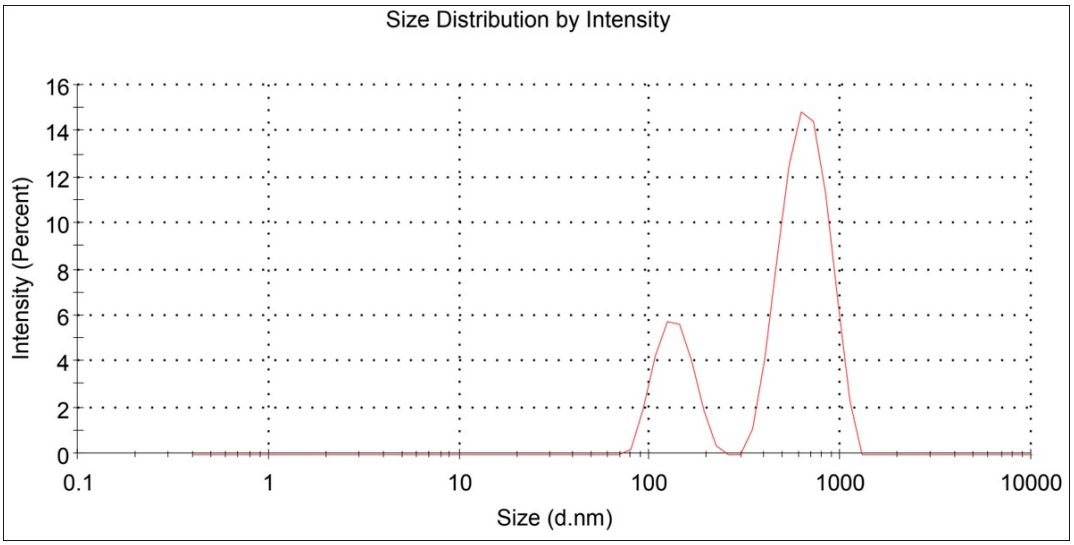

Figure A.3: Third reading of size distribution by intensity for empty micelles created with the sonification method for 3 kDa, first iteration of the triplicates, done by the DLS software done with attenuation factor 6. A table with information on peaks, intensity and standard deviation can be seen in Appendix B as readings 1.3.0.1 - 3

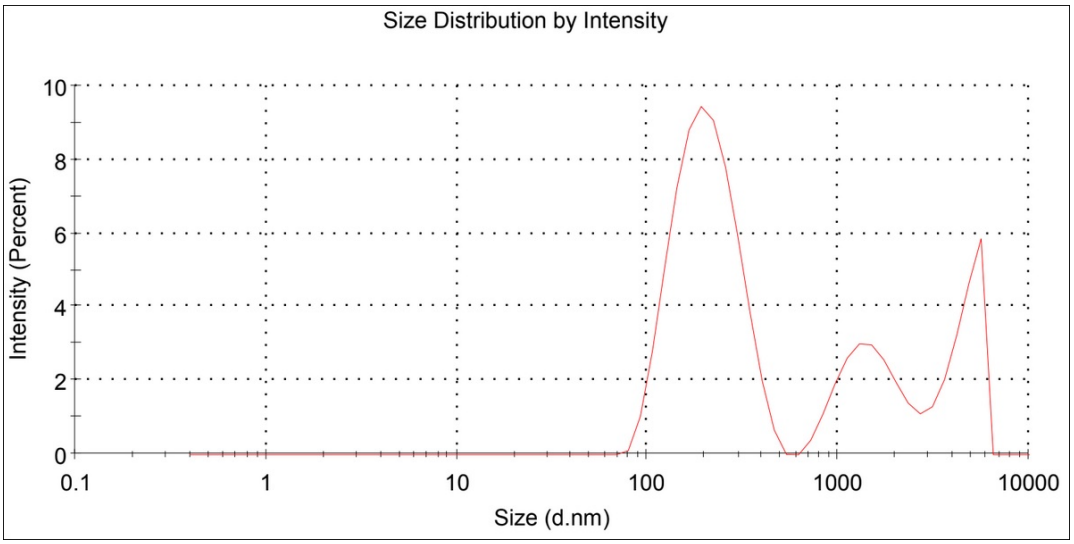

Figure A.4: First reading of size distribution by intensity for empty micelles created with the sonification method for 3 kDa, second iteration of the triplicates, done by the DLS software done with attenuation factor 6. A table with information on peaks, intensity and standard deviation can be seen in Appendix B as readings 1.3.0.2 - 1

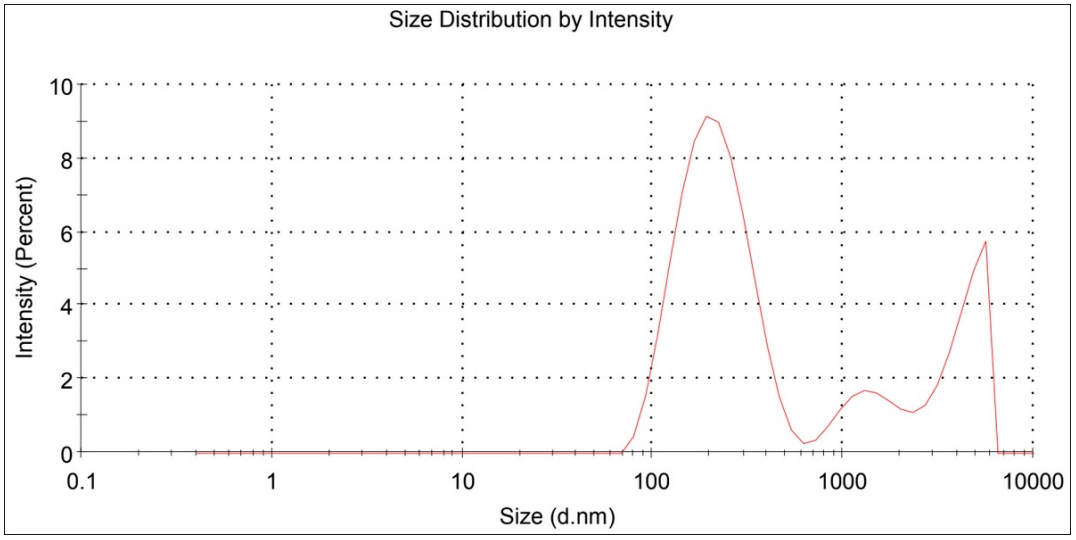

Figure A.5: Second reading of size distribution by intensity for empty micelles created with the sonification method for 3 kDa, second iteration of the triplicates, done by the DLS software done with attenuation factor 5. A table with information on peaks, intensity and standard deviation can be seen in Appendix B as readings 1.3.0.2 - 2

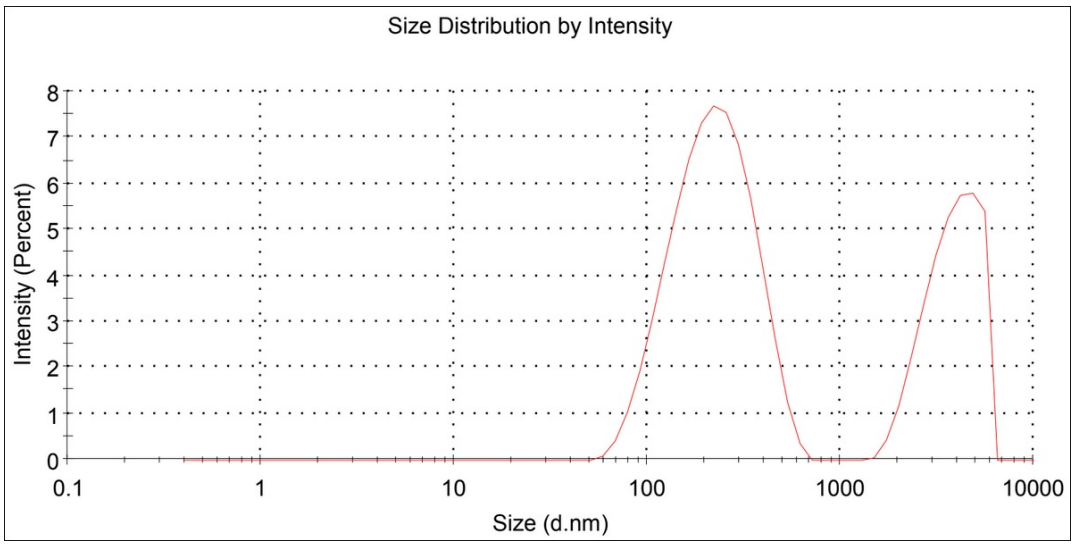

Figure A.6: Third reading of size distribution by intensity for empty micelles created with the sonification method for 3 kDa, second iteration of the triplicates, done by the DLS software done with attenuation factor 5. A table with information on peaks, intensity and standard deviation can be seen in Appendix B as readings 1.3.0.2 - 3

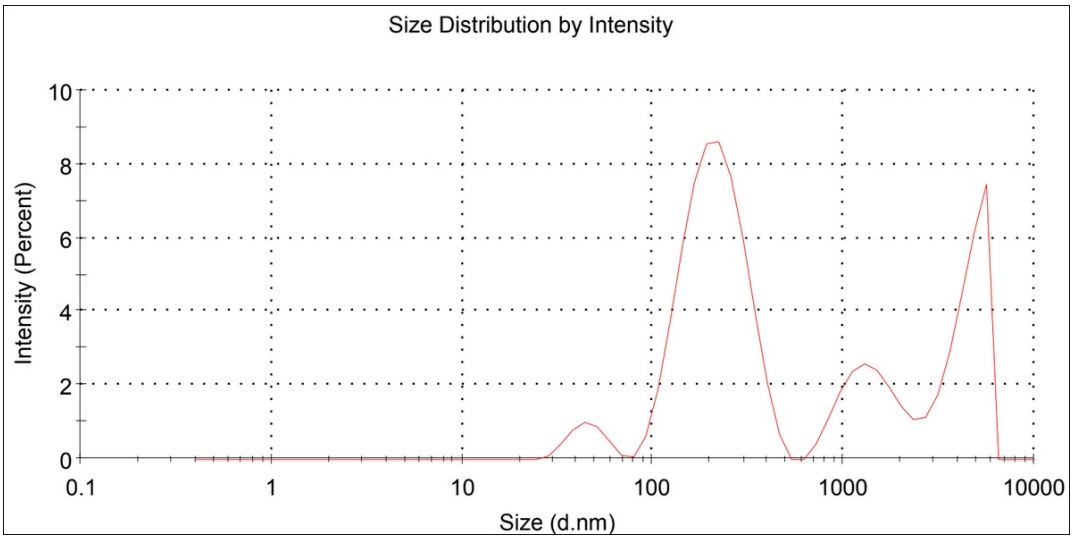

Figure A.7: First reading of size distribution by intensity for empty micelles created with the sonification method for 3 kDa, third iteration of the triplicates, done by the DLS software done with attenuation factor 6. A table with information on peaks, intensity and standard deviation can be seen in Appendix B as readings 1.3.0.3 - 1

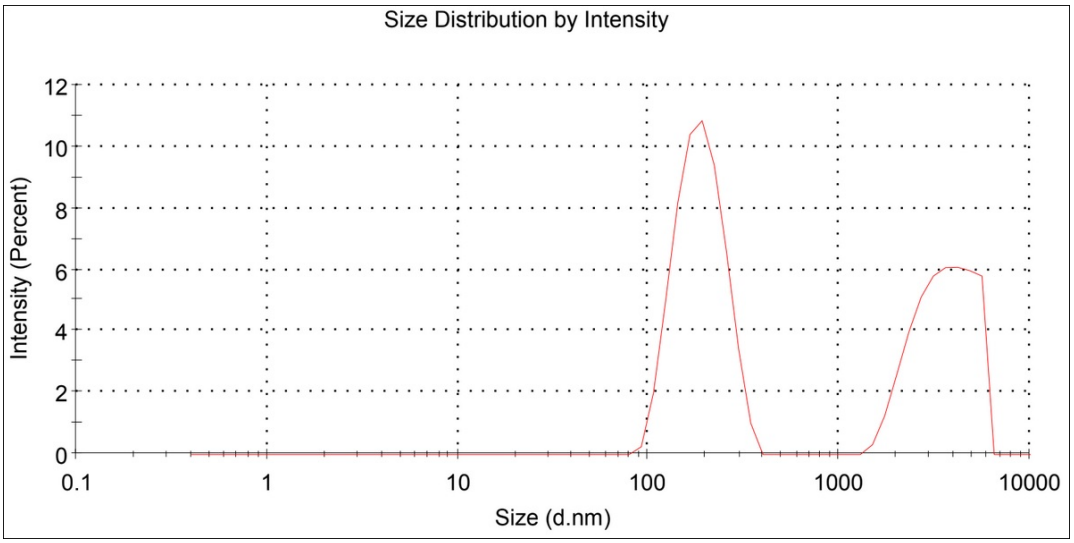

Figure A.8: Second reading of size distribution by intensity for empty micelles created with the sonification method for 3 kDa, third iteration of the triplicates, done by the DLS software done with attenuation factor 6. A table with information on peaks, intensity and standard deviation can be seen in Appendix B as readings 1.3.0.3 - 2

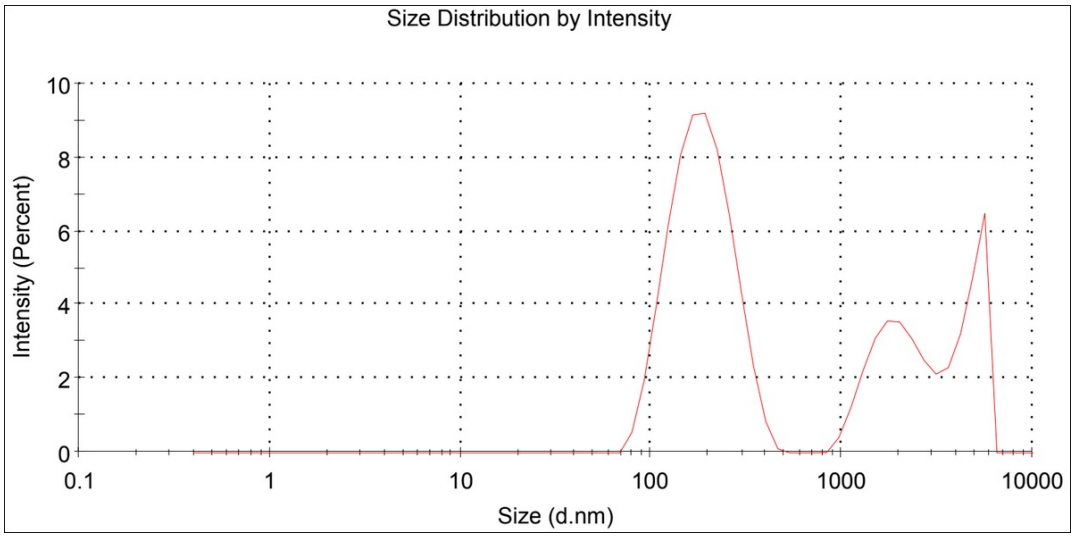

Figure A.9: Third reading of size distribution by intensity for empty micelles created with the sonification method for 3 kDa, third iteration of the triplicates, done by the DLS software done with attenuation factor 6. A table with information on peaks, intensity and standard deviation can be seen in Appendix B as readings 1.3.0.3 - 3

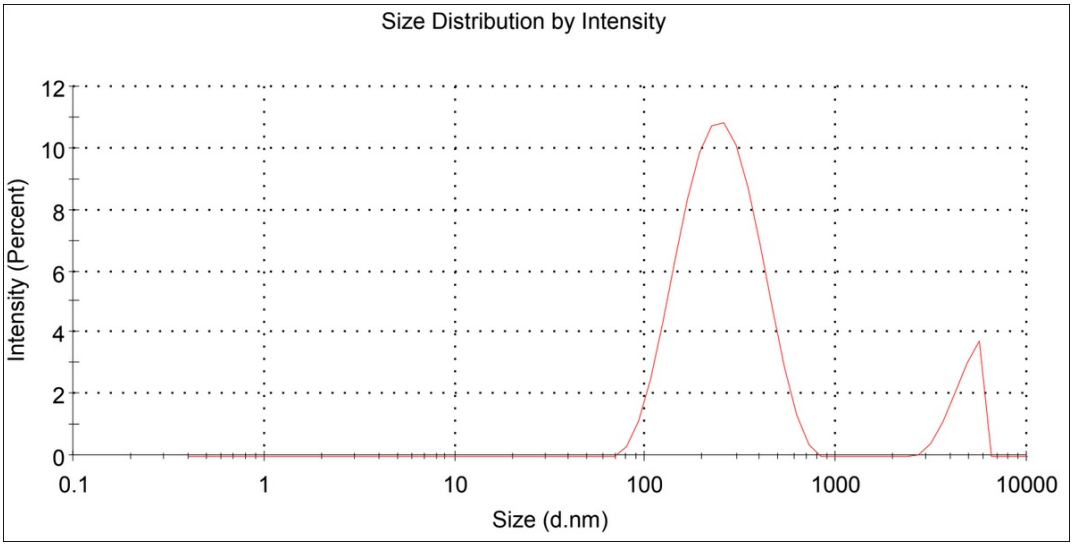

Figure A.10: First reading of size distribution by intensity for loaded micelles created with the sonification method for 3 kDa, first iteration of the triplicates, done by the DLS software done with attenuation factor 5. A table with information on peaks, intensity and standard deviation can be seen in Appendix B as readings 1.3.1.1 - 1

A.1.2 Co-solvent evaporation method

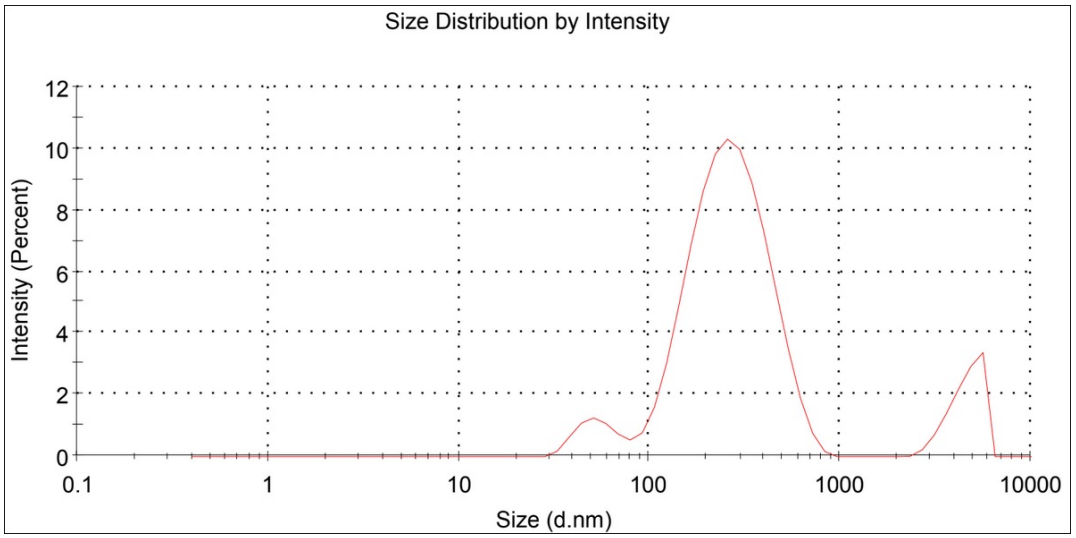

Figure A.11: Second reading of size distribution by intensity for loaded micelles created with the sonification method for 3 kDa, first iteration of the triplicates, done by the DLS software done with attenuation factor 5. A table with information on peaks, intensity and standard deviation can be seen in Appendix B as readings 1.3.1.1 - 2

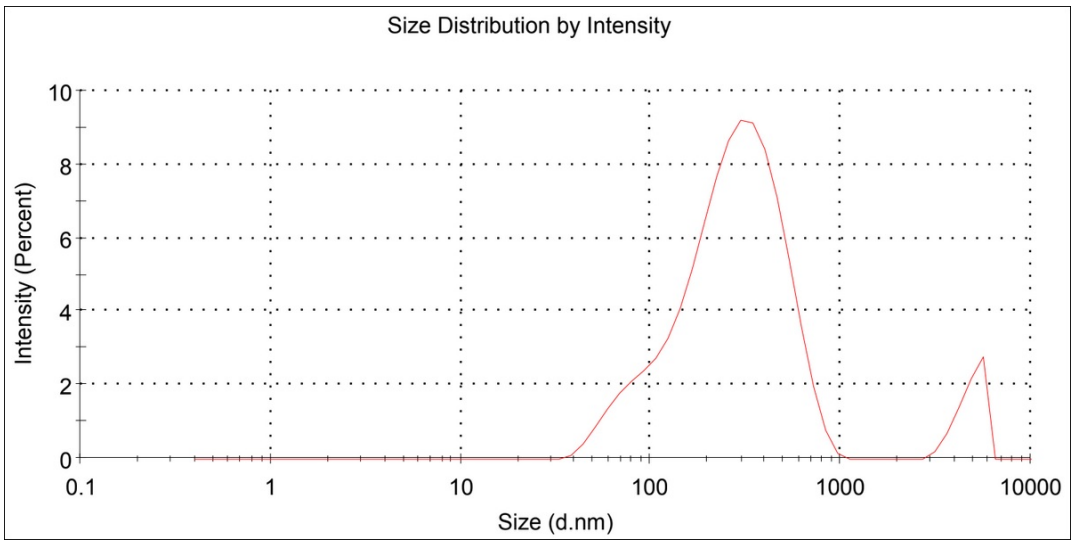

Figure A.12: Third reading of size distribution by intensity for loaded micelles created with the sonification method for 3 kDa, first iteration of the triplicates, done by the DLS software done with attenuation factor 5. A table with information on peaks, intensity and standard deviation can be seen in Appendix B as readings 1.3.1.1 - 3

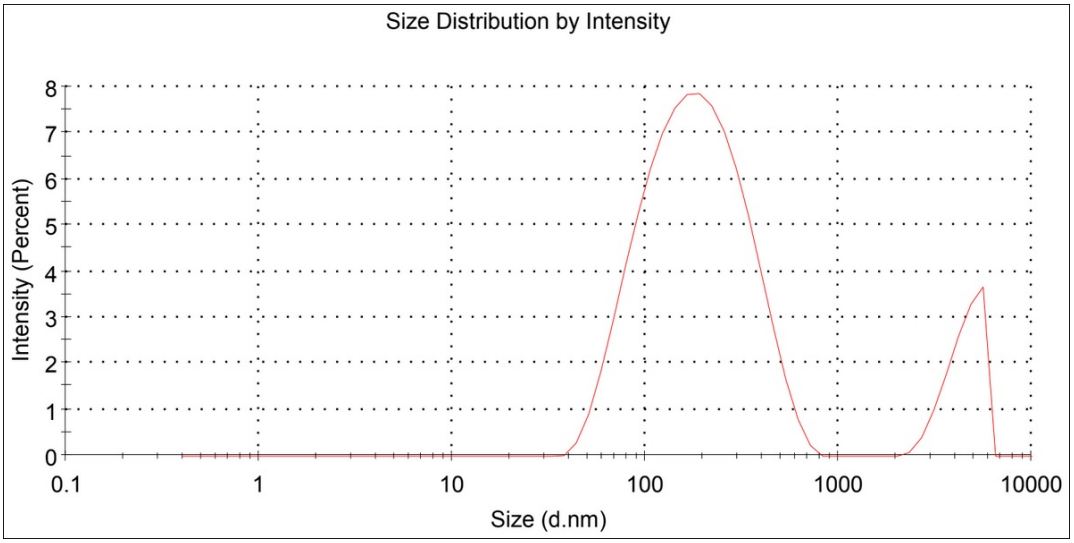

Figure A.13: First reading of size distribution by intensity for loaded micelles created with the sonification method for 3 kDa, second iteration of the triplicates, done by the DLS software done with attenuation factor 6. A table with information on peaks, intensity and standard deviation can be seen in Appendix B as readings 1.3.1.2 - 1

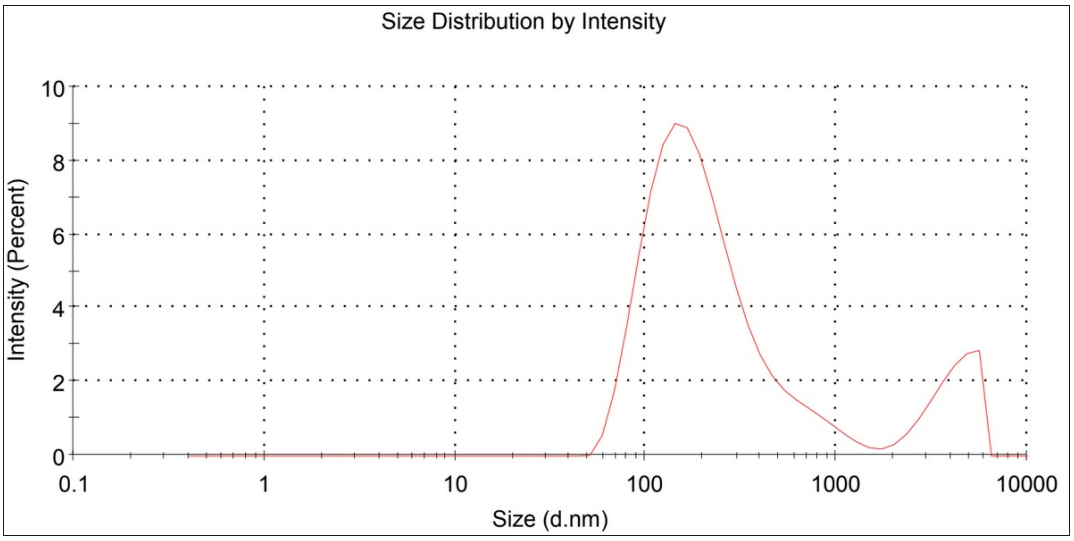

Figure A.14: Second reading of size distribution by intensity for loaded micelles created with the sonification method for 3 kDa, second iteration of the triplicates, done by the DLS software done with attenuation factor 6. A table with information on peaks, intensity and standard deviation can be seen in Appendix B as readings 1.3.1.2 - 2

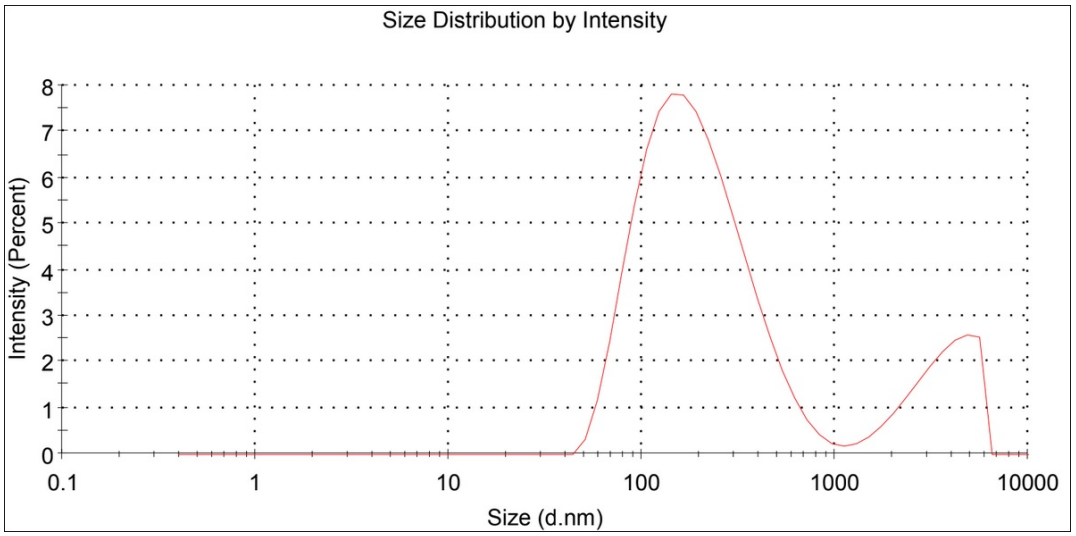

Figure A.15: Third reading of size distribution by intensity for loaded micelles created with the sonification method for 3 kDa, second iteration of the triplicates, done by the DLS software done with attenuation factor 6. A table with information on peaks, intensity and standard deviation can be seen in Appendix B as readings 1.3.1.2 - 3

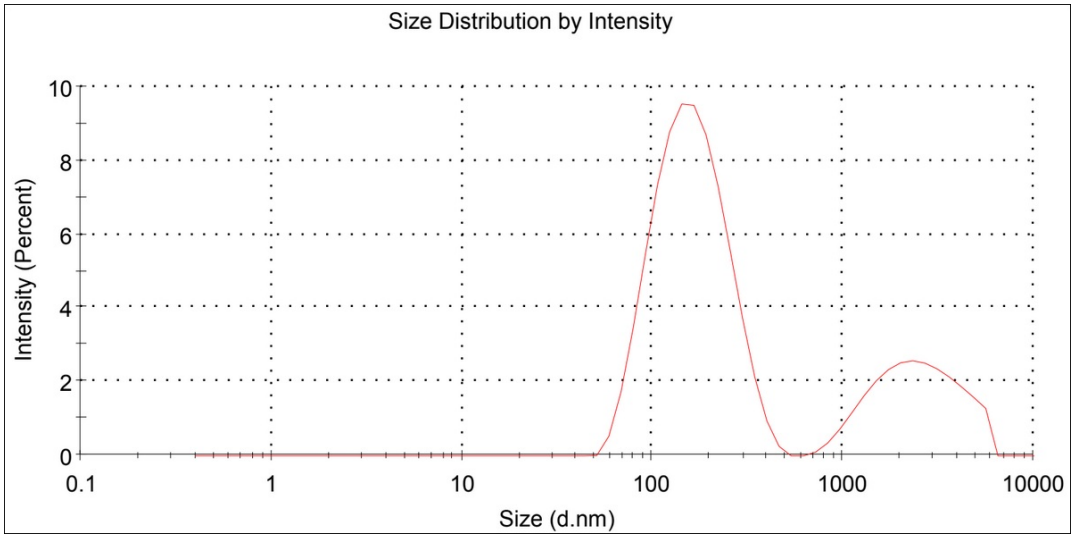

Figure A.16: First reading of size distribution by intensity for loaded micelles created with the sonification method for 3 kDa, third iteration of the triplicates, done by the DLS software done with attenuation factor 5. A table with information on peaks, intensity and standard deviation can be seen in Appendix B as readings 1.3.1.3 - 1

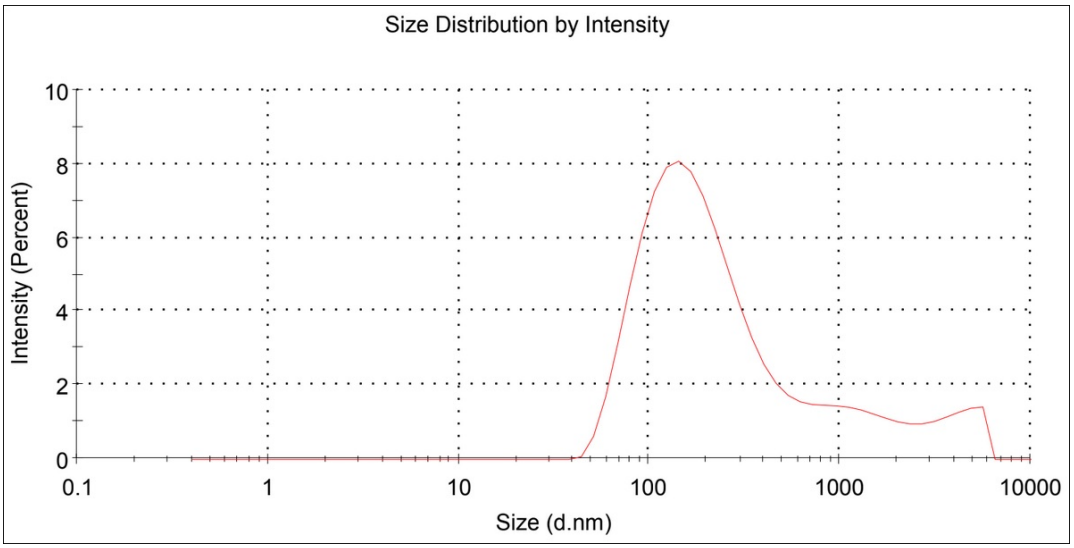

Figure A.17: Second reading of size distribution by intensity for loaded micelles created with the sonification method for 3 kDa, third iteration of the triplicates, done by the DLS software done with attenuation factor 5. A table with information on peaks, intensity and standard deviation can be seen in Appendix B as readings 1.3.1.3 - 2

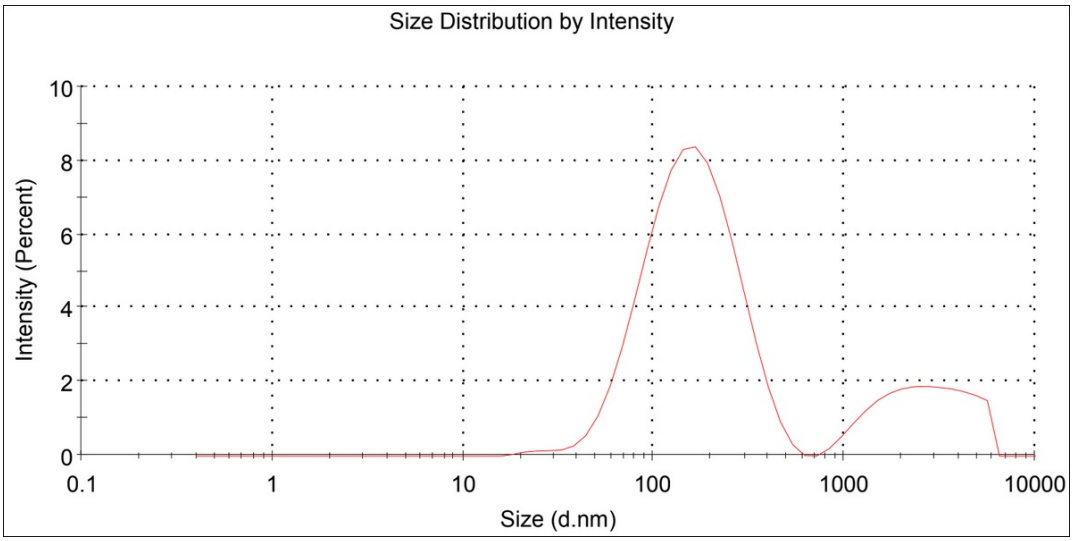

Figure A.18: Third reading of size distribution by intensity for loaded micelles created with the sonification method for 3 kDa, third iteration of the triplicates, done by the DLS software done with attenuation factor 5. A table with information on peaks, intensity and standard deviation can be seen in Appendix B as readings 1.3.1.3 - 3

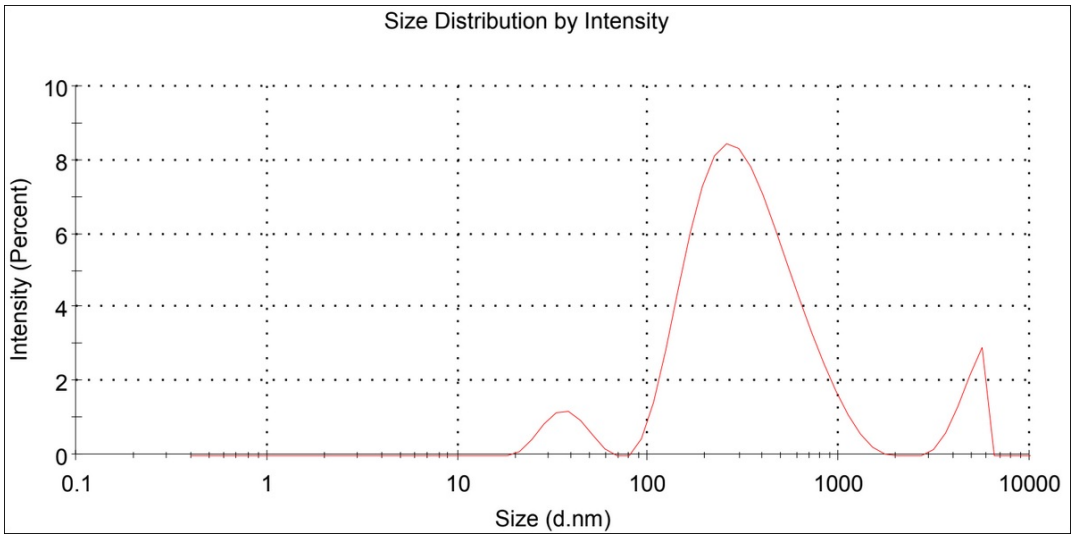

Figure A.19: First reading of size distribution by intensity for empty micelles created with the co-solvent evaporation method for 3 kDa, first iteration of the triplicates, done by the DLS software done with attenuation factor 7. A table with information on peaks, intensity and standard deviation can be seen in Appendix B as readings 2.3.0.1 - 1

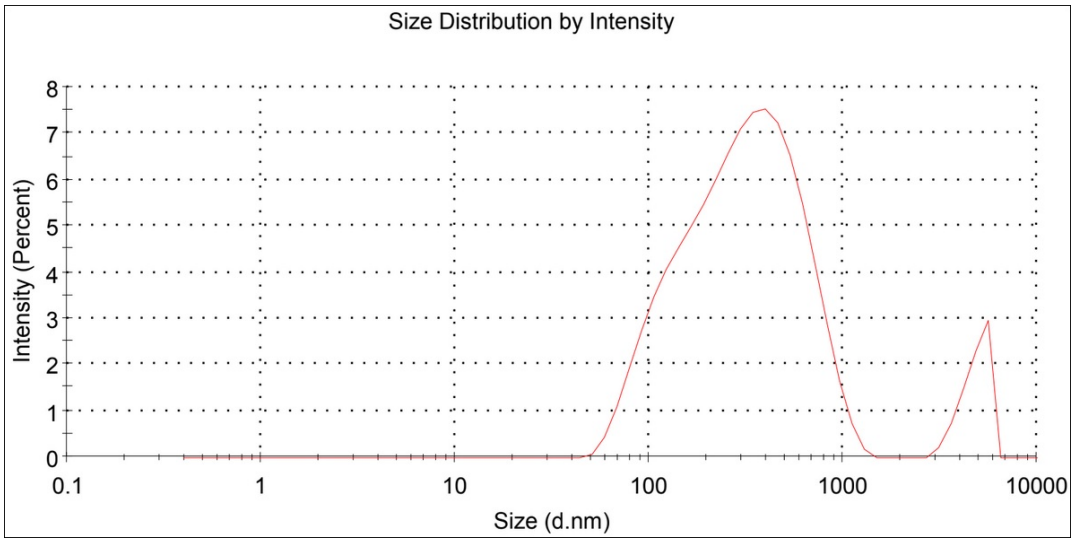

Figure A.20: Second reading of size distribution by intensity for empty micelles created with the co-solvent evaporation method for 3 kDa, first iteration of the triplicates, done by the DLS software done with attenuation factor 7. A table with information on peaks, intensity and standard deviation can be seen in Appendix B as readings 2.3.0.1 - 2

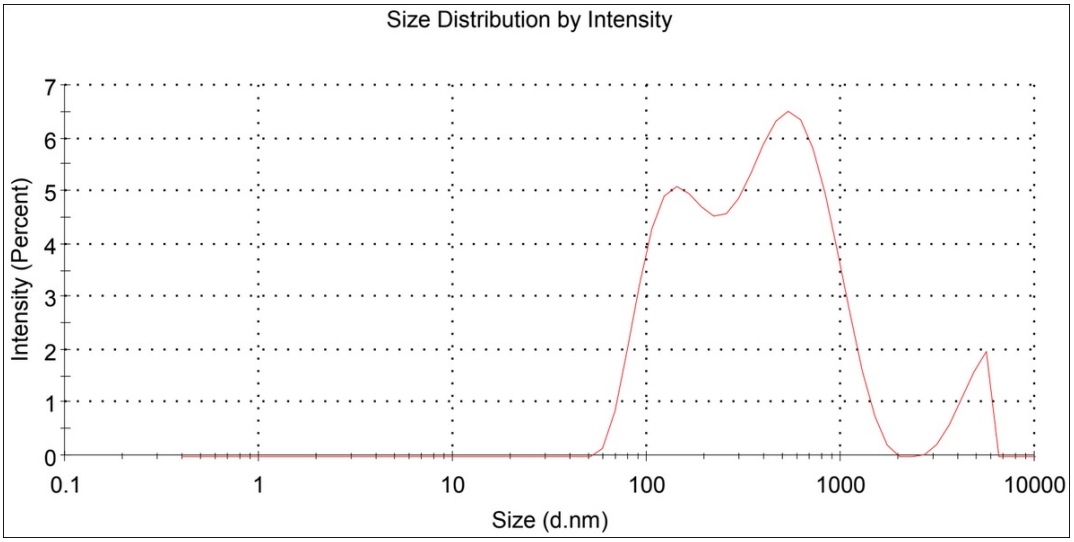

Figure A.21: Third reading of size distribution by intensity for empty micelles created with the co-solvent evaporation method for 3 kDa, first iteration of the triplicates, done by the DLS software done with attenuation factor 7. A table with information on peaks, intensity and standard deviation can be seen in Appendix B as readings 2.3.0.1 - 3

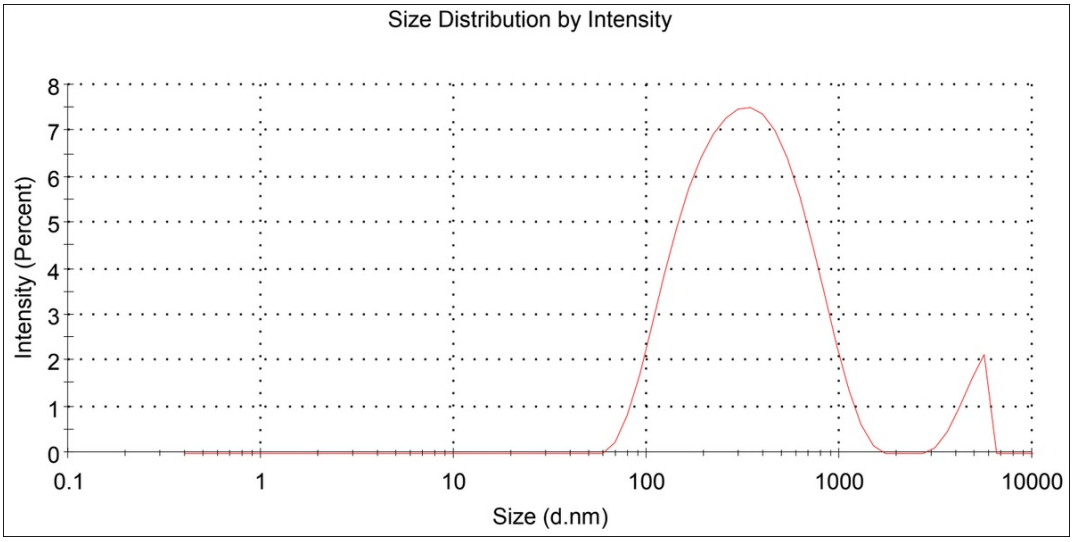

Figure A.22: First reading of size distribution by intensity for empty micelles created with the co-solvent evaporation method for 3 kDa, second iteration of the triplicates, done by the DLS software done with attenuation factor 7. A table with information on peaks, intensity and standard deviation can be seen in Appendix B as readings 2.3.0.2 - 1

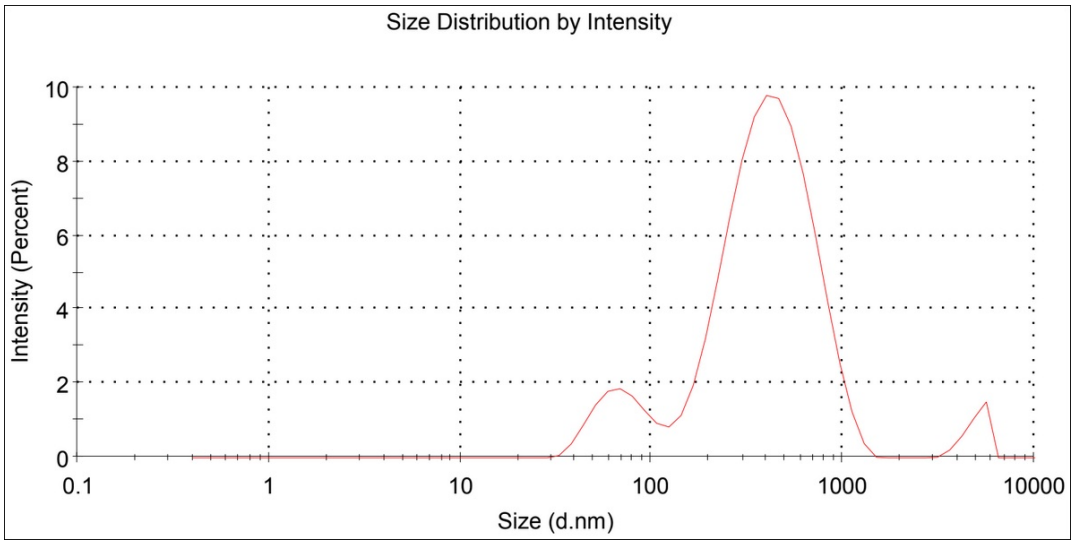

Figure A.23: Second reading of size distribution by intensity for empty micelles created with the co-solvent evaporation method for 3 kDa, second iteration of the triplicates, done by the DLS software done with attenuation factor 7. A table with information on peaks, intensity and standard deviation can be seen in Appendix B as readings 2.3.0.2 - 2

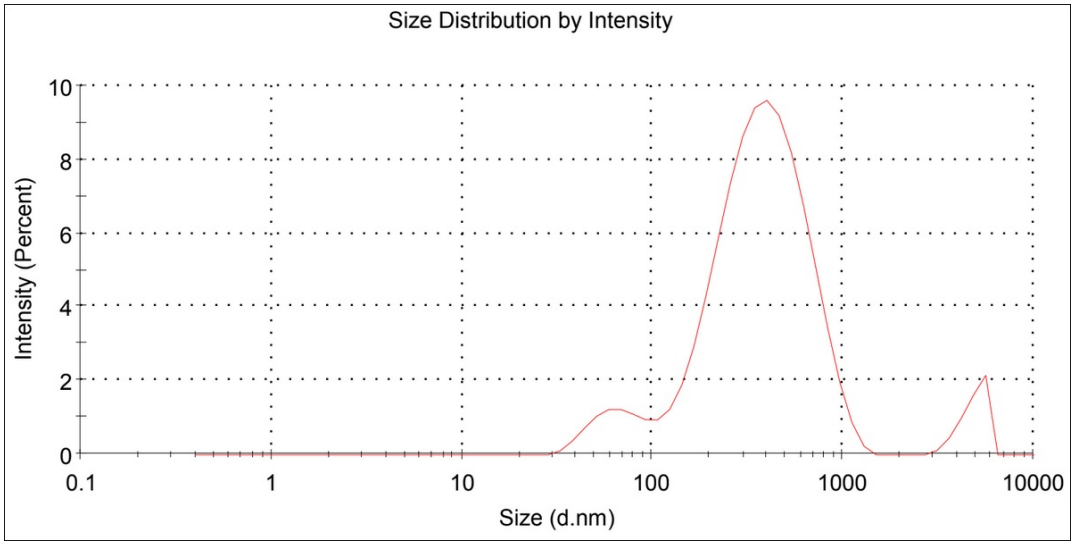

Figure A.24: Third reading of size distribution by intensity for empty micelles created with the co-solvent evaporation method for 3 kDa, second iteration of the triplicates, done by the DLS software done with attenuation factor 7. A table with information on peaks, intensity and standard deviation can be seen in Appendix B as readings 2.3.0.2 - 3

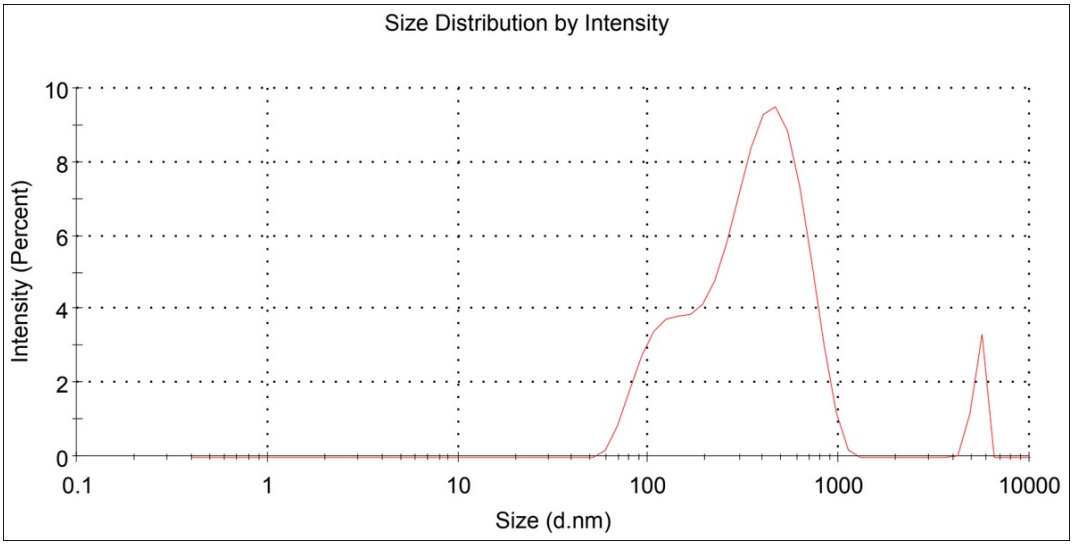

Figure A.25: First reading of size distribution by intensity for empty micelles created with the co-solvent evaporation method for 3 kDa, third iteration of the triplicates, done by the DLS software done with attenuation factor 6. A table with information on peaks, intensity and standard deviation can be seen in Appendix B as readings 2.3.0.3 - 1

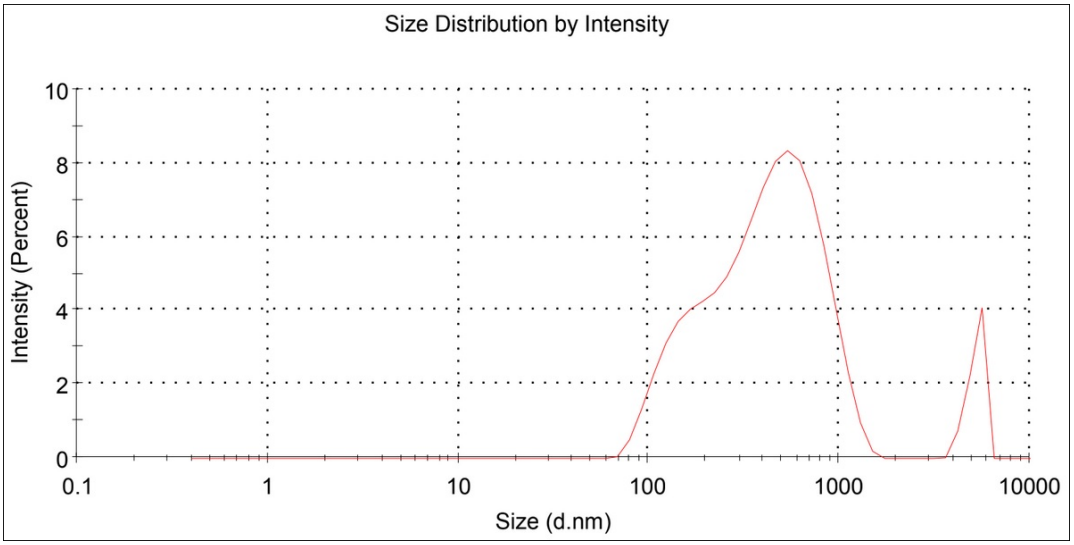

Figure A.26: Second reading of size distribution by intensity for empty micelles created with the co-solvent evaporation method for 3 kDa, third iteration of the triplicates, done by the DLS software done with attenuation factor 6. A table with information on peaks, intensity and standard deviation can be seen in Appendix B as readings 2.3.0.3 - 2

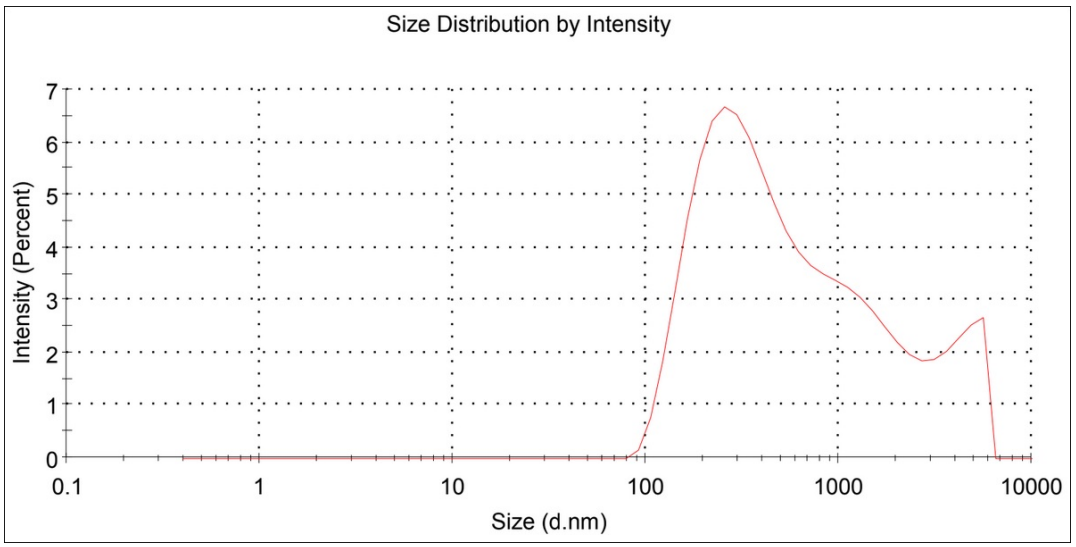

Figure A.27: Third reading of size distribution by intensity for empty micelles created with the co-solvent evaporation method for 3 kDa, third iteration of the triplicates, done by the DLS software done with attenuation factor 6. A table with information on peaks, intensity and standard deviation can be seen in Appendix B as readings 2.3.0.3 - 3

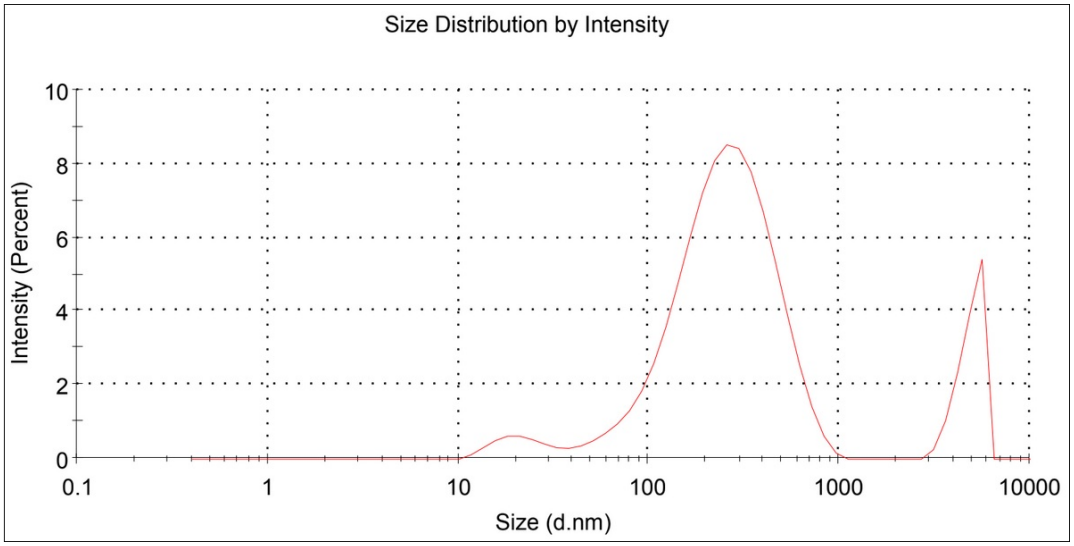

Figure A.28: First reading of size distribution by intensity for loaded micelles created with the co-solvent evaporation method for 3 kDa, first iteration of the triplicates, done by the DLS software done with attenuation factor 8. A table with information on peaks, intensity and standard deviation can be seen in Appendix B as readings 2.3.1.1 - 1

A.2 6 kDa polymeric micelles

A.2.1 Sonification method

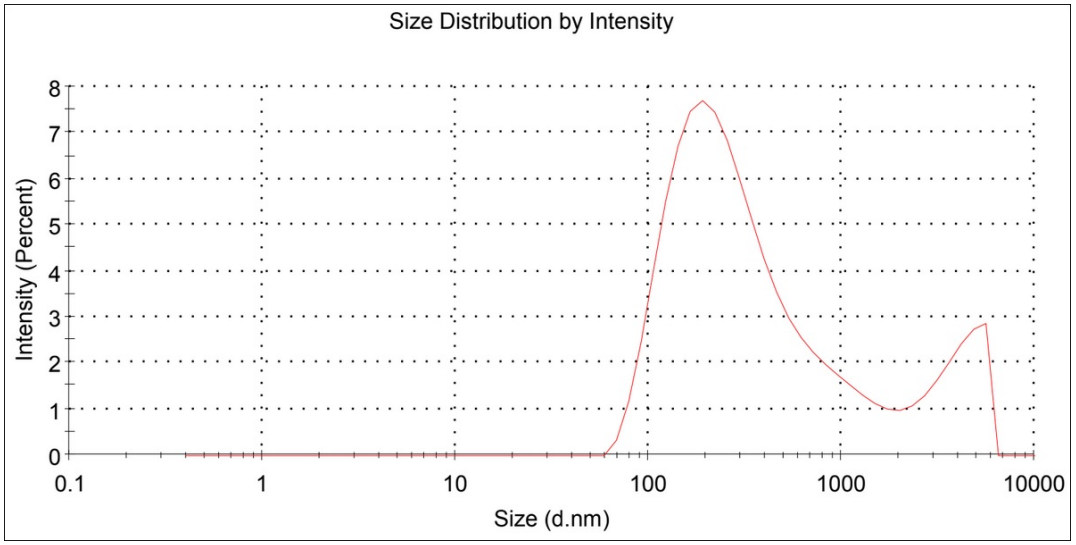

Figure A.29: Second reading of size distribution by intensity for loaded micelles created with the co-solvent evaporation method for 3 kDa, first iteration of the triplicates, done by the DLS software done with attenuation factor 8. A table with information on peaks, intensity and standard deviation can be seen in Appendix B as readings 2.3.1.1 - 2

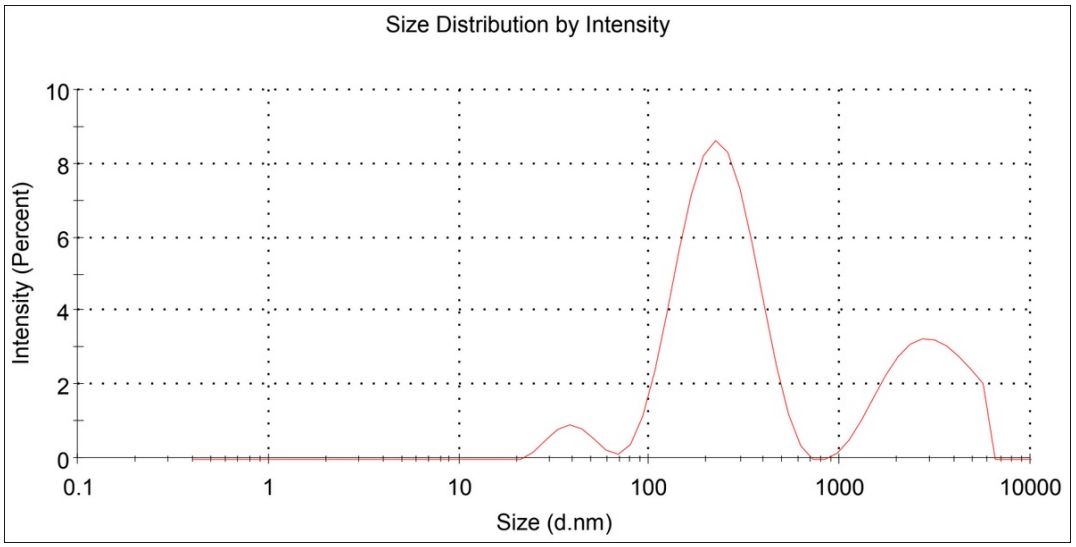

Figure A.30: Third reading of size distribution by intensity for loaded micelles created with the co-solvent evaporation method for 3 kDa, first iteration of the triplicates, done by the DLS software done with attenuation factor 8. A table with information on peaks, intensity and standard deviation can be seen in Appendix B as readings 2.3.1.1 - 3

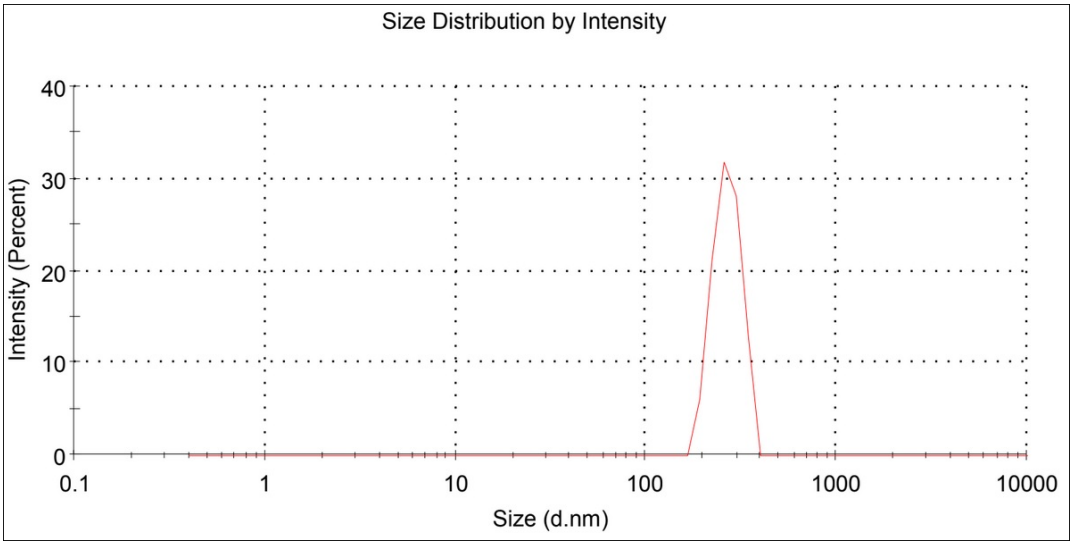

Figure A.31: First reading of size distribution by intensity for loaded micelles created with the co-solvent evaporation method for 3 kDa, second iteration of the triplicates, done by the DLS software done with attenuation factor 9. A table with information on peaks, intensity and standard deviation can be seen in Appendix B as readings 2.3.1.2 - 1

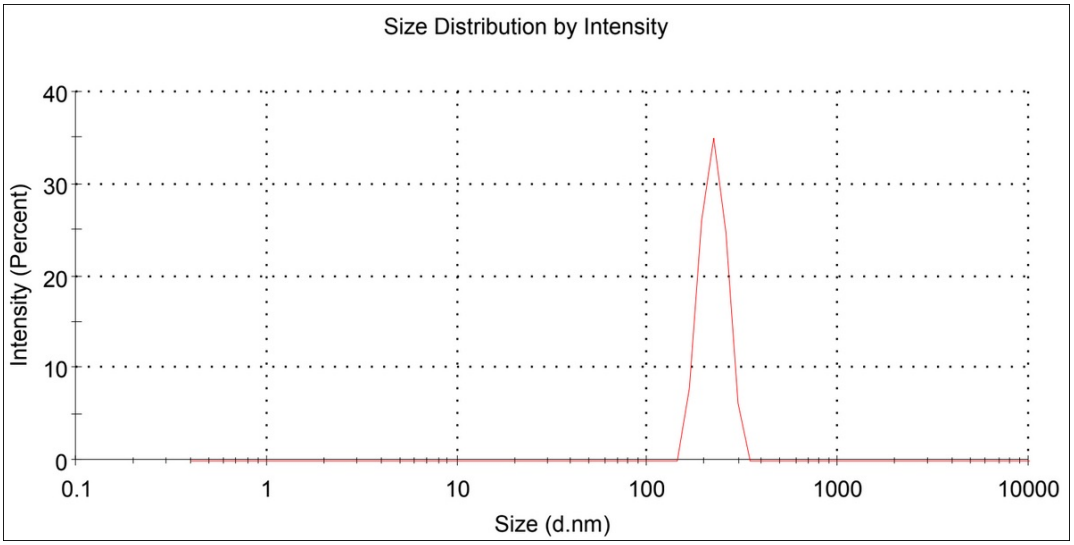

Figure A.32: Second reading of size distribution by intensity for loaded micelles created with the co-solvent evaporation method for 3 kDa, second iteration of the triplicates, done by the DLS software done with attenuation factor 9. A table with information on peaks, intensity and standard deviation can be seen in Appendix B as readings 2.3.1.2 - 2

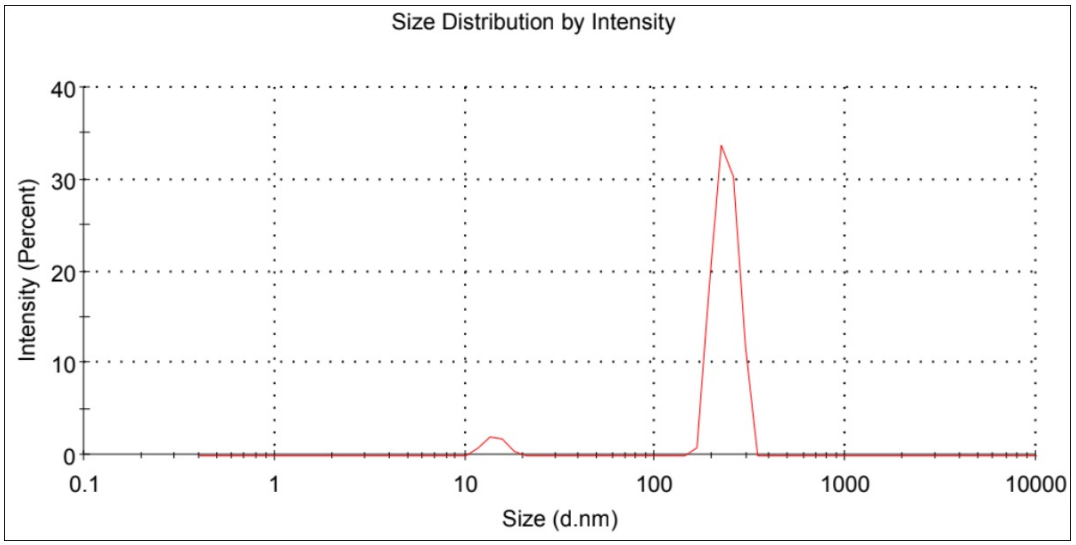

Figure A.33: Third reading of size distribution by intensity for loaded micelles created with the co-solvent evaporation method for 3 kDa, second iteration of the triplicates, done by the DLS software done with attenuation factor 9. A table with information on peaks, intensity and standard deviation can be seen in Appendix B as readings 2.3.1.2 - 3

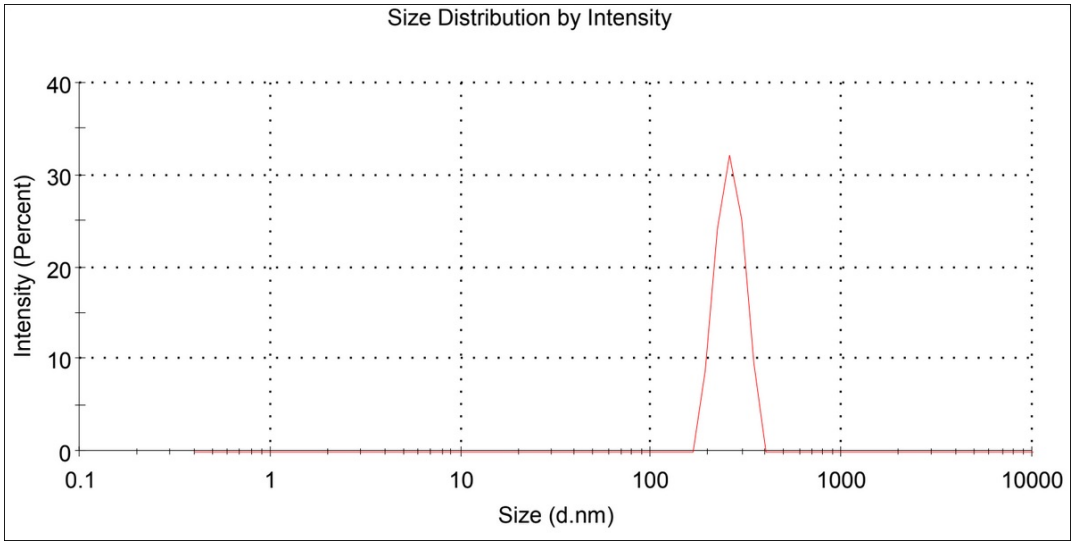

Figure A.34: First reading of size distribution by intensity for loaded micelles created with the co-solvent evaporation method for 3 kDa, third iteration of the triplicates, done by the DLS software done with attenuation factor 9. A table with information on peaks, intensity and standard deviation can be seen in Appendix B as readings 2.3.1.3 - 1

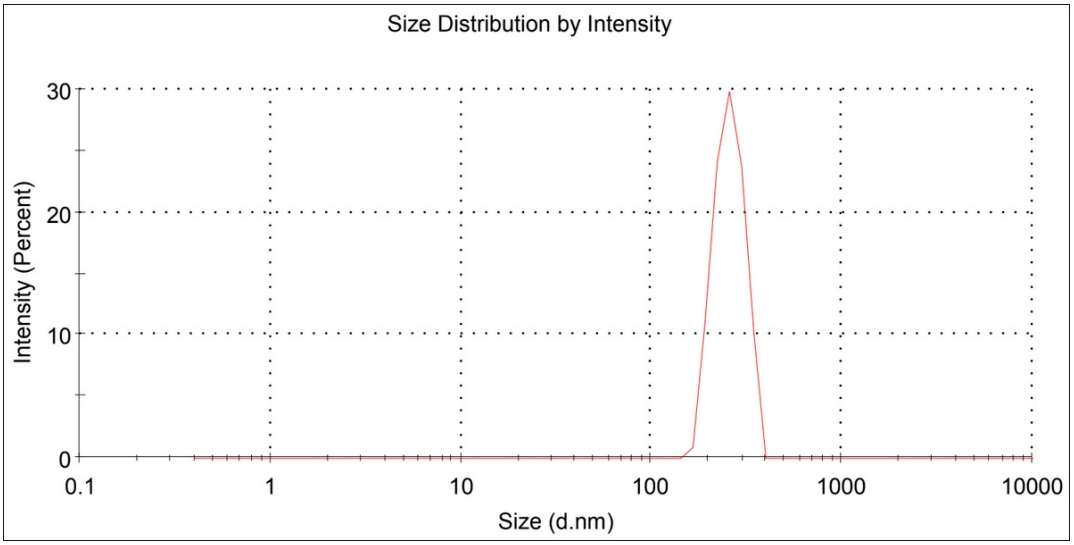

Figure A.35: Second reading of size distribution by intensity for loaded micelles created with the co-solvent evaporation method for 3 kDa, third iteration of the triplicates, done by the DLS software done with attenuation factor 9. A table with information on peaks, intensity and standard deviation can be seen in Appendix B as readings 2.3.1.3 - 2

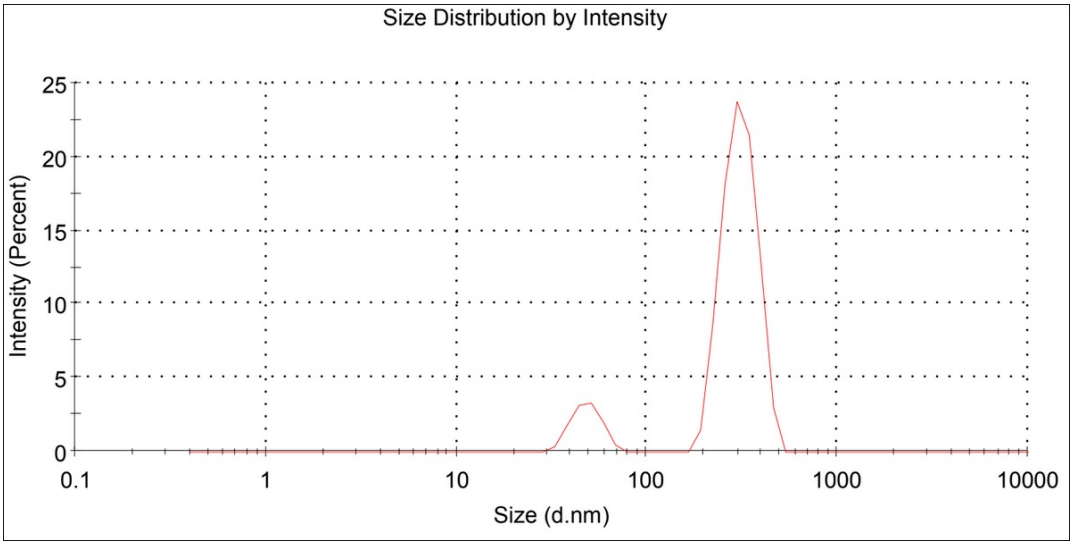

Figure A.36: Third reading of size distribution by intensity for loaded micelles created with the co-solvent evaporation method for 3 kDa, third iteration of the triplicates, done by the DLS software done with attenuation factor 9. A table with information on peaks, intensity and standard deviation can be seen in Appendix B as readings 2.3.1.3 - 3

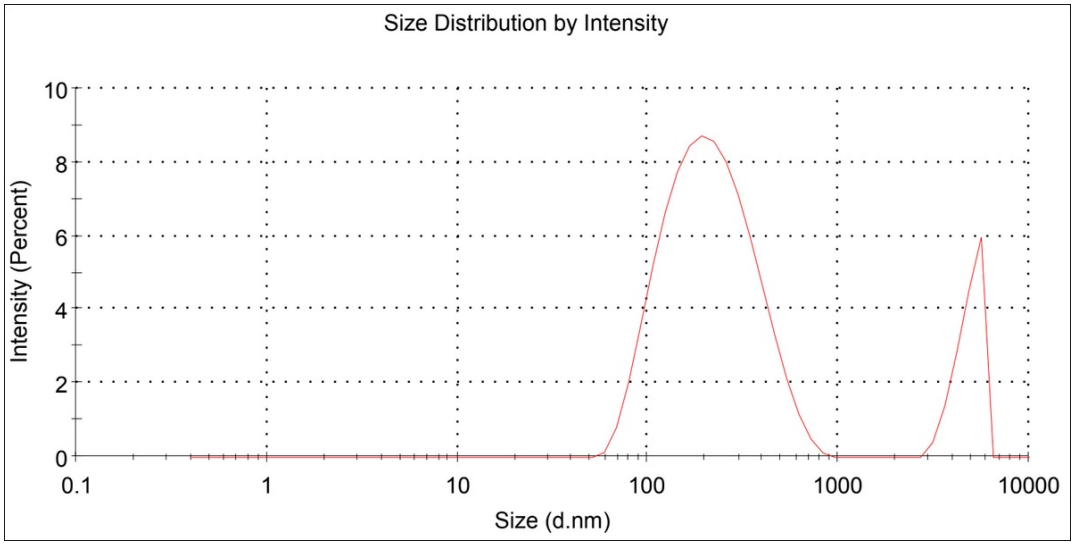

Figure A.37: First reading of size distribution by intensity for empty micelles created with the sonification method for 6 kDa, first iteration of the triplicates, done by the DLS software done with attenuation factor 6. A table with information on peaks, intensity and standard deviation can be seen in Appendix B as readings 1.6.0.1 - 1

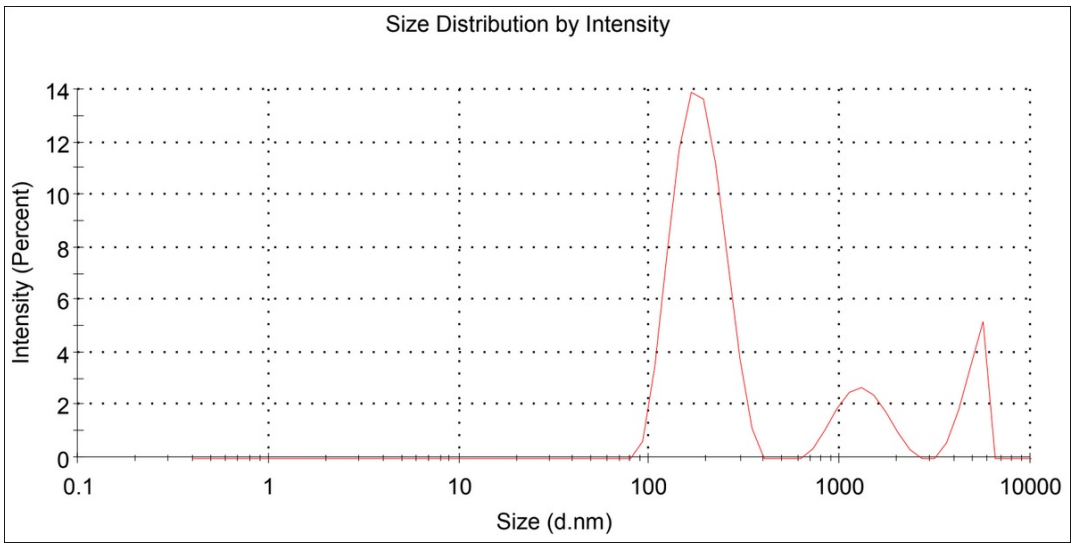

Figure A.38: Second reading of size distribution by intensity for empty micelles created with the sonification method for 6 kDa, first iteration of the triplicates, done by the DLS software done with attenuation factor 6. A table with information on peaks, intensity and standard deviation can be seen in Appendix B as readings 1.6.0.1 - 2

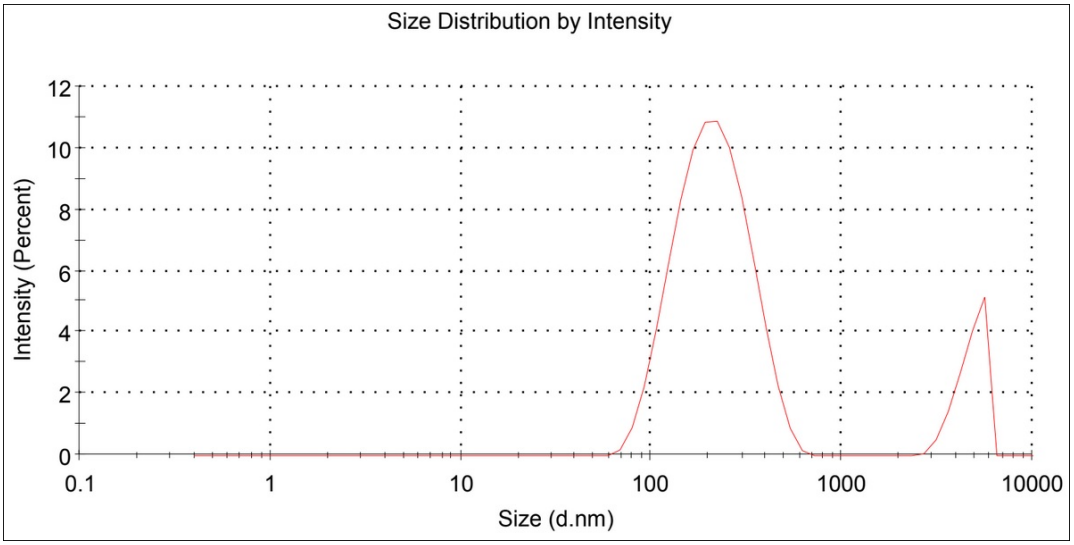

Figure A.39: Third reading of size distribution by intensity for empty micelles created with the sonification method for 6 kDa, first iteration of the triplicates, done by the DLS software done with attenuation factor 6. A table with information on peaks, intensity and standard deviation can be seen in Appendix B as readings 1.6.0.1 - 3

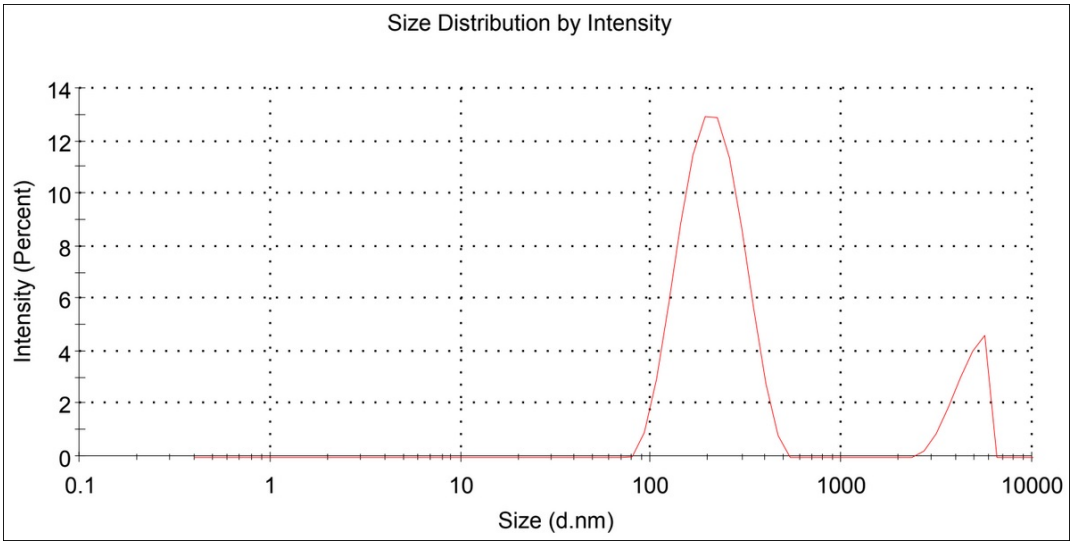

Figure A.40: First reading of size distribution by intensity for empty micelles created with the sonification method for 6 kDa, second iteration of the triplicates, done by the DLS software done with attenuation factor 6. A table with information on peaks, intensity and standard deviation can be seen in Appendix B as readings 1.6.0.2 - 1

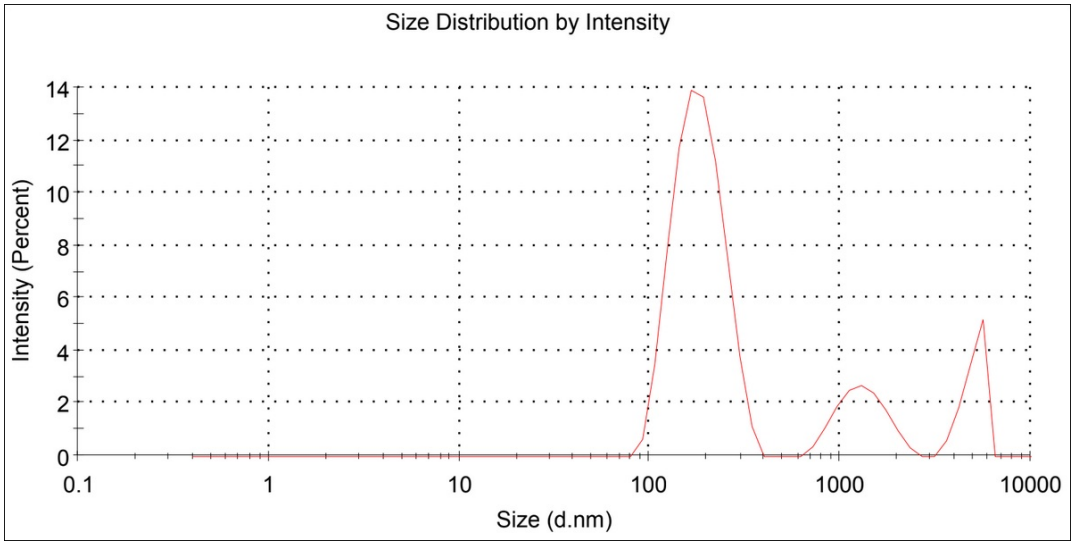

Figure A.41: Second reading of size distribution by intensity for empty micelles created with the sonification method for 6 kDa, second iteration of the triplicates, done by the DLS software done with attenuation factor 6. A table with information on peaks, intensity and standard deviation can be seen in Appendix B as readings 1.6.0.2 - 2

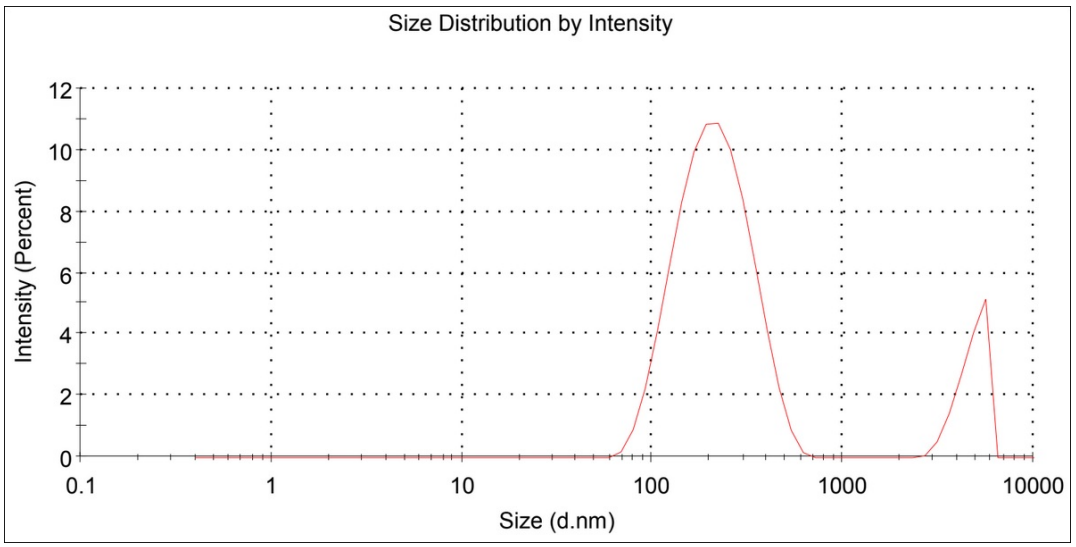

Figure A.42: Third reading of size distribution by intensity for empty micelles created with the sonification method for 6 kDa, second iteration of the triplicates, done by the DLS software done with attenuation factor 6. A table with information on peaks, intensity and standard deviation can be seen in Appendix B as readings 1.6.0.2 - 3

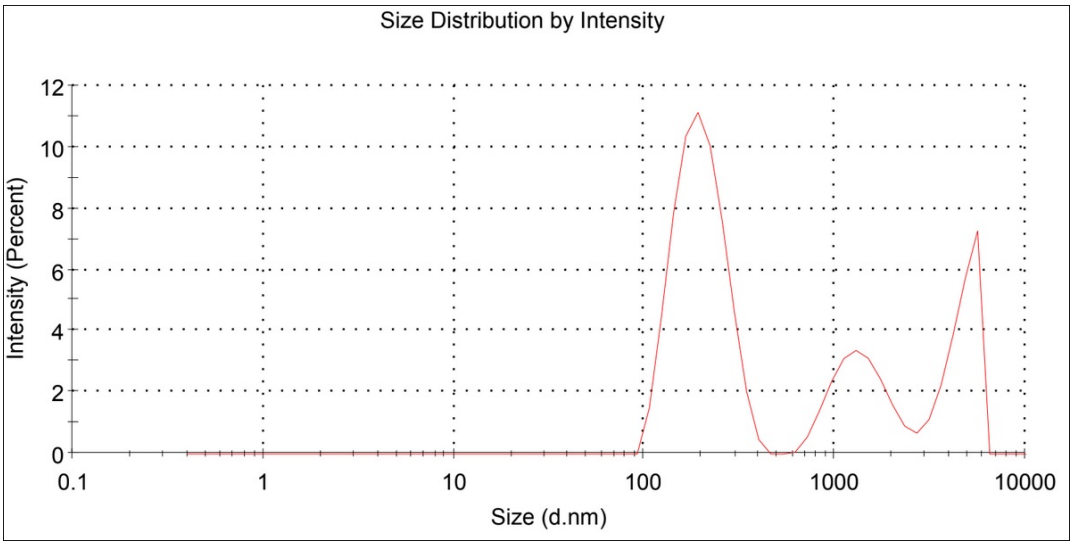

Figure A.43: First reading of size distribution by intensity for empty micelles created with the sonification method for 6 kDa, third iteration of the triplicates, done by the DLS software done with attenuation factor 6. A table with information on peaks, intensity and standard deviation can be seen in Appendix B as readings 1.6.0.3 - 1

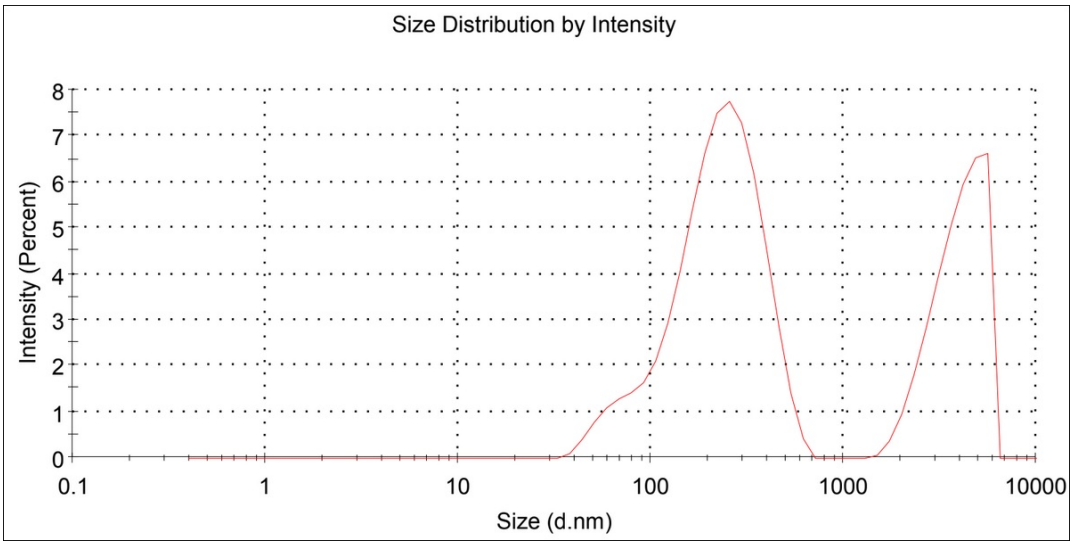

Figure A.44: Second reading of size distribution by intensity for empty micelles created with the sonification method for 6 kDa, third iteration of the triplicates, done by the DLS software done with attenuation factor 6. A table with information on peaks, intensity and standard deviation can be seen in Appendix B as readings 1.6.0.3 - 2

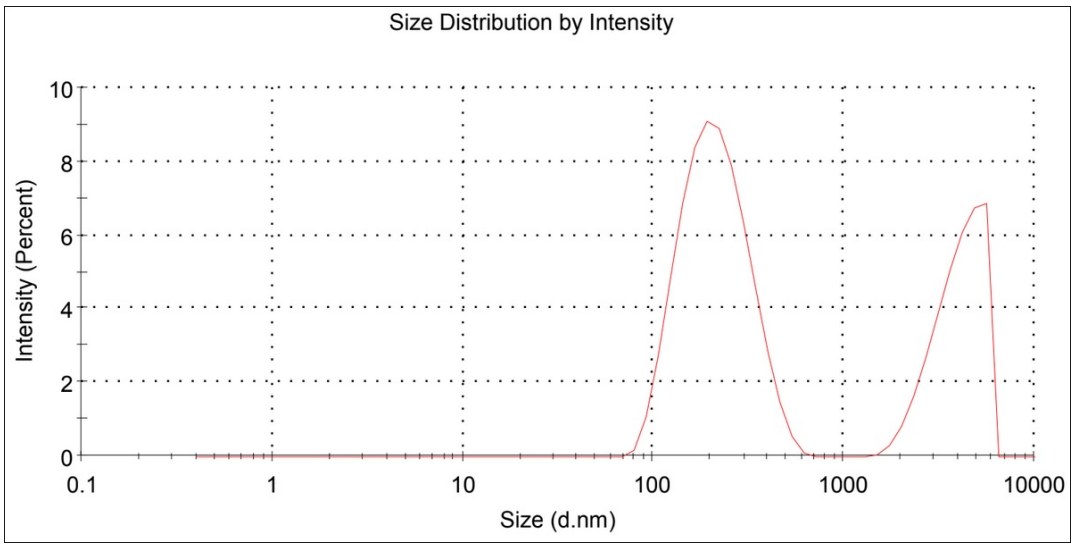

Figure A.45: Third reading of size distribution by intensity for empty micelles created with the sonification method for 6 kDa, third iteration of the triplicates, done by the DLS software done with attenuation factor 6. A table with information on peaks, intensity and standard deviation can be seen in Appendix B as readings 1.6.0.3 - 3

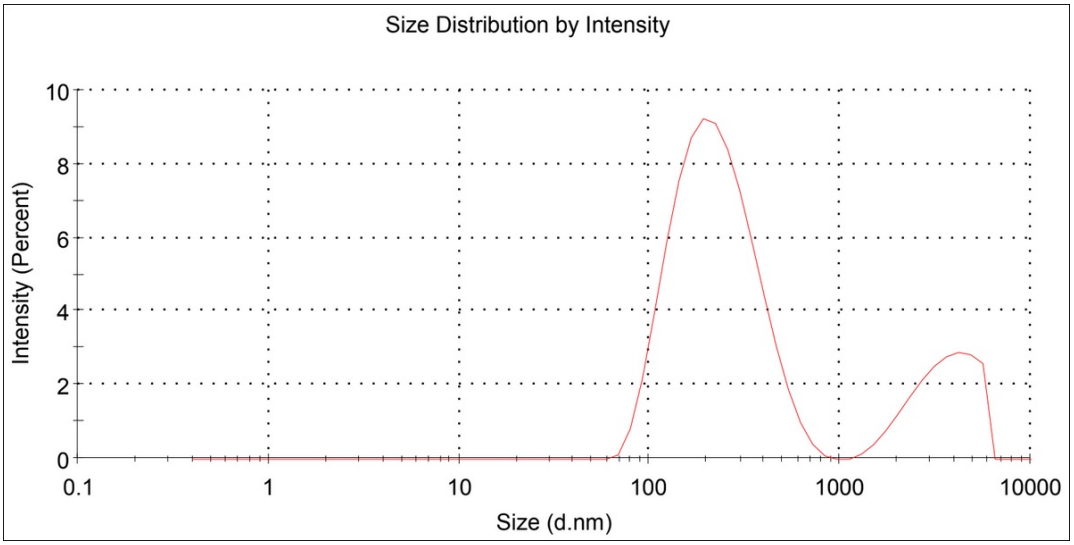

Figure A.46: First reading of size distribution by intensity for loaded micelles created with the sonification method for 6 kDa, first iteration of the triplicates, done by the DLS software done with attenuation factor 5. A table with information on peaks, intensity and standard deviation can be seen in Appendix B as readings 1.6.1.1 - 1

A.2.2 Co-solvent evaporation method

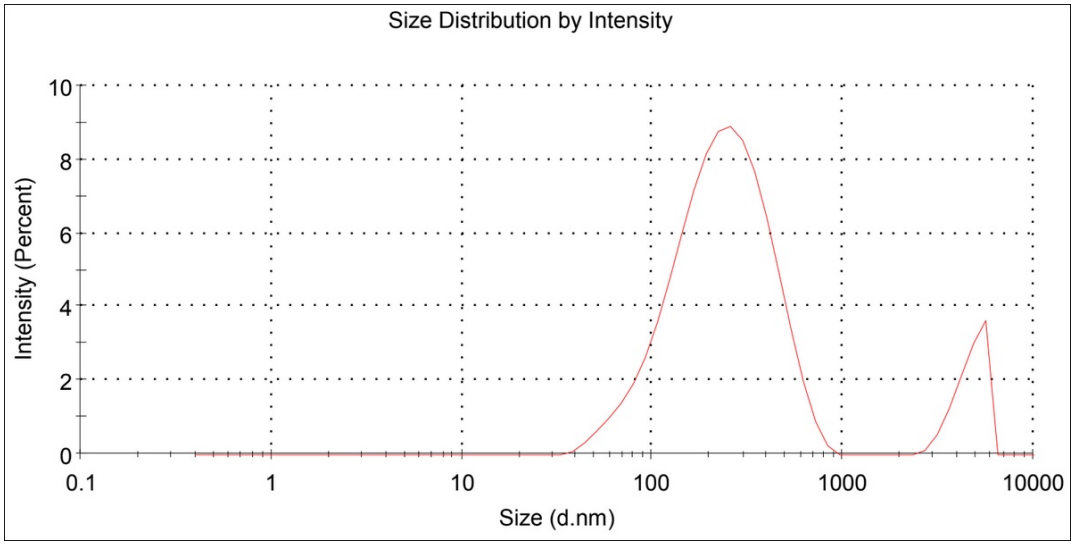

Figure A.47: Second reading of size distribution by intensity for loaded micelles created with the sonification method for 6 kDa, first iteration of the triplicates, done by the DLS software done with attenuation factor 6. A table with information on peaks, intensity and standard deviation can be seen in Appendix B as readings 1.6.1.1 - 2

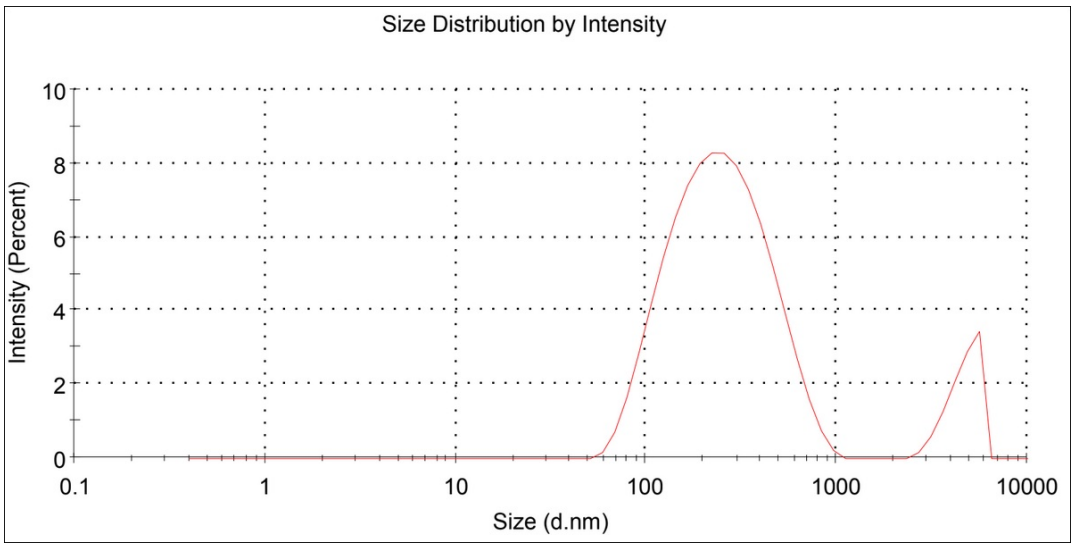

Figure A.48: Third reading of size distribution by intensity for loaded micelles created with the sonification method for 6 kDa, first iteration of the triplicates, done by the DLS software done with attenuation factor 6. A table with information on peaks, intensity and standard deviation can be seen in Appendix B as readings 1.6.1.1 - 3

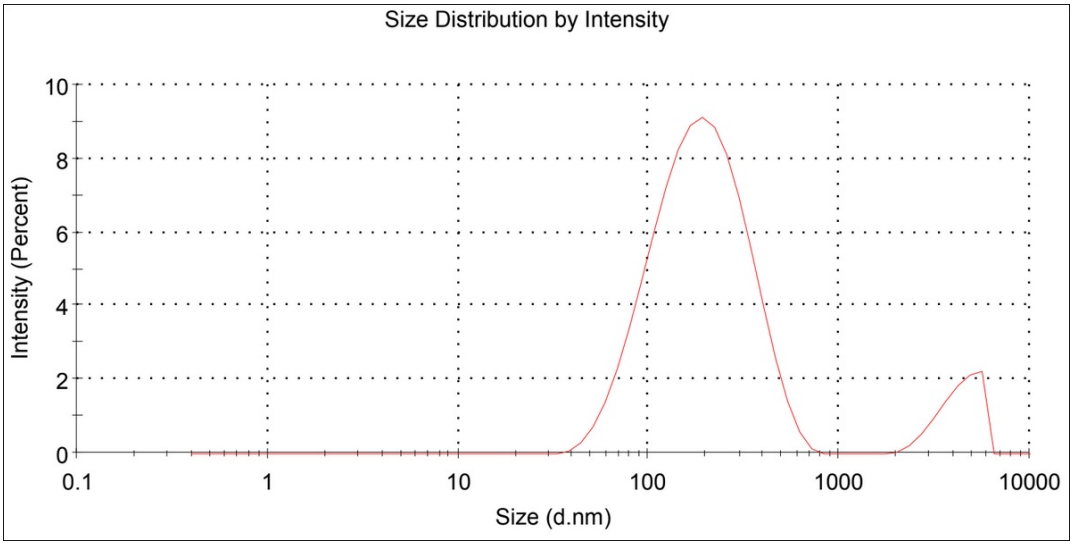

Figure A.49: First reading of size distribution by intensity for loaded micelles created with the sonification method for 6 kDa, second iteration of the triplicates, done by the DLS software done with attenuation factor 6. A table with information on peaks, intensity and standard deviation can be seen in Appendix B as readings 1.6.1.2 - 1

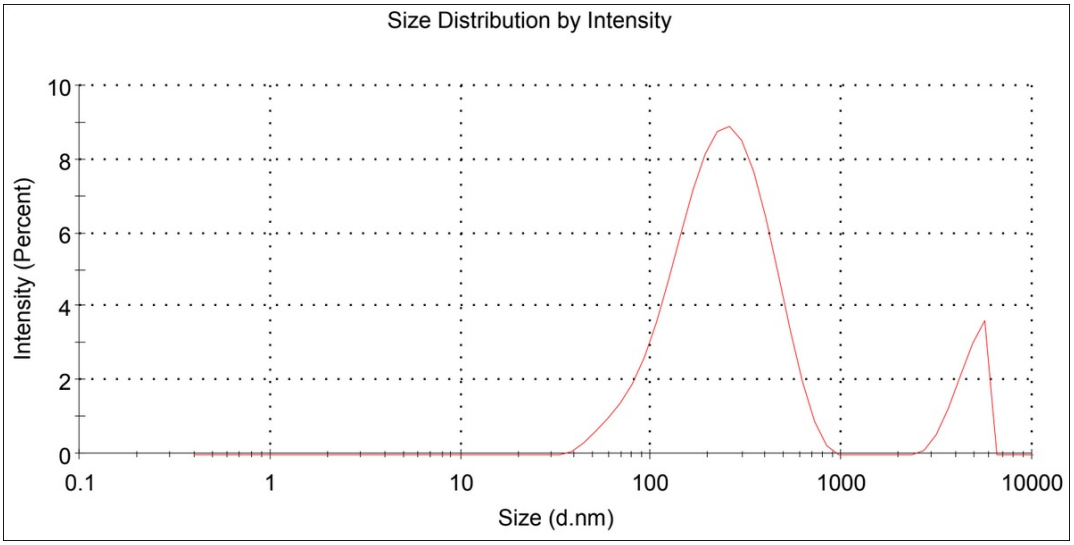

Figure A.50: Second reading of size distribution by intensity for loaded micelles created with the sonification method for 6 kDa, second iteration of the triplicates, done by the DLS software done with attenuation factor 6. A table with information on peaks, intensity and standard deviation can be seen in Appendix B as readings 1.6.1.2 - 2

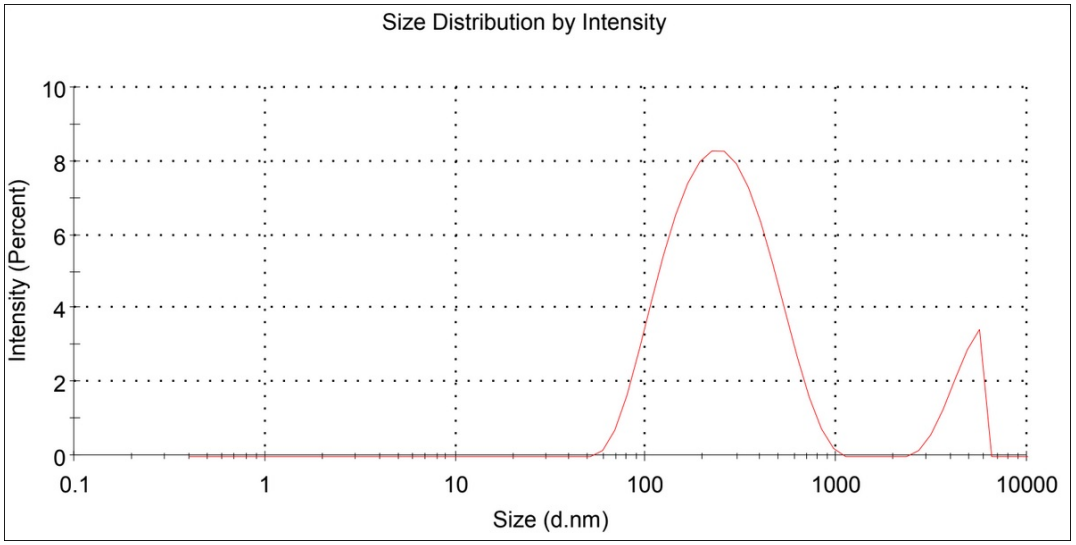

Figure A.51: Third reading of size distribution by intensity for loaded micelles created with the sonification method for 6 kDa, second iteration of the triplicates, done by the DLS software done with attenuation factor 6. A table with information on peaks, intensity and standard deviation can be seen in Appendix B as readings 1.6.1.2 - 3

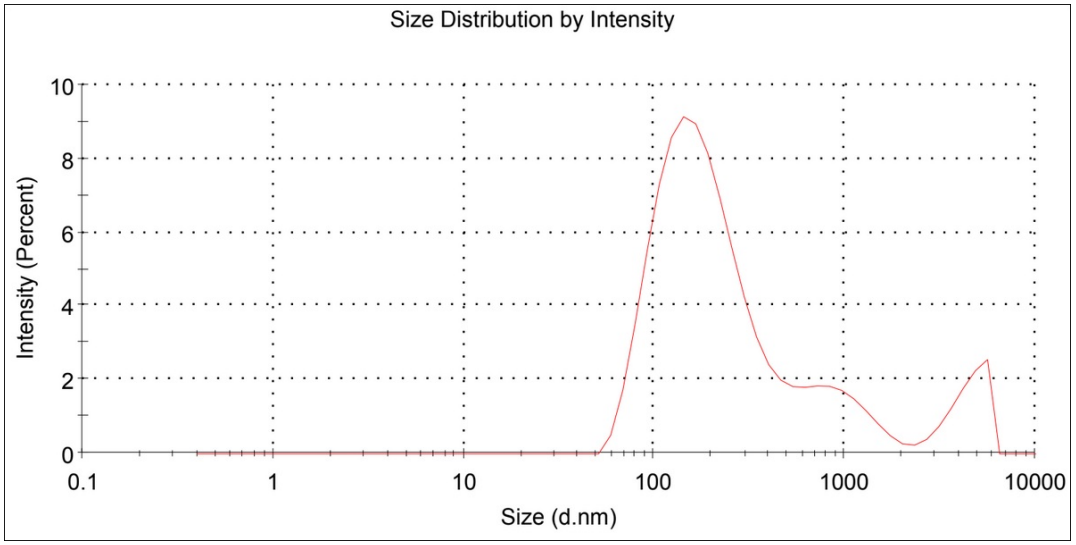

Figure A.52: First reading of size distribution by intensity for loaded micelles created with the sonification method for 6 kDa, third iteration of the triplicates, done by the DLS software done with attenuation factor 6. A table with information on peaks, intensity and standard deviation can be seen in Appendix B as readings 1.6.1.3 - 1

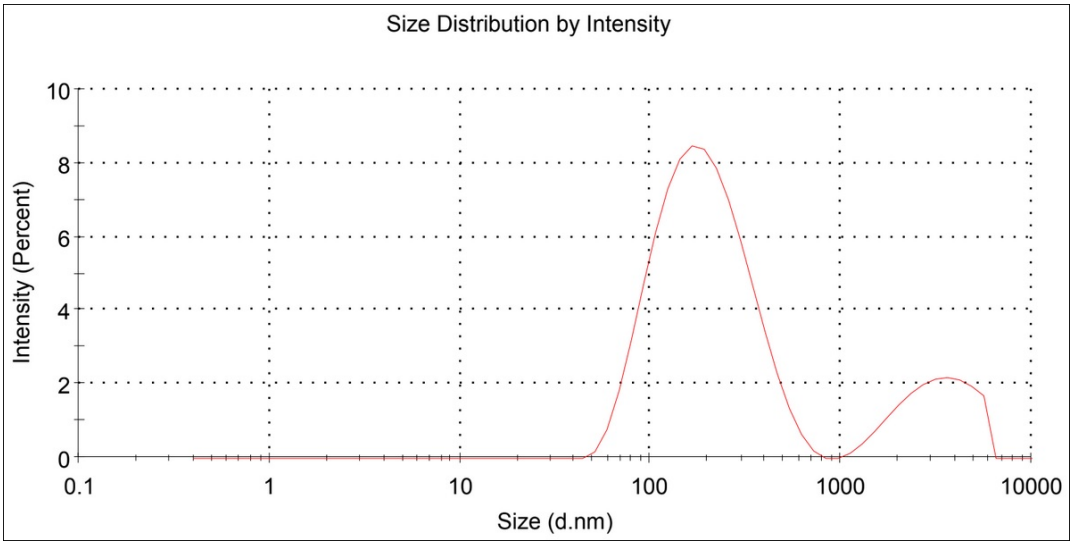

Figure A.53: Second reading of size distribution by intensity for loaded micelles created with the sonification method for 6 kDa, third iteration of the triplicates, done by the DLS software done with attenuation factor 6. A table with information on peaks, intensity and standard deviation can be seen in Appendix B as readings 1.6.1.3 - 2

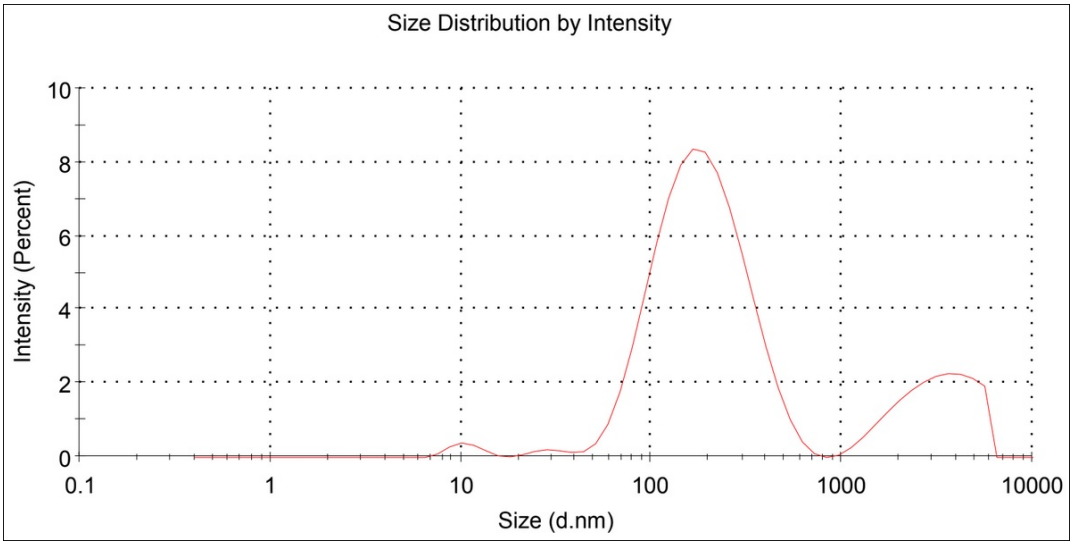

Figure A.54: Third reading of size distribution by intensity for loaded micelles created with the sonification method for 6 kDa, third iteration of the triplicates, done by the DLS software done with attenuation factor 6. A table with information on peaks, intensity and standard deviation can be seen in Appendix B as readings 1.6.1.3 - 3

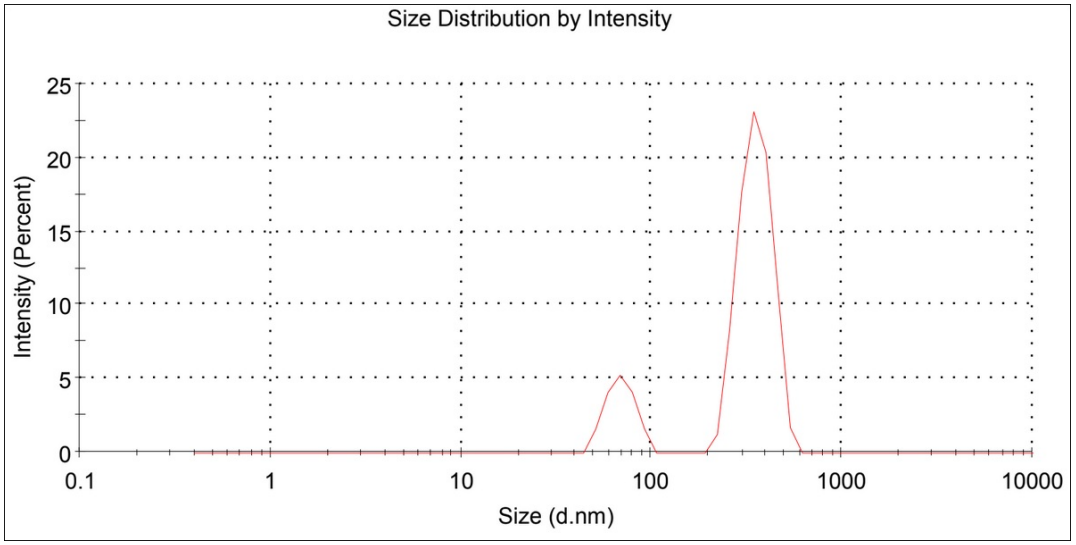

Figure A.55: First reading of size distribution by intensity for empty micelles created with the co-solvent evaporation method for 6 kDa, first iteration of the triplicates, done by the DLS software done with attenuation factor 7. A table with information on peaks, intensity and standard deviation can be seen in Appendix B as readings 2.6.0.1 - 1

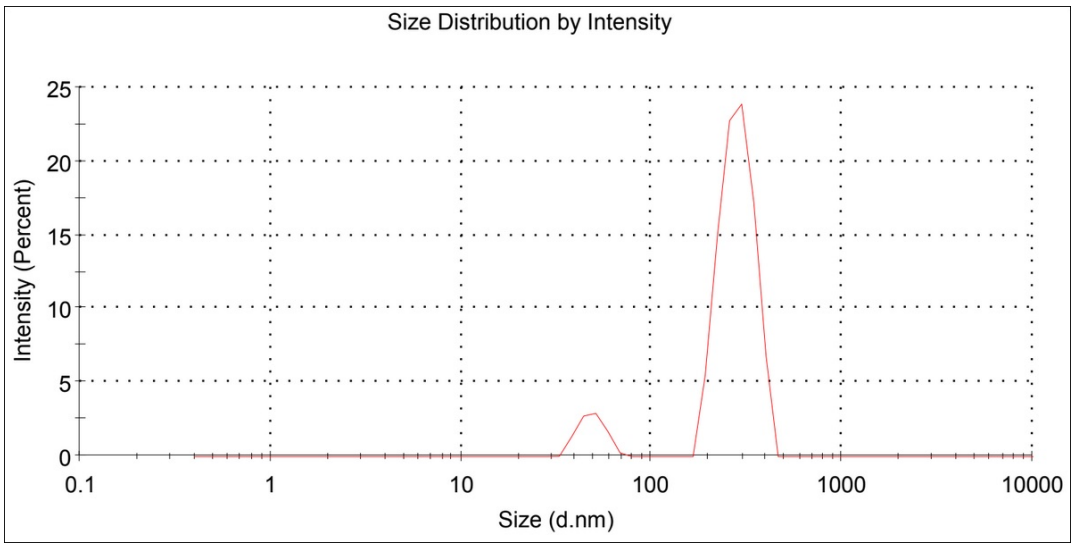

Figure A.56: Second reading of size distribution by intensity for empty micelles created with the co-solvent evaporation method for 6 kDa, first iteration of the triplicates, done by the DLS software done with attenuation factor 8. A table with information on peaks, intensity and standard deviation can be seen in Appendix B as readings 2.6.0.1 - 2

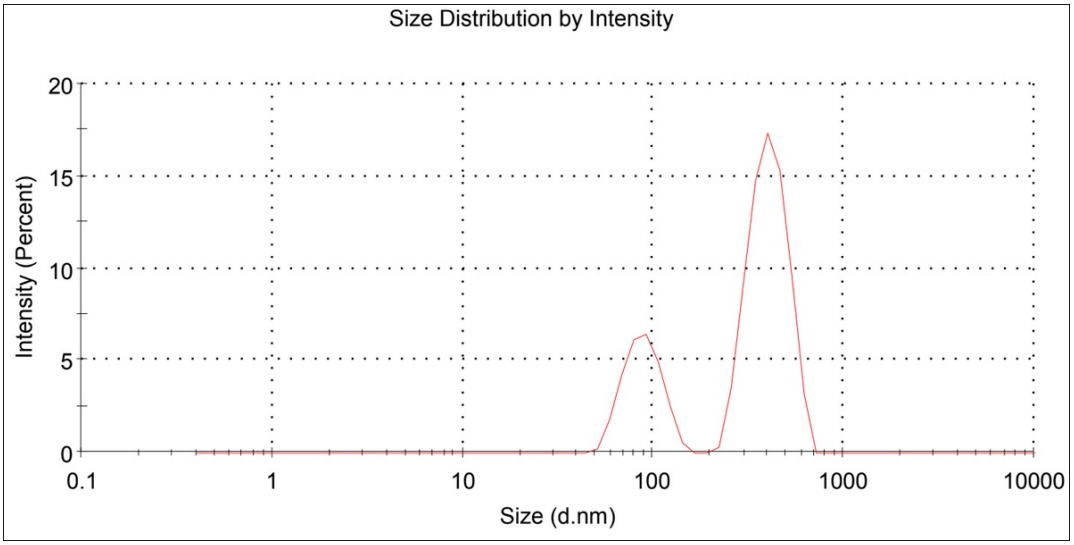

Figure A.57: Third reading of size distribution by intensity for empty micelles created with the co-solvent evaporation method for 6 kDa, first iteration of the triplicates, done by the DLS software done with attenuation factor 8. A table with information on peaks, intensity and standard deviation can be seen in Appendix B as readings 2.6.0.1 - 3

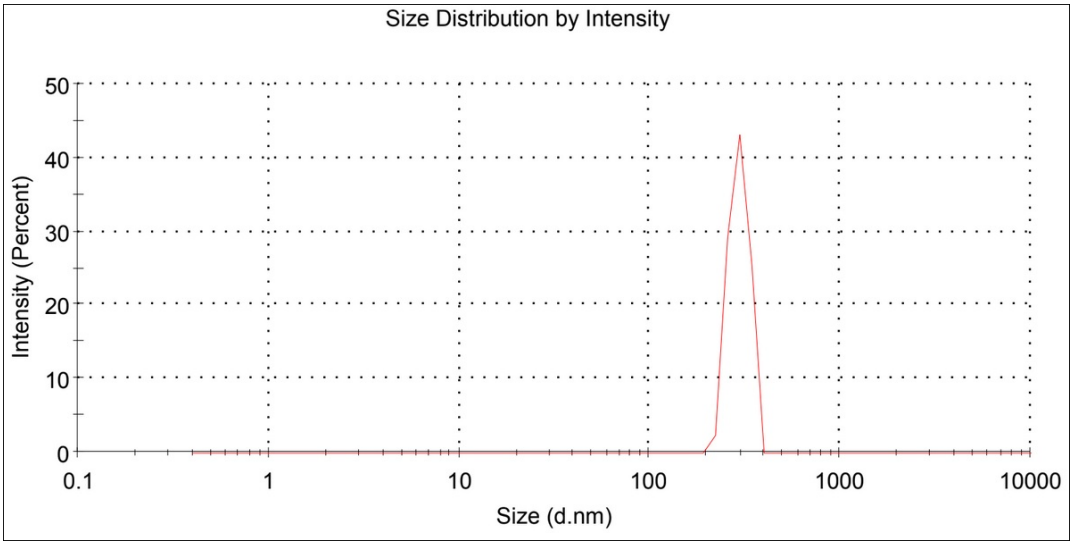

Figure A.58: First reading of size distribution by intensity for empty micelles created with the co-solvent evaporation method for 6 kDa, second iteration of the triplicates, done by the DLS software done with attenuation factor 8. A table with information on peaks, intensity and standard deviation can be seen in Appendix B as readings 2.6.0.2 - 1

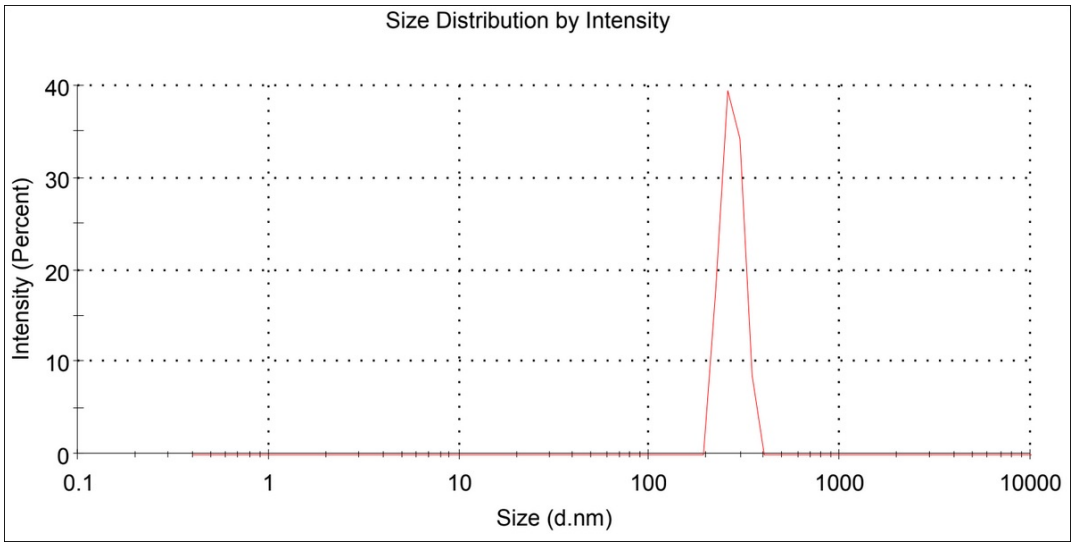

Figure A.59: Second reading of size distribution by intensity for empty micelles created with the co-solvent evaporation method for 6 kDa, second iteration of the triplicates, done by the DLS software done with attenuation factor 8. A table with information on peaks, intensity and standard deviation can be seen in Appendix B as readings 2.6.0.2 - 2

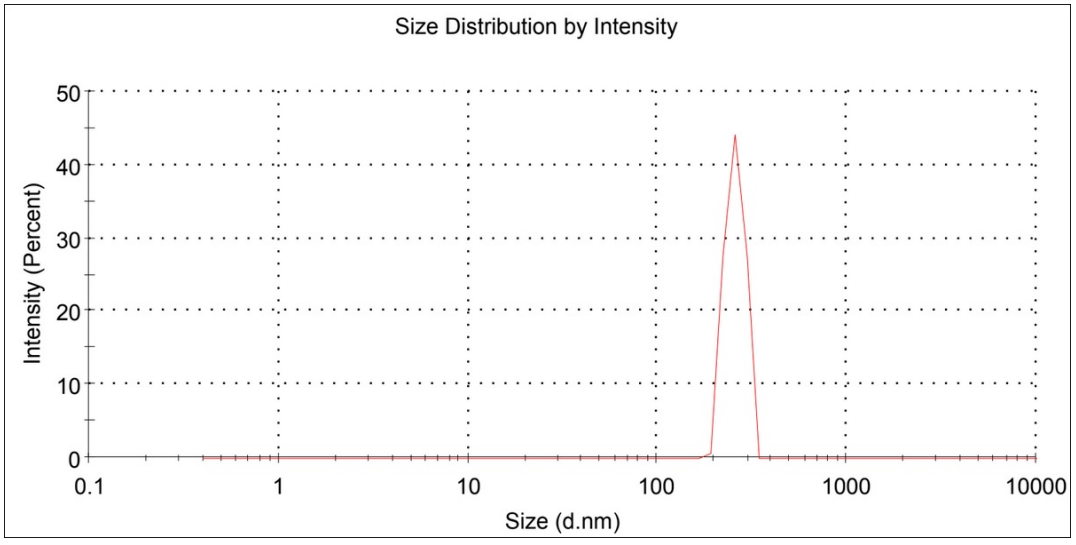

Figure A.60: Third reading of size distribution by intensity for empty micelles created with the co-solvent evaporation method for 6 kDa, second iteration of the triplicates, done by the DLS software done with attenuation factor 8. A table with information on peaks, intensity and standard deviation can be seen in Appendix B as readings 2.6.0.2 - 3

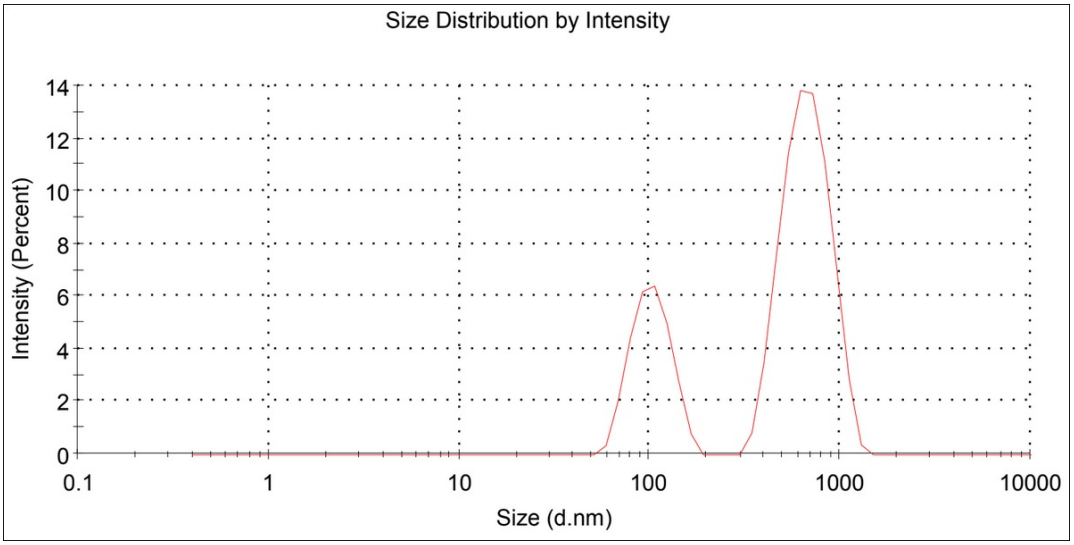

Figure A.61: First reading of size distribution by intensity for empty micelles created with the co-solvent evaporation method for 6 kDa, third iteration of the triplicates, done by the DLS software done with attenuation factor 7. A table with information on peaks, intensity and standard deviation can be seen in Appendix B as readings 2.6.0.3 - 1

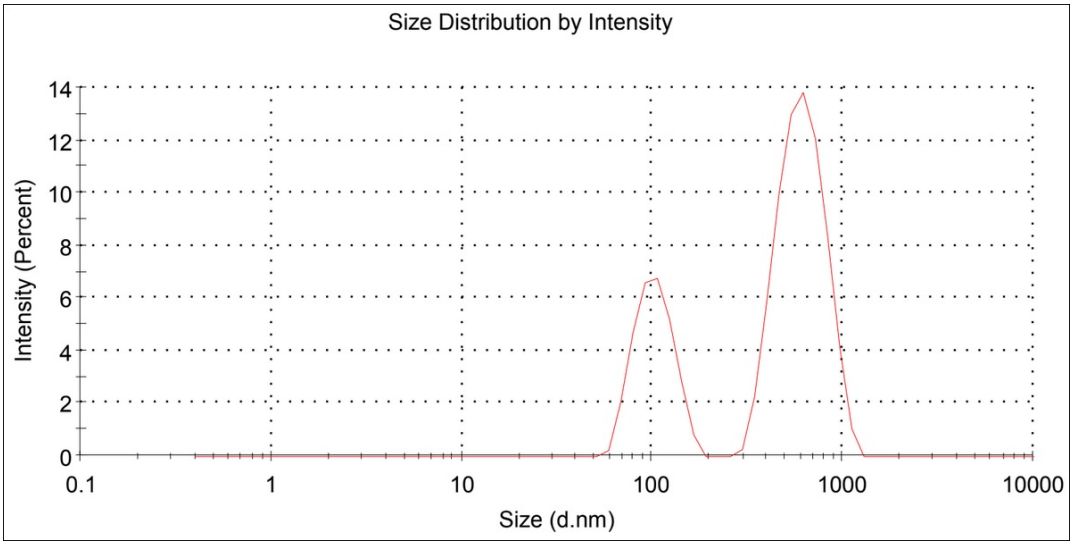

Figure A.62: Second reading of size distribution by intensity for empty micelles created with the co-solvent evaporation method for 6 kDa, third iteration of the triplicates, done by the DLS software done with attenuation factor 7. A table with information on peaks, intensity and standard deviation can be seen in Appendix B as readings 2.6.0.3 - 2

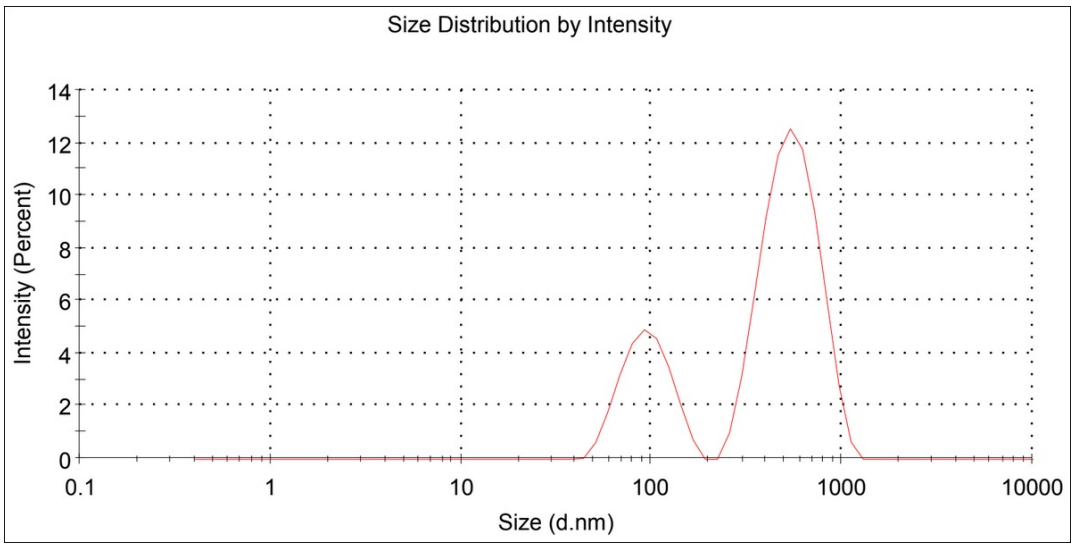

Figure A.63: Third reading of size distribution by intensity for empty micelles created with the co-solvent evaporation method for 6 kDa, third iteration of the triplicates, done by the DLS software done with attenuation factor 7. A table with information on peaks, intensity and standard deviation can be seen in Appendix B as readings 2.6.0.3 - 3

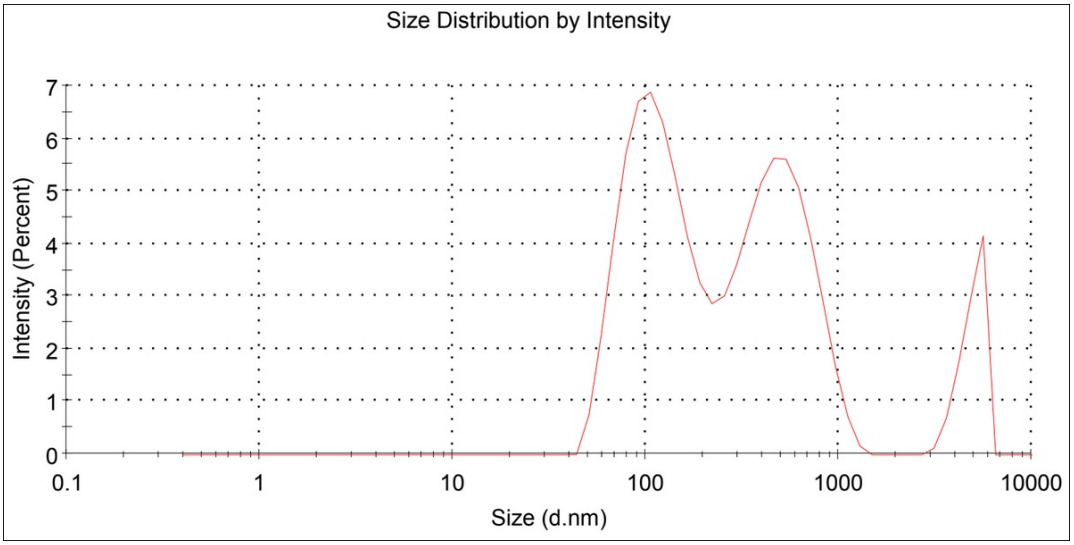

Figure A.64: First reading of size distribution by intensity for loaded micelles created with the co-solvent evaporation method for 6 kDa, first iteration of the triplicates, done by the DLS software done with attenuation factor 8. A table with information on peaks, intensity and standard deviation can be seen in Appendix B as readings 2.6.1.1 - 1

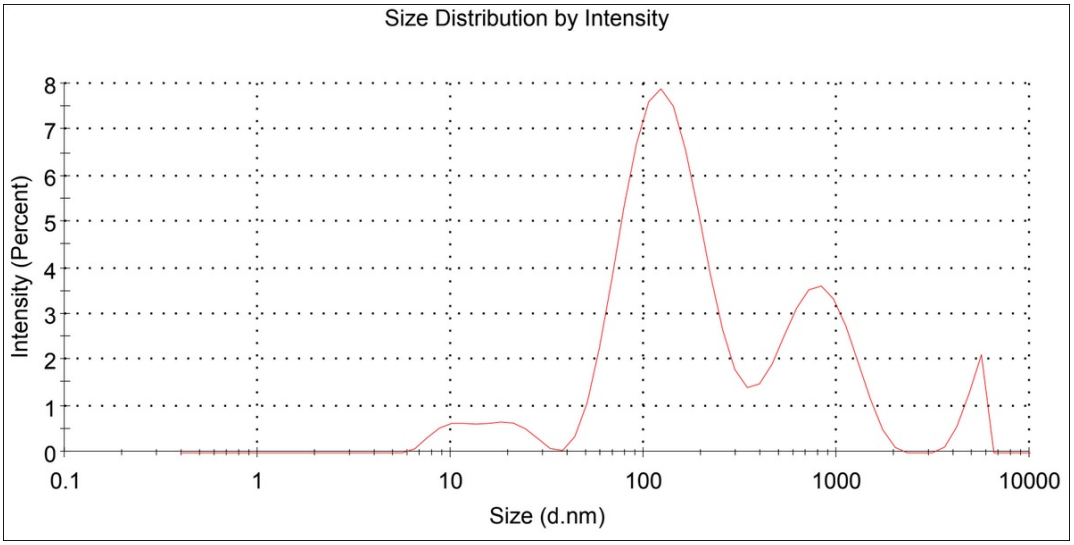

Figure A.65: Second reading of size distribution by intensity for loaded micelles created with the co-solvent evaporation method for 6 kDa, first iteration of the triplicates, done by the DLS software done with attenuation factor 7. A table with information on peaks, intensity and standard deviation can be seen in Appendix B as readings 2.6.1.1 - 2

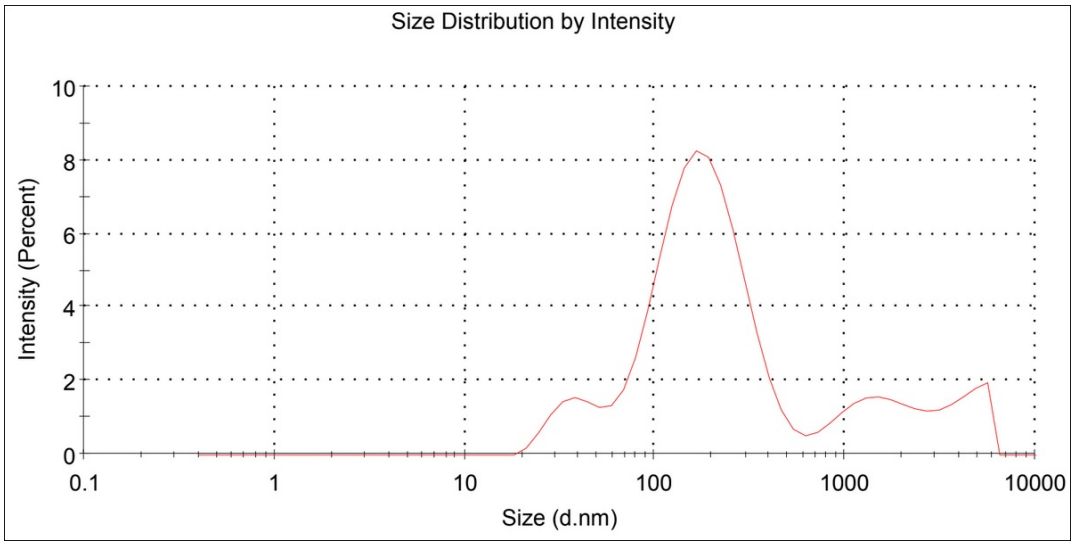

Figure A.66: Third reading of size distribution by intensity for loaded micelles created with the co-solvent evaporation method for 6 kDa, first iteration of the triplicates, done by the DLS software done with attenuation factor 7. A table with information on peaks, intensity and standard deviation can be seen in Appendix B as readings 2.6.1.1 - 3

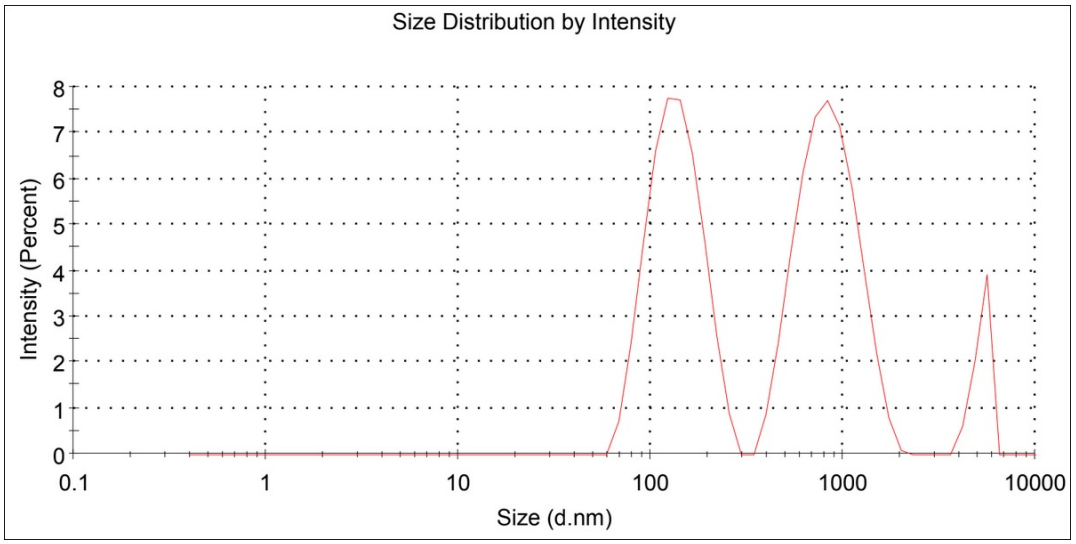

Figure A.67: First reading of size distribution by intensity for loaded micelles created with the co-solvent evaporation method for 6 kDa, second iteration of the triplicates, done by the DLS software done with attenuation factor 7. A table with information on peaks, intensity and standard deviation can be seen in Appendix B as readings 2.6.1.2 - 1

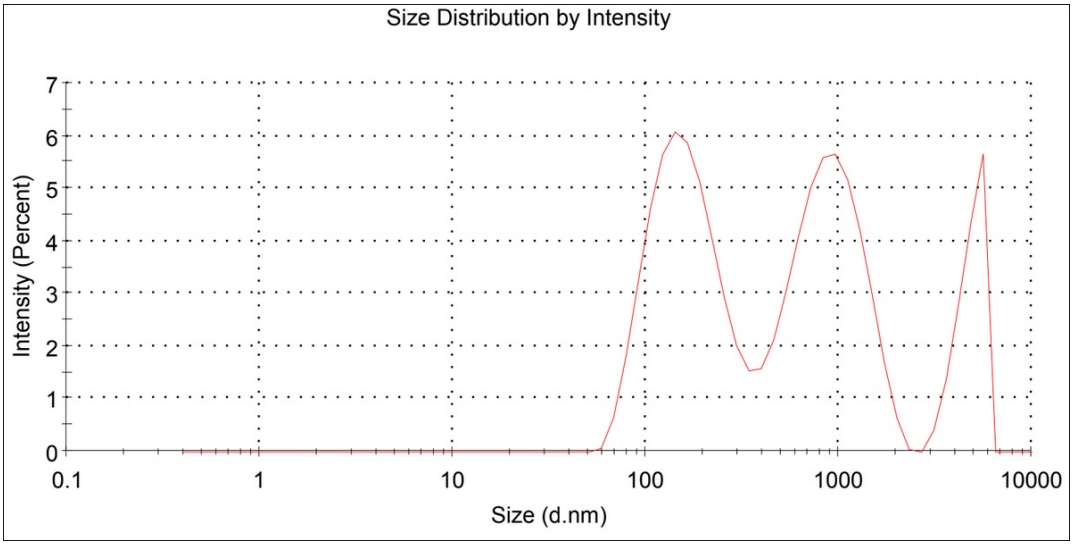

Figure A.68: Second reading of size distribution by intensity for loaded micelles created with the co-solvent evaporation method for 6 kDa, second iteration of the triplicates, done by the DLS software done with attenuation factor 7. A table with information on peaks, intensity and standard deviation can be seen in Appendix B as readings 2.6.1.2 - 2

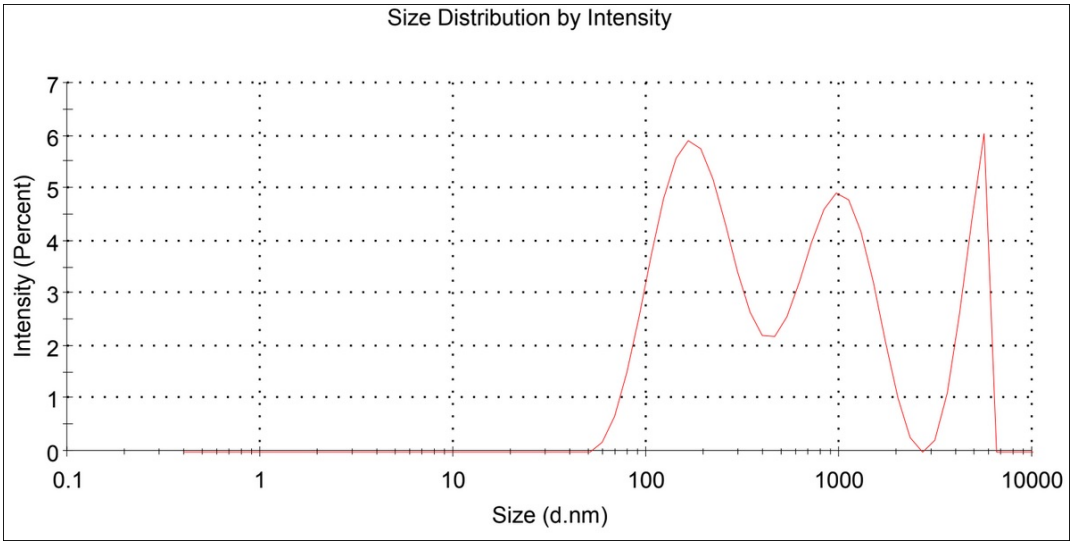

Figure A.69: Third reading of size distribution by intensity for loaded micelles created with the co-solvent evaporation method for 6 kDa, second iteration of the triplicates, done by the DLS software done with attenuation factor 7. A table with information on peaks, intensity and standard deviation can be seen in Appendix B as readings 2.6.1.2 - 3

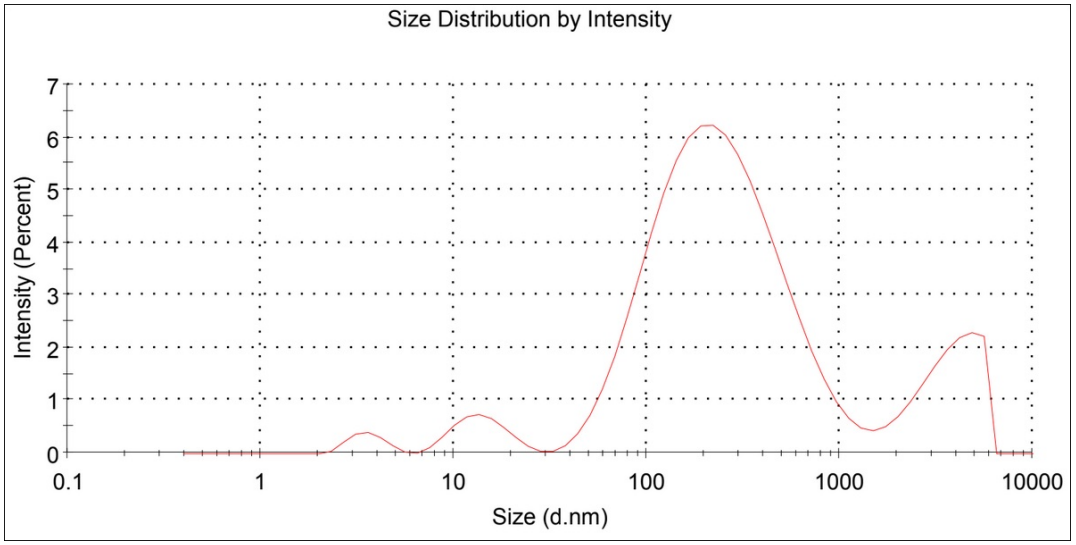

Figure A.70: First reading of size distribution by intensity for loaded micelles created with the co-solvent evaporation method for 6 kDa, third iteration of the triplicates, done by the DLS software done with attenuation factor 6. A table with information on peaks, intensity and standard deviation can be seen in Appendix B as readings 2.6.1.3 - 1

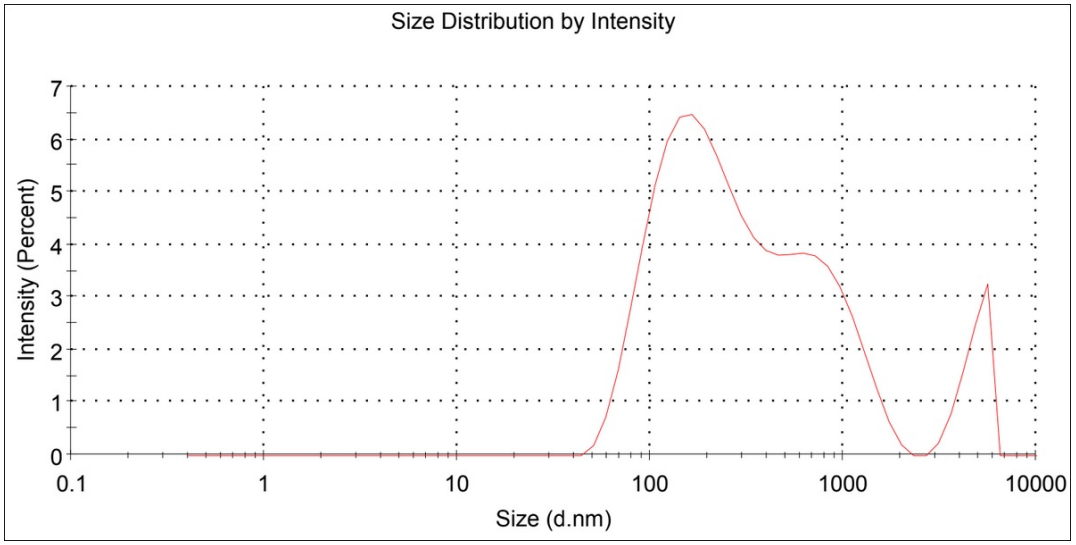

Figure A.71: Second reading of size distribution by intensity for loaded micelles created with the co-solvent evaporation method for 6 kDa, third iteration of the triplicates, done by the DLS software done with attenuation factor 6. A table with information on peaks, intensity and standard deviation can be seen in Appendix B as readings 2.6.1.3 - 2

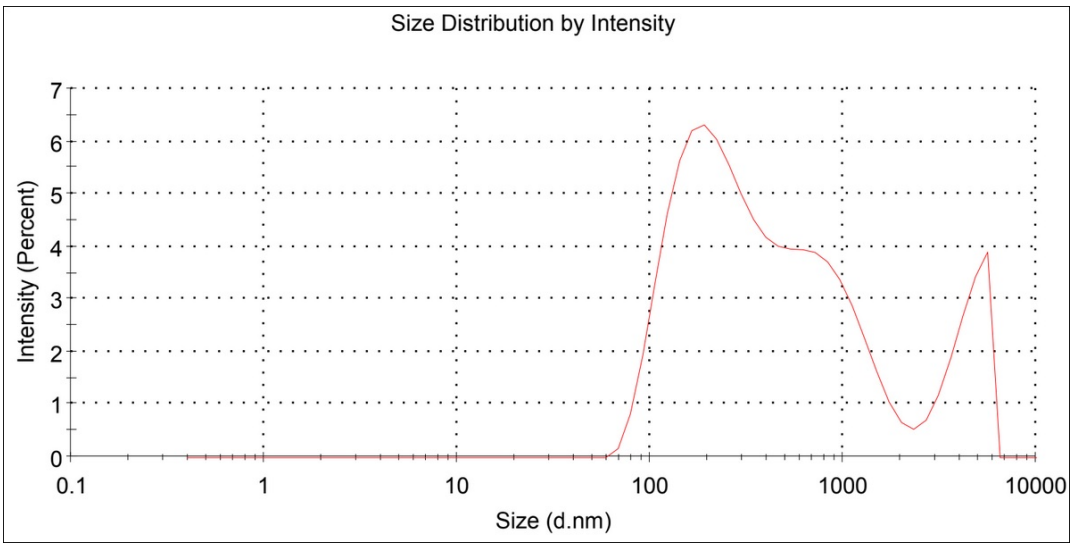

Figure A.72: Third reading of size distribution by intensity for loaded micelles created with the co-solvent evaporation method for 6 kDa, third iteration of the triplicates, done by the DLS software done with attenuation factor 6. A table with information on peaks, intensity and standard deviation can be seen in Appendix B as readings 2.6.1.3 - 3

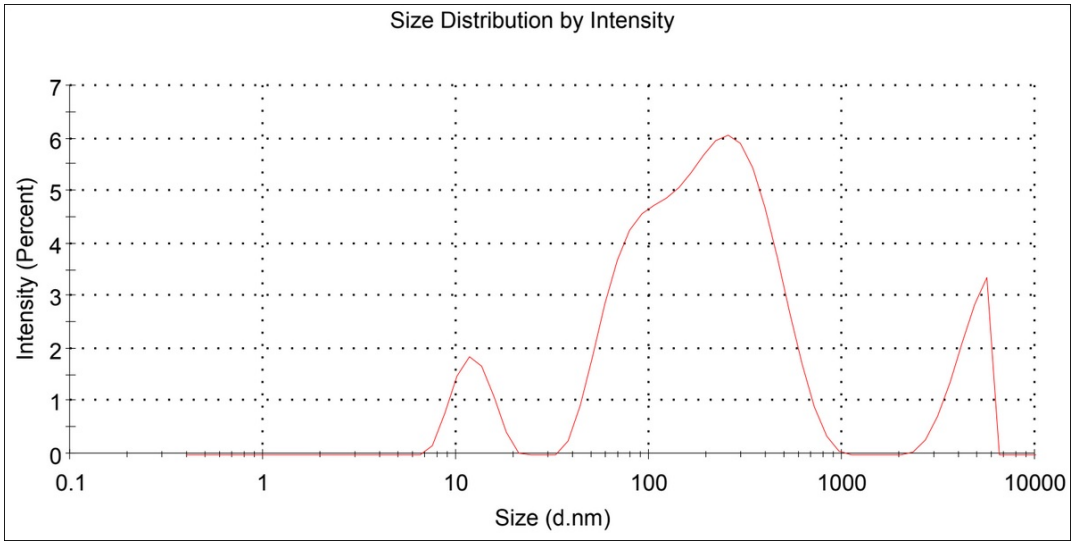

Figure A.73: First reading of size distribution by intensity for empty micelles created with the sonification method for 12 kDa, first iteration of the triplicates, done by the DLS software done with attenuation factor 6. A table with information on peaks, intensity and standard deviation can be seen in Appendix B as readings 1.12.0.1 - 1

A.3 12 kDa polymeric micelles

A.3.1 Sonification method

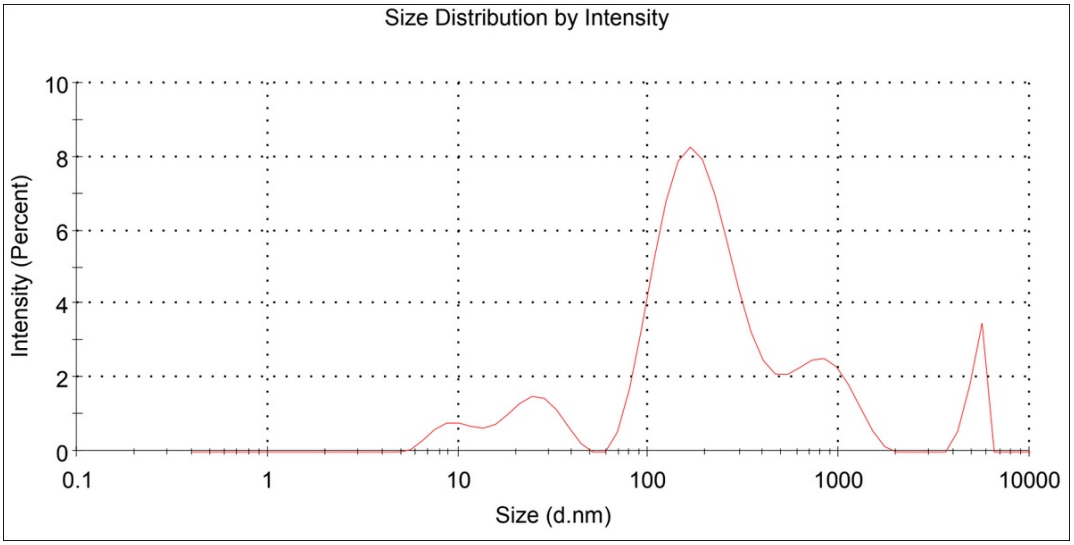

Figure A.74: Second reading of size distribution by intensity for empty micelles created with the sonification method for 12 kDa, first iteration of the triplicates, done by the DLS software done with attenuation factor 6. A table with information on peaks, intensity and standard deviation can be seen in Appendix B as readings 1.12.0.1 - 2

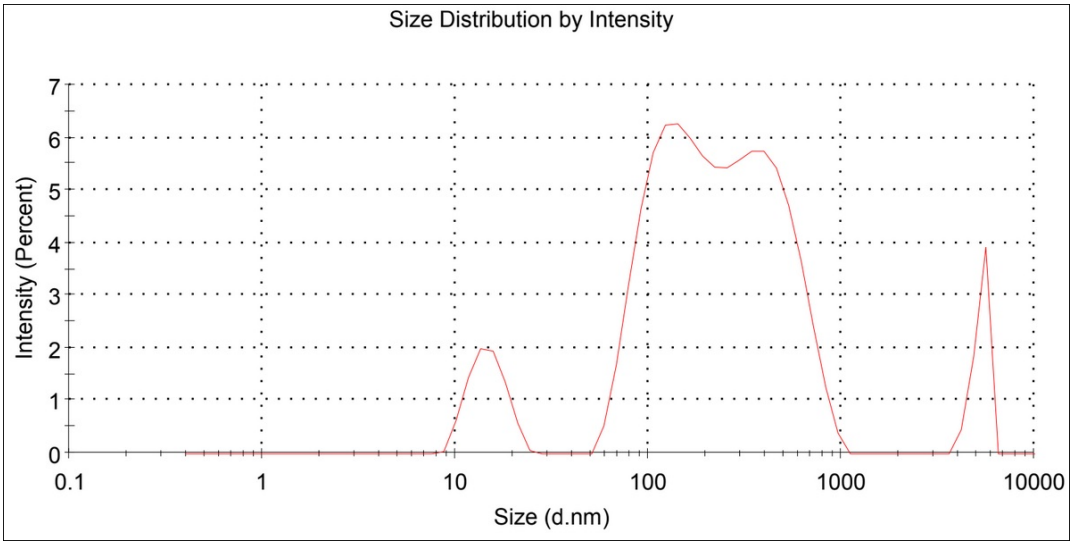

Figure A.75: Third reading of size distribution by intensity for empty micelles created with the sonification method for 12 kDa, first iteration of the triplicates, done by the DLS software done with attenuation factor 6. A table with information on peaks, intensity and standard deviation can be seen in Appendix B as readings 1.12.0.1 - 3

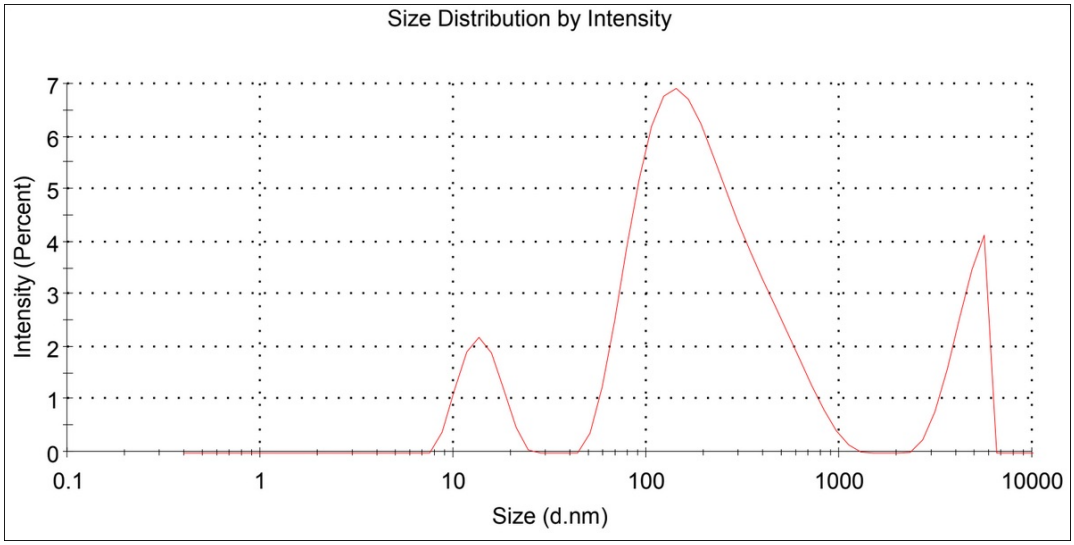

Figure A.76: First reading of size distribution by intensity for empty micelles created with the sonification method for 12 kDa, second iteration of the triplicates, done by the DLS software done with attenuation factor 7. A table with information on peaks, intensity and standard deviation can be seen in Appendix B as readings 1.12.0.2 - 1

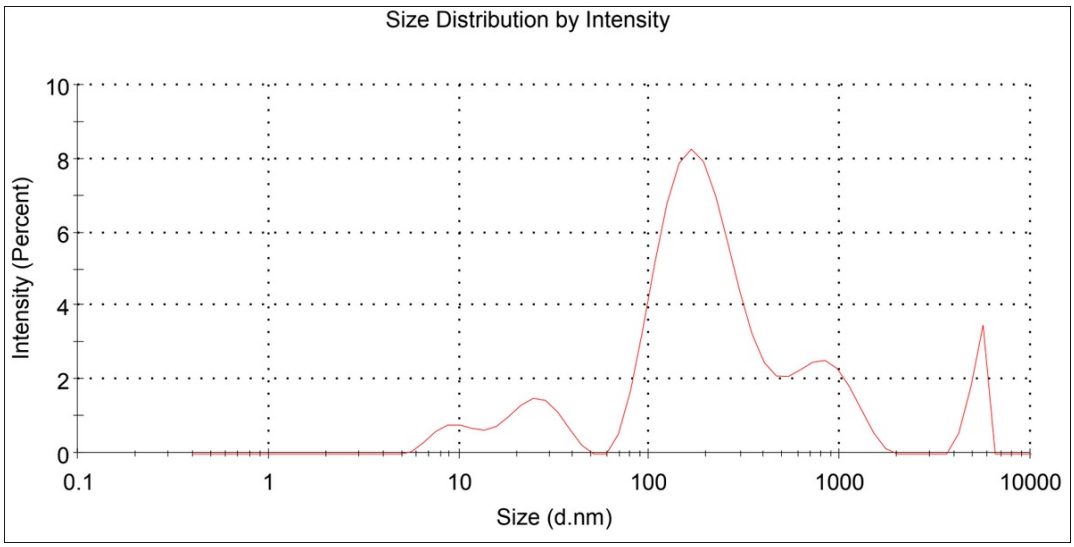

Figure A.77: Second reading of size distribution by intensity for empty micelles created with the sonification method for 12 kDa, second iteration of the triplicates, done by the DLS software done with attenuation factor 7. A table with information on peaks, intensity and standard deviation can be seen in Appendix B as readings 1.12.0.2 - 2

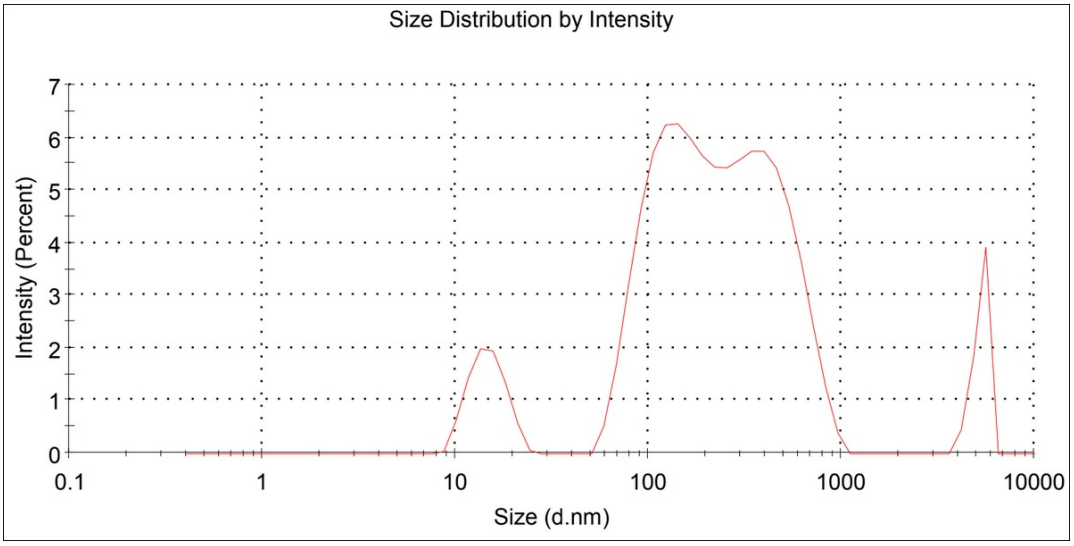

Figure A.78: Third reading of size distribution by intensity for empty micelles created with the sonification method for 12 kDa, second iteration of the triplicates, done by the DLS software done with attenuation factor 7. A table with information on peaks, intensity and standard deviation can be seen in Appendix B as readings 1.12.0.2 - 3

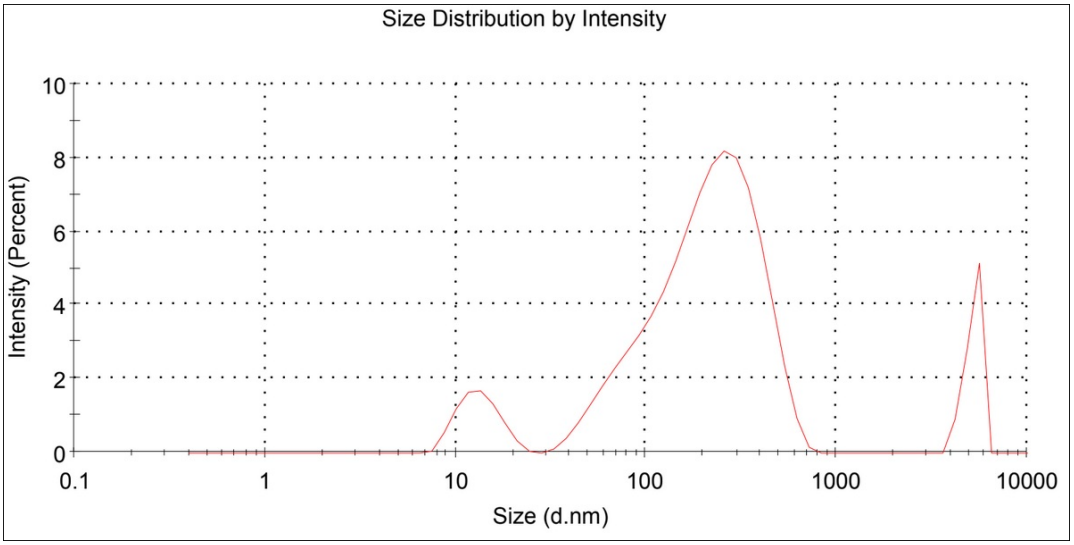

Figure A.79: First reading of size distribution by intensity for empty micelles created with the sonification method for 12 kDa, third iteration of the triplicates, done by the DLS software done with attenuation factor 7. A table with information on peaks, intensity and standard deviation can be seen in Appendix B as readings 1.12.0.3 - 1

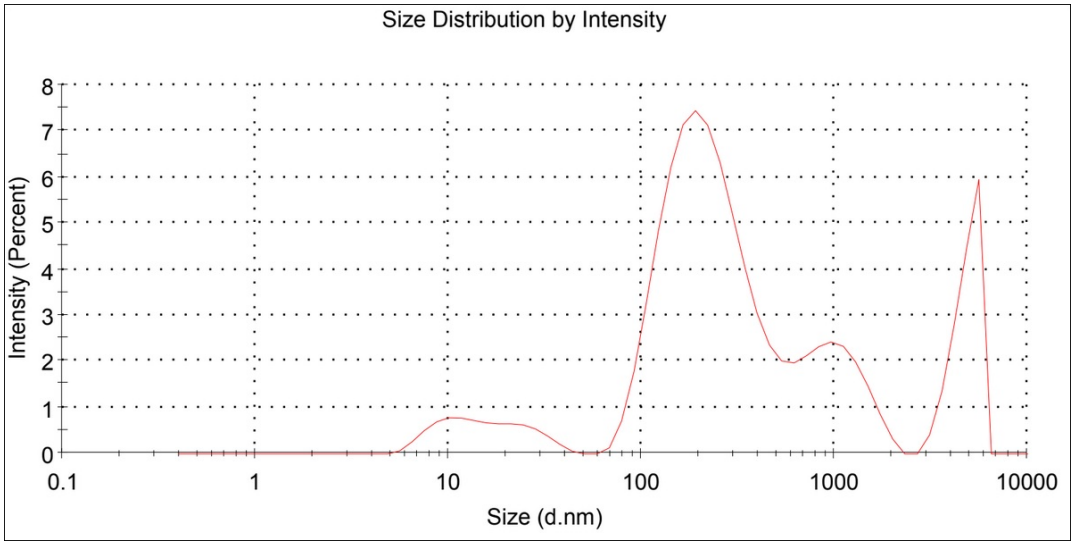

Figure A.80: Second reading of size distribution by intensity for empty micelles created with the sonification method for 12 kDa, third iteration of the triplicates, done by the DLS software done with attenuation factor 7. A table with information on peaks, intensity and standard deviation can be seen in Appendix B as readings 1.12.0.3 - 2

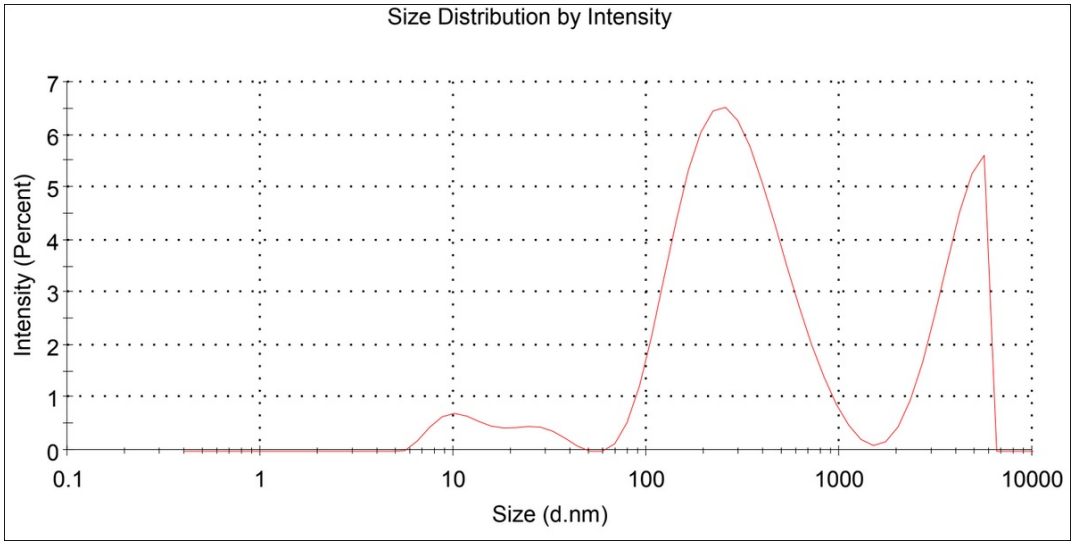

Figure A.81: Third reading of size distribution by intensity for empty micelles created with the sonification method for 12 kDa, third iteration of the triplicates, done by the DLS software done with attenuation factor 7. A table with information on peaks, intensity and standard deviation can be seen in Appendix B as readings 1.12.0.3 - 3

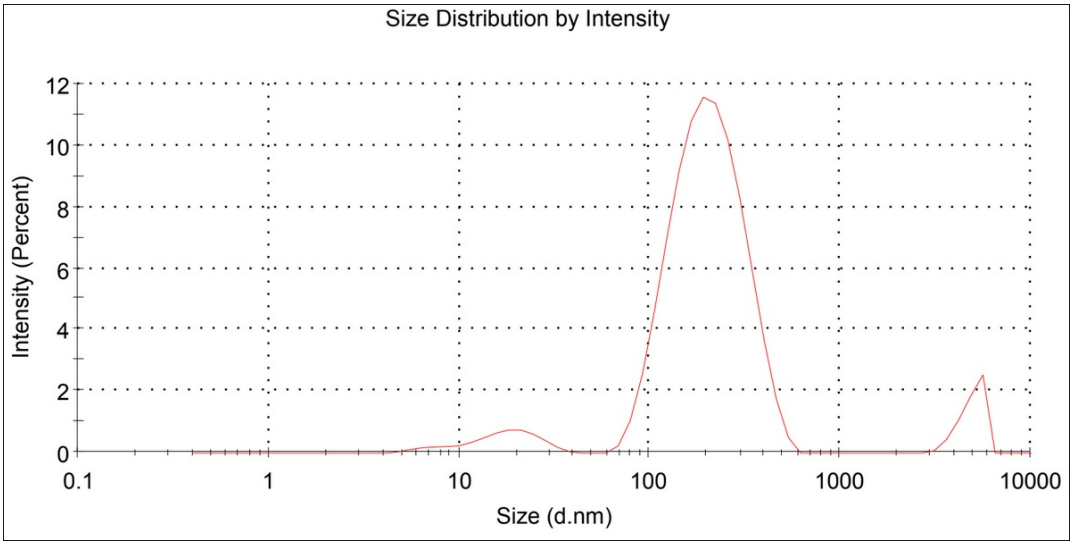

Figure A.82: First reading of size distribution by intensity for loaded micelles created with the sonification method for 12 kDa, first iteration of the triplicates, done by the DLS software done with attenuation factor 6. A table with information on peaks, intensity and standard deviation can be seen in Appendix B as readings 1.12.1.1 - 1

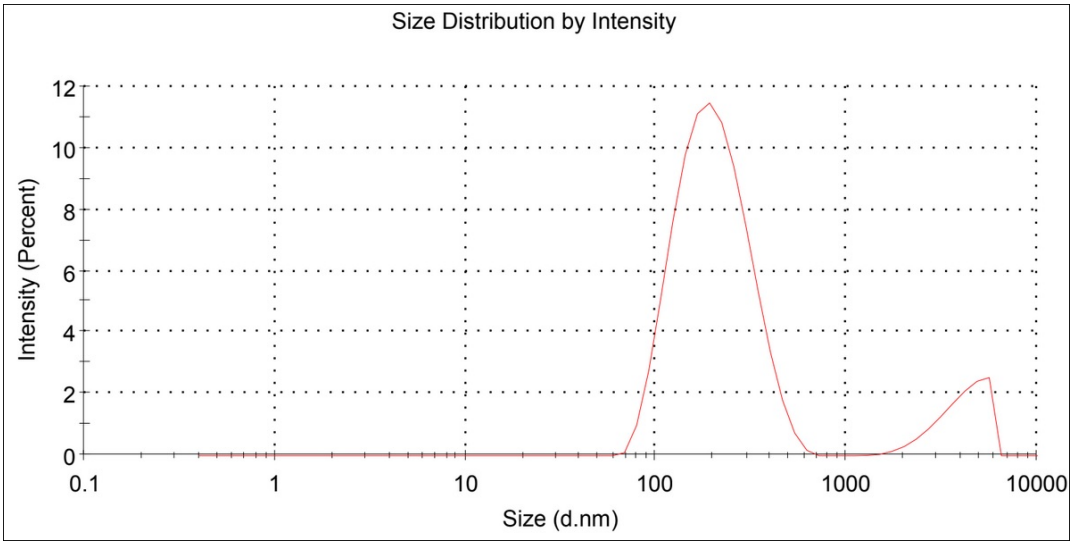

Figure A.83: Second reading of size distribution by intensity for loaded micelles created with the sonification method for 12 kDa, first iteration of the triplicates, done by the DLS software done with attenuation factor 6. A table with information on peaks, intensity and standard deviation can be seen in Appendix B as readings 1.12.1.1 - 2

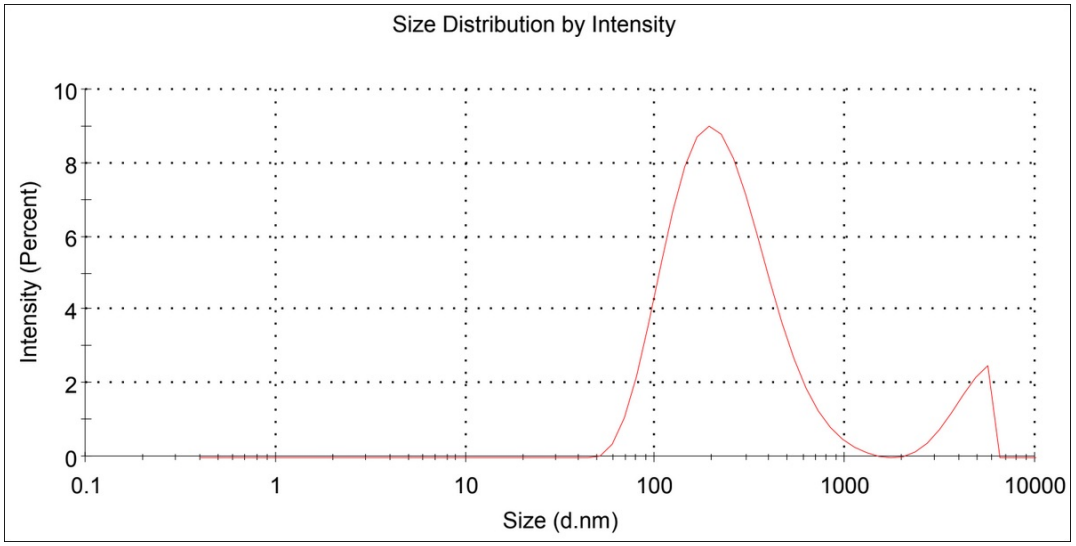

Figure A.84: Third reading of size distribution by intensity for loaded micelles created with the sonification method for 12 kDa, first iteration of the triplicates, done by the DLS software done with attenuation factor 6. A table with information on peaks, intensity and standard deviation can be seen in Appendix B as readings 1.12.1.1 - 3

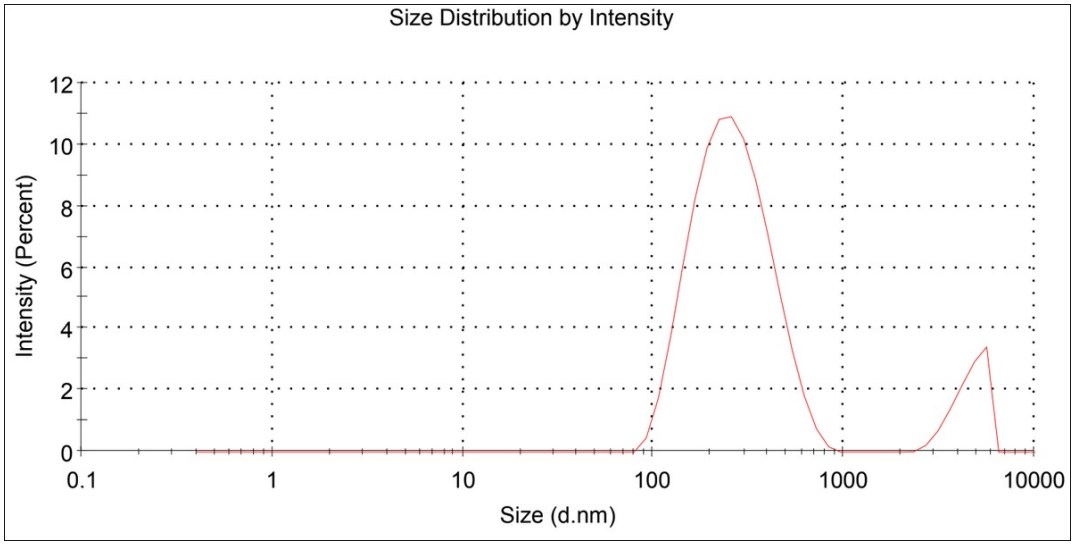

Figure A.85: First reading of size distribution by intensity for loaded micelles created with the sonification method for 12 kDa, second iteration of the triplicates, done by the DLS software done with attenuation factor 6. A table with information on peaks, intensity and standard deviation can be seen in Appendix B as readings 1.12.1.2 - 1

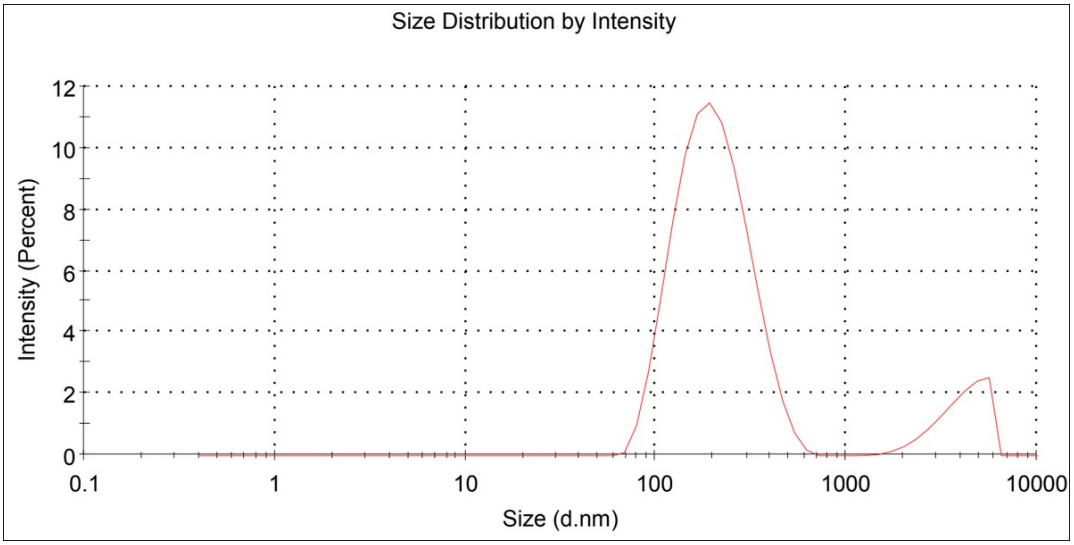

Figure A.86: Second reading of size distribution by intensity for loaded micelles created with the sonification method for 12 kDa, second iteration of the triplicates, done by the DLS software done with attenuation factor 6. A table with information on peaks, intensity and standard deviation can be seen in Appendix B as readings 1.12.1.2 - 2

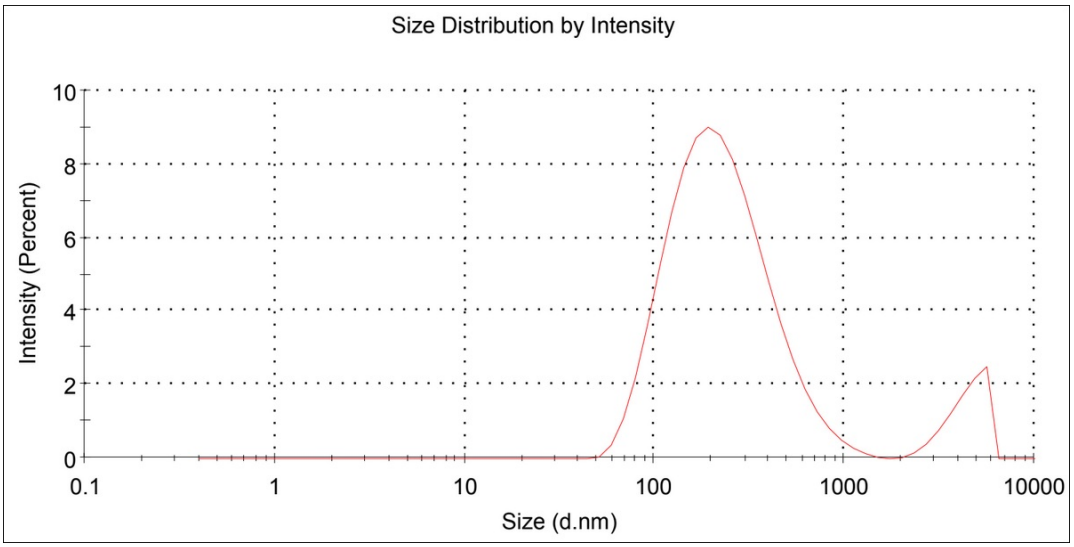

Figure A.87: Third reading of size distribution by intensity for loaded micelles created with the sonification method for 12 kDa, second iteration of the triplicates, done by the DLS software done with attenuation factor 6. A table with information on peaks, intensity and standard deviation can be seen in Appendix B as readings 1.12.1.2 - 3

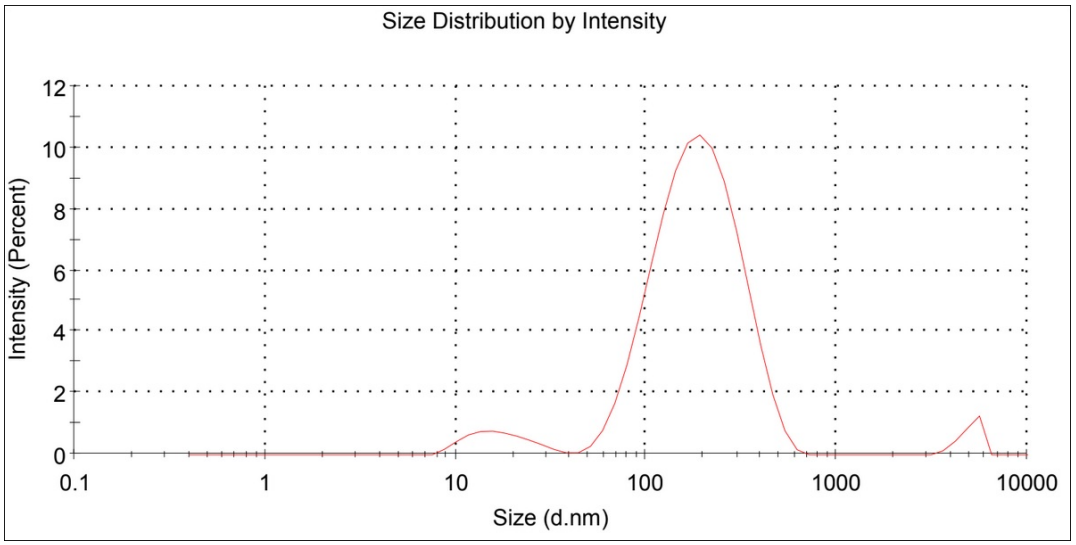

Figure A.88: First reading of size distribution by intensity for loaded micelles created with the sonification method for 12 kDa, third iteration of the triplicates, done by the DLS software done with attenuation factor 6. A table with information on peaks, intensity and standard deviation can be seen in Appendix B as readings 1.12.1.3 - 1

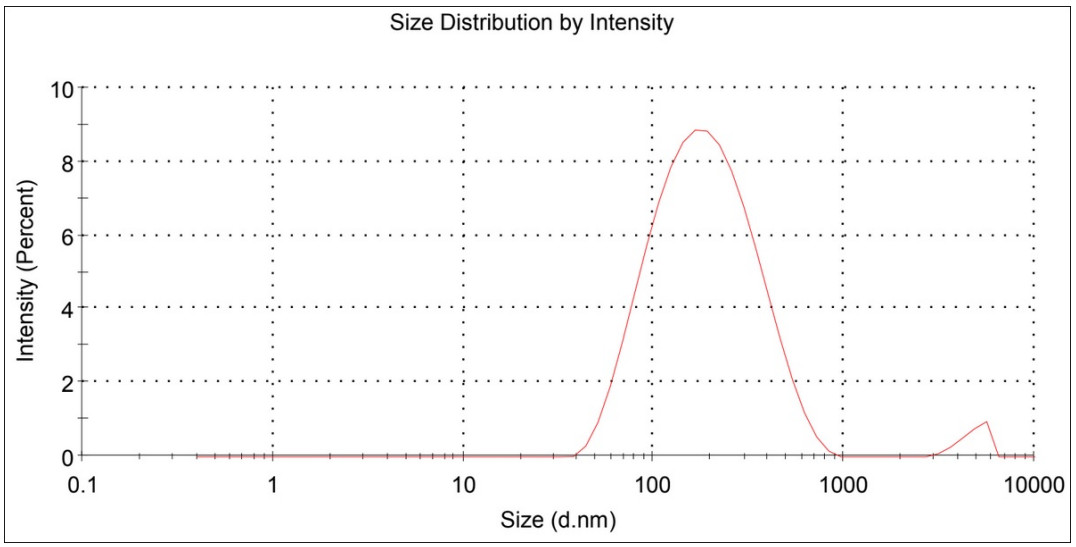

Figure A.89: Second reading of size distribution by intensity for loaded micelles created with the sonification method for 12 kDa, third iteration of the triplicates, done by the DLS software done with attenuation factor 6. A table with information on peaks, intensity and standard deviation can be seen in Appendix B as readings 1.12.1.3 - 2

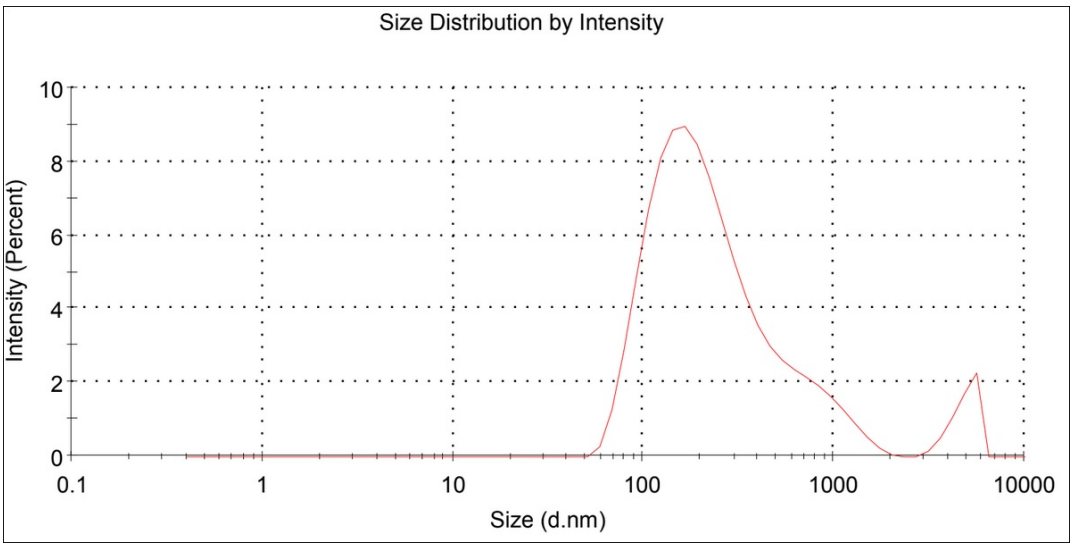

Figure A.90: Third reading of size distribution by intensity for loaded micelles created with the sonification method for 12 kDa, third iteration of the triplicates, done by the DLS software done with attenuation factor 6. A table with information on peaks, intensity and standard deviation can be seen in Appendix B as readings 1.12.1.3 - 3

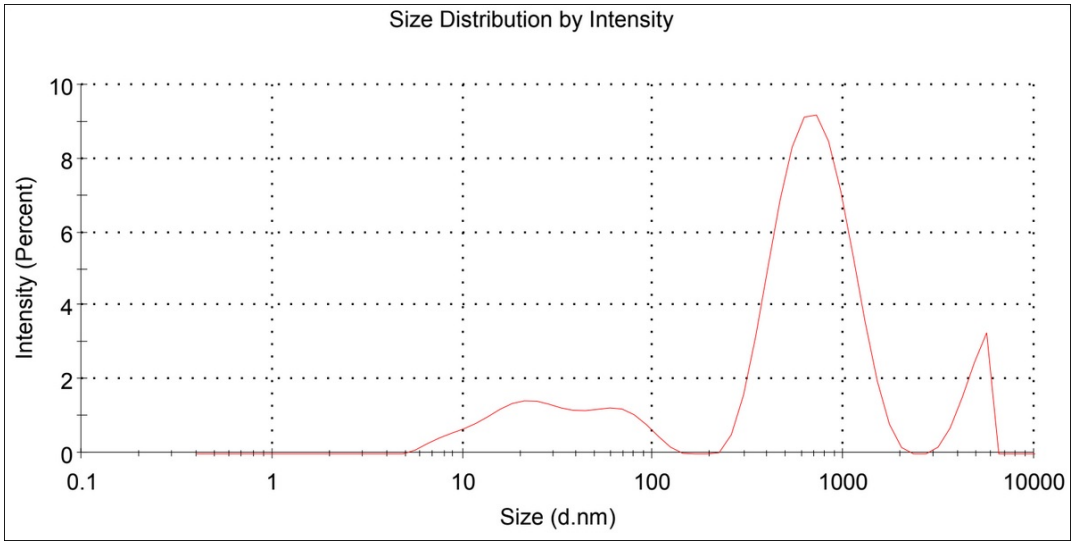

Figure A.91: First reading of size distribution by intensity for empty micelles created with the co-solvent evaporation method for 12 kDa, first iteration of the triplicates, done by the DLS software done with attenuation factor 7. A table with information on peaks, intensity and standard deviation can be seen in Appendix B as readings 2.12.0.1 - 1

A.4 Co-solvent evaporation method

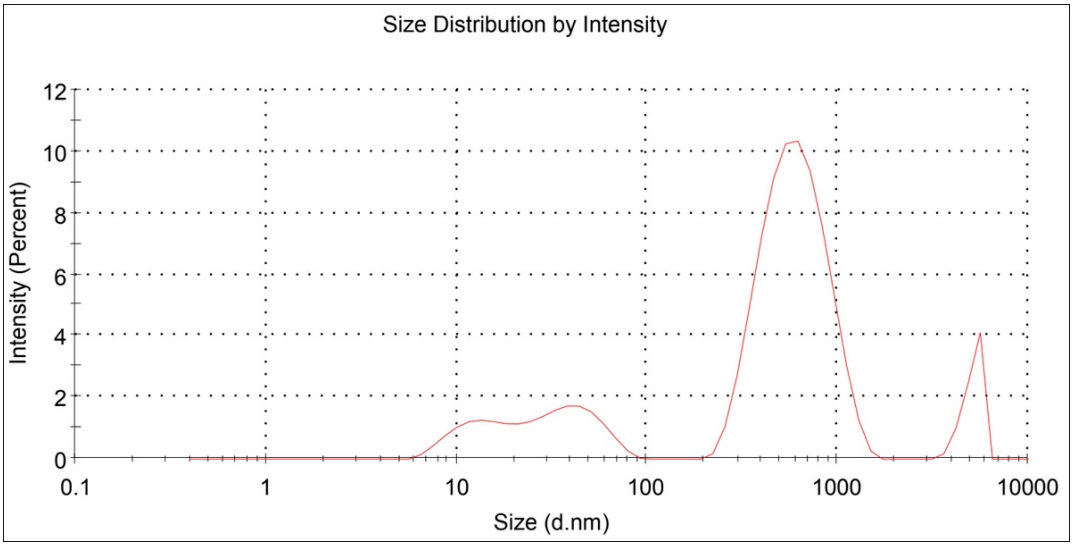

Figure A.92: Second reading of size distribution by intensity for empty micelles created with the co-solvent evaporation method for 12 kDa, first iteration of the triplicates, done by the DLS software done with attenuation factor 7. A table with information on peaks, intensity and standard deviation can be seen in Appendix B as readings 2.12.0.1 - 2

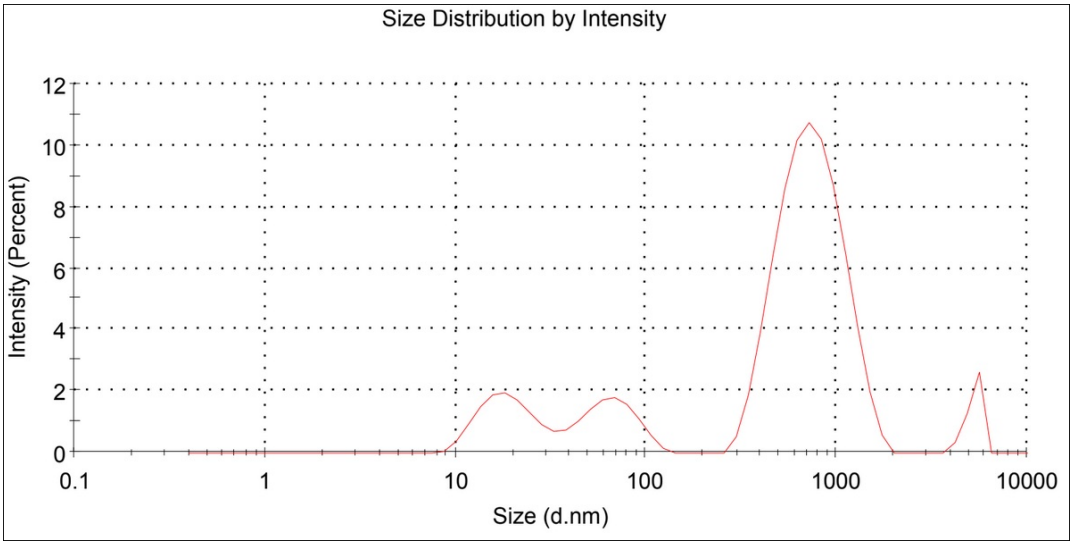

Figure A.93: Third reading of size distribution by intensity for empty micelles created with the co-solvent evaporation method for 12 kDa, first iteration of the triplicates, done by the DLS software done with attenuation factor 7. A table with information on peaks, intensity and standard deviation can be seen in Appendix B as readings 2.12.0.1 - 3

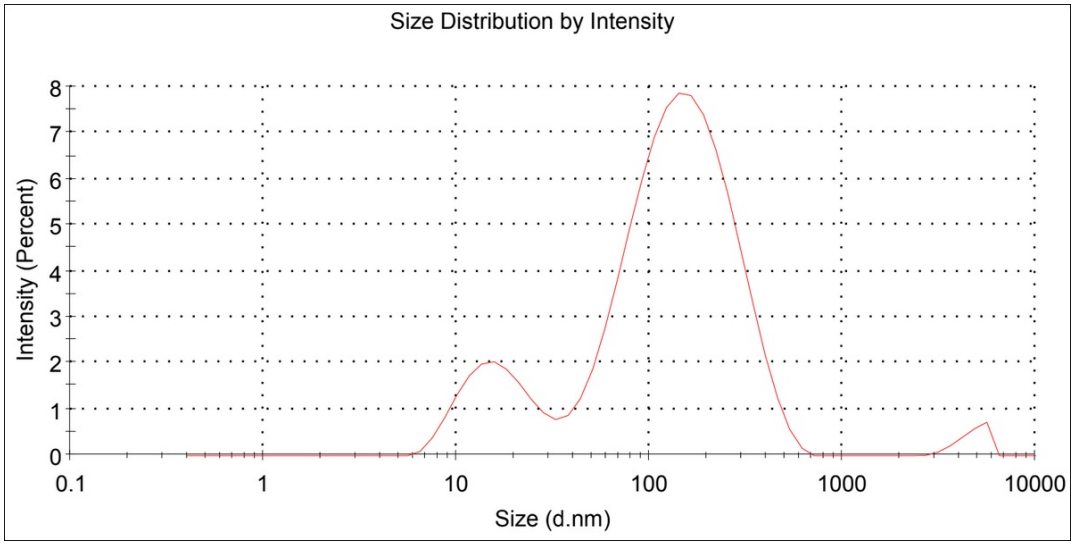

Figure A.94: First reading of size distribution by intensity for empty micelles created with the co-solvent evaporation method for 12 kDa, second iteration of the triplicates, done by the DLS software done with attenuation factor 8. A table with information on peaks, intensity and standard deviation can be seen in Appendix B as readings 2.12.0.2 - 1

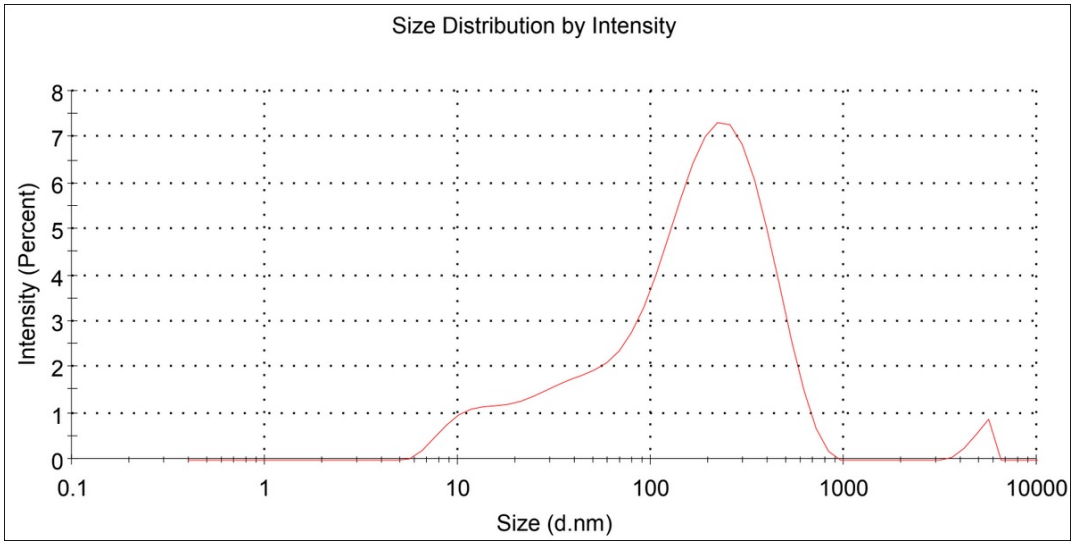

Figure A.95: Second reading of size distribution by intensity for empty micelles created with the co-solvent evaporation method for 12 kDa, second iteration of the triplicates, done by the DLS software done with attenuation factor 8. A table with information on peaks, intensity and standard deviation can be seen in Appendix B as readings 2.12.0.2 - 2

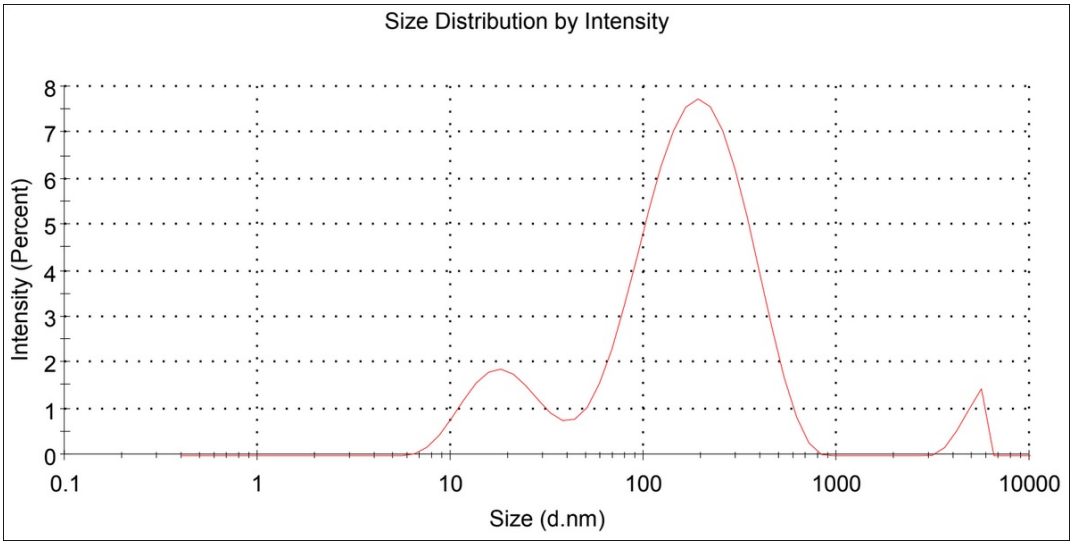

Figure A.96: Third reading of size distribution by intensity for empty micelles created with the co-solvent evaporation method for 12 kDa, second iteration of the triplicates, done by the DLS software done with attenuation factor 8. A table with information on peaks, intensity and standard deviation can be seen in Appendix B as readings 2.12.0.2 - 3

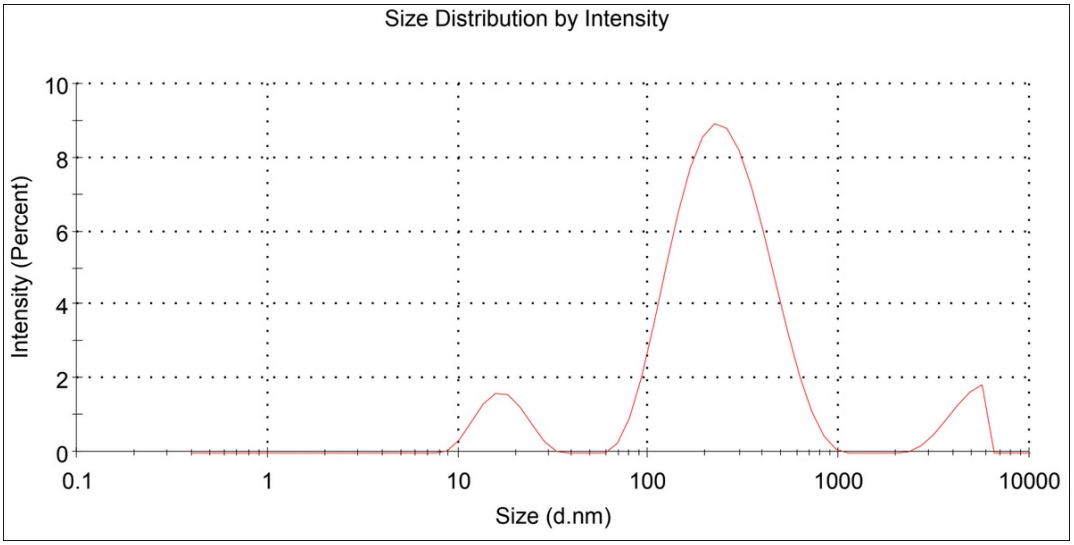

Figure A.97: First reading of size distribution by intensity for empty micelles created with the co-solvent evaporation method for 12 kDa, third iteration of the triplicates, done by the DLS software done with attenuation factor 8. A table with information on peaks, intensity and standard deviation can be seen in Appendix B as readings 2.12.0.3 - 1

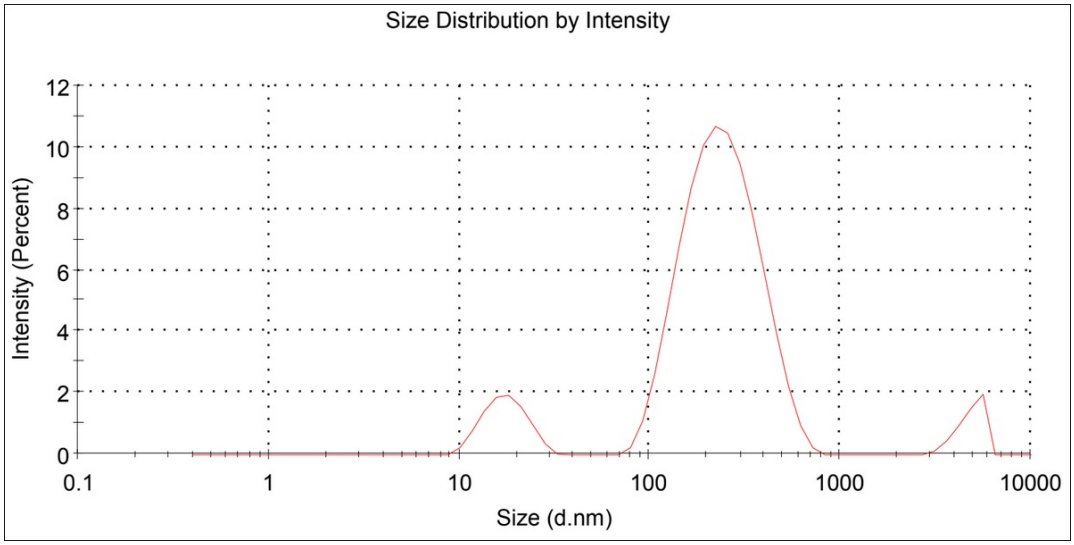

Figure A.98: Second reading of size distribution by intensity for empty micelles created with the co-solvent evaporation method for 12 kDa, third iteration of the triplicates, done by the DLS software done with attenuation factor 8. A table with information on peaks, intensity and standard deviation can be seen in Appendix B as readings 2.12.0.3 - 2

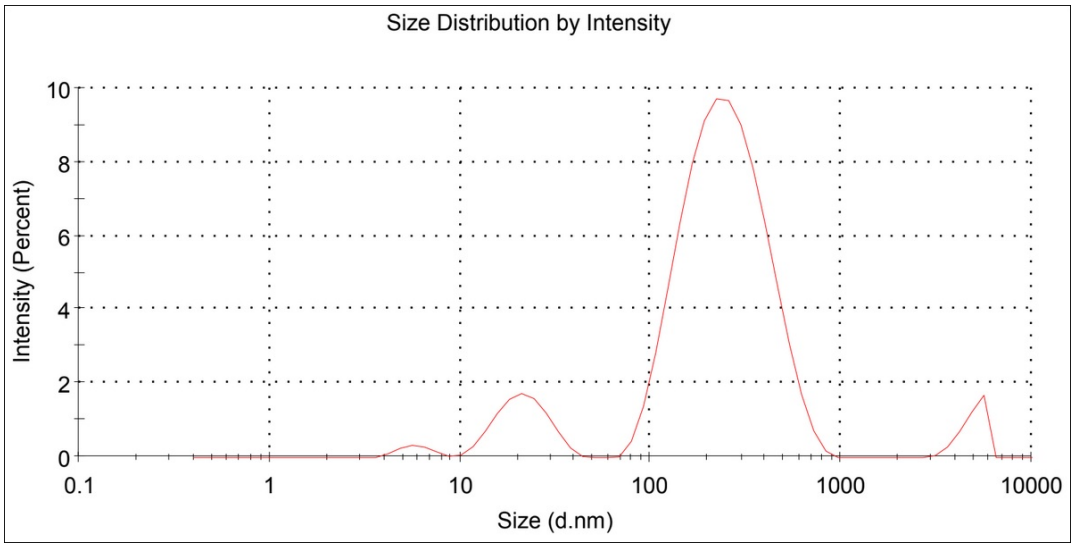

Figure A.99: Third reading of size distribution by intensity for empty micelles created with the co-solvent evaporation method for 12 kDa, third iteration of the triplicates, done by the DLS software done with attenuation factor 8. A table with information on peaks, intensity and standard deviation can be seen in Appendix B as readings 2.12.0.3 - 3

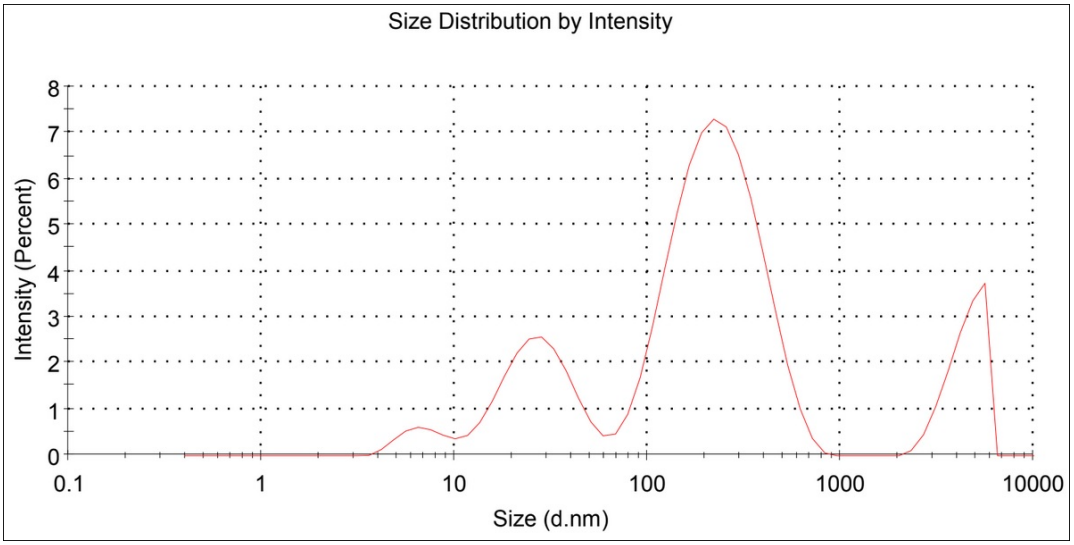

Figure A.100: First reading of size distribution by intensity for loaded micelles created with the co-solvent evaporation method for 12 kDa, first iteration of the triplicates, done by the DLS software done with attenuation factor 7. A table with information on peaks, intensity and standard deviation can be seen in Appendix B as readings 2.12.1.1 - 1

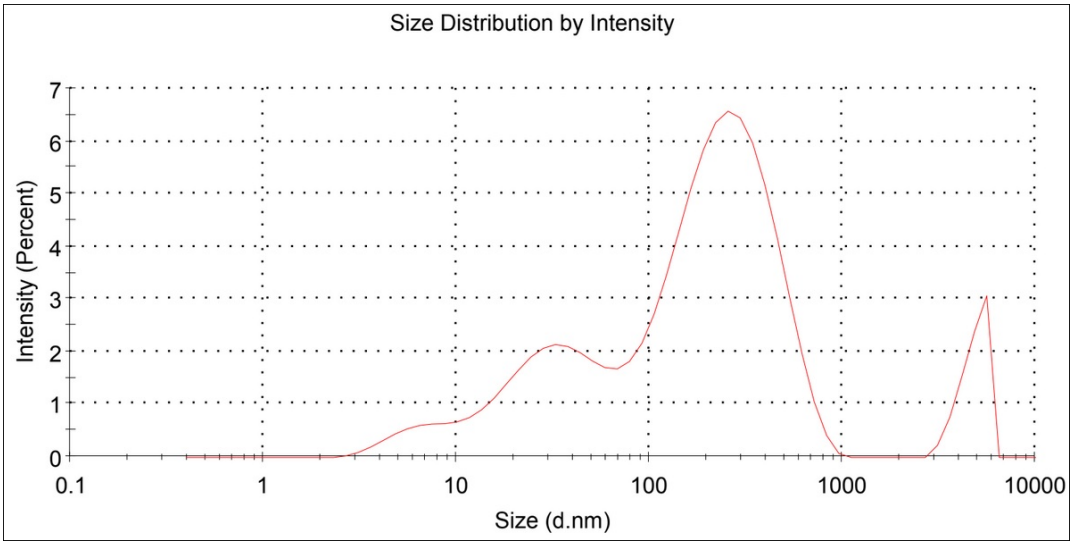

Figure A.101: Second reading of size distribution by intensity for loaded micelles created with the co-solvent evaporation method for 12 kDa, first iteration of the triplicates, done by the DLS software done with attenuation factor 7. A table with information on peaks, intensity and standard deviation can be seen in Appendix B as readings 2.12.1.1 - 2

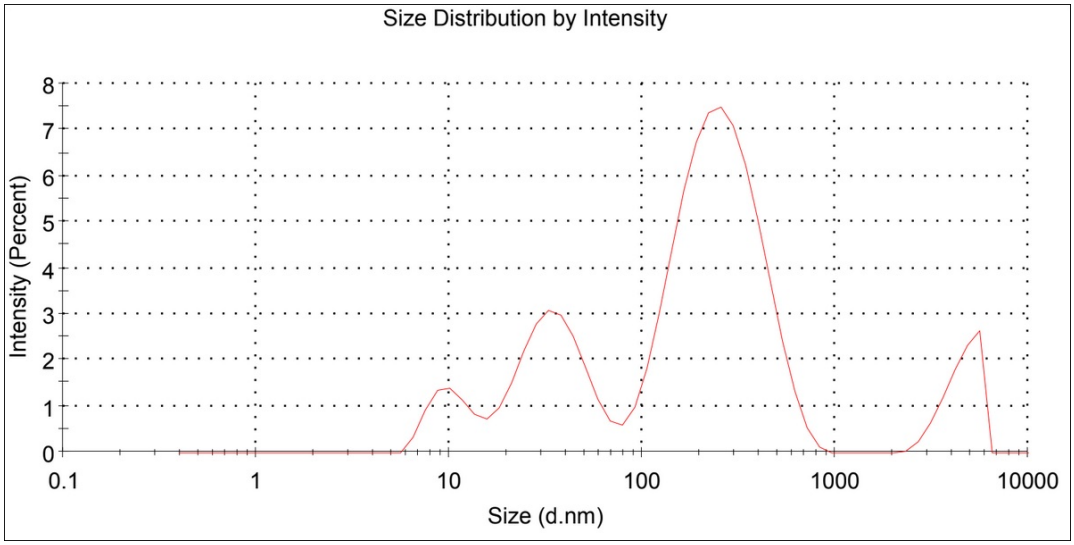

Figure A.102: Third reading of size distribution by intensity for loaded micelles created with the co-solvent evaporation method for 12 kDa, first iteration of the triplicates, done by the DLS software done with attenuation factor 7. A table with information on peaks, intensity and standard deviation can be seen in Appendix B as readings 2.12.1.1 - 3

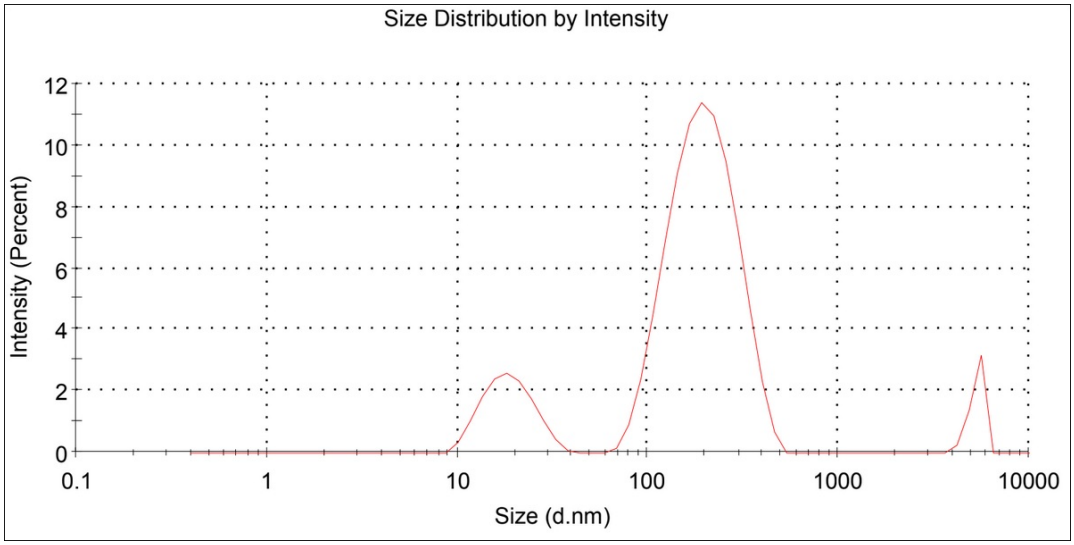

Figure A.103: First reading of size distribution by intensity for loaded micelles created with the co-solvent evaporation method for 12 kDa, second iteration of the triplicates, done by the DLS software done with attenuation factor 7. A table with information on peaks, intensity and standard deviation can be seen in Appendix B as readings 2.12.1.2 - 1

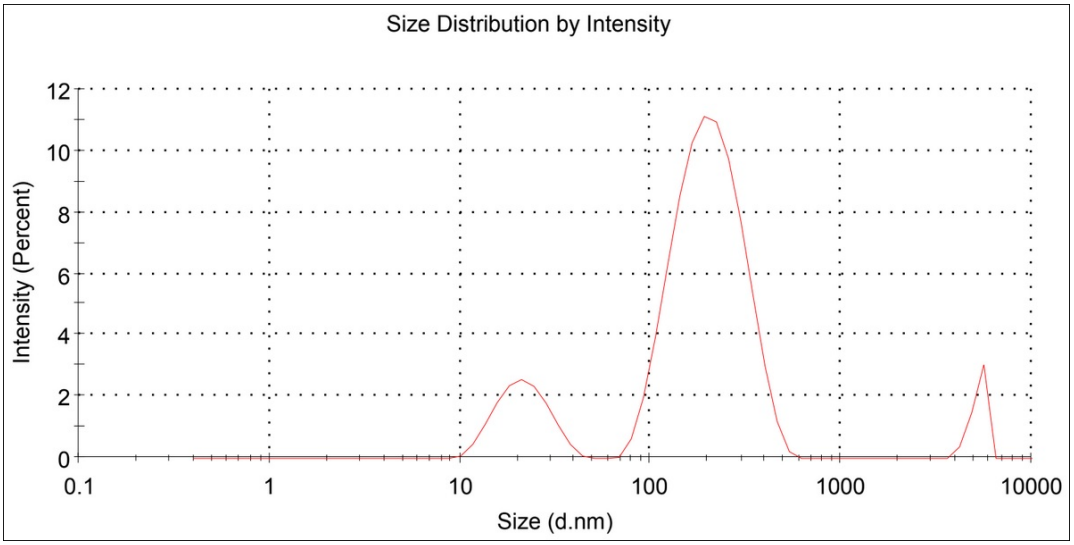

Figure A.104: Second reading of size distribution by intensity for loaded micelles created with the co-solvent evaporation method for 12 kDa, second iteration of the triplicates, done by the DLS software done with attenuation factor 7. A table with information on peaks, intensity and standard deviation can be seen in Appendix B as readings 2.12.1.2 - 2

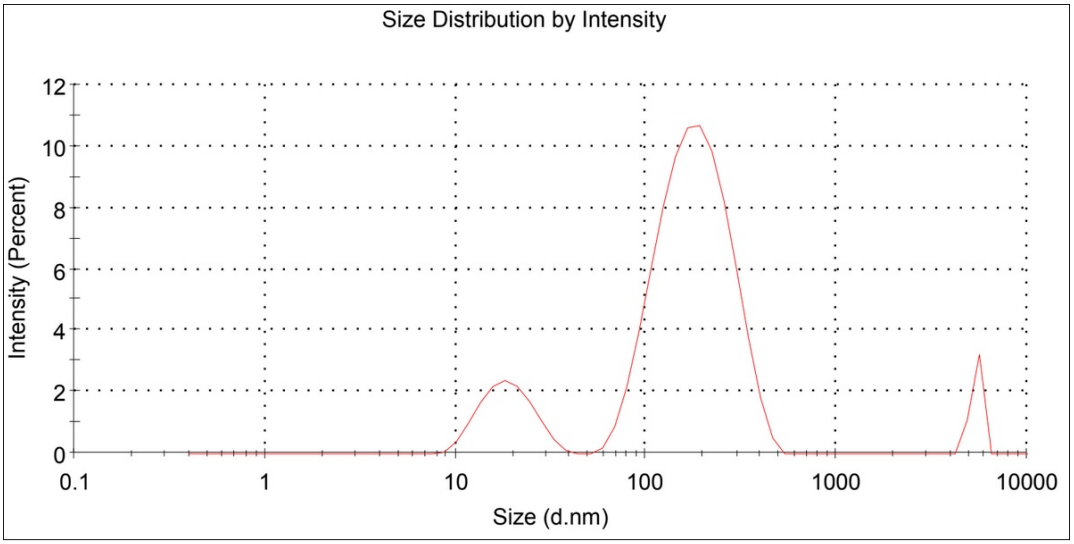

Figure A.105: Third reading of size distribution by intensity for loaded micelles created with the co-solvent evaporation method for 12 kDa, second iteration of the triplicates, done by the DLS software done with attenuation factor 7. A table with information on peaks, intensity and standard deviation can be seen in Appendix B as readings 2.12.1.2 - 3

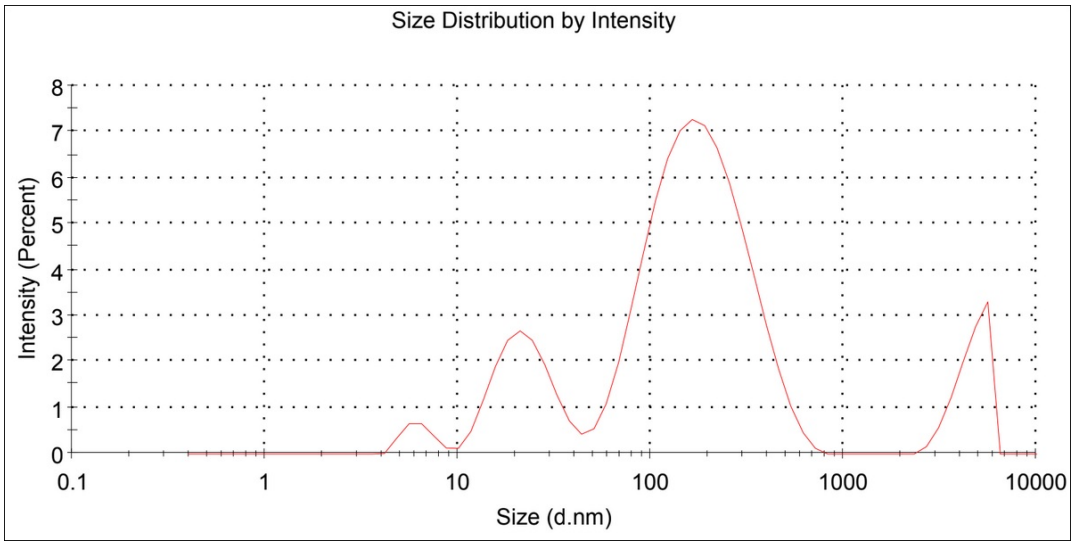

Figure A.106: First reading of size distribution by intensity for loaded micelles created with the co-solvent evaporation method for 12 kDa, third iteration of the triplicates, done by the DLS software done with attenuation factor 7. A table with information on peaks, intensity and standard deviation can be seen in Appendix B as readings 2.12.1.3 - 1

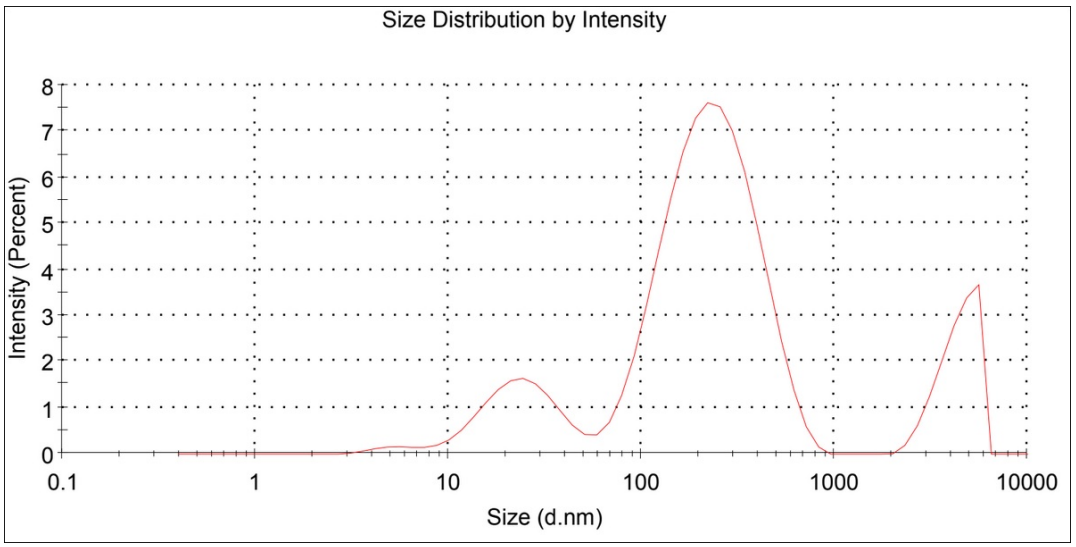

Figure A.107: Second reading of size distribution by intensity for loaded micelles created with the co-solvent evaporation method for 12 kDa, third iteration of the triplicates, done by the DLS software done with attenuation factor 7. A table with information on peaks, intensity and standard deviation can be seen in Appendix B as readings 2.12.1.3 - 2

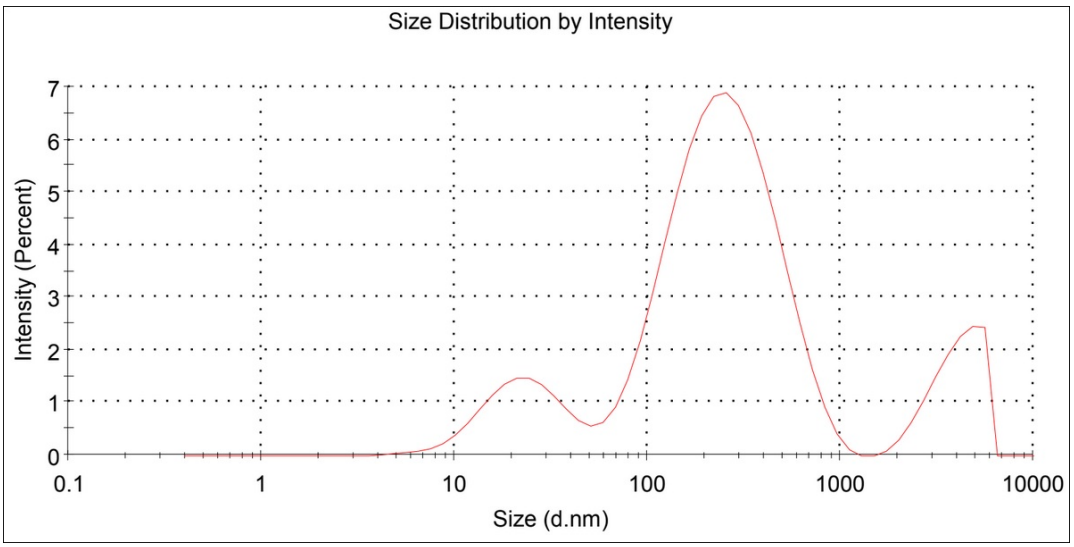

Figure A.108: Third reading of size distribution by intensity for loaded micelles created with the co-solvent evaporation method for 12 kDa, third iteration of the triplicates, done by the DLS software done with attenuation factor 7. A table with information on peaks, intensity and standard deviation can be seen in Appendix B as readings 2.12.1.3 - 3

Appendix B

DLS tables

Here the tables created from the 3 readings the DLS does of the individual samples read. It is given with the information of Z-average (size dependency to the intensity), peak size (which is the size at the highest intensity point in the graph), St. Dev (the standard deviation of the size) and PdI (the polydispersity index, or dispersion, given by the DLS software) and intensity (the percentage of the peak present in the total reading). Z-average and polydispersity is for the whole sample reading and includes each individual peak present, and thus if there are more than one peak present it will be presented in a "separate" part of the tables below, only 3 peaks are presented with data from the software. This will then become the a part of the tables while each peak is presented in the b part of the table, as such: Table A.1.1 a & b, as can be seen in table B.2.

Table B.1: The 3 readings done by the DLS of the BSA-polymer conjugate, with the average presented as Av - BSA.

READING (SAMPLE)	Z-AVERAGE	PEAK SIZE	ST. DEV	PDI
1 - BSA	135,8	148,80	42,35	0,087
2 - BSA	135,8	153,20	53,84	0,112
3 - BSA	136,7	148,60	41,83	0,079
AV - BSA	136,1	150,2	46,39	0,093

Table B.2: The 3 readings done by the DLS on the first iteration of the triplicates of empty micelles created with sonification method, of 3 kDa pvp-od, with the individual peaks present in each reading. Which also includes the average of all 3 readings presented as Av - 1.3.0.1.

READING - SAMPLE	Z-AVERAGE	PDL
1 - 1.3.0.1	579,0	0,499
2 - 1.3.0.1	428,8	0,503
3 - 1.3.0.1	533,3	0,515
AV - 1.3.0.1	513,7	0,506

a)

Reading - Sample - Peak	Peak size	Intensity	St. Dev
1 - 1.3.0.1 - 1	893,4	66,1	249,4
1 - 1.3.0.1 - 2	151,5	32,4	36,5
1 - 1.3.0.1 - 3	5560	1,4	0,00
2 - 1.3.0.1 - 1	408,2	89,9	114,0
2 - 1.3.0.1 - 2	81,5	9,1	14,6
2 - 1.3.0.1 -3	5560	1,0	6,1*10-5
3 - 1.3.0.1 - 1	662,8	75,8	177,1
3 - 1.3.0.1 - 2	134,9	24,2	29,7
Av - 1.3.0.1 -1	624,8	76,9	270,8
Av - 1.3.0.1 - 2	138,2	22,3	40,6
Av - 1.3.0.1 - 3	5560	0,8	0,0

b)

Table B.3: The 3 readings done by the DLS on the second iteration of the triplicates of empty micelles created with sonification method, of 3 kDa pvp-od, with the individual peaks present in each reading. Which also includes the average of all 3 readings presented as Av - 1.3.0.2.

READING - SAMPLE	Z-AVERAGE	PDL
1 - 1.3.0.2	309,1	0,692
2 - 1.3.0.2	289,2	0,701
3 - 1.3.0.2	300,4	0,731
Av - 1.3.0.2	299,6	0,708

a)

Reading - Sample - Peak	Peak size	Intensity	St. Dev
1 - 1.3.0.2 - 1	210,7	63,2	77,4
1 - 1.3.0.2 - 2	1506	18,9	505,8
1 - 1.3.0.2 - 3	4539	18,0	920,1
2 - 1.3.0.2 - 1	221,2	67,7	93,6
2 - 1.3.0.2 - 2	4237	21,3	1020
2 - 1.3.0.2 - 3	1422	11,0	467,7
3 - 1.3.0.2 - 1	236,9	66,2	108,2
3 - 1.3.0.2 - 2	3880	33,8	1097
Av - 1.3.0.2 - 1	223,0	65,2	94,6
Av - 1.3.0.2 - 2	4067	25,5	1138
Av - 1.3.0.2 - 3	1371	9,4	390,0

b)

Table B.4: The 3 readings done by the DLS on the third iteration of the triplicates of empty micelles created with sonification method, of 3 kDa pvp-od, with the individual peaks present in each reading. Which also includes the average of all 3 readings presented as Av - 1.3.0.3.

READING - SAMPLE	Z-AVERAGE	PDL
1 - 1.3.0.3	331,7	0,798
2 - 1.3.0.3	306,9	0,857
3 - 1.3.0.3	337,5	0,663
Av - 1.3.0.3	325,3	0,772

a)

Reading - Sample - Peak	Peak size	Intensity	St. Dev
1 - 1.3.0.3 - 1	218,8	56,4	77,5
1 - 1.3.0.3 - 2	4441	24,7	987,6
1 - 1.3.0.3 - 3	1393	15,1	426,5
2 - 1.3.0.3 - 1	190,6	57,0	53,5
2 - 1.3.0.3 - 2	3637	43,0	116
3 - 1.3.0.3 - 1	190,8	60,1	68,5
3 - 1.3.0.3 - 2	1961	21,4	590,9
3 - 1.3.0.3 - 3	4607	18,5	863,7
Av - 1.3.0.3 - 1	199,8	58,5	68,6
Av - 1.3.0.3 - 2	3391	40,2	1492
Av - 1.3.0.3 - 3	45,4	1,3	9,1

b)

Table B.5: The 3 readings done by the DLS on the first iteration of the triplicates of loaded micelles created with sonification method, of 3 kDa pvp-od, with the individual peaks present in each reading. Which also includes the average of all 3 readings presented as Av - 1.3.1.1.

READING - SAMPLE	Z-AVERAGE	PDL
1 - 1.3.1.1	239,1	0,530
2 - 1.3.1.1	240,0	0,548
3 - 1.3.1.1	235,8	0,537
Av - 1.3.1.1	238,3	0,538

a)

Reading - Sample - Peak	Peak size	Intensity	St. Dev
1 - 1.3.1.1 - 1	264,6	89,6	118,7
1 - 1.3.1.1 - 2	4733	10,4	766,8
2 - 1.3.1.1 - 1	284,0	83,8	128,8
2 - 1.3.1.1 - 2	4590	10,8	837,2
2 - 1.3.1.1 - 3	53,96	5,5	12,60
3 - 1.3.1.1 - 1	297,5	92,7	166,1
3 - 1.3.1.1 - 2	4800	7,3	725,6
Av - 1.3.1.1 - 1	277,9	90,5	142,7
Av - 1.3.1.1 - 2	4696	9,5	789,1

b)

Table B.6: The 3 readings done by the DLS on the second iteration of the triplicates of loaded micelles created with sonification method, of 3 kDa pvp-od, with the individual peaks present in each reading. Which also includes the average of all 3 readings presented as Av - 1.3.1.2.

READING - SAMPLE	Z-AVERAGE	PDL
1 - 1.3.1.2	176,1	0,558
2 - 1.3.1.2	178,9	0,551
3 - 1.3.1.2	178,9	0,566
Av - 1.3.1.2	177,9	0,558

a)

Reading - Sample - Peak	Peak size	Intensity	St. Dev
1 - 1.3.1.2 - 1	206,3	87,2	120,8
1 - 1.3.1.2 - 2	4500	12,8	882,5
2 - 1.3.1.2 - 1	241,6	86,4	213,8
2 - 1.3.1.2 - 2	4107	13,6	1079
3 - 1.3.1.2 - 1	216,6	83,2	148,5
3 - 1.3.1.2 - 2	3657	16,8	1259
Av - 1.3.1.2 - 1	220,2	85,4	160,2
Av - 1.3.1.2 - 2	4024	14,6	1176

b)

Table B.7: The 3 readings done by the DLS on the third iteration of the triplicates of loaded micelles created with sonification method, of 3 kDa pvp-od, with the individual peaks present in each reading. Which also includes the average of all 3 readings presented as Av - 1.3.1.3.

READING - SAMPLE	Z-AVERAGE	PDL
1 - 1.3.1.3	182,1	0,412
2 - 1.3.1.3	173,7	0,416
3 - 1.3.1.3	173,6	0,394
Av - 1.3.1.3	176,5	0,407

a)

Reading - Sample - Peak	Peak size	Intensity	St. Dev
1 - 1.3.1.3 - 1	169,1	74,8	72,9
1 - 1.3.1.3 - 2	2642	25,2	1266
2 - 1.3.1.3 - 1	329,6	91,9	418,8
2 - 1.3.1.3 - 2	3901	8,1	1096
3 - 1.3.1.3 - 1	172,1	79,8	90,9
3 - 1.3.1.3 - 2	2826	20,2	1348
Av - 1.3.1.3 - 1	178,3	78,2	98,5
Av - 1.3.1.3 - 2	2577	21,8	1407

b)

Table B.8: The 3 readings done by the DLS on the first iteration of the triplicates of empty micelles created with co-solvent evaporation method, of 3 kDa pvp-od, with the individual peaks present in each reading. Which also includes the average of all 3 readings presented as Av - 2.3.0.1.

READING - SAMPLE	Z-AVERAGE	PDL
1 - 2.3.0.1	266,8	0,448
2 - 2.3.0.1	262,0	0,447
3 - 2.3.0.1	263,8	0,454
Av - 2.3.0.1	264,2	0,450

a)

Reading - Sample - Peak	Peak size	Intensity	St. Dev
1 - 2.3.0.1 - 1	366,9	87,3	233,8
1 - 2.3.0.1 - 2	4844	7,2	711,5
1 - 2.3.0.1 - 3	36,89	5,5	8,81
2 - 2.3.0.1 - 1	353,6	92,3	224,4
2 - 2.3.0.1 - 2	4800	7,7	728,0
3 - 2.3.0.1 - 1	567,0	61,4	291,1
3 - 2.3.0.1 - 2	144,0	33,3	45,0
3 - 2.3.0.1 - 3	4725	5,3	772,4
Av - 2.3.0.1 - 1	382,6	91,4	264,0
Av - 2.3.0.1 - 2	4795	6,8	736,1
Av - 2.3.0.1 - 3	36,31	1,8	8,0

Table B.9: The 3 readings done by the DLS on the second iteration of the triplicates of empty micelles created with co-solvent evaporation method, of 3 kDa pvp-od, with the individual peaks present in each reading. Which also includes the average of all 3 readings presented as Av - 2.3.0.2.

READING - SAMPLE	Z-AVERAGE	PDL
1 - 2.3.0.2	237,0	0,528
2 - 2.3.0.2	262,4	0,559
3 - 2.3.0.2	274,3	0,502
Av - 2.3.0.2	257,9	0,530

a)

Reading - Sample - Peak	Peak size	Intensity	St. Dev
1 - 2.3.0.2 - 1	380,5	94,6	247,0
1 - 2.3.0.2 - 2	4833	5,4	713,4
2 - 2.3.0.2 - 1	456,2	85,6	219,6
2 - 2.3.0.2 - 2	72,7	11,0	23,1
2 - 2.3.0.2 - 3	4941	3,4	646,4
3 - 2.3.0.2 - 1	419,5	87,1	210,9
3 - 2.3.0.2 - 2	69,0	7,6	20,7
3 - 2.3.0.2 - 3	4840	5,3	709,4
Av - 2.3.0.2 - 1	396,6	95,3	237,2
Av - 2.3.0.2 - 2	4862	4,7	697,8
Av - 2.3.0.1 - 3	36,31	1,8	8,0

Table B.10: The 3 readings done by the DLS on the third iteration of the triplicates of empty micelles created with co-solvent evaporation method, of 3 kDa pvp-od, with the individual peaks present in each reading. Which also includes the average of all 3 readings presented as Av - 2.3.0.3.

READING - SAMPLE	Z-AVERAGE	PDL
1 - 2.3.0.3	315,1	0,573
2 - 2.3.0.3	376,9	0,555
3 - 2.3.0.3	389,2	0,499
Av - 2.3.0.3	360,4	0,542

a)

Reading - Sample - Peak	Peak size	Intensity	St. Dev
1 - 2.3.0.3 - 1	373,8	95,4	209,6
1 - 2.3.0.3 - 2	5346	4,6	355,5
2 - 2.3.0.3 - 1	458,9	92,9	273,5
2 - 2.3.0.3 - 2	5165	7,1	498,5
3 - 2.3.0.3 - 1	647,6	87,0	602,6
3 - 2.3.0.3 - 2	4113	13,0	998,0
Av - 2.3.0.3 - 1	489,9	91,8	411,5
Av - 2.3.0.3 - 2	4639	8,2	970,3

Table B.11: The 3 readings done by the DLS on the first iteration of the triplicates of loaded micelles created with co-solvent evaporation method, of 3 kDa pvp-od, with the individual peaks present in each reading. Which also includes the average of all 3 readings presented as Av - 2.3.1.1.

READING - SAMPLE	Z-AVERAGE	PDL
1 - 2.3.1.1	256,4	0,606
2 - 2.3.1.1	221,8	0,678
3 - 2.3.1.1	220,0	0,782
Av - 2.3.1.1	232,7	0,689

a)

Reading - Sample - Peak	Peak size	Intensity	St. Dev
1 - 2.3.1.1 - 1	283,4	83,3	156,3
1 - 2.3.1.1 - 2	4865	13,0	699,8
1 - 2.3.1.1 - 3	22,45	3,7	7,2
2 - 2.3.1.1 - 1	373,0	85,1	364,3
2 - 2.3.1.1 - 2	3945	14,9	1148
3 - 2.3.1.1 - 1	241,4	67,4	103,3
3 - 2.3.1.1 - 2	3008	28,4	1245
3 - 2.3.1.1 - 3	40,18	4,2	10,2
Av - 2.3.1.1 - 1	282,7	76,7	179,4
Av - 2.3.1.1 - 2	3504	20,2	1435
Av - 2.3.1.1 - 3	34,75	3,1	13,6

Table B.12: The 3 readings done by the DLS on the second iteration of the triplicates of loaded micelles created with co-solvent evaporation method, of 3 kDa pvp-od, with the individual peaks present in each reading. Which also includes the average of all 3 readings presented as Av - 2.3.1.2.

READING - SAMPLE	Z-AVERAGE	PDL
1 - 2.3.1.2	550,4	266,2
2 - 2.3.1.2	507,9	221,3
3 - 2.3.1.2	649,4	234,4
Av - 2.3.1.2	569,2	240,7

Table B.13: The 3 readings done by the DLS on the third iteration of the triplicates of loaded micelles created with co-solvent evaporation method, of 3 kDa pvp-od, with the individual peaks present in each reading. Which also includes the average of all 3 readings presented as Av - 2.3.1.3.

READING - SAMPLE	Z-AVERAGE	PDL
1 - 2.3.1.3	458,2	259,4
2 - 2.3.1.3	487,8	257,2
3 - 2.3.1.3 Peak 1 (Intensity %) ———— Peak 2 (Intensity %)	515,4	308,9 (88,8) ———— 48,36 (11,2)
Av - 2.3.1.2 Peak 1 (Intensity %) ———— Peak 2 (Intensity %)	487,1	273,9 (96,3) ———— 48,36 (3,7)

Table B.14: The 3 readings done by the DLS on the first iteration of the triplicates of empty micelles created with sonification method, of 6 kDa pvp-od, with the individual peaks present in each reading. Which also includes the average of all 3 readings presented as Av - 1.6.0.1.

READING - SAMPLE	Z-AVERAGE	PDL
1 - 1.6.0.1	246,0	0,551
2 - 1.6.0.1	254,6	0,594
3 - 1.6.0.1	224,2	0,580
Av - 1.6.0.1	238,6	0,575

a)

Reading - Sample - Peak	Peak size	Intensity	St. Dev
1 - 1.6.0.1 - 1	233,3	84,8	126,0
1 - 1.6.0.1 - 2	4818	15,2	722,0
2 - 1.6.0.1 - 1	184,6	74,7	53,2
2 - 1.6.0.1 - 2	1320	14,1	366,7
2 - 1.6.0.1 - 3	4977	11,2	622,9
3 - 1.6.0.1 - 1	223,8	86,1	95,8
3 - 1.6.0.1 - 2	4755	13,9	760,3
Av - 1.6.0.1 - 1	215,6	81,7	100,8
Av - 1.6.0.1 - 2	4840	13,4	715,4
Av - 1.6.0.1 - 3	1301	4,9	388,1

Table B.15: The 3 readings done by the DLS on the first iteration of the triplicates of empty micelles created with sonification method, of 6 kDa pvp-od, with the individual peaks present in each reading. Which also includes the average of all 3 readings presented as Av - 1.6.0.2.

READING - SAMPLE	Z-AVERAGE	PDL
1 - 1.6.0.2	211,7	0,557
2 - 1.6.0.2	197,0	0,505
3 - 1.6.0.2	189,4	0,485
Av - 1.6.0.2	199,4	0,516

a)

Reading - Sample - Peak	Peak size	Intensity	St. Dev
1 - 1.6.0.2 - 1	216,3	85,3	76,0
1 - 1.6.0.2 - 2	4607	14,7	823,6
2 - 1.6.0.2 - 1	221,5	88,3	94,64
2 - 1.6.0.2 - 2	4686	10,0	792,1
2 - 1.6.0.2 - 3	41,78	1,7	8,9
3 - 1.6.0.2 - 1	195,0	90,3	65,6
3 - 1.6.0.2 - 2	4887	9,7	678,5
Av - 1.6.0.2 - 1	210,7	88,0	80,42
Av - 1.6.0.2 - 2	4709	11,5	784,7
Av - 1.6.0.2 - 3	41,78	0,6	8,9

Table B.16: The 3 readings done by the DLS on the third iteration of the triplicates of empty micelles created with sonification method, of 6 kDa pvp-od, with the individual peaks present in each reading. Which also includes the average of all 3 readings presented as Av - 1.6.0.3.

READING - SAMPLE	Z-AVERAGE	PDL
1 - 1.6.0.3	339,3	0,704
2 - 1.6.0.3	314,6	0,748
3 - 1.6.0.3	301,7	0,706
Av - 1.6.0.3	318,5	0,719

a)

Reading - Sample - Peak	Peak size	Intensity	St. Dev
1 - 1.6.0.3 - 1	200,2	59,6	59,05
1 - 1.6.0.3 - 2	4650	20,8	848,6
1 - 1.6.0.3 - 3	1403	19,5	464,1
2 - 1.6.0.3 - 1	240,1	65,8	115,6
2 - 1.6.0.3 - 2	4025	34,2	1096
3 - 1.6.0.3 - 1	22,2	65,9	90,0
3 - 1.6.0.3 - 2	4073	34,1	1079
Av - 1.6.0.3 - 1	223,0	63,3	97,2
Av - 1.6.0.3 - 2	4074	31,0	1155
Av - 1.6.0.3 - 3	1266	5,7	300,2

Table B.17: The 3 readings done by the DLS on the first iteration of the triplicates of loaded micelles created with sonification method, of 6 kDa pvp-od, with the individual peaks present in each reading. Which also includes the average of all 3 readings presented as Av - 1.6.1.1.

READING - SAMPLE	Z-AVERAGE	PDL
1 - 1.6.1.1	241,9	0,413
2 - 1.6.1.1	228,0	0,505
3 - 1.6.1.1	229,9	0,544
Av - 1.6.1.1	315,1	0,573

a)

Reading - Sample - Peak	Peak size	Intensity	St. Dev
1 - 1.6.1.1 - 1	238,8	80,0	119,2
1 - 1.6.1.1 - 2	3597	20,0	1198
2 - 1.6.1.1 - 1	258,9	89,3	141,7
2 - 1.6.1.1 - 2	4673	10,7	799,4
3 - 1.6.1.1 - 1	275,1	89,5	158,5
3 - 1.6.1.1 - 2	4640	10,5	816,6
Av - 1.6.1.1 - 1	373,8	95,4	209,6
Av - 1.6.1.1 - 2	5346	4,6	355,5

Table B.18: The 3 readings done by the DLS on the second iteration of the triplicates of loaded micelles created with sonification method, of 6 kDa pvp-od, with the individual peaks present in each reading. Which also includes the average of all 3 readings presented as Av - 1.6.1.2.

READING - SAMPLE	Z-AVERAGE	PDL
1 - 1.6.1.2	178,4	0,360
2 - 1.6.1.2	176,6	0,379
3 - 1.6.1.2	176,7	0,361
Av - 1.6.1.2	177,2	0,367

a)

Reading - Sample - Peak	Peak size	Intensity	St. Dev
1 - 1.6.1.2 - 1	208,0	90,6	113,1
1 - 1.6.1.2 - 2	4300	9,4	968,7
2 - 1.6.1.2 - 1	193,0	7,3	79,32
2 - 1.6.1.2 - 2	3981	12,7	1091
3 - 1.6.1.2 - 1	191,3	90,5	89,45
3 - 1.6.1.2 - 2	4551	9,5	864,3
Av - 1.6.1.2 - 1	197,5	89,5	95,49
Av - 1.6.1.2 - 2	4247	10,5	1019

Table B.19: The 3 readings done by the DLS on the third iteration of the triplicates of loaded micelles created with sonification method, of 6 kDa pvp-od, with the individual peaks present in each reading. Which also includes the average of all 3 readings presented as Av - 1.6.1.3.

READING - SAMPLE	Z-AVERAGE	PDL
1 - 1.6.1.3	178,8	0,556
2 - 1.6.1.3	190,2	0,402
3 - 1.6.1.3	194,0	0,417
Av - 1.6.1.3	187,6	0,458

a)

Reading - Sample - Peak	Peak size	Intensity	St. Dev
1 - 1.6.1.3 - 1	200,4	79,6	120,3
1 - 1.6.1.3 - 2	1017	11,5	381,4
1 - 1.6.1.3 - 3	4429	9,0	945,0
2 - 1.6.1.3 - 1	207,0	82,4	113,3
2 - 1.6.1.3 - 2	3283	17,6	1242
3 - 1.6.1.3 - 1	201,0	78,7	107,2
3 - 1.6.1.3 - 2	3254	19,2	1285
3 - 1.6.1.3 - 3	10,8	1,3	2,1
Av - 1.6.1.3 - 1	216,7	82,1	146,2
Av - 1.6.1.3 - 2	3240	17,2	1418
Av - 1.6.1.3 - 3	10,8	0,4	2,1

Table B.20: The 3 readings done by the DLS on the firstiteration of the triplicates of empty micelles created with co-solvent evaporation method, of 6 kDa pvp-od, with the individual peaks present in each reading. Which also includes the average of all 3 readings presented as Av - 2.6.0.1.

READING - SAMPLE	Z-AVERAGE	PDL
1 - 2.6.0.1	561,0	0,738
2 - 2.6.0.1	402,7	0,718
3 - 2.6.0.1	381,4	0,852
Av - 2.6.0.1	448,4	0,770

a)

Reading - Sample - Peak	Peak size	Intensity	St. Dev
1 - 2.6.0.1 - 1	353,9	83,2	67,3
1 - 2.6.0.1 - 2	69,1	16,8	11,4
2 - 2.6.0.1 - 1	282,9	91,0	55,0
2 - 2.6.0.1 - 2	48,7	9,0	7,5
3 - 2.6.0.1 - 1	405,3	73,1	90,4
3 - 2.6.0.1 - 2	88,8	26,9	19,5
Av - 2.6.0.1 - 1	343,0	82,5	87,0
Av - 2.6.0.1 - 2	75,67	17,5	21,8

Table B.21: The 3 readings done by the DLS on the second iteration of the triplicates of lempty micelles created with co-solvent evaporation method, of 6 kDa pvp-od, with the individual peaks present in each reading. Which also includes the average of all 3 readings presented as Av - 2.6.0.2.

Reading (sample)	Z-average	Peak size	St. Dev	PdI
1 - 2.6.0.2	903,5	293,6	34,0	0,728
2 - 2.6.0.2	1015	270,2	34,6	0,810
3 - 2.6.0.2	1000	256,1	28,5	0,829
Av - 2.6.0.2	973,0	273,3	36,0	0,789

Table B.22: The 3 readings done by the DLS on the third iteration of the triplicates of empty micelles created with co-solvent evaporation method, of 6 kDa pvp-od, with the individual peaks present in each reading. Which also includes the average of all 3 readings presented as Av - 2.6.0.3.

READING - SAMPLE	Z-AVERAGE	PDL
1 - 2.6.0.3	361,5	0,568
2 - 2.6.0.3	340,8	0,542
3 - 2.6.0.3	334,9	0,531
Av - 2.6.0.3	345,7	0,547

a)

Reading - Sample - Peak	Peak size	Intensity	St. Dev
1 - 2.6.0.3 - 1	678,0	72,1	185,7
1 - 2.6.0.3 - 2	103,1	27,9	23,7
2 - 2.6.0.3 - 1	618,1	70,8	169,4
2 - 2.6.0.3 - 2	103,2	29,2	23,4
3 - 2.6.0.3 - 1	555,4	74,1	175,8
3 - 2.6.0.3 - 2	95,8	25,9	26,7
Av - 2.6.0.3 - 1	616,6	72,3	184,1
Av - 2.6.0.3 - 2	100,9	27,7	24,8

Table B.23: The 3 readings done by the DLS on the first iteration of the triplicates of loaded micelles created with co-solvent evaporation method, of 6 kDa pvp-od, with the individual peaks present in each reading. Which also includes the average of all 3 readings presented as Av - 2.6.1.1.

READING - SAMPLE	Z-AVERAGE	PDL
1 - 2.6.1.1	187,9	0,621
2 - 2.6.1.1	138,1	0,715
3 - 2.6.1.1	135,5	0,804
Av - 2.6.1.1	153,9	0,713

a)

Reading - Sample - Peak	Peak size	Intensity	St. Dev
1 - 2.6.1.1 - 1	117,9	46,9	44,4
1 - 2.6.1.1 - 2	503,8	43,7	211,7
1 - 2.6.1.1 - 3	4900	9,4	676,4
2 - 2.6.1.1 - 1	139,6	62,8	65,2
2 - 2.6.1.1 - 2	810,7	26,8	330,3
2 - 2.6.1.1 - 3	5067	4,0	574,9
3 - 2.6.1.1 - 1	191,2	71,1	101,4
3 - 2.6.1.1 - 2	1525	12,6	597,8
3 - 2.6.1.1 - 3	4161	8,9	998,3
Av - 2.6.1.1 - 1	171,7	70,7	107,2
Av - 2.6.1.1 - 2	896,3	21,0	478,3
Av - 2.6.1.1 - 3	4636	7,4	895,4

Table B.24: The 3 readings done by the DLS on the second iteration of the triplicates of loaded micelles created with co-solvent evaporation method, of 6 kDa pvp-od, with the individual peaks present in each reading. Which also includes the average of all 3 readings presented as Av - 2.6.1.2.

READING - SAMPLE	Z-AVERAGE	PDL
1 - 2.6.1.2	320,7	0,536
2 - 2.6.1.2	382,3	0,530
3 - 2.6.1.2	372,6	0,591
Av - 2.6.1.2	358,5	0,552

a)

Reading - Sample - Peak	Peak size	Intensity	St. Dev
1 - 2.6.1.2 - 1	865,6	48,9	296,2
1 - 2.6.1.2 - 2	138,3	44,5	41,8
1 - 2.6.1.2 - 3	5192	6,6	480,0
2 - 2.6.1.2 - 1	165,5	43,0	56,9
2 - 2.6.1.2 - 2	914,3	42,7	374,8
2 - 2.6.1.2 - 3	4804	14,4	727,9
3 - 2.6.1.2 - 1	202,9	49,6	98,2
3 - 2.6.1.2 - 2	1009	36,3	397,3
3 - 2.6.1.2 - 3	4878	14,1	689,4
Av - 2.6.1.2 - 1	162,0	44,2	64,1
Av - 2.6.1.2 - 2	902,8	44,1	367,5
Av - 2.6.1.2 - 3	4906	11,7	687,2

Table B.25: The 3 readings done by the DLS on the third iteration of the triplicates of loaded micelles created with co-solvent evaporation method, of 6 kDa pvp-od, with the individual peaks present in each reading. Which also includes the average of all 3 readings presented as Av - 2.6.1.3.

READING - SAMPLE	Z-AVERAGE	PDL
1 - 2.6.1.3	165,7	0,845
2 - 2.6.1.3	190,0	0,802
3 - 2.6.1.3	260,1	0,737
Av - 2.6.1.3	205,3	0,795

a)

Reading - Sample - Peak	Peak size	Intensity	St. Dev
1 - 2.6.1.3 - 1	292,1	80,2	235,2
1 - 2.6.1.3 - 2	3733	14,2	1213
1 - 2.6.1.3 - 3	14,21	4,1	4,3
2 - 2.6.1.3 - 1	206,4	64,2	108,9
2 - 2.6.1.3 - 2	823,5	27,7	326,7
2 - 2.6.1.3 - 3	4808	8,1	727,5
3 - 2.6.1.3 - 1	463,1	85,7	415,9
3 - 2.6.1.3 - 2	4382	14,3	979,5
Av - 2.6.1.3 - 1	398,0	86,4	383,8
Av - 2.6.1.3 - 2	4342	11,7	1001
Av - 2.6.1.3 - 3	14,2	1,4	4,3

Table B.26: The 3 readings done by the DLS on the first iteration of the triplicates of empty micelles created with sonification method, of 12 kDa pvp-od, with the individual peaks present in each reading. Which also includes the average of all 3 readings presented as Av - 1.12.0.1

READING - SAMPLE	Z-AVERAGE	PDL
1 - 1.12.0.1	137,9	0,679
2 - 1.12.0.1	165,0	0,695
3 - 1.12.0.1	209,0	0,530
Av - 1.12.0.1	170,6	0,635

a)

Reading - Sample - Peak	Peak size	Intensity	St. Dev
1 - 1.12.0.1 - 1	227,9	81,7	155,1
1 - 1.12.0.1 - 2	4569	10,8	864,5
1 - 1.12.0.1 - 3	12,4	7,5	2,7
2 - 1.12.0.1 - 1	208,4	66,8	107,1
2 - 1.12.0.1 - 2	856,9	15,1	266,4
2 - 1.12.0.1 - 3	24,9	8,5	7,5
3 - 1.12.0.1 - 1	151,9	48,2	56,3
3 - 1.12.0.1 - 2	437,6	38,3	157,1
3 - 1.12.0.1 - 3	14,8	7,7	3,1
Av - 1.12.0.1 - 1	276,0	83,2	223,3
Av - 1.12.0.1 - 2	16,7	9,2	7,4
Av - 1.12.0.1 - 3	4908	7,6	755,8

Table B.27: The 3 readings done by the DLS on the second iteration of the triplicates of empty micelles created with sonification method, of 12 kDa pvp-od, with the individual peaks present in each reading. Which also includes the average of all 3 readings presented as Av - 1.12.0.2

READING - SAMPLE	Z-AVERAGE	PDL
1 - 1.12.0.2	146,2	0,641
2 - 1.12.0.2	179,7	0,650
3 - 1.12.0.2	216,5	0,646
Av - 1.12.0.2	180,8	0,646

a)

Reading - Sample - Peak	Peak size	Intensity	St. Dev
1 - 1.12.0.2 - 1	231,6	77,9	172,0
1 - 1.12.0.2 - 2	4614	12,8	834,1
1 - 1.12.0.2 - 3	14,0	9,3	3,2
2 - 1.12.0.2 - 1	252,6	72,8	198,8
2 - 1.12.0.2 - 2	4586	16,5	852,1
2 - 1.12.0.2 - 3	11,2	6,3	3,1
3 - 1.12.0.2 - 1	290,0	74,0	241,7
3 - 1.12.0.2 - 2	4824	15,8	721,7
3 - 1.12.0.2 - 3	22,2	7,5	5,4
Av - 1.12.0.2 - 1	257,2	75,1	207,1
Av - 1.12.0.2 - 2	4677	15,1	810,8
Av - 1.12.0.2 - 3	16,9	9,9	8,3

Table B.28: The 3 readings done by the DLS on the third iteration of the triplicates of empty micelles created with sonification method, of 12 kDa pvp-od, with the individual peaks present in each reading. Which also includes the average of all 3 readings presented as Av - 1.12.0.3

READING - SAMPLE	Z-AVERAGE	PDL
1 - 1.12.0.3	193,8	0,581
2 - 1.12.0.3	296,6	0,515
3 - 1.12.0.3	342,0	0,487
Av - 1.12.0.3	277,5	0,527

a)

Reading - Sample - Peak	Peak size	Intensity	St. Dev
1 - 1.12.0.3 - 1	234,7	83,5	129,5
1 - 1.12.0.3 - 2	5172	8,9	489,5
1 - 1.12.0.3 - 3	13,5	7,7	3,3
2 - 1.12.0.3 - 1	240,7	62,3	125,7
2 - 1.12.0.3 - 2	1036	15,5	338,1
2 - 1.12.0.3 - 3	4822	14,7	723,6
3 - 1.12.0.3 - 1	324,1	68,5	208,4
3 - 1.12.0.3 - 2	4170	27,9	1067
3 - 1.12.0.3 - 3	11,6	4,2	3,4
Av - 1.12.0.3 - 1	318,9	76,5	277,8
Av - 1.12.0.3 - 2	4553	16,2	972,1
Av - 1.12.0.3 - 3	16,1	73	7,7

Table B.29: The 3 readings done by the DLS on the first iteration of the triplicates of loaded micelles created with sonification method, of 12 kDa pvp-od, with the individual peaks present in each reading. Which also includes the average of all 3 readings presented as Av - 1.12.1.1

READING - SAMPLE	Z-AVERAGE	PDL
1 - 1.12.1.1	181,4	0,376
2 - 1.12.1.1	188,1	0,388
3 - 1.12.1.1	197,8	0,408
Av - 1.12.1.1	189,1	0,391

a)

Reading - Sample - Peak	Peak size	Intensity	St. Dev
1 - 1.12.1.1 - 1	214,8	88,8	89,2
1 - 1.12.1.1 - 2	4893	6,0	678,9
1 - 1.12.1.1 - 3	17,6	5,2	7,0
2 - 1.12.1.1 - 1	211,9	88,1	92,0
2 - 1.12.1.1 - 2	4104	11,9	1098
3 - 1.12.1.1 - 1	254,8	91,0	169,6
3 - 1.12.1.1 - 2	4429	9,0	943,8
Av - 1.12.1.1 - 1	227,7	89,3	126,1
Av - 1.12.1.1 - 2	4385	9,0	1018
Av - 1.12.1.1 - 3	17,6	1,7	7,0

Table B.30: The 3 readings done by the DLS on the second iteration of the triplicates of loaded micelles created with sonification method, of 12 kDa pvp-od, with the individual peaks present in each reading. Which also includes the average of all 3 readings presented as Av - 1.12.1.2

READING - SAMPLE	Z-AVERAGE	PDL
1 - 1.12.1.2	263,3	0,581
2 - 1.12.1.2	229,4	0,543
3 - 1.12.1.2	228,9	0,408
Av - 1.12.1.2	231,5	0,511

a)

Reading - Sample - Peak	Peak size	Intensity	St. Dev
1 - 1.12.1.2 - 1	277,1	89,1	126,1
1 - 1.12.1.2 - 2	4594	10,9	840,0
2 - 1.12.1.2 - 1	300,5	93,3	185,4
2 - 1.12.1.2 - 2	5014	6,7	604,8
3 - 1.12.1.2 - 1	246,1	80,8	111,4
3 - 1.12.1.2 - 2	3326	19,2	1257
Av - 1.12.1.2 - 1	277,9	87,8	154,2
Av - 1.12.1.2 - 2	4010	12,2	1274

Table B.31: The 3 readings done by the DLS on the third iteration of the triplicates of loaded micelles created with sonification method, of 12 kDa pvp-od, with the individual peaks present in each reading. Which also includes the average of all 3 readings presented as Av - 1.12.1.3

READING - SAMPLE	Z-AVERAGE	PDL
1 - 1.12.1.3	146,8	0,387
2 - 1.12.1.3	142,5	0,411
3 - 1.12.1.3	182,3	0,443
Av - 1.12.1.3	157,2	0,413

a)

Reading - Sample - Peak	Peak size	Intensity	St. Dev
1 - 1.12.1.3 - 1	202,8	92,2	98,0
1 - 1.12.1.3 - 2	17,6	5,1	6,4
1 - 1.12.1.3 - 3	4991	2,7	613,4
2 - 1.12.1.3 - 1	211,5	97,4	128,6
2 - 1.12.1.3 - 2	4770	2,6	744,2
3 - 1.12.1.3 - 1	290,1	94,3	265,4
3 - 1.12.1.3 - 2	4829	5,7	717,9
Av - 1.12.1.3 - 1	234,8	94,6	183,6
Av - 1.12.1.3 - 2	4855	3,6	704,8
Av - 1.12.1.3 - 3	17,6	1,7	6,5

Table B.32: The 3 readings done by the DLS on the first iteration of the triplicates of empty micelles created with co-solvent evaporation method, of 12 kDa pvp-od, with the individual peaks present in each reading. Which also includes the average of all 3 readings presented as Av - 2.12.0.1

READING - SAMPLE	Z-AVERAGE	PDL
1 - 2.12.0.1	304,7	0,788
2 - 2.12.0.1	378,6	0,544
3 - 2.12.0.1	362,0	0,622
Av - 2.12.0.1	348,4	0,651

a)

Reading - Sample - Peak	Peak size	Intensity	St. Dev
1 - 2.12.0.1 - 1	734,5	70,5	311,0
1 - 2.12.0.1 - 2	22,7	14,	10,8
1 - 2.12.0.1 - 3	4837	8,1	710,7
2 - 2.12.0.1 - 1	619,9	71,8	234,4
2 - 2.12.0.1 - 2	40,3	12,3	14,5
2 - 2.12.0.1 - 3	14,0	8,3	4,2
3 - 2.12.0.1 - 1	765,0	73,7	285,8
3 - 2.12.0.1 - 2	19,2	11,3	6,0
3 - 2.12.0.1 - 3	64,4	10,8	20,7
Av - 2.12.0.1 - 1	706,7	71,9	285,7
Av - 2.12.0.1 - 2	19,1	11,8	7,3
Av - 2.12.0.1 - 3	57,7	9,7	20,6

Table B.33: The 3 readings done by the DLS on the second iteration of the triplicates of empty micelles created with co-solvent evaporation method, of 12 kDa pvp-od, with the individual peaks present in each reading. Which also includes the average of all 3 readings presented as Av - 2.12.0.2

READING - SAMPLE	Z-AVERAGE	PDL
1 - 2.12.0.2	78,73	0,582
2 - 2.12.0.2	100,5	0,624
3 - 2.12.0.2	106,1	0,553
Av - 2.12.0.2	95,1	0,587

a)

Reading - Sample - Peak	Peak size	Intensity	St. Dev
1 - 2.12.0.2 - 1	169,4	83,3	99,5
1 - 2.12.0.2 - 2	17,1	14,7	6,6
1 - 2.12.0.2 - 3	4743	2,0	758,0
2 - 2.12.0.2 - 1	201,2	98,2	152,1
2 - 2.12.0.2 - 2	5043	1,8	586,4
3 - 2.12.0.2 - 1	210,8	82,8	123,8
3 - 2.12.0.2 - 2	19,8	14,1	7,8
3 - 2.12.0.2 - 3	4964	3,2	630,5
Av - 2.12.0.2 - 1	201,4	84,2	127,1
Av - 2.12.0.2 - 2	18,3	13,5	7,2
Av - 2.12.0.2 - 3	4921	2,3	669,7

Table B.34: The 3 readings done by the DLS on the third iteration of the triplicates of empty micelles created with co-solvent evaporation method, of 12 kDa pvp-od, with the individual peaks present in each reading. Which also includes the average of all 3 readings presented as Av - 2.12.0.3

READING - SAMPLE	Z-AVERAGE	PDL
1 - 2.12.0.3	166,6	0,587
2 - 2.12.0.3	157,9	0,658
3 - 2.12.0.3	164,9	0,513
Av - 2.12.0.3	163,2	0586

a)

Reading - Sample - Peak	Peak size	Intensity	St. Dev
1 - 2.12.0.3 - 1	269,2	85,4	144,0
1 - 2.12.0.3 - 2	17,3	8,1	4,6
1 - 2.12.0.3 - 3	4504	6,4	881,6
2 - 2.12.0.3 - 1	254,5	85,9	112,6
2 - 2.12.0.3 - 2	17,8	9,1	4,4
2 - 2.12.0.3 - 3	4827	5,0	714,5
3 - 2.12.0.3 - 1	267,6	85,5	129,6
3 - 2.12.0.3 - 2	21,8	9,4	6,4
3 - 2.12.0.3 - 3	4897	4,0	677,0
Av - 2.12.0.3 - 1	263,7	85,6	129,5
Av - 2.12.0.3 - 2	19,1	8,9	5,6
Av - 2.12.0.3 - 3	4710	5,1	799,8

Table B.35: The 3 readings done by the DLS on the first iteration of the triplicates of loaded micelles created with co-solvent evaporation method, of 12 kDa pvp-od, with the individual peaks present in each reading. Which also includes the average of all 3 readings presented as Av - 2.12.1.1

READING - SAMPLE	Z-AVERAGE	PDL
1 - 2.12.1.1	153,1	0,461
2 - 2.12.1.1	147,0	0,392
3 - 2.12.1.1	133,7	0,425
Av - 2.12.1.1	144,6	0,426

a)

Reading - Sample - Peak	Peak size	Intensity	St. Dev
1 - 2.12.1.1 - 1	250,2	65,7	125,4
1 - 2.12.1.1 - 2	27,9	18,2	11,0
1 - 2.12.1.1 - 3	4482	13,1	893,4
2 - 2.12.1.1 - 1	273,7	67,1	153,7
2 - 2.12.1.1 - 2	30,5	25,0	18,3
2 - 2.12.1.1 - 3	4798	7,9	729,0
3 - 2.12.1.1 - 1	272,2	63,7	129,5
3 - 2.12.1.1 - 2	36,7	20,8	14,5
3 - 2.12.1.1 - 3	4537	8,8	867,0
Av - 2.12.1.1 - 1	265,2	65,3	137,5
Av - 2.12.1.1 - 2	32,8	20,4	14,5
Av - 2.12.1.1 - 3	4582	9,9	855,0

Table B.36: The 3 readings done by the DLS on the second iteration of the triplicates of loaded micelles created with co-solvent evaporation method, of 12 kDa pvp-od, with the individual peaks present in each reading. Which also includes the average of all 3 readings presented as Av - 2.12.1.2

READING - SAMPLE	Z-AVERAGE	PDL
1 - 2.12.1.2	176,7	0,315
2 - 2.12.1.2	180,6	0,267
3 - 2.12.1.2	169,4	0,348
Av - 2.12.1.2	175,6	0,310

a)

Reading - Sample - Peak	Peak size	Intensity	St. Dev
1 - 2.12.1.2 - 1	204,2	81,3	78,16
1 - 2.12.1.2 - 2	19,0	13,9	5,5
1 - 2.12.1.2 - 3	5267	4,8	429,8
2 - 2.12.1.2 - 1	213,4	81,0	83,6
2 - 2.12.1.2 - 2	21,9	14,1	6,6
2 - 2.12.1.2 - 3	5222	4,9	461,7
3 - 2.12.1.2 - 1	190,0	82,4	78,2
3 - 2.12.1.2 - 2	19,2	13,3	5,8
3 - 2.12.1.2 - 3	5366	4,3	330,7
Av - 2.12.1.2 - 1	202,5	81,6	80,6
Av - 2.12.1.2 - 2	20,1	13,8	6,1
Av - 2.12.1.2 - 3	5282	4,7	418,2

Table B.37: The 3 readings done by the DLS on the second iteration of the triplicates of loaded micelles created with co-solvent evaporation method, of 12 kDa pvp-od, with the individual peaks present in each reading. Which also includes the average of all 3 readings presented as Av - 2.12.1.3

READING - SAMPLE	Z-AVERAGE	PDL
1 - 2.12.1.3	108,6	0,615
2 - 2.12.1.3	174,0	0,533
3 - 2.12.1.3	178,9	0,472
Av - 2.12.1.3	153,8	0,540

a)

Reading - Sample - Peak	Peak size	Intensity	St. Dev
1 - 2.12.1.3 - 1	199,1	72,1	111,3
1 - 2.12.1.3 - 2	22,8	15,6	7,5
1 - 2.12.1.3 - 3	4640	10,0	818,0
2 - 2.12.1.3 - 1	254,9	72,5	133,4
2 - 2.12.1.3 - 2	4409	13,9	923,4
2 - 2.12.1.3 - 3	25,8	12,9	11,7
3 - 2.12.1.3 - 1	284,6	74,9	173,6
3 - 2.12.1.3 - 2	4051	12,6	1069
3 - 2.12.1.3 - 3	24,2	12,5	11,0
Av - 2.12.1.3 - 1	246,7	73,1	146,6
Av - 2.12.1.3 - 2	24,3	13,5	9,9
Av - 2.12.1.3 - 3	4349	12,1	978,8

Appendix C

Table for Cytotoxic Assay

Table C.1: Table showing the given values from the life/death assay kit. With sample name given with the method used, concentration, polymeric length and if it is loaded [L] or empty [E]. It also gives the calculated percentages, standard deviation and the mean.

Sample	Mean	Standard deviation	Value	Dead cells (%)
[L] 12 kDa co-solvent 0.08 mg/ml	69,59	3,42	-2,92	-1,86
[L] 12 kDa co-solvent 0.04 mg/ml	73,73	1,99	1,22	0,78
[E] 12 kDa co-solvent 0.08 mg/ml	77.80	2,45	3,30	2,10
[E] 12 kDa co-solvent 0.04 mg/ml	77,80	3,73	5,28	3,36
[L] 12 kDa sonification 0.08 mg/ml	75,09	2,42	2,57	1,63
[L] 12 kDa sonification 0.04 mg/ml	74,47	1,13	1,96	1,24
[E] 12 kDa sonification 0.08 mg/ml	77,72	1,99	5,21	3,31
[E] 12 kDa sonification 0.04 mg/ml	78,52	0,48	6,00	3,81
BSA-conjugates 0.08 mg/ml	74,21	1,96	1,69	1,07
BSA-conjugates 0,04 mg/ml	74,30	0,92	1,78	1,13
[E] 6 kDa co-solvent 0.08 mg/ml	80,71	2,85	8,20	5,21
[L] 6 kDa co-solvent 0.08 mg/ml	92,04	1,88	19,53	12,40
[E] 6 kDa sonification 0.08 mg/ml	142,26	1,21	69,75	44,30
Positive control	229,93	12,73	157,42	100,00
Negative control	72,52	2.92	0,00	0,00

Table C.2: Table containing the mean, standard deviation and percentage of dead cells for empty micelles formed by 6 kDa pvp-od polymers with the sonification method incubating for 24 hours on fibroblast cells.

	Concentration (mg/ml)				
	5	0.1	0.08	0.04	0.01
Mean	165.87	159.63	138.84	99.63	82.57
St.dev	11.32	0.91	17.68	14.05	1.47
Dead cells (%)	42.56	39.55	29.52	10.60	2.38

Table C.3: Table containing the mean, standard deviation and percentage of dead cells after for empty micelles formed by 6 kDa pvp-od polymers with the sonification method incubating for 24 hours on glioblastoma cells.

	Concentration (mg/ml)				
	5	0.1	0.08	0.04	0.01
Mean	162.06	157.58	171.41	82.91	79.94
St.dev	18.05	7.75	22.87	3.34	7.26
Dead cells (%)	31.15	29.26	35.09	-2.22	-3.47

Table C.4: Table containing the mean, standard deviation and percentage of dead cells after for empty micelles formed by 6 kDa pvp-od polymers with the sonification method incubating for 24 hours on fibroblast cells.

	Concentration (mg/ml)				
	5	0.1	0.08	0.04	0.01
Mean	125.32	143.58	141.98	112.86	93.72
St.dev	5.83	13.22	10.94	19.33	6.04
Dead cells (%)	23.00	31.81	31.03	16.99	7.75

Table C.5: Table containing the mean, standard deviation and percentage of dead cells after for empty micelles formed by 6 kDa pvp-od polymers with the sonification method incubating for 24 hours on glioblastoma cells.

	Concentration (mg/ml)				
	5	0.1	0.08	0.04	0.01
Mean	125.32	160.85	166.46	135.71	92.42
St.dev	5.83	11.65	11.79	26.29	4.01
Dead cells (%)	15.66	30.64	33.00	20.04	1.79

Table C.6: Table containing the mean, standard deviation and percentage of dead cells after incubation for empty micelles formed by 6 kDa pvp-od polymers with the co-solvent evaporation method, incubating for 24 hours on fibroblast cells.

	Concentration (mg/ml)		
	0.08	0.04	0.01
Mean	89.34	99.50	95.41
St.dev	5.49	16.87	4.62
Dead cells (%)	5.64	10.54	8.57

Table C.7: Table containing the mean, standard deviation and percentage of dead cells after incubation for empty micelles formed by 6 kDa pvp-od polymers with the co-solvent evaporation method, incubating for 24 hours on glioblastoma cells.

	Concentration (mg/ml)		
	0.08	0.04	0.01
Mean	100.36	83.48	89.83
St.dev	15.30	6.87	6.67
Dead cells (%)	5.14	-1.98	0.70

Table C.8: Table containing the mean, standard deviation and percentage of dead cells after incubation for empty micelles formed by 12 kDa pvp-od polymers with the co-solvent evaporation method, incubating for 24 hours on fibroblast cells.

	Concentration (mg/ml)			
	0.1	0.08	0.04	0.01
Mean	128.57	111.34	97.33	98.85
St.dev	16.01	13.69	12.50	16.61
Dead cells (%)	24.57	16.26	9.50	10.23

Table C.9: Table containing the mean, standard deviation and percentage of dead cells after incubation for empty micelles formed by 12 kDa pvp-od polymers with the co-solvent evaporation method, incubating for 24 hours on glioblastoma cells.

	Concentration (mg/ml)			
	0.1	0.08	0.04	0.01
Mean	87.25	96.04	86.66	78.76
St.dev	4.10	7.26	9.36	5.52
Dead cells (%)	-0.39	3.32	-0.64	-3.97

Table C.10: Table containing the mean, standard deviation and percentage of dead cells after incubation for empty micelles formed by 12 kDa pvp-od polymers with the co-solvent evaporation method, incubating for 24 hours on fibroblast cells.

	Concentration (mg/ml)			
	0.1	0.08	0.04	0.01
Mean	137.93	103.47	97.92	99.08
St.dev	5.84	7.81	5.62	5.79
Dead cells (%)	29.08	12.46	9.78	10.34

Table C.11: Table containing the mean, standard deviation and percentage of dead cells after incubation for empty micelles formed by 12 kDa pvp-od polymers with the co-solvent evaporation method, incubating for 24 hours on glioblastoma cells.

	Concentration (mg/ml)			
	0.1	0.08	0.04	0.01
Mean	167.69	85.00	89.29	88.03
St.dev	9.06	8.47	5.49	7.59
Dead cells (%)	33.52	-1.34	0.47	-0.06